BUMP CONTROL DESIGN PROTOCOL FOR ROOM-AND-PILLAR RETREAT MINING

by

Alan A. Campoli

Dissertation submitted to the Faculty of the Virginia Polytechnic Institute and State University in partial fulfillment of the requirements for the degree of

DOCTOR OF PHILOSOPHY

in

Mining Engineering

APPROVED:

C. Haycocks, Chairman

M. G. Karfakis

E. R. Palowitch

E. Topuz

M. E. Karmis

May, 1994

Blacksburg, Virginia

BUMP CONTROL DESIGN PROTOCOL FOR ROOM-AND-PILLAR RETREAT MINING

by

Alan A. Campoli

Dr. Christopher Haycocks

Department of Mining and Minerals Engineering

ABSTRACT

A stress control design protocol was developed to minimize coal mine bumps, which are the explosive failure of highly stressed pillars. The protocol was developed for room-and-pillar retreat mining conducted with available continuous miner technology. The inability of existing coal pillar equations to accurately represent the wide total extraction pillars required, forced the development of the pseudoductile coal pillar strength model. A confined pillar core is assumed to reach a maximum stress when surrounded by a yielded perimeter. The width of the yielded perimeter is assumed to increase linearly with increased coalbed thickness. The pseudoductile model was employed in the development of supercritical and subcritical width section design criteria. The supercritical design procedure assumes an infinitely long pillar line, composed of uniformly sized pillars, extracted against an infinitely wide gob area. Tributary area theory was combined with a linear shear angle concept to estimate the loads applied to total extraction pillars adjacent to gob areas. The boundary element code MULSIM/NL was utilized in the development and implementation of a systematic subcritical design procedure to apply the stress shield

concept to retreat room-and-pillar coal mining, under bump hazard. The complex distribution of gob side abutment load between the side abutment pillars and the chain pillars in the total extraction zone made computer simulation a necessity. Section layouts were determined for the mining of a 6 ft thick coalbed under overburden up to 2,200 ft thick. The sections consist of total extraction areas separated by continuous abutment pillars. A spreadsheet program LAYOUT was created to summarize and provide for efficient utilization of the bump control design protocol. Based on overburden thickness, coalbed thickness, abutment load linear shear angle, and pillar dimensions entered by the user, LAYOUT calculates a stability factor for the first and second pillar row outbye the expanding gob for supercritical width sections. If the overburden and coalbed thickness conditions do not allow a supercritical section design, LAYOUT develops a subcritical design.

DEDICATION

I would like to dedicate this work to three individuals have made vital contributions, without which success would have been impossible. Mr. Claude A. Goode, Research Supervisor, Explosives Group, Pittsburgh Research Center, Bureau of Mines is at once my mentor, friend, and the closest thing I have to a father in this world. His encouragement and vision for this work in its early stages will never be forgotten. Mr. Michael Gauna, Mining Engineer, Consolidation Coal Company, St. Louis, Missouri who while Engineering Manager at Island Creek Coal Company, Oakwood Division had the courage to implement a very successful bump control longwall gate road design that many so called experts said would cause bumps of "biblical proportion." Finally, Mr. Fred C. VanDyke, Coal Mine Inspector, Mine Safety and Health Administration, Princeton, WV who while an Engineering Technician with the Bureau of Mines put five years of his life into the collection of valuable field data.

ACKNOWLEDGMENTS

I would like to express my gratitude to Dr. Christopher Haycocks, Dr. Michael E. Karmis, Dr. Mario Karfakis, Dr. Ertugrul Topuz, and Dr. Eugene R. Palowitch for their help and guidance during the course of my research. Special thanks to my Bureau of Mines Managers: Dr. David R. Forshey, Associate Director--Research; Mr. John N. Murphy, Research Director, Pittsburgh Research Center; Mr. Gerald L. Finfinger, Research Supervisor, Ground and Methane Control Group; and Mr. Anthony T. Iannacchione, Group Supervisor, Rock Mechanics for their technical and organizational support of this effort.

The Ground and Methane Control Group, Pittsburgh Research Center, Bureau of Mines provided the vehicle for the this research, which began in 1984 with the Tri-State Mountain Bump Workshop held in Princeton, WV. Significant contributions to this work been made by numerous Bureau employees and representatives from: the Island Creek Coal Company; Olga Coal Company; LTV Steel Company; U.S. Steel Mining Company; Milburn Colliery Company; W-P Coal Company; and the Mine Safety and Health Administration, Bruceton Safety Technology Center.

Mrs. Kimberly Mitchell's careful and time consuming preparation of this manuscript is most appreciated.

TABLE OF CONTENTS

LIST OF FIGURES

Page

Page

Page

Page

LIST OF TABLES

Chapter I

INTRODUCTION

1.1 Problem Definition and Significance

A coal mine bump is the violent failure of coal pillar(s) due to overstress, during retreat mining. The phenomenon has been the subject of research in the United States and abroad for over 100 years. The Southern Appalachian Region of the United States experienced fatalities from bumps during room-and-pillar mining as early as 1923 in the Cumberland Plateau District of eastern Kentucky and Virginia (Rice, 1935), and in the Gary District of West Virginia in 1930 (Talman and Schroder, 1958). Bumps have resulted in 14 fatalities from 1959 to the present in the eastern states of Kentucky, West Virginia, and Pennsylvania (Campoli, et al., 1993).

Risk of coal mine bumps becomes critical when the mined coalbed is under significant overburden and encased in rigid associated strata. In general, a bump-prone coalbed is located under overburden in excess of 500 ft thick, and is confined by a massive sandstone or conglomerate roof and a strong floor that does not heave readily.

Previous research can be divided into methodologies to either predict or prevent coal mine bumps. The prediction of coal mine bumps within an existing or planned mine must be based on sound geologic knowledge of the formation containing the mined coalbed. Geologic information combined with historical bump occurrence information can isolate high stress areas likely to bump. Once the circumstances

likely to surround bump occurrence have been outlined, various modeling, geophysical, and geotechnical techniques are available to further define the location and magnitude of the potential bump hazard.

All coal mine bumps are the result of dangerous accumulations and release of coalbed stress. Coal mine bumps can prevented by limiting the magnitude of coalbed stress through mining method modifications and/or localized destressing procedures. Destressing transfers stress from one portion of a mine structure to another by fracturing or softening coal and/or associated strata. Coal, or in some instances roof and/or floor rock, is intentionally fractured and made to fail, thereby, reducing the ability of the fractured zone to carry the load. Volley firing, hydraulic fracturing, and auger drilling are the destressing methods commonly employed in coal mines. The relative effectiveness of each method depends largely on local mine conditions. Conceptually the principle is simple, but in practice, controlling the rate and magnitude of load transfer is difficult. The timing of destressing is critical. Performed too late, the act of destressing can be dangerous in itself as it may trigger a bump. Performed too early, the coalbed may reconsolidate and accumulate the necessary strain energy required to bump upon coal cutting.

1.2 Objective and Scope

The goal of this research was to facilitate safe and efficient room-and-pillar retreat mining of bump-prone coalbeds, without resorting to costly and hazardous

destressing methodologies. This was accomplished by limiting the coalbed stress adjacent to expanding gob areas through mining method modification. Specifically, the development of a bump control protocol based on section layout design changes, using the assumption that coal mine layout changes are the only factor under significant control of the mine operator. The protocol was developed within the limits imposed by existing continuous miner technology to ensure the research would be of practical value to mines currently extracting deep bump prone coalbeds.

Retreat mining requires that the coal in areas of total extraction support the combination of development and gob side abutment loads. The greater the percent extraction during development mining the less support remains to support these loads during retreat mining. Retreat longwall total extraction zones are very large coal pillars that provide for maximum support. Continuous miner technology requires the total extraction area be cut into small coal pillars to facilitate ventilation, haulage, and roof support functions during retreat mining. It is for this reason that longwall technology has been recommended over continuous miner technology when mining deep, bump prone coalbeds (Campoli, et. al, 1993). However, longwall sections have very high capital costs and require large and geologically consistent coal reserves. Continuous miner sections capital costs are one eighth that of longwall sections and can economically mine smaller and geologically inconsistent coal reserves. The price for this increased flexibility and reduced capital costs is decreased production capacity and increased ground control problems.

1.3 Methodology

Development of the stress limit design protocol required an understanding of: 1) the total extraction pillar size limitations imposed by continuous miner technology; 2) the strength and failure characteristics of coal mine pillar under bump prone geologic conditions; and 3) the magnitude and distribution of gob side abutment load. The stress limit concept is simple, keep the stress in the pillars adjacent to the gob below that which results in explosive coal bumps. This can be accomplished by maximizing coal pillar strength or minimizing abutment loads. But the maximum total extraction pillar size is determined by continuous miner technology limitations, not ground control considerations.

Thus, the first step in the design process is to determine the limits of total extraction pillar sizes. The second step is to estimate the strength of these pillars. The third step is to construct mining layouts that limited the abutment stress applied to the total extraction pillars, to below that which caused bumps. Finally, a spreadsheet computer program will be created to summarize and provide for efficient utilization of the bump control design protocol.

Chapter II

LITERATURE REVIEW

2.1 Occurrence and Classification of Bumps

The violent failure of coals due to excessive stress, were described as early as 1730 in collieries in the northern regions of England. The first North American incidents occurred in mines in the Crowsnest Pass Field of British Columbia in 1909 (Lessley, 1983). The Southern Appalachian Region of the United States experienced fatalities from bumps during room-and-pillar mining as early as 1923 in the Cumberland Plateau District of eastern Kentucky and Virginia (Rice, 1935), and in the Gary District of West Virginia in 1930 (Talman and Schroder, 1958).

Bumps and related high stress failures occur whenever coal is mined under significant overburden thickness. Thus, numerous bump classification systems have been advanced worldwide (Herd, 1930; Hargraves, 1958; Fine, 1964; Lama, 1967; Crouch and Fairhurst, 1973). U.S. Bureau of Mines researchers classify violent failures in coal mines as bounces, bursts, and outbursts (Campoli, et al., 1987; Haramy and McDonnell, 1988). A bounce is the sudden forceful impact or vibration of a coal pillar which may be accompanied by rib or face movement. A burst is the instantaneous explosive failure of coal or associated strata. An outburst is the spontaneous ejection of coal and gas from the solid face. The ejected coal is pulverized in the process. The gas released is a mixture of predominantly methane

and carbon dioxide. Outbursts result in a cavity ahead of, or to one side of the entry. During an outburst, large quantities of gas are emitted. Subsequently, there is a rapid reduction in the gas emission rate over time (Campoli, et al., 1985).

Rice (1935) perceived two types of bumps, differentiated by the mechanism triggering failure of the coal. Pressure bumps were described as the sudden failure of a pillar or pillar remnant due to static overloading resulting in failure once the coal's strength was exceeded. Rice thought the second category of violent failure, shock bumps, occurred more frequently. Shock bumps resulted from dynamic loading of the pillar brought about by dramatic changes in the distribution of stress in the overlying strata. Holland and Thomas (1954) discounted the importance of the distinction between shock and pressure bumps and noted that the majority of bumps actually occurred in pillars subjected to the highest level of static loading.

2.2 Pillar Loading and Bump Mechanism

When an opening is developed in a coalbed, a portion of the natural ground support is removed, and the load of the superjacent strata over the mined out area must be carried by the coal that remains. The subjacent strata also react to that added load through the coal. The natural tendency of the roof, floor, and coal pillars is to close this opening. In actuality, coal pillars bearing substantial load will deteriorate resulting in perimeter yielding and sloughing. This widens the unsupported span and transmits an additional load onto the remaining structurally competent coal. Figure

2.1 is an idealized illustration of the adjustment of the stress field to the loss of equilibrium and the creation of high loading at the edge of the coal pillar due to stress concentration.

The load transferred to a pillar is determined by the percent of extraction and the thickness of the overburden. The stress distribution in the pillar, however, is governed by the physical properties of the roof, floor, and coalbed, along with pillar geometry. The probable stress distribution on a wide pillar is idealized in figure 2.2. Idealistically, the pillar has sufficient roof contact area to carry the load without failure and sufficient floor bearing area to resist the load. It is further postulated that the roof-and-floor are resistant to yielding. As coal generally is a friable material, the edges of the pillar yield. Thus, the stresses are low at the yielding edges of the pillar and increase rapidly over a short distance toward the core of the pillar. The state of stress in the core zone of the pillar is a function of its width and the length of time it has been supporting the roof. In a wide pillar it is postulated that the stress level is substantially lower in the pillar core than near the edges.

Figure 2.3 indicates the idealized stress pattern over a narrow pillar. As a narrow pillar takes load, the pillar yields and the roof-and-floor tend to converge. Under this condition, the pillar is incapable of carrying subsequent loadings. As a result, solid coal bears the additional weight. The formation of a secondary arch as

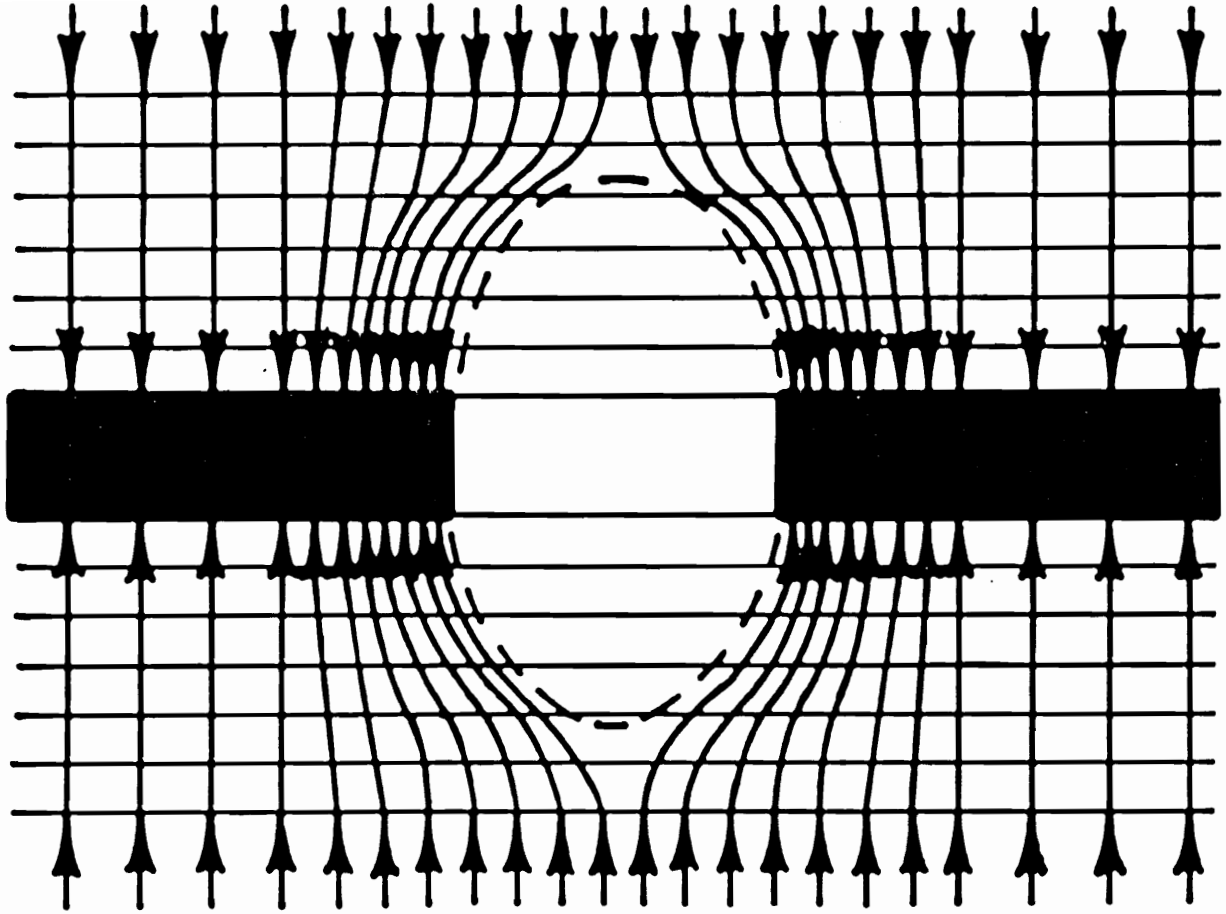

Figure 2.1—Adjustment of stress around a single entry (After Campoli, et al., 1987).

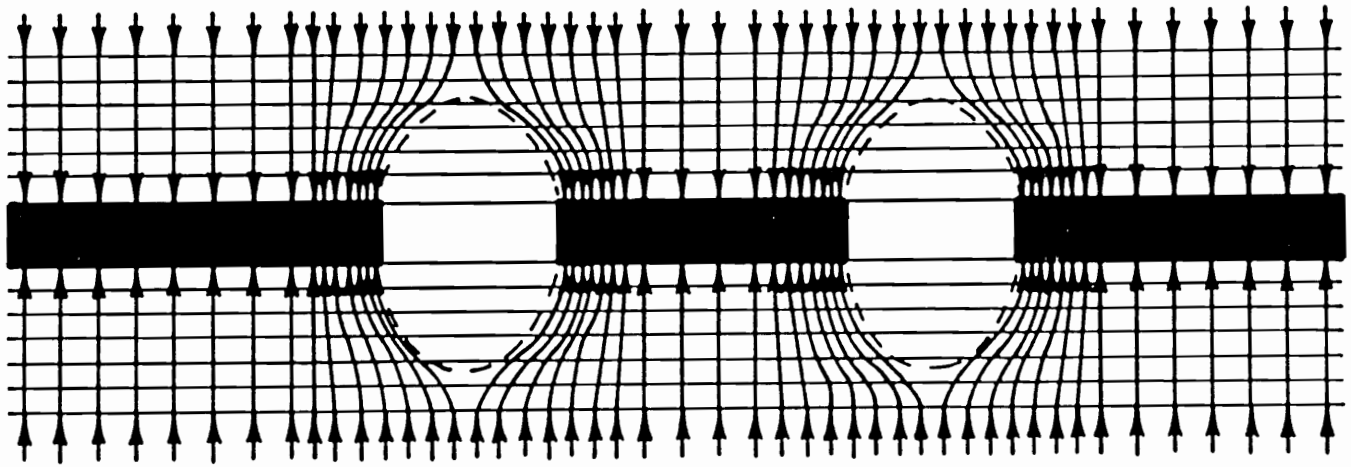

Figure 2.2—Adjustment of stress around a wide pillar (After Campoli, et al., 1987).

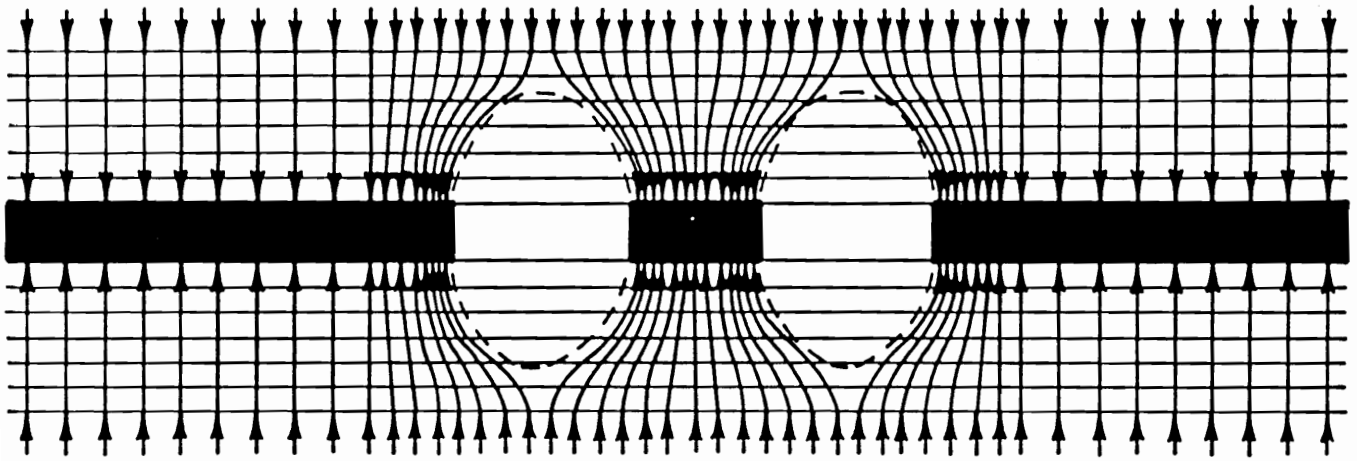

Figure 2.3—Adjustment of stress around a narrow pillar (After Campoli, et al., 1987).

shown in figure 2.4 is time dependent, being a function of the nature of the strata (Goode, et al., 1984). This natural stress arch has been used to stabilize roof strata in coal and potash mines (Serata, 1991). Carr, et al. (1984) described the solution of longwall gateroad roof stability problems through application of a yield-abutment-yield gateroad design, in the 2,000 ft deep Mary Lee Coalbed. Coal mine bumps were mitigated in the Pocahontas No. 4 Coalbed in Southern West Virginia by extracting thin yield pillars against a wide abutment pillar in the 1950's (Campoli, et al., 1987).

The pillar loading hypotheses just presented for development of a pillar section are similar for retreat mining, with the addition of abutment zone forces. While the stress distribution in the gob is difficult to measure, the effect of the associated abutment pressures on the active pillar section is indicated by convergence directly outby the pillar line. Roof-to-floor convergence, brought on by the approaching pillar line, represents the total movement of the roof, floor, and pillar system. Depending on the physical properties of the coalbed, the characteristics of the adjacent strata and the depth of cover, the lateral extent of the zone of convergence may vary from a few tens of feet to hundreds of feet.

Coal pillars exposed to high abutment zone pressures will either yield or support the load, depending on their size and strength. A bump hazard may develop in a pillar of intermediate size, especially when surrounded by smaller yielding pillars. A pillar of this size yields around its periphery. The destressed coal around

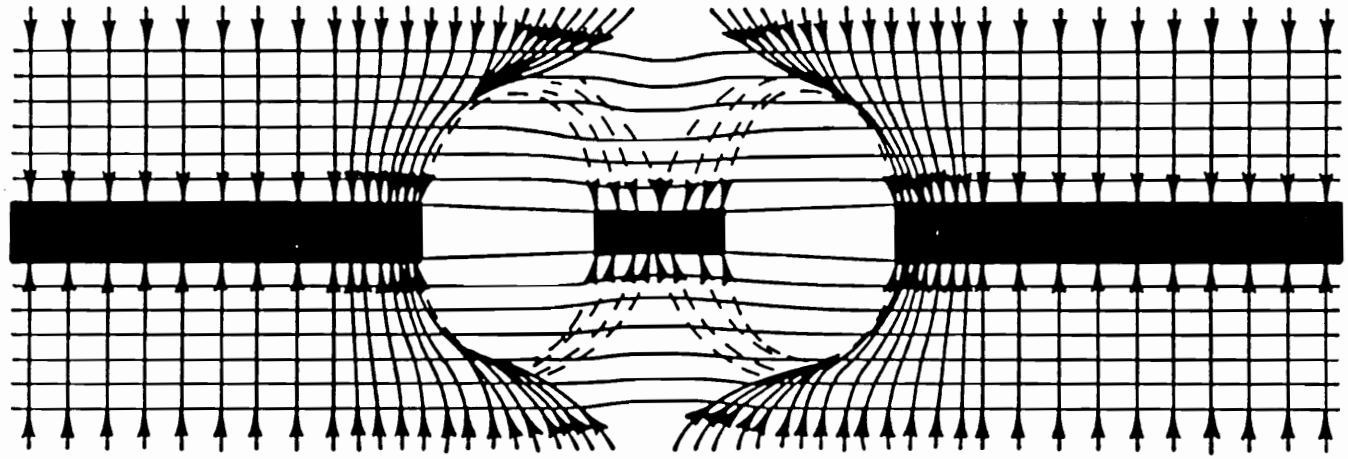

Figure 2.4—Adjustment of stress due to the yielding of a narrow pillar (After Campoli, et al., 1987).

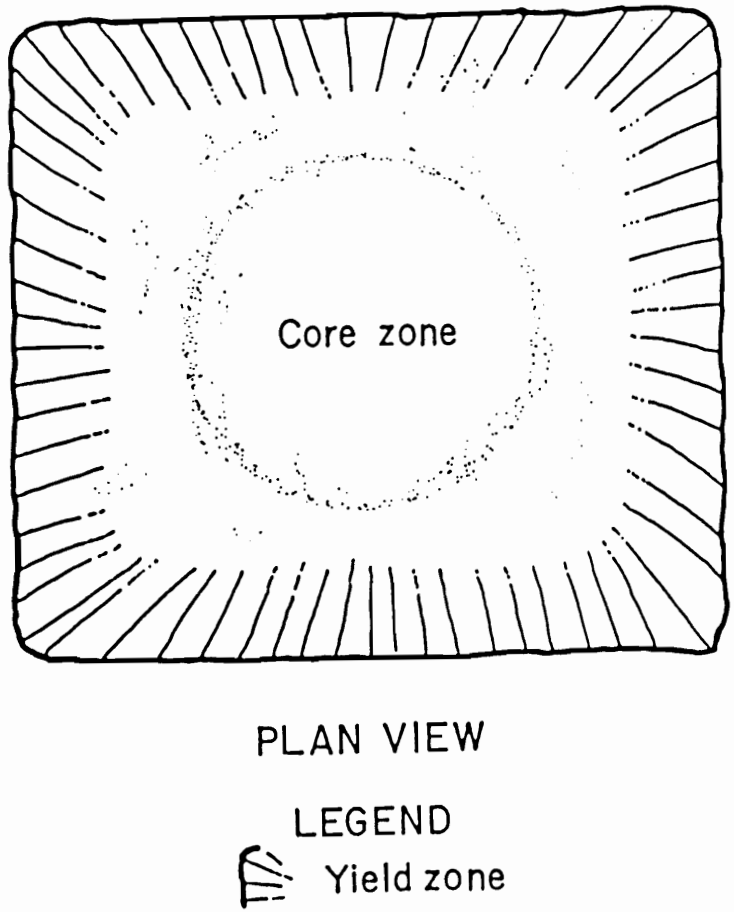

Figure 2.5—Idealized diagram of core confinement loading of a critical size pillar (After Campoli, et al., 1987).

the perimeter confines the pillar core. Figure 2.5 is an idealized plan view of the conditions in such a pillar. The lateral forces exerted by the pressurized core are counterbalanced by the lateral confinement provided by the yielded perimeter (Campoli, et al., 1987).

It has been shown by Holland (1958) and Phillips (1944), that coal pillars deformed in the above fashion store elastic strain energy. The unconfined outer perimeter stores little strain energy. As the distance from the pillar edge increases, the amount of energy stored per unit volume of coal increases dramatically until a maximum is reached. Beyond that point, the energy stored per unit volume of the coal decreases towards the inner core of the pillar.

If the stiffness of the pillar is greater than the stiffness of the loading system, violent failure of the pillar will occur when the stress within the pillar reaches the pillar strength (Blake, 1972). The situation depicted in case A of figure 2.6 is the storage of excess energy, as represented in the cross-hatched region, to continue to load the pillar without the introduction of additional external force. If the stiffness of the loading system is greater than that of the pillar as is shown in case B of figure 2.6, nonviolent or gradual failure or yielding occurs. Insufficient strain energy is stored within the loading system to cause further deformation of the pillar. A similar conclusion had been reached by Holland (1942) when he stated that when a coal seam is the weakest member in the strata in which the energy is released, it will absorb and serve as the relief valve of the energy released.

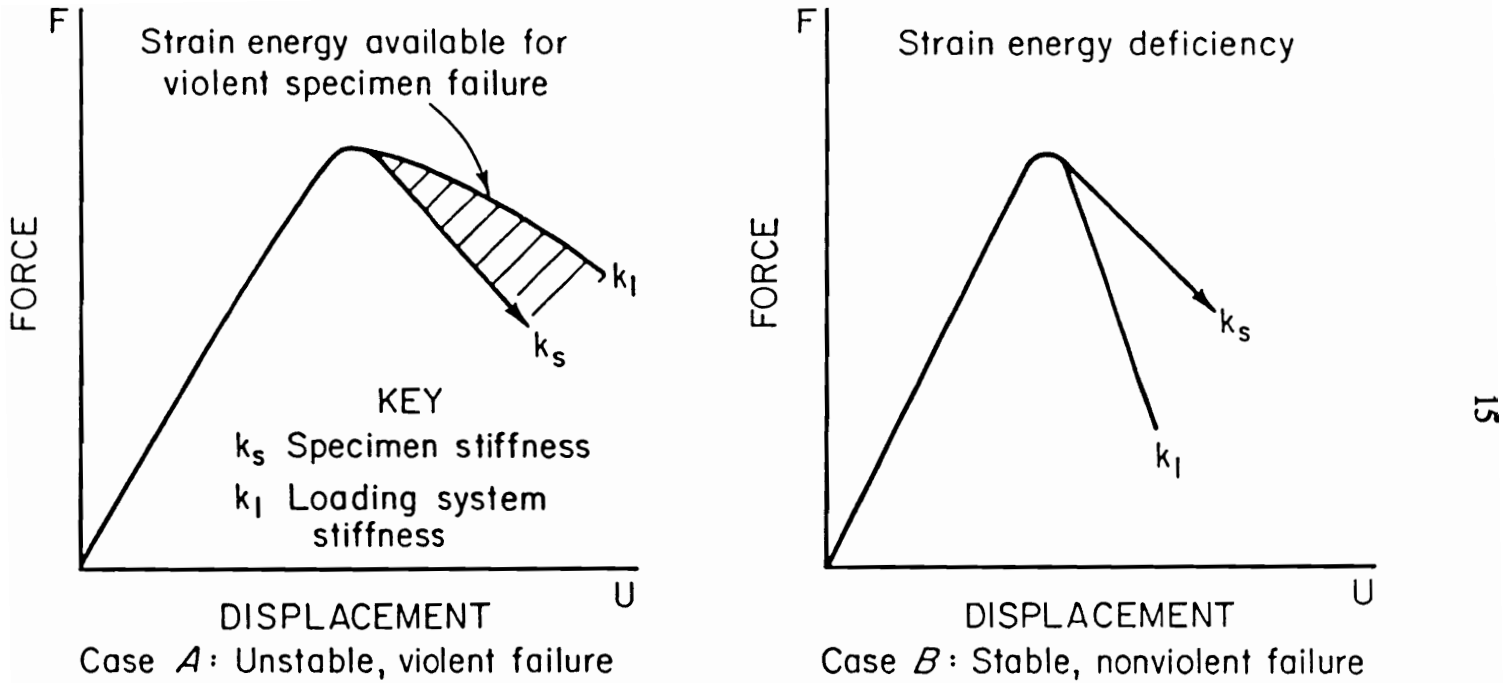

Figure 2.6—Effect of loading system stiffness on the mode of specimen failure (After Blake, 1972).

The energy storage concept will be addressed in the discussion of the boundary element method program MULSIM/NL. MULSIM/NL was developed to assist in alleviating safety hazards associated with bumps in U.S. coal mines and was documented by Zipf (1992a). The program provides a means to calculate stress, displacement, and energy changes for various mining configurations under bump-prone conditions. These program outputs permit the evaluation of mine designs that may decrease the risk of coal mine bumps. MULSIM/NL calculates detailed energy changes due to mining. The basis for these calculations is the energy release rate concept advanced by Cook (1966), later by Walsh (1977), and most recently by Salamon (1984), and Brady and Brown (1985). The incidence and severity of rock bursts in South African has been correlated with the energy dissipation per unit area mined (Hodgson and Joughin, 1966).

2.3 Physical Properties of Bump-Prone Coal and Associated Strata

The relative stiffness of the loading system is determined by the physical properties of the coalbed and associated strata, the geology, and the mining method employed. The relative importance of variations in coalbed physical properties on bump occurrence has been the focus of numerous investigations. Rice (1935) and Holland and Thomas (1954) insisted a structurally strong coal was necessary for bump occurrence. However, Talman and Schroder (1958) documented frequent bumps in

the relatively soft Pocahontas No. 4 Coalbed in West Virginia; as did Lessley (1983) in the soft Pocahontas No. 3 Coalbed in Virginia.

Babcock and Bickel (1984) showed that stress can produce bumps in many coals if constraint is necessary for pillar survival and is suddenly lost. Model coal pillars from 15 different coalbeds in 6 states were tested; 13 of these coals were made to bump by removing confinement.

Several geological conditions are believed to cause bumps in the Eastern coalfields where the overburden is 500 ft or more thick. A strong, overlying stratum, usually a massive sandstone or a conglomerate, occurs immediately above or close to the coalbed. The floor is strong and does not heave readily. These assumptions were drawn from an examination of 117 bump incidents during the period from 1925 to 1950, performed by Holland and Thomas (1954). Table 2.1 is a synopsis of bump fatalities in the United States since 1964. The geological conditions meet the criterion for depth in 100 pct of the occurrences, for sandstone roof in 90 pct, and for stiff floor in 80 pct (Goode, et al., 1984).

The minimum overburden thickness required to cause bumping varies with the coalbed studied: Herd (1930), Springhill No. 2 Mine in Nova Scotia, 1,900 ft; Rice (1935), Harlan Coalbed in southwestern Virginia and Eastern Kentucky, 1,000 ft; and Talman and Schroder (1958), Pocahontas No. 4 Coalbed in southern West Virginia, 700 ft.

Table 2.1—Description of areas where bumps have resulted in U.S. fatalities since 1964 (After Goode, et al., 1984)

Date	State	Seam	Cover (ft)	Coal Thickness (in)	Roof Thickness (ft)	Description	Thickness (ft)	Floor Description
11/29/83	WV	Chilton	752	42	55	Sandstone	--	Sandstone
							2	Shale
10/18/83	WV	Pocahontas No. 4	935	72	60	Massive sandstone		Massive sandstone
8/12/82	UT	Blind Canyon	1,400	168	--	Sandstone		
					2	Laminated shale		
12/8/78	WV	Pocahontas No. 4	1,475	84	200	Massive sandstone	--	Massive sandstone
								Shale
							2	
4/27/78	CO	Sub-seam No. 3	1,400	72	--	--	90	Hard sandstone
					1-1/2	Sandy shale		
11/4/77	VA	Tiller		120		Hard shale and sandstone		
10/4/77	CO	Middle B	2,850	108				
5/23/75	CO	Coal Basin B	2,000	84		Hard sandstone		Weak bottom shale, coal
5/15/74	VA	Pocahontas No. 3	2,400	56	60	Massive sandstone		Sandy shale
					25	Sandy shale		
4/14/70	UT	Castle Gate D	1,500	150		Firm sandstone		Sandy shale
11/6/69	WV	Cedar Grove		72	40	Sandstone		Dense fireclay
10/3/69	CO	Coal Basin B	2,300	84		Sandstone		Coal
8/29/69	CO	Coal Basin B	2,000	84		Laminated Shale		Soft shale and coal
12/13/67	VA	Tiller	1,100	54	25	Medium-grained sandstone		Hard dense shale
1/11/67	CO	"C" coalbed	1,500	84		Coal-bearing shale, laminated shale and sandstone		Laminated shale and sandstone
1/31/66	WV	Pocahontas No. 4	750	80	20	Sandstone	--	Sandstone
					2	Shale	5	Sandy shale
9/2/65	WV	Pocahontas No. 4	1,000	60		Massive sandstone	--	Massive sandstone
							4	Sandy shale
8/12/65	KY	Harlan	1,500	50		Massive sandstone		Dense shale
6/3/64	UT	Sunnyside	2,000					
2/25/64	WV	Eagle	845	53		Massive sandstone		Dense shale

The presence of massive, competent strata in close proximity to the coalbed within a given stratigraphic column, is a condition noted by numerous observers of bumping tendencies in coal mines. Rice (1935) noted massive sandstone beds above the Harlan Coalbed of the Cumberland Field. Peparakis (1958) sandstone units above and below the Sunnyside Coalbed in Utah. Talman and Schroder (1958) described the Pocahontas No. 4 Coalbed as overlain by the 100 ft thick Eckman sandstone and underlain by a fine-grained sandy shale. Lessley (1983) described the hard sandstones above and below the Pocahontas No. 3 Coalbed in southwestern Virginia. Mining in each of these coalbeds has resulted in coal mine bump fatalities since 1964 (tab. 2.1). The Pocahontas No. 3 and 4 Coalbeds were the subject of detailed rock mechanics studies which are described in subsequent chapters.

Geologic structure has never been considered a significant factor in bump-prone coalbeds of the eastern coalfields in the United States. Rice (1935), Holland and Thomas (1954), and Talman and Schroder (1958) made little or no reference to the occurrence of faults, folds, or joint structure. In fact, the lack of structure has been advanced as a cause of coal mine bumps by Iannacchione (1988).

Geologic structure has been correlated with coal and gas outbursts (Hargraves, 1958; Shepherd, et al., 1981; Campoli, et al., 1985). Extensive geological investigations of the Sunnyside District in Utah (Osterwald, 1962) as well as seismic monitoring of rock noises (Dunrud and Osterwald, 1965) indicated that the most numerous and intense bumps occurred within approximately 500 ft of the areas of the mine traversed by the Sunnyside fault system.

The Sunnyside Mine is committed to the use of two entry yielding gateroads as are many coal mines in the western United States. DeMarco, 1994 states "While it is true that tailgate pillar bumps in yielding entry systems are virtually nonexistent in western U. S. operations today, legitimate concerns have been raised regarding the influence of these gate designs may have on end-panel bumps. Because overburden loads are diverted away from the softened groundmass around about the entry system and onto the nearby, stiffer panel abutments, one can reasonably conclude that the frequency and severity of face bumps near the tailgate will also increase." The stress shield concept was employed in the 2,000 ft deep VP No. 3 Mine to mitigate just such face bumps (Campoli, et al., 1990).

2.4 Mine Design

Of the many factors that control coal mine bumps, the mine design is the only factor under significant control of the mine operator. The successful design must either shield the workings from excessive stress or reduce the bearing capacity of the coalbed in the area of active extraction. Superposition of abutment loading from adjacent gob areas are the primary cause of excessive stress concentrations. Dangerous stress concentrations may also be developed if large pillars are surrounded by smaller yielding pillars (fig. 2.7). Multiple-seam mining can contribute to coal mine bump hazard (Kripakov, et al., 1988; Heasley and Zelanko, 1992). Mining above or below the mined coalbed may superimpose abutment zones from different mining levels.

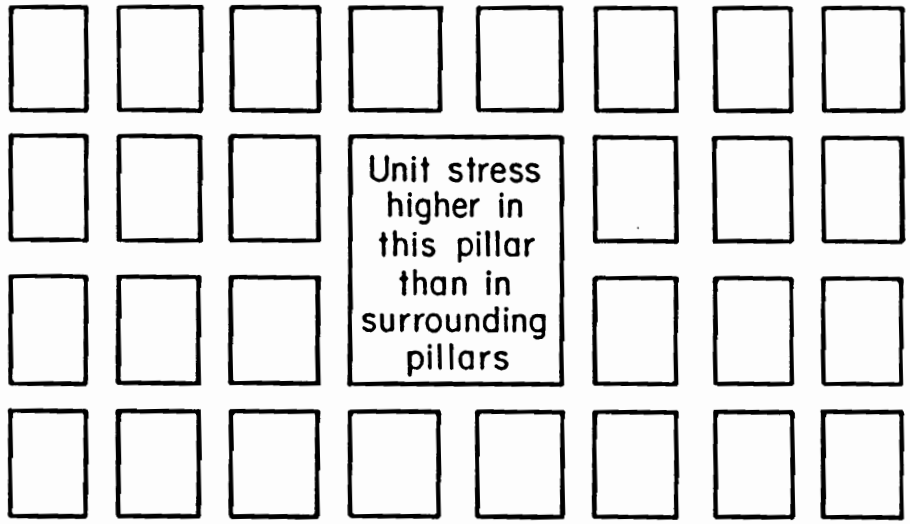

Figure 2.7—Conditions under which a large pillar may be overloaded when surrounded by a number of small pillars (After Holland and Thomas, 1954).

2.4.1 Longwall Mining

Haramy and McDonnell (1988) characterized the frequency of bump events based on the mining method and place of occurrence (fig. 2.8). They indicate bumps occur three times more often during room-and-pillar mining than during longwall mining. The configuration of a longwall mine is responsible for this increased bump resistance; a thin web is sliced off a very large pillar. This web is removed from the relatively low stress edge of the longwall panel, not the highly stressed core zone. Thus, longwall mining is generally recommended over room-and-pillar mining for deep mines with bump-prone associated strata (Campoli, et al., 1987). However, as the depth of overburden increases, catastrophic longwall face bumps can become a reality.

Again, the successful design must either shield the workings from excessive stress or reduce the bearing capacity of the coalbed in the area of active extraction. Retreat longwall mining with conventionally designed gate roads have successfully eliminated longwall face bumps at the VP No. 3 Mine, Vansant, VA, under 2,200 ft of overburden (Campoli, et al., 1990a). This study will be discussed in a subsequent chapter. Advancing longwall or retreat longwall mining combined with in-mine bump prediction and prevention technology have been successfully employed in the Dutch Creek Mine, Redstone, CO, under nearly 3,000 ft of overburden (Haramy, et al., 1988).

Figure 2.8—Bump frequency by mining method and place of occurrence (After Haramy and McDonnell, 1988).

2.4.2 Room-and-Pillar Mining

Holland and Thomas (1954) reported that a statistical survey of 117 bumps documented in various room-and-pillar coal mines indicated that nearly 90 pct of the bumps were either definitely, or probably, located within pillar line points as shown in figure 2.9. In this situation, the high stress area is not shielded from excessive stress. If no attempt is made to reduce the bearing capacity of the pillars, their mining presents an extreme bump hazard. The angle formed by the pillar line at this location results in the active working place being subjected to two superimposed abutment zones. To counter this difficulty, Holland and Thomas (1954) recommended keeping pillar lines as straight as possible and pillars of a uniform shape and size. These recommendations have been reiterated by Rice (1935), Phillips (1944), Campbell (1958), Jacobi (1966), and Campoli, et al, (1987).

The above recommendations are inadequate as the depth of overburden increases. Again, the successful design must either shield the workings from excessive stress or reduce the bearing capacity of the coalbed in the area of active extraction.

Two room-and-pillar mining methods have been developed to shield the working face from excessive stress. The Olga Method was developed at the Olga Mine, McDowell Co., WV. This novel retreat mining system, which conducted mining over three pillar rows outby the gob, distributed abutment loads up to six pillar rows outby the newly formed gob.

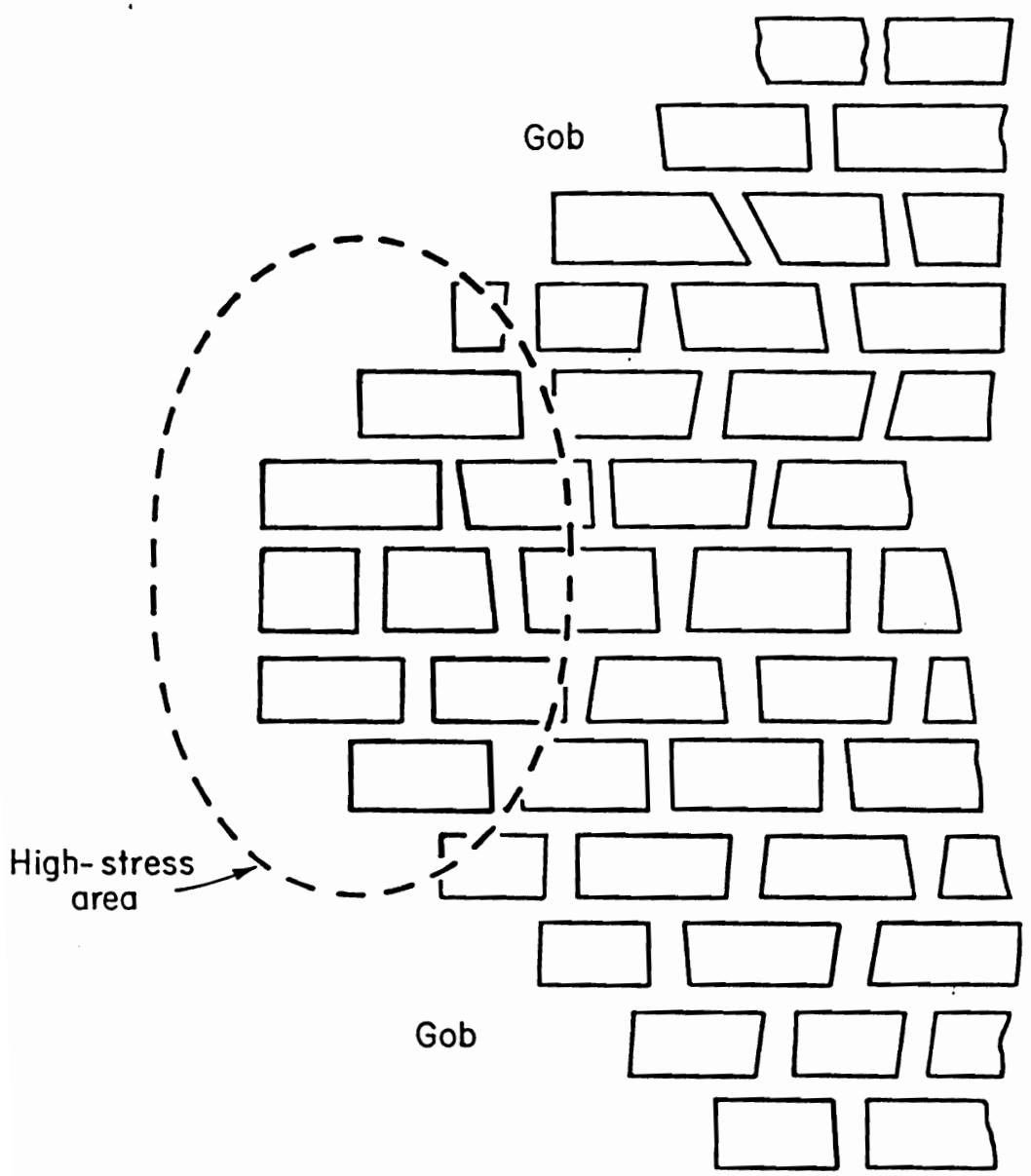

Figure 2.9—High stress area caused by convergence of two active pillar lines (After Holland and Thomas, 1954).

The Thin Pillar Method was developed at the Gary No. 2 Mine, McDowell Co., WV. This system designed in the 1950s to combat bumps during the mining of barrier blocks is still in use today. Splitting is limited to the active gob edge of the barrier pillar. The rigid portion of the barrier pillar carries the main roof load, and its gob side becomes crushed and softened. All barrier splitting is confined to the yielded portion of the barrier pillar and mining in the highly stressed core is avoided. In-mine bump prediction and prevention techniques were employed with both these methods. Both of these approaches will be discussed in more detail subsequently.

2.5 Prediction of Coal Mine Bumps

The prediction of coal mine bumps within an existing or planned mine must be based on sound geologic knowledge of the formation containing the mined coalbed. Variations in the depth of overburden and the proximity of strong stiff strata to the coalbed are critical information. Bump control is but one of many factors in designing the mining method. The thickness of a shale formation between the mined coalbed and a massive sandstone member may determine where bump control is a critical design factor. Geologic information combined with historical bump occurrence information can isolate high stress areas likely to bump. Once the circumstances likely to surround bump occurrence have been outlined, various modeling, geophysical, and geotechnical techniques are available to further define the location and magnitude of the potential bump hazard.

2.5.1 Modeling

Modeling the mine environment to predict the magnitude of bump hazard, requires estimating the stress and displacement response of the coalbed and associated strata to the changing mine geometry. Early techniques of stress analysis utilized closed-form mathematical solutions and photoelastic models, which required laborious solutions performed by mathematically skilled analysts. The computer programs of the 1960's were based on fairly simple concepts of elasticity, but required considerable computational effort. The availability of increasing computational power and efficiency, encouraged the development of increasingly sophisticated and varied computer programs capable of modeling complicated problems. The selection and application of these programs will be addressed in a subsequent chapter.

The numerical methods used in rock mechanics are either boundary or domain methods. Boundary element methods divide the boundary of the rock mass into elements with the interior viewed as an infinite continuum. Domain methods divide the rock mass into geometrically simple zones with the reaction of the rock mass modeled by the composite reaction of these simple zones (Hoek, et al., 1991).

The displacement discontinuity approach to the boundary-element method explicitly models joints. A widely used application of displacement discontinuity boundary-element method is in the modeling of tabular ore bodies. The entire ore seam is represented as a joint, initially filled, with ore that may have a stiffness different from that of the host rock. Mining is stimulated by reducing the stiffness of the ore to zero in those areas where mining has occurred and examining the resulting

stress redistribution to the surrounding pillars. The MULSIM/NL program, which functions in this fashion, will be discussed in detail with an example of its utility to the design of room-and-pillar retreat mining methods for bump control (Zipf, 1992b).

2.5.2 Microseismic

The microseismic method is a geophysical approach that detects subaudible rock noise associated with yielding or fracturing of rock. In the late 1930s, Obert and Duvall (1945) discovered naturally occurring rock noise while measuring seismic velocities in mine pillars. Stress redistribution in coal and rock results from fracturing induced by either geological or mining stresses. The microseismic method is used to detect high-stress zones and potentially unstable areas and is based on experimental evidence that show that rock, under load, undergoes small-scale displacements which result in the release of seismic and sometimes acoustic energy (Obert and Duvall, 1967).

Rock noise level increases with increased stress and is maximum at the ultimate stress. The slopes of the noise level curves are compared to normalize the difference between rock types and their associated failure mechanisms (Blake, et al., 1974). A very low activity period immediately prior to bumps in underground mines has been noted by several researchers (Condon and Munson, 1987). While some bumps are preceded by rapid increases in the microseismic noise level, others show no increase; and occasionally rapid noise level increases are measured, but no bumps occur (Blake, 1983).

The microseismic wave contains both compressional (P) and shear (S) waves. Most of the energy is in the S-wave. A good coupling between the geophone and the rock is required for good response to S-wave arrivals. Energy calculations from field data generally require both the P- and S-waves.

Qualitative analysis of microseismic data requires the accurate determination of each rock noise source location. The laminated sedimentary geology of coal measure rock results in nonuniform wave fronts. Source location is very sensitive to the geophone array geometry. Ideally, a three-dimensional array that surrounds the study area is recommended for more accurate event locations. Incomplete geophone arrays result if areas of the mine are not accessible because of bad ground conditions or mining method geometry (Haramy and McDonnell, 1988).

An event releases seismic energy which travels outward from the source in all directions. The arrival times to each geophone provide the basis for calculating the coordinates of each rock noise event. Event concentrations locate areas of structural readjustment to stress. The stress state, rock mass strength, and failure criterion are not considered. Structural stability analysis is based on the rock-noise count, energy-release rate, source location, and seismic velocity data. Complete analysis requires knowledge of the structure loading and the mining induced load transfer. Structural loading in conjunction with the microseismic data may indicate how the mine structure is reacting to mining activities and if failure is expected (Blake, et al., 1974).

Haramy and McDonnell (1988) analyzed microseismic activity against known bump occurrences in an advancing longwall mines. In general, bumps occurred in areas that experienced a decrease in documented microseismic activity prior to the bump. However, the low microseismic activity zones were not a direct indicator of an impending bump. These researchers stated: "Many questions still exist regarding the use of acoustic emissions in bump detection; why do some bumps occur in nonactive zones while others do not; interpretation of the acoustic emission data is highly dependent on individual observers and site-specific conditions."

2.5.3 Drilling Yield

Neyman, et al., (1972), Krawiec and Stanislaw (1977), Kidybinski (1981), Haramy and McDonnell (1988), and Campoli, et al., (1990b) described the drilling of small diameter holes into pillars to probe for highly stressed coal. Auger holes are drilled horizontally into a coal pillar and the volume of drill cuttings from a given hole depth monitored. An increase in cuttings volume indicates increased stress at that depth. Based on the site-specific geological conditions, a threshold volume of cuttings indicates a dangerous accumulation of stress. Drilling in a stressed zone produces compression in the borehole. Such dynamic effects, as audible knocking and jamming of the drilling rod in the borehole are observed. The closer to the pillar edge a highly stressed zone is encountered, the greater the danger of bumping.

Based on past studies (Neyman, et al., 1972), the bump hazard is a function of the ratio between the depth to the high stress zone and the mining height. A safe

mining state is assumed if the increased stress zone is detected at a depth greater than 3.5 times the mining height. A bump hazard may exist, depending on the specific conditions, if the increased stress zone is detected at a distance between 1.5 and 3.5 the mining height. A critical bumping condition exists, if the increased stress zone is detected at a distance less than 1.5 times the mining height into the pillar. In this event, mining should cease and appropriate bump prevention techniques employed.

2.5.4 Roof-to-Floor Convergence

Roof-to-floor convergence measurements have been used to define the relative bump hazard against the expected location of abutment zones outby gob areas by numerous investigators. McCall (1934) in Nova Scotia and Shepard and Kellet (1973) in Doncaster reported that the lack of characteristic convergence indicated a stress concentration in pillars about to bump. Lessley (1983) and Campoli, et al., (1990b) employed convergence measurements to evaluate the success of bump prevention techniques. Neyman, et al., (1972) reported that convergence measurements were widely used in Polish mines for the detection of bump hazard, particularly in areas in which the hazard of shock bumping was high.

2.5.5 Direct Pillar Stress and Strain

A variety of instruments have been employed to detect zones of high stress or strain within coal seams. Barry, et al., (1967) monitored stress in the bump-prone areas of the Pocahontas No. 4 Coalbed in southern West Virginia using hydraulic

borehole pressure cells. Campoli, et al., (1990a) employed an advanced version of the hydraulic cell and wire rope extensometers, in bump-prone areas of the Pocahontas No. 3 Coalbed in Virginia, to measure coalbed stress and strain, respectively. The output from these hydraulic cells was calibrated to in situ stress values by a computer program developed by Heasley (1989). These efforts resulted in the development of a successful yield-abutment-yield gate road design which eliminated longwall face bumps at the study mine.

2.5.6 Microgravity

Fajklewicz (1983) advanced the microgravity method which uses changes in gravity intensity to infer changes in the density of coal structures. The resulting density distribution is a function of the change in rock mass volumetric strain. Strain energy released in the form of a bump is approximately equal to the change in gravity intensity. An incipient rock bump may be predicted by a negative gravity anomaly, while a positive gravity anomaly indicates a bump is not likely to occur. A negative gravity anomaly is caused by an increase in volume and hence a decrease in rock density.

2.6 Prevention of Coal Mine Bumps

All coal mine bumps are the result of dangerous accumulations of coalbed stress. Coalbed stress may be maintained at an acceptable level through mining method modifications and/or localized destressing procedures. The mine design

engineer must find the economic compromise between total extraction of the coalbed and not mining the coalbed. If total extraction is attempted by the advancing longwall method, no stress shield is afforded to the longwall panel. As a result, worker and equipment safety must be provided by localized destressing methods (Haramy and McDonnell, 1988). The alternative stress shield approach leaves abutment pillars in place to allow safe extraction of the longwall (Campoli, et al., 1990a).

Destressing is defined as the transferring of high stress concentrations from one portion of a mine structure to another by fracturing or softening rock or coal in order to control stress buildup. Destressing the active working face is the most logical method to preventing coal mine bumps. Coal, or in some instances roof and/or floor rock, is intentionally fractured and made to fail, thereby, reducing the ability of the fractured zone to carry the load. The load is transferred to another part of the mine structure. If stress cannot buildup in the destressed zone the area cannot bump violently. Conceptually, the principle is simple, but in practice controlling the rate and magnitude of load transfer is difficult. The act of destressing can be dangerous in itself as it may trigger a bump. Volley firing, hydraulic fracturing and auger drilling are the major destressing methods used commonly in coal mines. The relative effectiveness of each method depends largely on local mine conditions.

2.6.1 Volley Firing

Volley firing has successfully reduced the number of rock and coal bumps in underground mines (Haramy, et al., 1985). With this method, explosives are used to

fracture the coal to advance the abutment zone away from the active working face prior to face advance or entry development. Longwall faces are destressed by the detonation of 3 lb of permissible explosives in holes drilled in previously located high-stress zones (fig. 2.10). The drill pattern reported by Haramy and McDonnell (1988) consists of a series of 2-in-diam holes, 13 to 15 ft deep, drilled on approximately 4 ft centers. The daily advance of the face and the location and magnitude of the stress abutment ahead of the face fixes the required hole depth. Radial drilling pattern combinations of two or three holes can relieve high stress in both the face and rib areas.

Figure 2.11 displays a volley-fire, drill-hole pattern for a development section. The pattern is designed to move the maximum abutment stress ahead of development while minimizing reduction in the load bearing capacity of the pillars left behind. The depth and angle of the drill holes are determined by the pillar design and by the characteristics of the abutment zone.

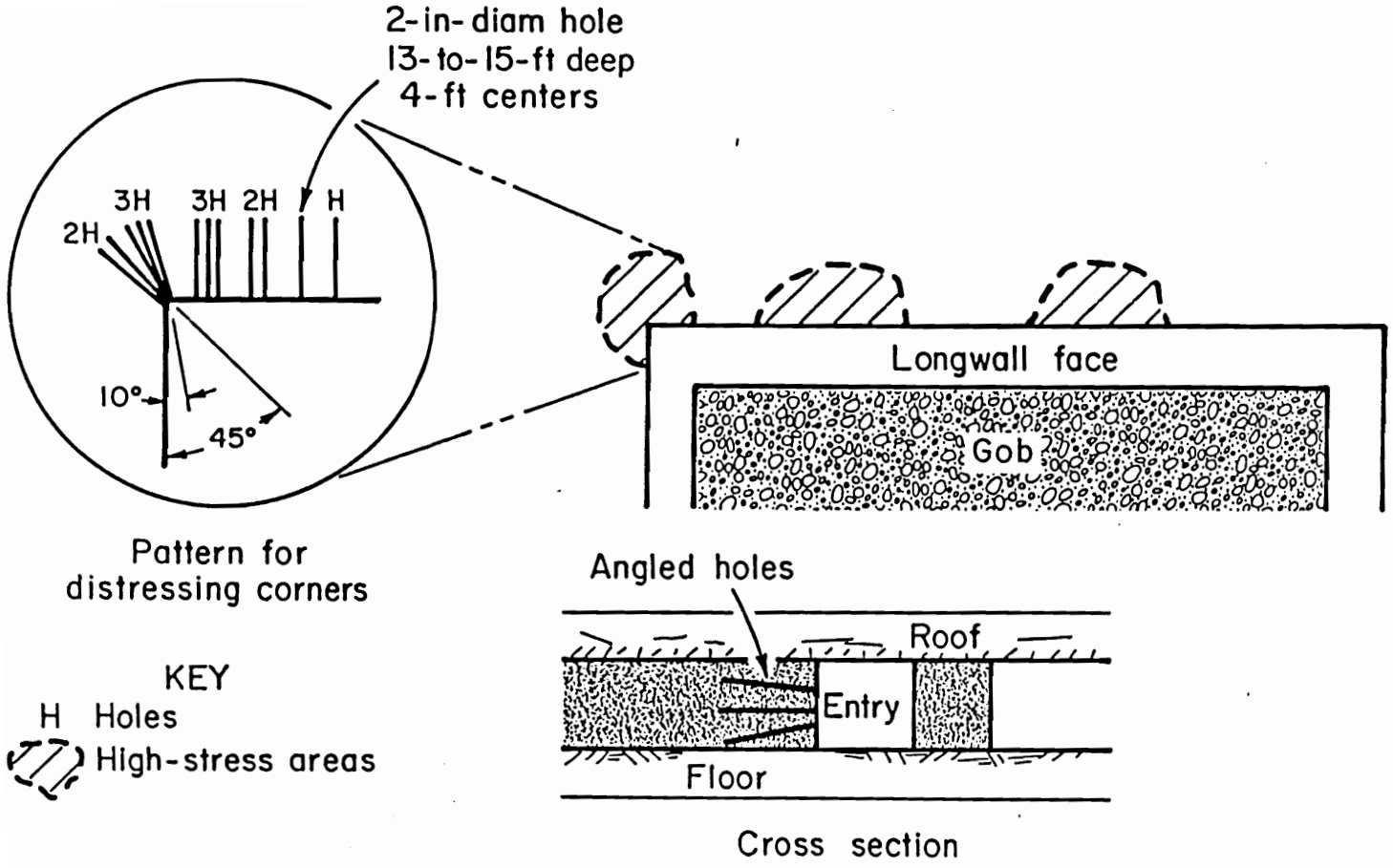

Figure 2.10—Volley firing drill hole pattern for longwall face and corners (After Haramy and McDonnell, 1988).

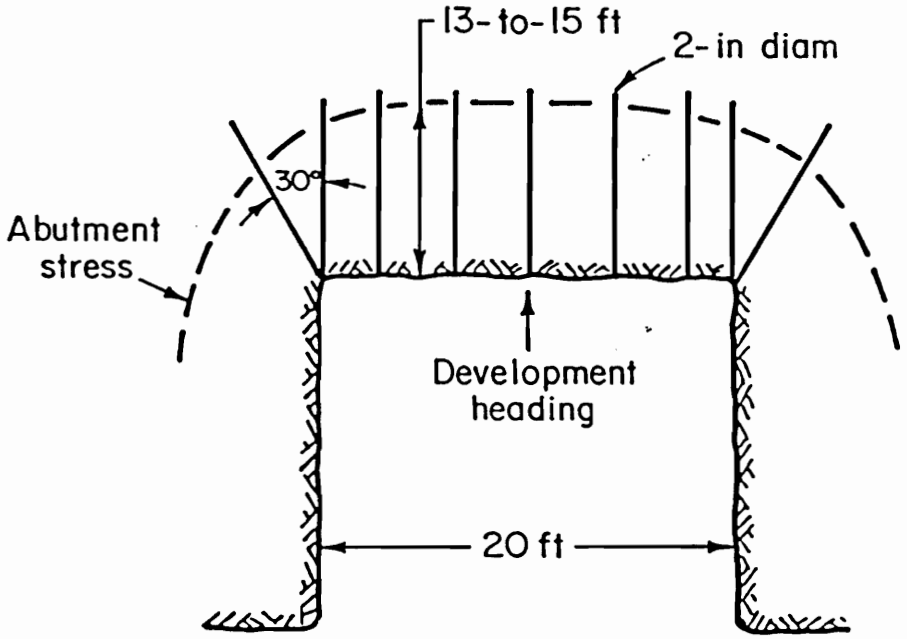

Figure 2.11—Volley firing drill hole pattern for development entries (After Haramy and McDonnell, 1988).

Volley firing was employed at the Olga Mine to reduce the load bearing capacity of coal pillars; and thus, their potential for storing strain energy, (Campoli, et al., 1990b). Three volley fire operations, (conducted in advance of the pillar splitting retreat mining system), were evaluated by roof-to-floor convergence monitoring, in the area to the right of barriers A and C (figs. 2.12 and 2.13). Red Diamond Gelatin B permissible dynamite was used. This blasting agent has the following characteristics: 1) density 1.35 g/cm^3; 2) detonation rate 16,000 ft/s; 3) detonation pressure 81,000 bar; 4) weight strength 955 cal/g; and 5) weight 211 g per stick. The high detonation rate ensures a heavy shock wave that will fracture the coalbed with minimal movement of the coal.

Each experiment consisted of two volleys. Roof-to-floor convergence station location, hole configuration, and dynamite load varied in the three tests (fig. 2.12). Tests 1, 2, and 3 were completed in sequence, within a 6 hour nonmining period. Figure 2.13 displays graphically the convergence induced by tests 1, 2, and 3. Roof-to-floor convergence due to mining was negligible. This was confirmed by the stabilization of the roof-to-floor convergence readings between volleys.

All three tests show a roof-to-floor convergence reaction to both volleys. This may indicate a softening of the subject pillars due to volley firing, resulting in a reduction of their stored energy. The minimum and maximum roof-to-floor convergence reactions occurred during test 1 in reaction to the minimum (14 sticks)

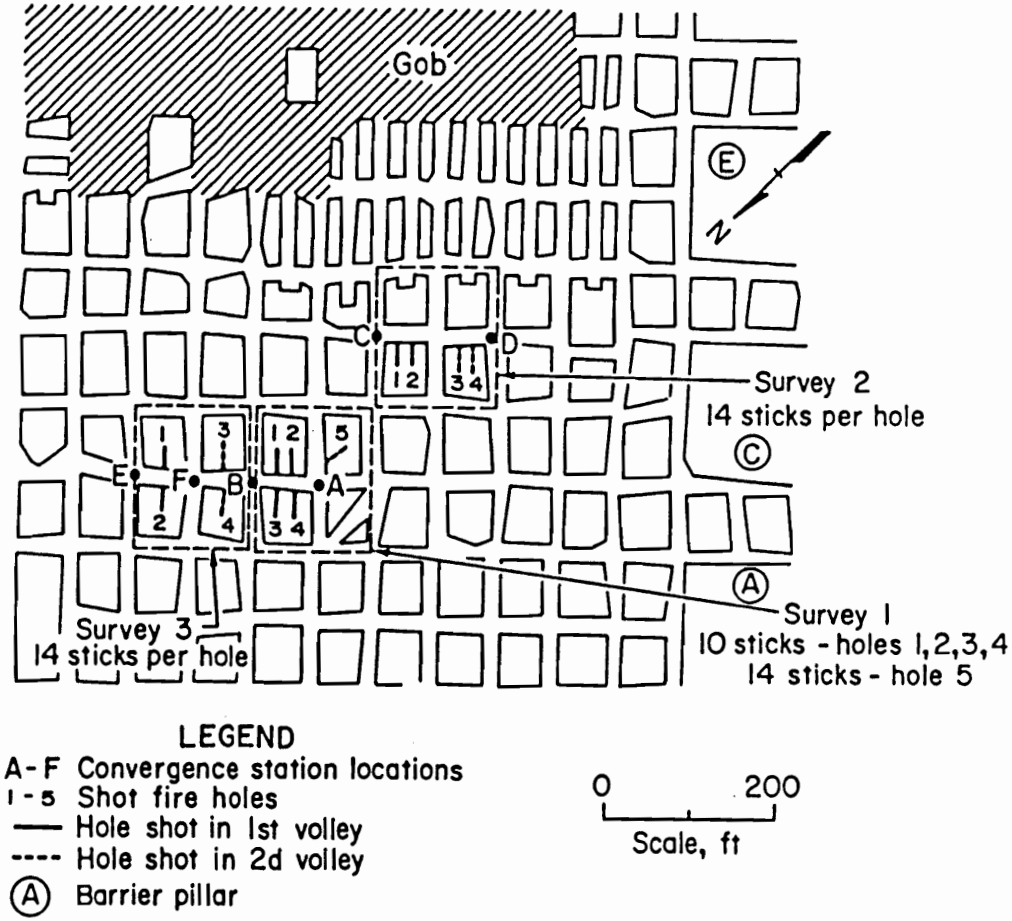

Figure 2.12—Shot fire roof-to-floor convergence survey locations and hole configurations, Olga Mine (After Campoli, et al., 1990b).

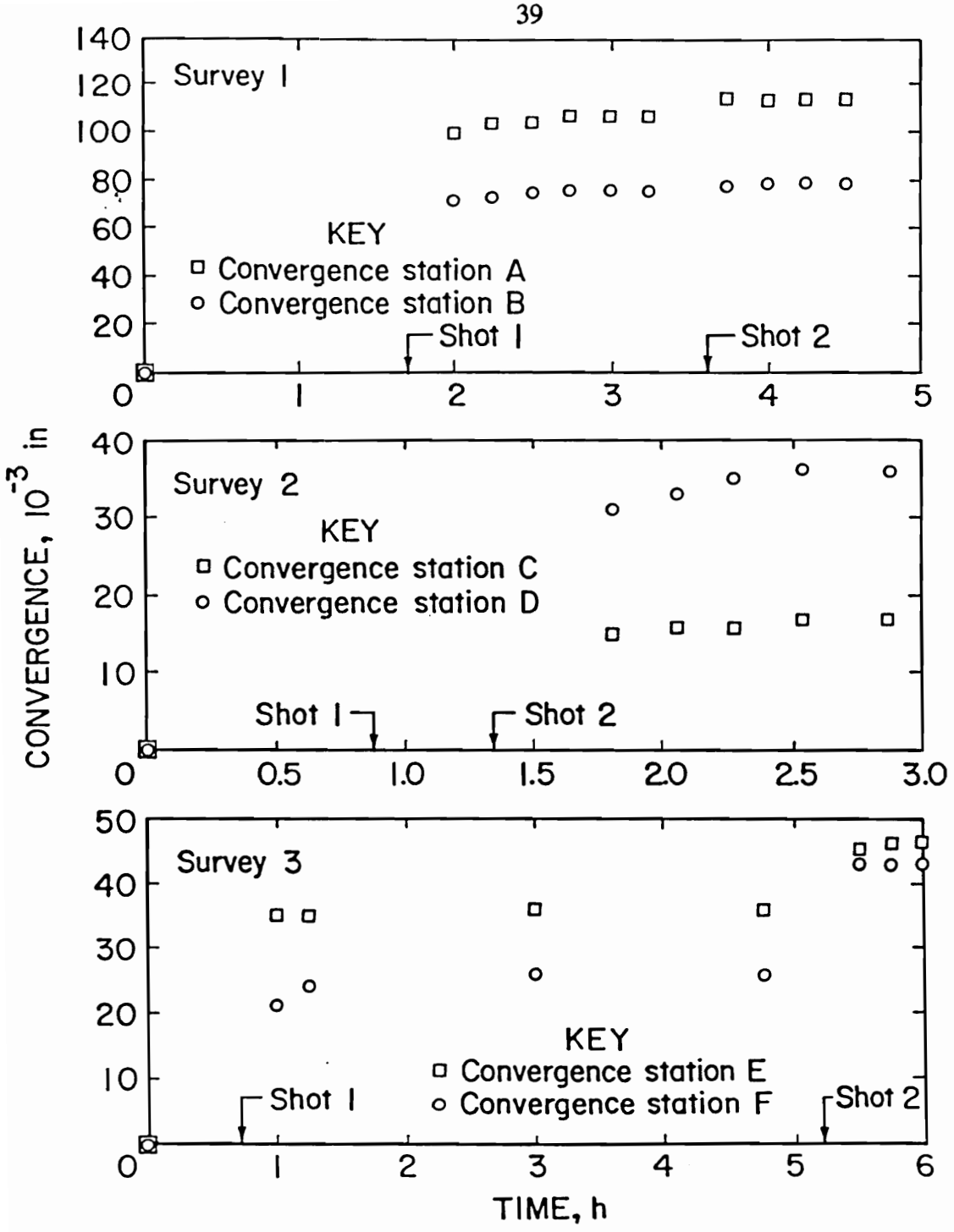

Figure 2.13—Roof-to-floor convergence versus time for shot fire surveys 1, 2, and 3, Olga Mine (After Campoli, et al., 1990b).

and maximum (40 sticks)dynamite loads. This observation suggests that the effectiveness of volley firing increases with the amount of explosives used. Other important variables not considered are pillar geometry, hole spacing, and the effect of simultaneous treatment of multiple pillars (Campoli, et al., 1990b).

Longwall gate road pillar bumps occurred at the Beatrice Mine, Oakwood, VA in areas of Pocahontas No. 3 Coalbed where the bottom was composed of dense sandy shales, (Campoli, 1987). The combination of the load transferred to the tailgate from the adjacent gob area formed by the previously removed panel, the abutment pressure in advance of the longwall plow face, and the unyielding bottom strata caused the bumps. The 100 by 100 ft pillars were too large to yield under load. Thus, the pillar stored energy until explosive failure occurred (fig. 2.14). The large pillar was softened where firm unyielding roof-and-floor strata were present under at least 2,200 ft of overburden. The ribs of the 100 by 100 ft pillar were drilled and shot as shown in figure 2.15.

2.6.2 Hydraulic Fracturing

High pressure injection of a fluid (i.e., water) can be used to hydraulically fracture high stressed areas in coalbeds and transfer dangerous accumulations of high stress away from mining. Hydraulic fracturing design is dictated by the in situ stress magnitude, host rock mechanical properties, rate of fluid injection, injection time, formation permeability and porosity, fracture fluid viscosity and pressure,

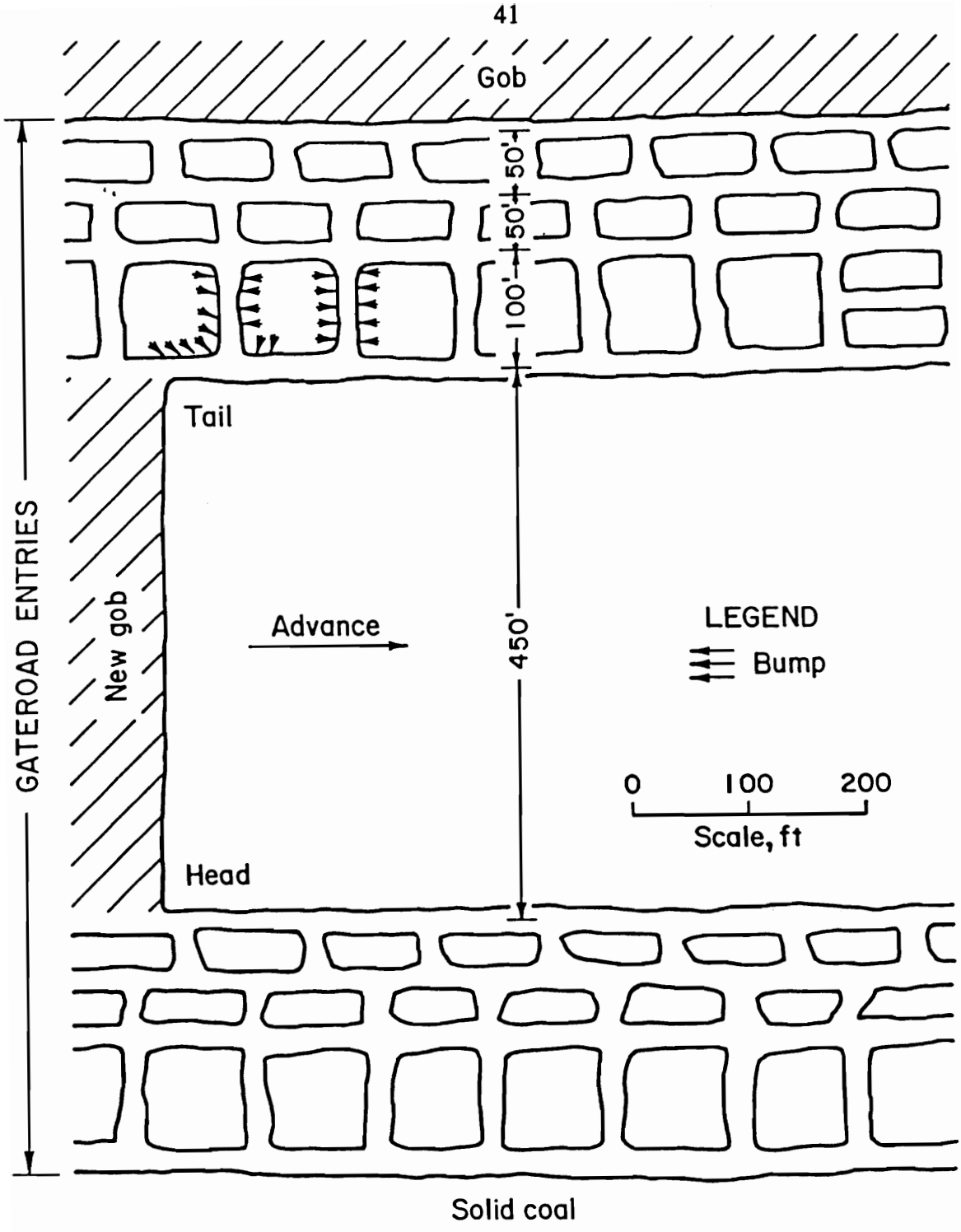

Figure 2.14—Plan view of longwall gate road entries and location of bump event, Beatrice Mine (After Campoli, et al., 1987).

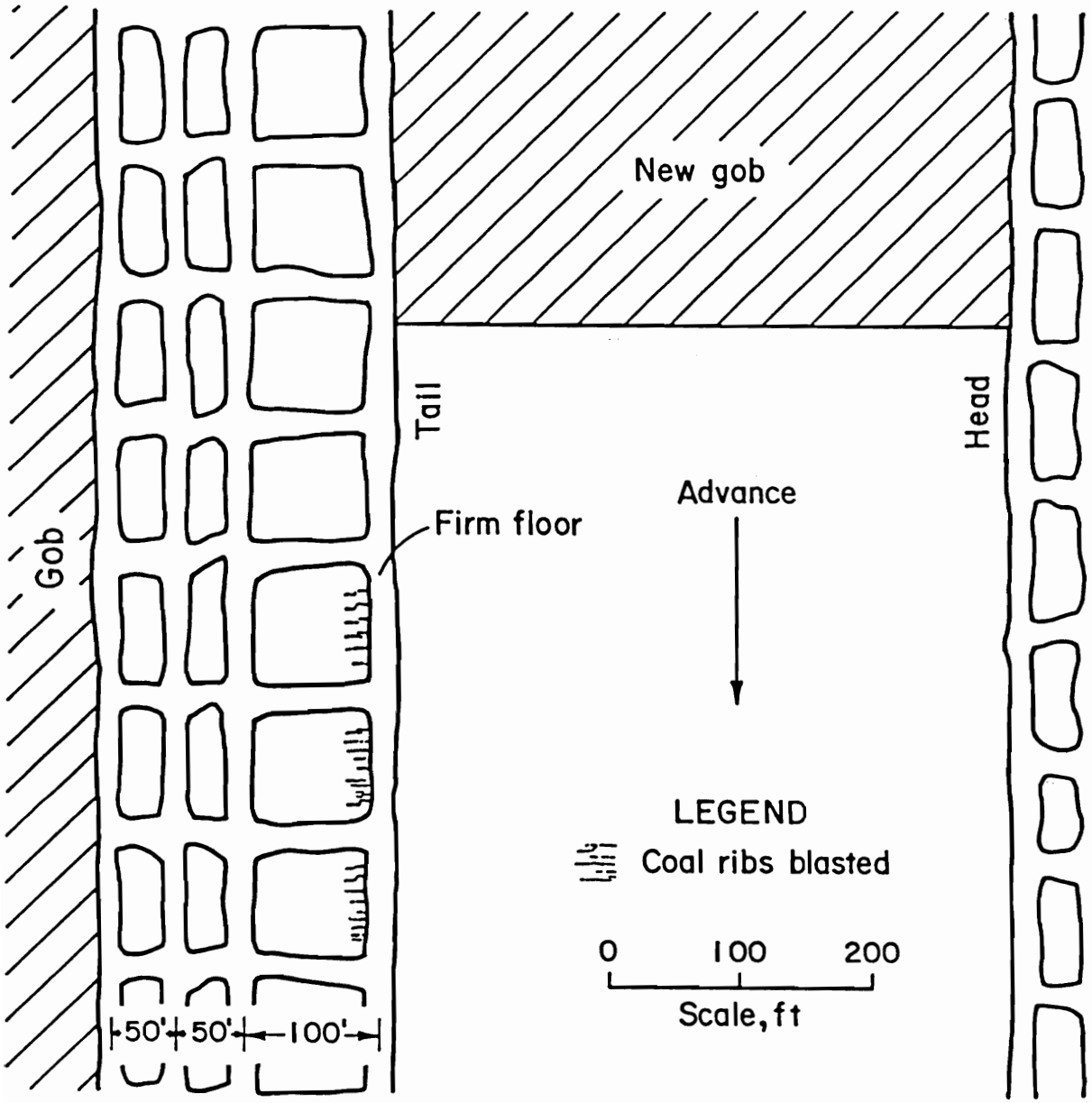

Figure 2.15—Plan view of volley fire softening technique, used on tail entry of longwall gate roads for bump control, Beatrice Mine (After Campoli, et al., 1987).

and total fluid volume injected. Thus, controlling the extent of the affected fracture zone is difficult.

Coeuillet (1964) reports the Poles have demonstrated successfully hydraulic fracturing of a roof ahead of a longwall face. Seismic events increased during injection; and a significant decrease in the number of seismic events that occurred during mining in zones where the roof had been hydraulically fractured as compared with zones that had not been prefractured.

Haramy and McDonnell (1988) reported on hydraulic fracturing of the rib of an advancing longwall panel (fig. 2.16). They calculated the pressure required for fracture to occur by the following equation:

$$F=(1-\nu)(x+\tau) \qquad (2.1)$$

where F = fluid pressure

ν = poisson's ratio

x = horizontal rock bed strength

τ = tensile strength

Campoli, et al., (1987) report the use of hydraulic fracturing during room-and-pillar mining in the Pocahontas No. 3 Coalbed in the Beatrice Mine, Oakwood, VA. Figure 2.17 shows the convergence contours outby the pillar line. Note the 2- to 3-in total convergence along the pillar line A to B and the 0.5- to 1.5-in total convergence at pillar C. Pillar C was infused by pumping water at 800 to 1,200 psi pressure, into the pillar at a rate of 10 gal/min. Figure 2.18 shows the effect of infusion on

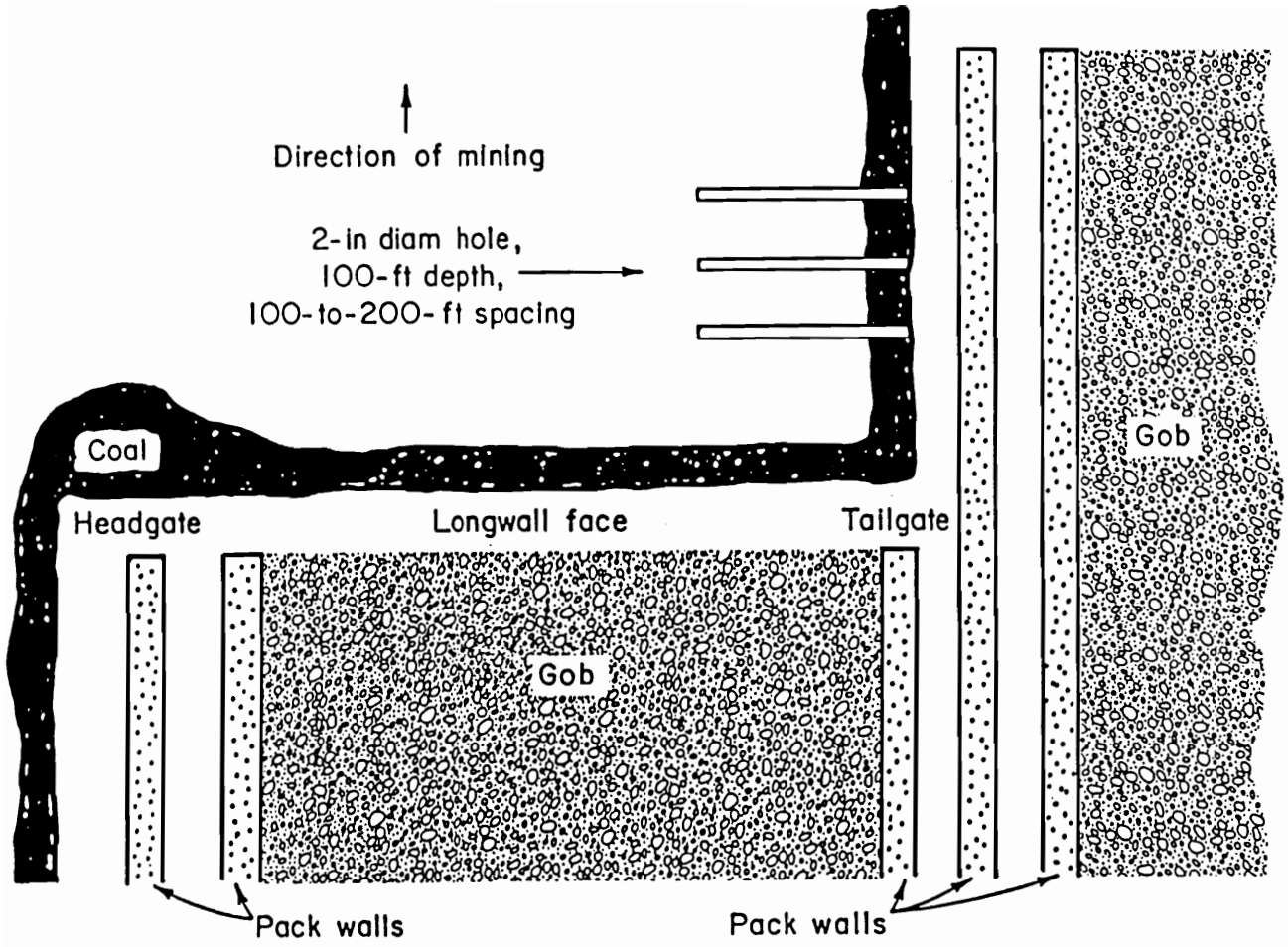

Figure 2.16—Hydraulic fracturing pattern ahead of longwall face (After Haramy and McDonnell, 1988).

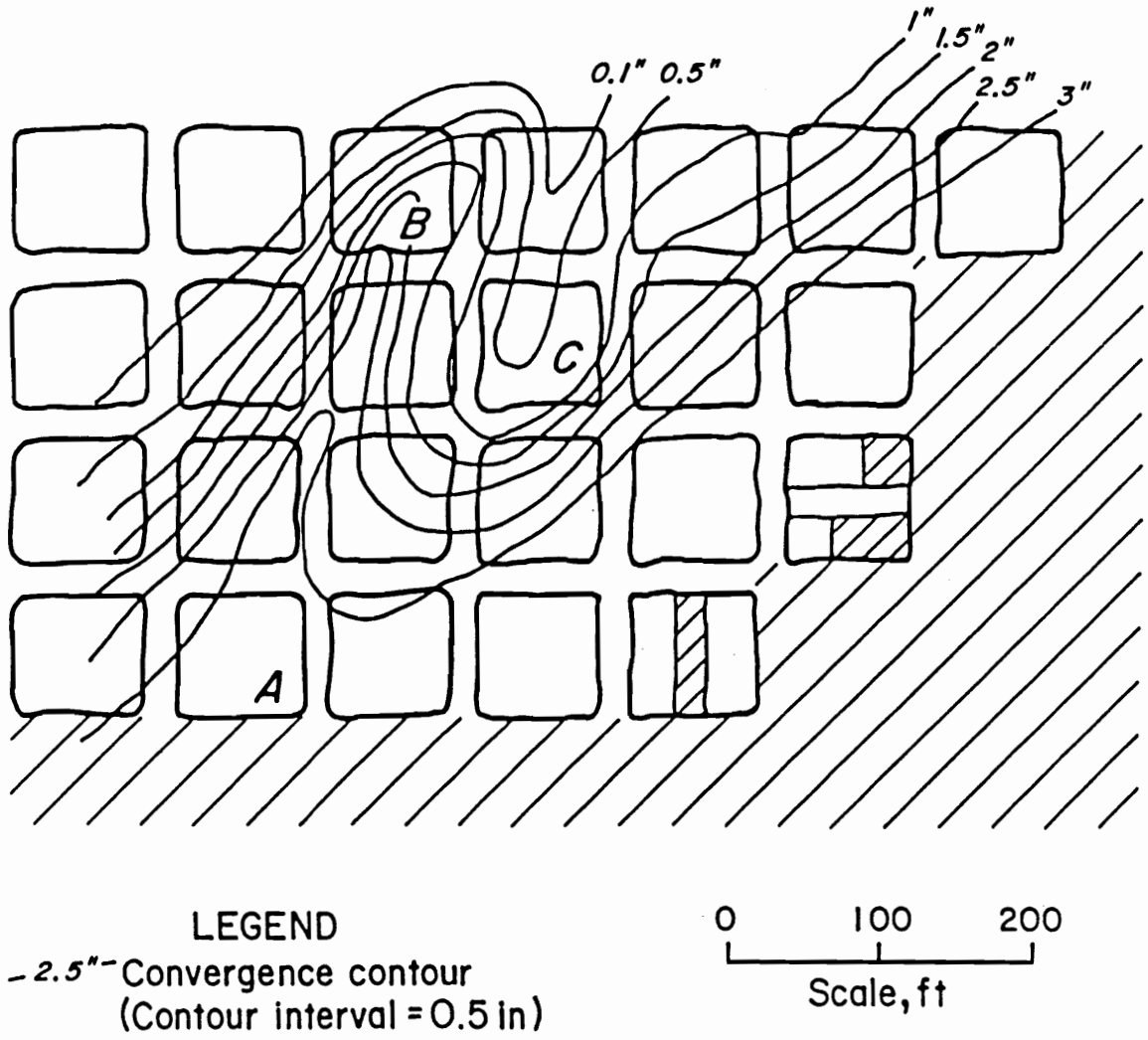

Figure 2.17—Convergence contour map for room-and-pillar retreat mining, Beatrice Mine (After Campoli, et al., 1987).

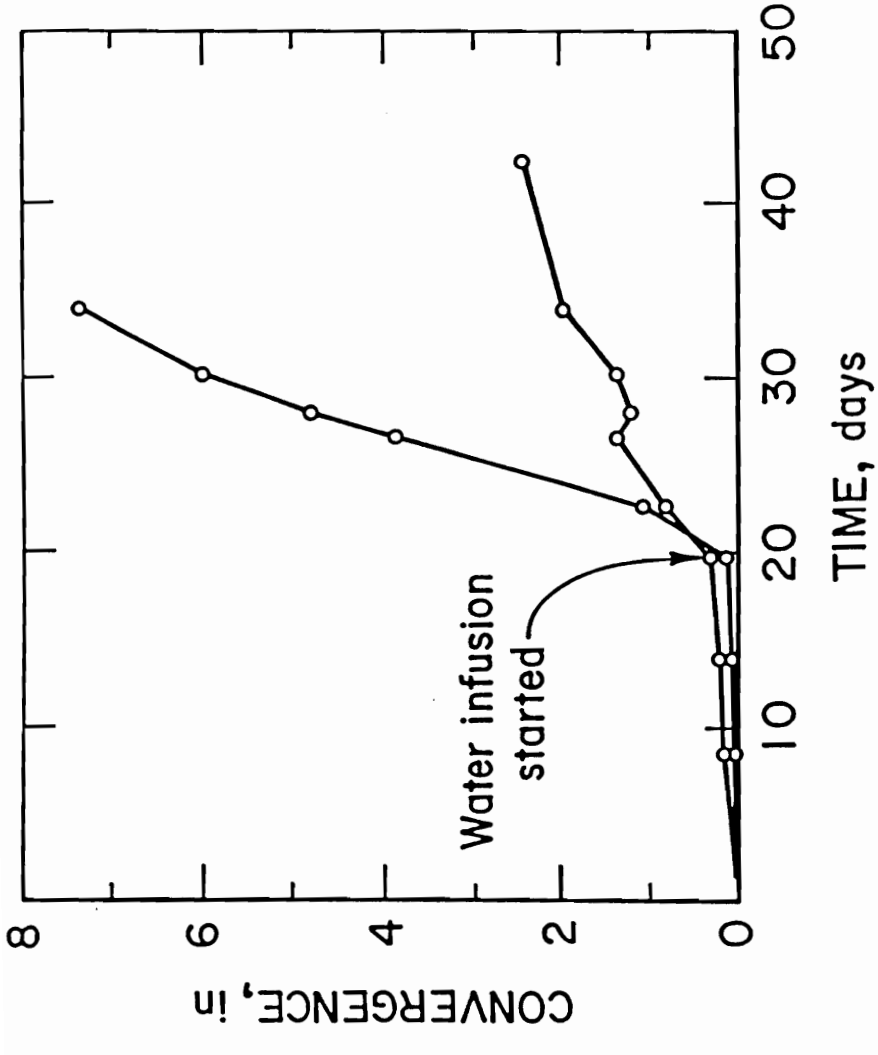

Figure 2.18—Graph of convergence effects of water infusion of pillar C (fig. 2.17), Beatrice Mine (After Campoli, et al., 1987).

the convergence rate around the pillar. The dramatic increase in the convergence rate resulting from the water infusion led mine officials to believe that the pillar was destressed. It was subsequently mined without incident.

2.6.3 Auger Drilling

Drilling horizontal auger boreholes into highly stressed coal removes large volumes of coal cuttings. The stress within the pillar causes the borehole to converge and provide a source of coal to the auger flights. Thus, this technique premines the highly stressed pillar core causing a transfer of stress. Long boreholes (50 to 80 ft) with large diameters (4.5 to 12 in) and spaced on 13- to 16-ft centers have been used to relieve stress at mining faces in foreign mines (Coeuillet, 1964; Sikora, et al., 1978; and Haramy, et al., 1985).

Talman and Shroder (1958) reported experiences with drilling large-diameter auger holes as a method for relieving stress in the Pocahontas No. 4 Coalbed, Gary No. 2 Mine, Gary, WV. These experiments were conducted to determine if 24-in diameter auger holes could be drilled safely. Figure 2.19-A shows a 180 by 170 ft pillar that was formed by the removal of a barrier pillar. The coalbed is 7 ft 4 in thick and the depth of cover is 1,100 ft. This pillar was destressed by auger drilling. Holes A, B, and C (fig. 2.19-B) were drilled to their predetermined depth of 95 ft from behind barricades. Upon completion of hole C, three entries following the auger holes were advanced 75 ft and connected by a crosscut. As the

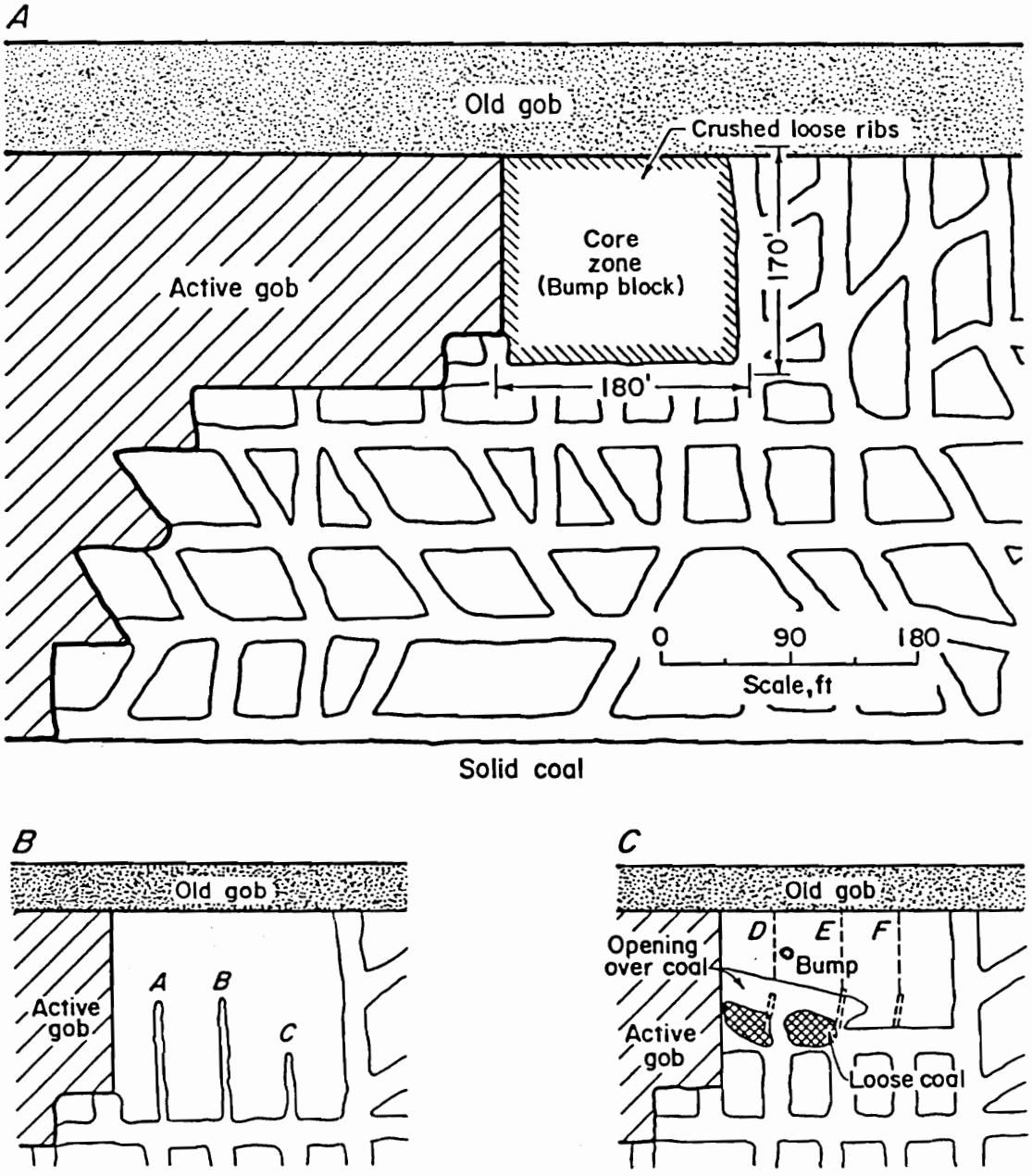

Figure 2.19—Results of auger drilling of bump block left by the thin pillar mining method, Gary No. 2 Mine (After Talman and Schroder, 1958).

crosscuts were being driven, the last 35 ft of the auger holes collapsed. Holes D, E, and F, which were continuations of holes A, B, and C were then drilled. Hole D (fig. 2.19-C) was at a depth of 149 ft in the crushed coal area of what was formerly hole A, when a heavy bump occurred. Approximately 1,000 tons of coal were thrown into the entry. An area 100 by 35 ft was opened over the coal pillar with a gap of 8 to 12 in. Because of the extreme precautions taken, no serious injuries resulted. Drilling resumed and another bump occurred in hole F, which totally destressed the pillar. The pillar was then extracted without further incident. Auger drilling was discontinued shortly thereafter because the operator considered this method to be both uneconomical and dangerous (Campoli, 1987).

Auger drilling was used also for localized stress reduction during room-and-pillar mining operations in the Pocahontas No. 3 Coalbed, Olga Mine, McDowell Co., WV. A post mounted air-driven drill having a 3.9 in diameter bit and 40-in-long pin-connected augers was used to drill holes at midseam height. Dry cuttings were removed by the right hand screw action of the augers. The volume of cuttings was measured and used as an indication of stress encountered at the drill depth. At the end of each auger section of penetration, the volume of cuttings produced were measured. A large volume of cuttings is thought to indicate highly stressed coal pillars and hence, bump hazard zones.

Eleven auger drilling operations were monitored for cutting volume yield and induced convergence effects. The holes averaged 24 ft in length. The effectiveness of auger drilling for destressing proved to be dependent on the state of stress within the treated pillar. Survey 1 was performed in a 55-by 70-ft chain pillar located between two barrier pillars (fig. 2.20). The pillar was surrounded by an array of coal cells and roof-to-floor convergence stations. At the time of this experiment, raw readings from the hydraulic coal cells within the subject pillar indicated pillar pressures ranging from 3,550 to 4,900 psig. Drilling of this "low" stress pillar produced only the expected cutting volume of 2 gal per steel advance (40 in) and did not significantly change the pillar pressure or induce roof-to-floor convergence in the adjacent rooms.

In surveys 9 and 10 under "high" stress conditions, two adjacent pillars were drilled (hole 9 followed by hole 10) prior to the second cut of pillar splitting (fig. 2.21). Coal cells located two pillar rows outby the test site displayed maximum raw pressures of approximately 13,000 psig before and after the experiment. The first 10 ft of both holes displayed similar behavior to the "low" stress test, i.e., expected cutting volume for a 3.9 in diameter bit and no induced roof-to-floor convergence (fig. 2.22). However, drilling in the 10 to 23 ft deep zone of the "high" stress pillars produced as much as 180 fold the expected cutting volume and 0.024 in of roof-to-floor convergence per steel advance (40 in).

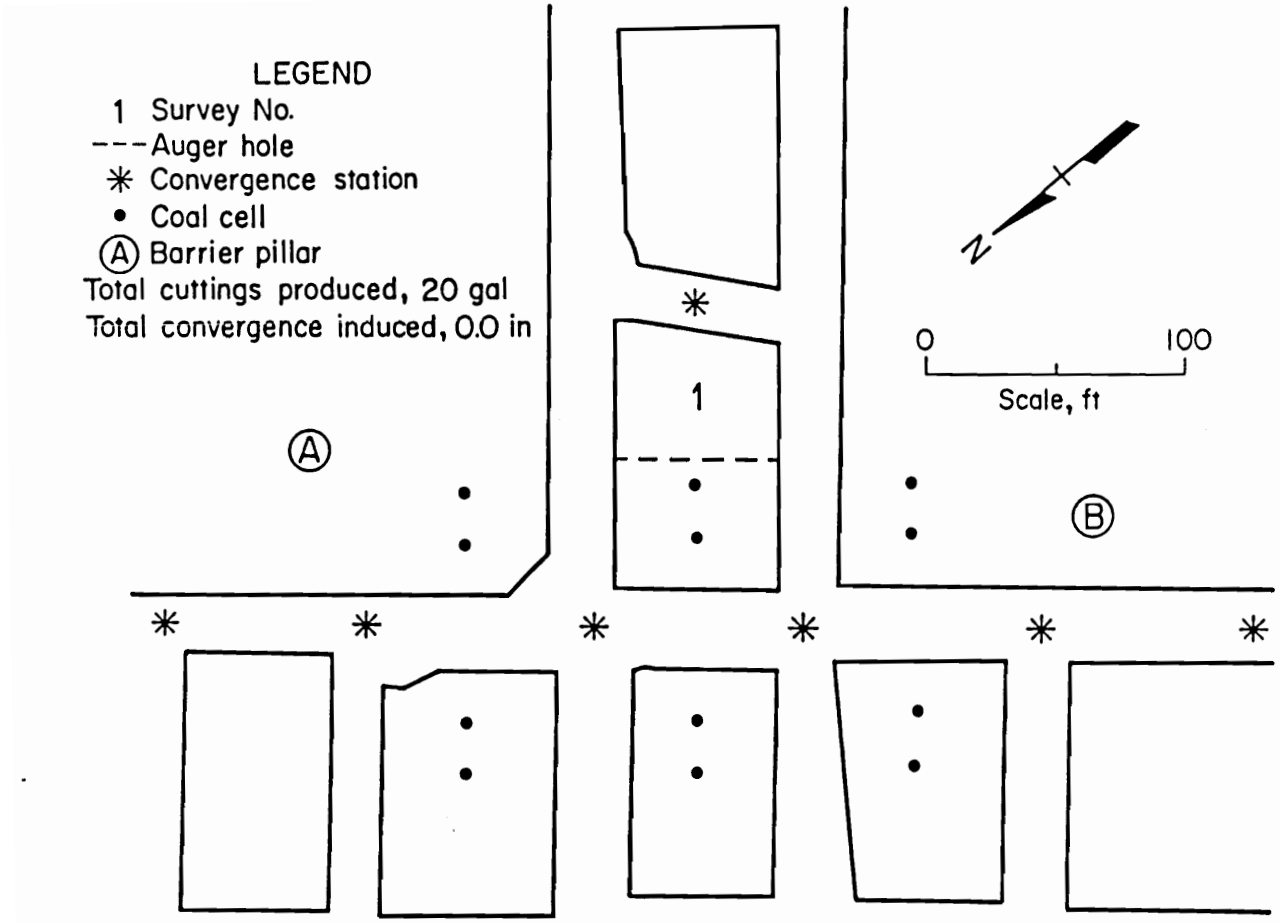

Figure 2.20—Plan view of auger drilling survey one, Olga Mine (After Campoli, et al., 1990b).

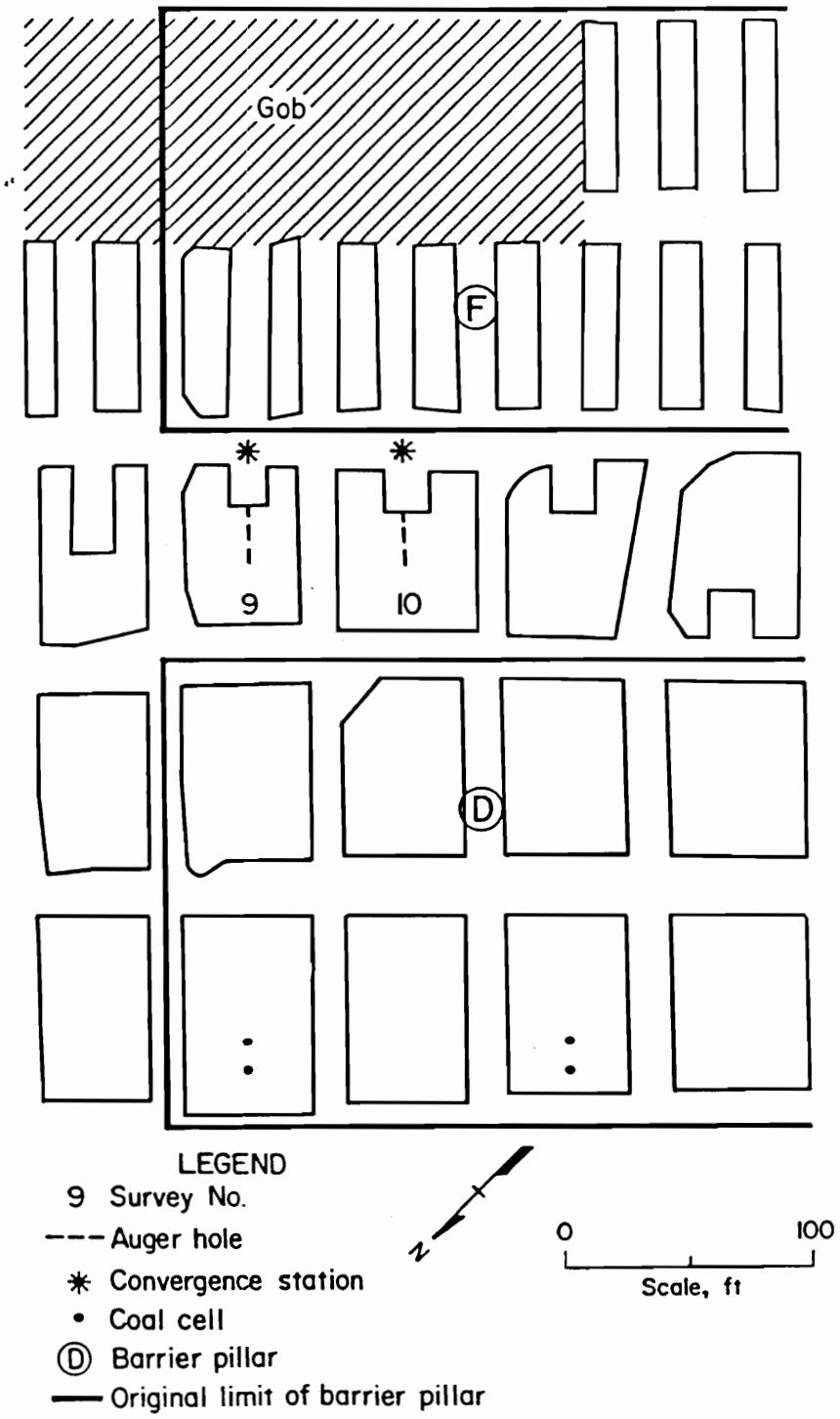

Figure 2.21—Plan view of auger drilling surveys nine and ten, Olga Mine (After Campoli, et al., 1990b).

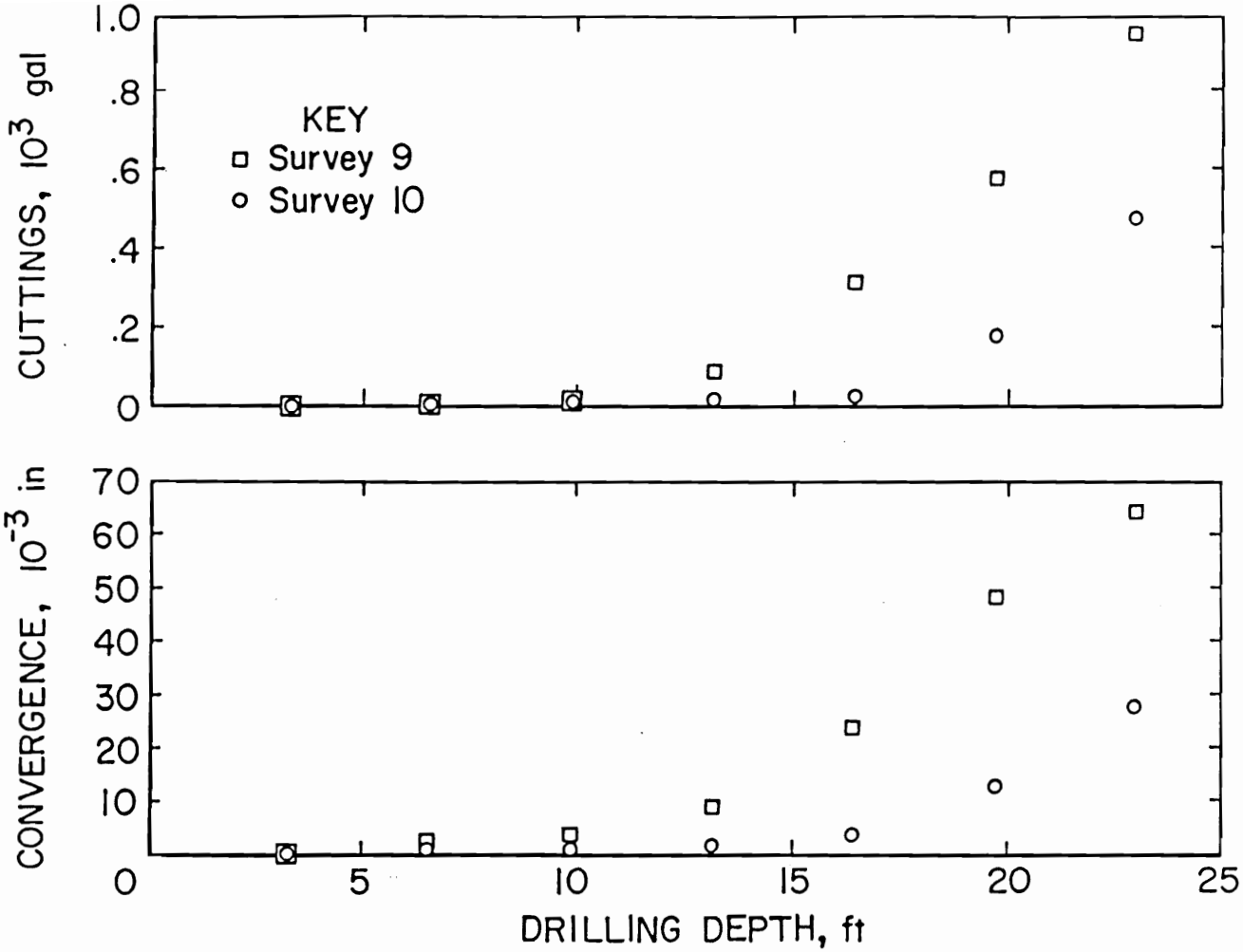

Figure 2.22—Cumulative cuttings volume and cumulative roof-to-floor convergence versus drilling depth for auger drilling surveys 9 and 10, Olga Mine (After Campoli, et al., 1990b).

Both the cumulative cutting volume and roof-to-floor convergence (fig. 2.22) data show that pillar 9 was under higher stress conditions than pillar 10, due possibly to the fact that pillar 9 was slightly smaller than pillar 10. Further analysis of cuttings volume and roof-to-floor convergence data per steel advance showed that a linear relationship existed between the two data sets. Only one point falls outside the 95 pct confidence interval (fig. 2.23) for the linear equation $y = 0.006(x) + 0.96$, with an R-square value of 0.88.

Mining of the "high" stress auger drilled cuts by continuous miner was observed. During the first 10 ft of advance of the continuous miner, the holes remained cylindrical. In the 10 to 20 ft deep drilled depth, the holes changed to V-shaped cavities, forming a fissure as wide as 30 in at the top of the coal pillar (fig. 2.24). It is postulated that the vertical stress in the pillar had been reduced significantly. If the stress field had not been reduced, the voids would have been closed. Only cylindrical holes were found in the "low" stress application. Thus, "high" pillar pressures are necessary if the auger drilling for stress reduction is to be effective (Campoli, et al., 1990b).

2.7 Numerical Methods in Rock Mechanics

The development of rock mechanics has followed closely the development of methods analyzing stresses and displacements in rock structures. Early techniques of stress analysis utilized closed-form mathematical solutions, which required laborious solutions performed by mathematically skilled analysts. The computer programs

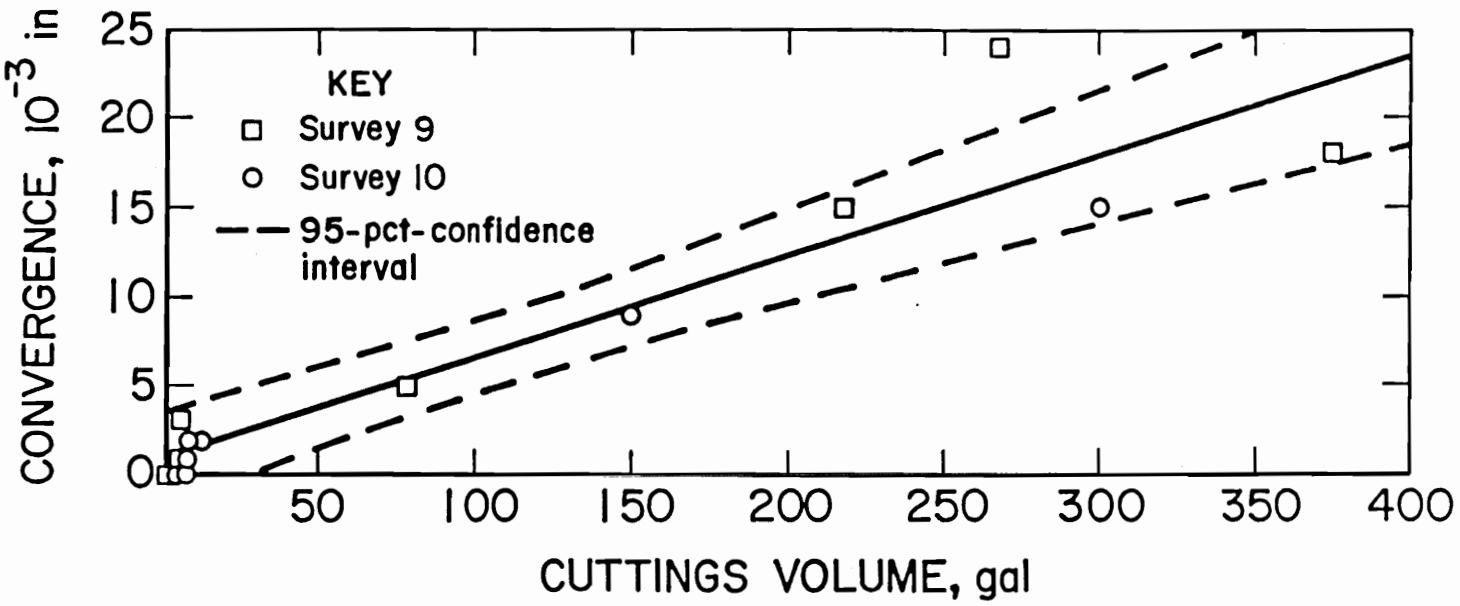

Figure 2.23—Roof-to-floor convergence versus cutting volume produced per steel advance (surveys 9 and 10), Olga Mine (After Campoli, et al., 1990b).

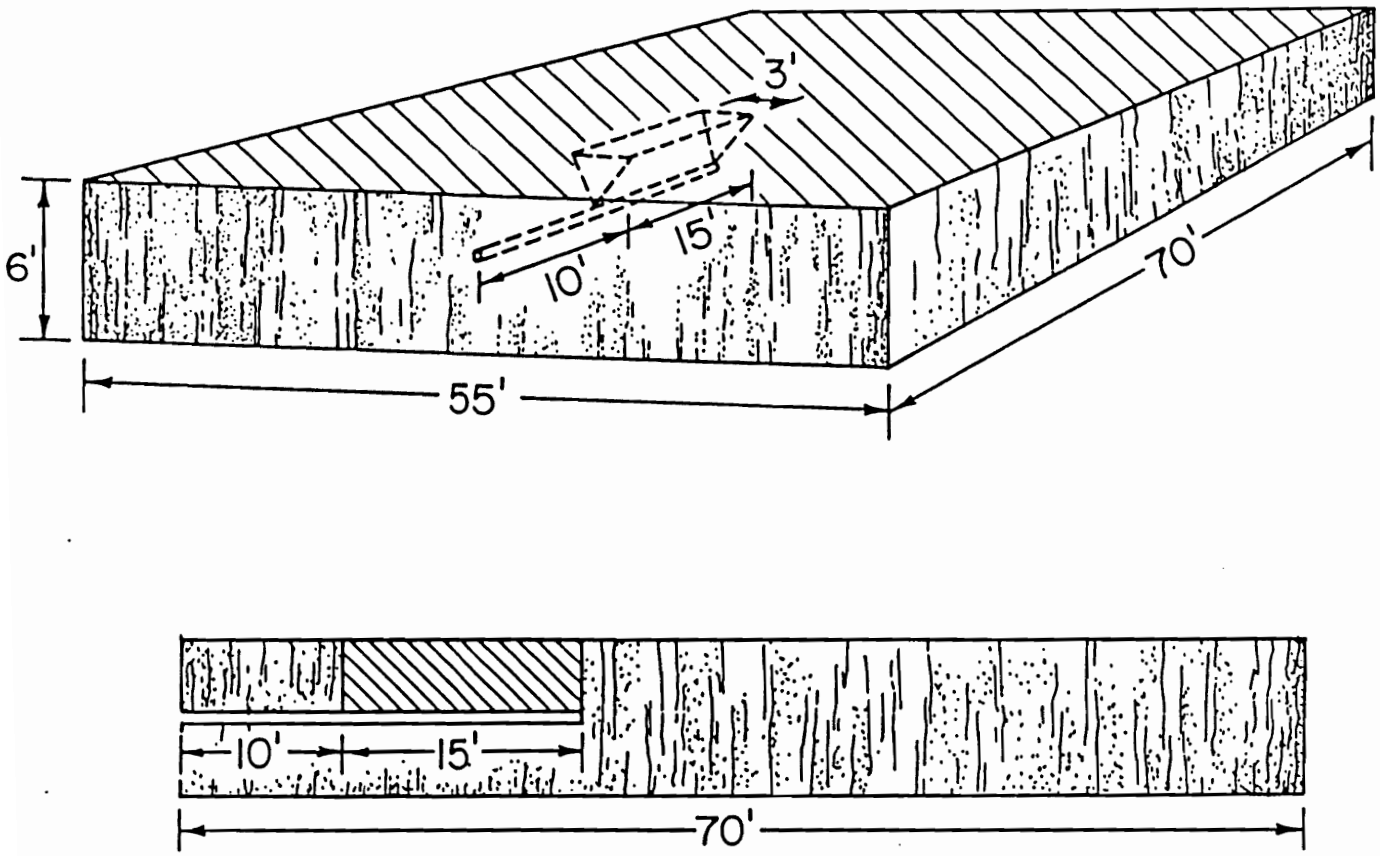

Figure 2.24—Illustration of the effect of auger drilling in "high" stress pillars,. Olga Mine (After Campoli, et al., 1990b).

of the 1960's were based on fairly simple concepts of elasticity and required considerable computational effort. Increasing computational power and efficiency encouraged the development of increasingly sophisticated and varied programs capable of modeling complicated problems. As the sophistication of these programs increased the knowledge required of the user decreased. It is, therefore, critical that the mining engineer understand both the strengths and the weaknesses of the approach selected for any specific application (Hoek, et al., 1991).

The behavior of the rock mass is dependent on the mechanical and structural properties of the mass and the shape of the excavation created. The rock mass may respond elastically, plastically, or fracture. The rock mechanist cannot represent every conceivable response of the rock mass in the model. Hence, the model will always be a simplification of the real life situation.

The rock mass response to load is classified as either continuous or discontinuous (fig. 2.25). The rock mechanist must determine which regions will be assumed to be continuous and which will be assumed to be discontinuous. The magnitude of displacement on a plane determines if it is treated as a discontinuity. The next step in the modeling process is the development of constitutive relations which relate stress and strain. A homogeneous region is composed of one material and is governed by one constitutive relation. A heterogenous region is composed of multiple materials and requires a constitutive relation for each material. Isotropic behavior is assumed for simplicity in most models. Orthotropic behavior

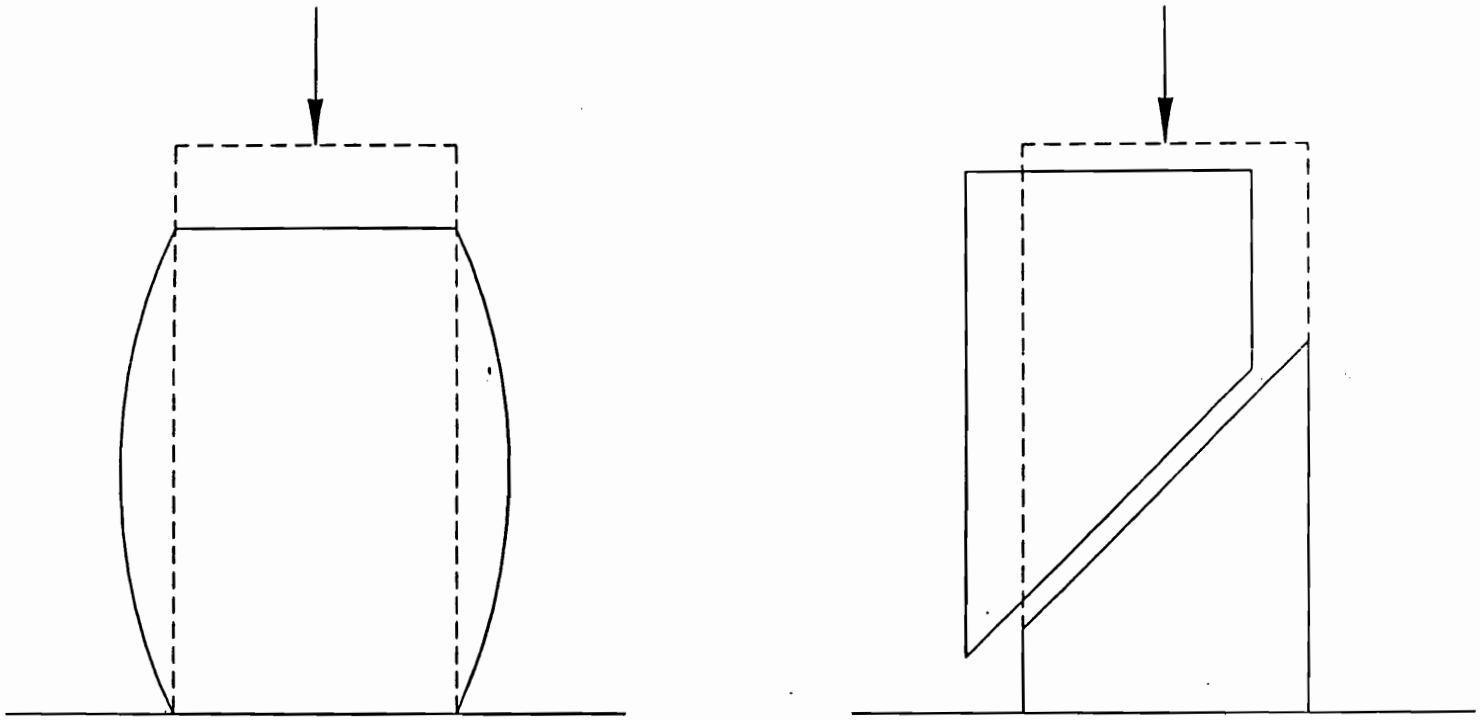

Figure 2.25—Continuous (left) and discontinuous (right) behavior of uniaxially loaded specimens (After Hoek, et al., 1991).

is more complex and is reserved for pronounced directional differences in material behavior.

Mathematical relations between stress and displacement, such as Hooke's law, can be developed into closed-form solutions. These solutions represent the complex behavior of the rock mass in the form of equations. Closed-form solutions that recognize the heterogeneous nature of rock and its various failure modes have led the development of the science of rock mechanics. Brady and Brown (1985) reviewed the current science of rock mechanics as it applies to underground mining. Closed-form solutions provide the basis for and testing of numerical models.

The closed-form solution technique is of limited use in modeling the behavior of heterogeneous and fractured rock masses, especially when the rock mass is penetrated by irregularly shaped mine openings. Approximate solutions to such problems may be obtained from computer based methods. Numerical methods divide the problem into a number of smaller physical and mathematical components and then sum the influence of the components to approximate the behavior of the whole system. The problem is formulated as a set of simultaneous equations that are solved by a variety of matrix solution techniques. The matrix technique solves problems efficiently with simple constitutive laws. Models of more complex behavior are solved by the explicit or dynamic relaxation technique. Explicit solution assumes that a disturbance at a point in space is initially felt only by points in the immediate vicinity. Over succeeding computational steps, the disturbance spreads until equilibrium is established. This technique does not require the solution of a matrix

for each step. Explicit solution results in improved efficiency, numerical stability and accuracy, when complex constitutive relations and severe gradients are modeled. Either solution technique can be used for any of the following methods.

The numerical methods used in rock mechanics are either boundary or domain methods. The boundary of the rock mass is divided into elements and the interior is viewed as an infinite continuum in boundary element methods. The rock mass is divided into geometrically simple zones in domain methods. The reaction of the rock mass is modeled by the composite reaction of these simple zones (Hoek, et al., 1991).

Domain methods require a significant amount of effort to discretize the model (fig. 2.26). Discretization of complex models can become extremely difficult. In contrast, boundary methods require that only the excavation boundary be discretized and the surrounding rock mass is treated as an infinite continuum (fig. 2.26). Fewer elements are required in the boundary method, thereby, reducing the required computer memory and operator skill.

Domain methods require significant separation of the outer boundaries and mine openings to minimize errors due to these interactions. No outer boundaries are required in boundary methods as the far-field conditions are only specified as stresses. Representing the rock mass as an infinite continuum is the main strength of boundary methods. This significant simplification generally prohibits the modeling of multiple

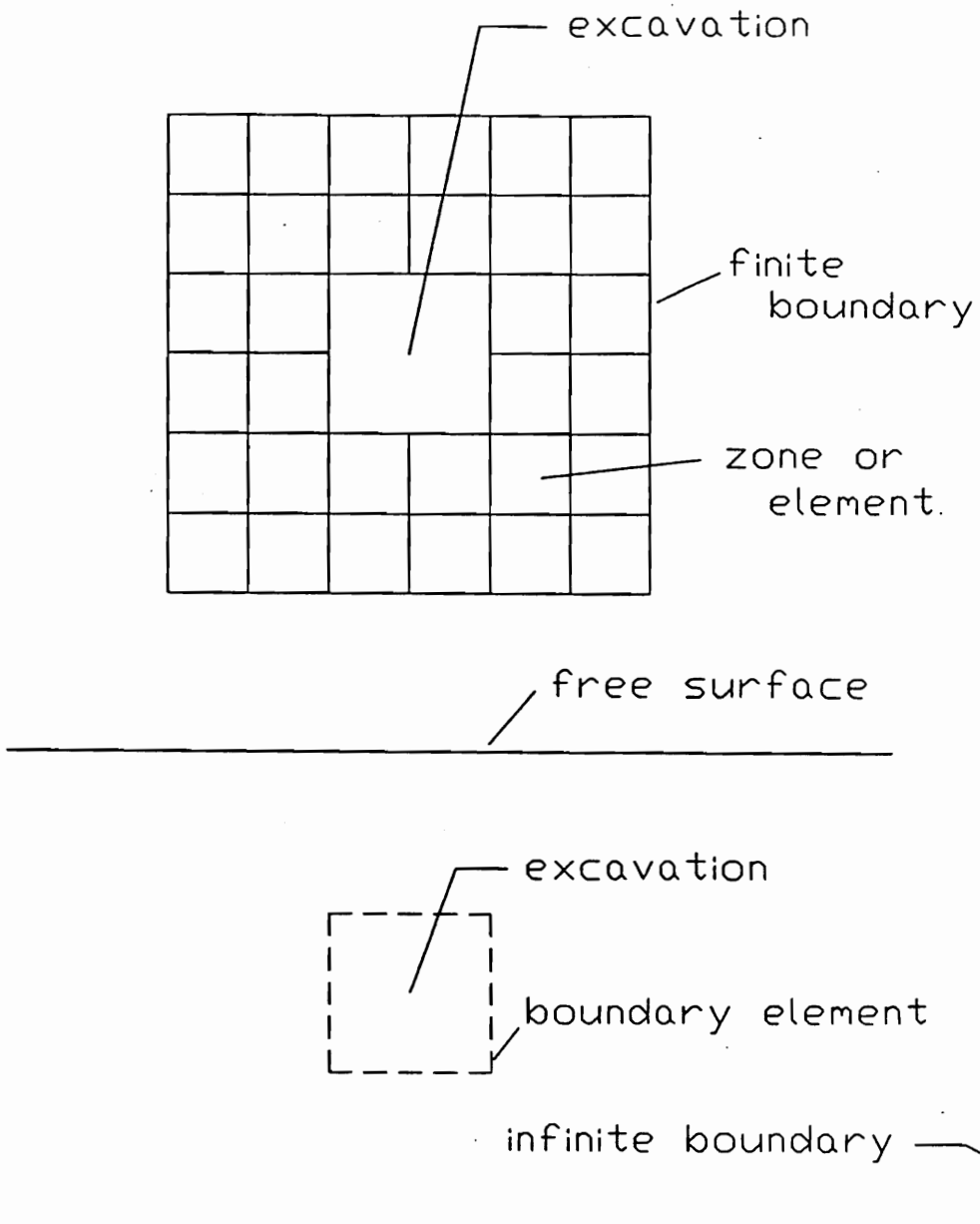

Figure 2.26—Division of model into elements in domain methods (top) and definition of excavation boundary in boundary methods (bottom) (After Hoek, et al., 1991).

material types and the interaction of rock mass and artificial support. These types of problems are generally addressed with domain methods.

2.7.1 Boundary-Element Method

The boundary-element method discretizes only the boundaries of the problem geometry (entry surfaces, joints, and material interfaces). There are three approaches to boundary-element modeling, namely the indirect, direct, and displacement discontinuity methods. The indirect or fictitious stress method finds the stresses on the boundary first and separate relations are applied subsequently to find boundary displacements. The direct method finds unknown stress and/or displacements from the specified boundary conditions. The displacement discontinuity method represents the result of pulling apart a slit in an elastic continuum.

The boundary-element method is the solution of a mathematical relationship between the conditions on the surface of an element and the conditions at all points within the remaining medium. Therefore, each element can have an effect on every other element. A system of linear equations is assembled, the members of the fully populated coefficient matrix represent the influence of one element on another. Dissimilarly, finite-element matrices typically are banded. Given a specific size, fully populated matrices take longer to solve than banded matrices. However, the boundary-element method typically requires fewer elements as only the boundary is discretized.

The boundary-element method determines the state at a point within the medium solely from the conditions at the discretized boundaries. The problem can be devised so that the far-field stresses are not influenced by the creation of an opening. Finite-element techniques require the approximation of far-field conditions. The fact that a boundary element represents an influence to infinity can also be a disadvantage. For a heterogenous rock mass consisting of multiple variations in structural properties over short distances, it usually is advisable to use one of the other numerical methods (Hoek, et al., 1991).

The displacement discontinuity approach, to the boundary-element method, explicitly models joints. A widely used application of displacement discontinuity boundary elements is in the modeling of tabular ore bodies. The entire ore body is represented as a joint, initially filled with ore that may have a different stiffness from that of the host rock. A mining operation is stimulated by reducing the stiffness of the ore to zero in those areas where mining has occurred and examining the resulting stress redistribution to the surrounding pillars. The MULSIM/NL program, which functions in this fashion, will be discussed in detail and applied to the design of room-and-pillar retreat mining methods for bump control.

2.7.2 Finite-Element Method

Boundary-element formulations relate conditions on a surface to the points within the body. In contrast, the finite-element method relates the conditions at a few points within the medium (nodal points) to the state within a finite closed region

formed by these points (the element). The physical problem is modeled numerically by discretizing the problem region into elements (fig. 2.27).

The strength of finite-element method lies in its ability to solve problems involving multiple materials and/or nonlinear material properties (changes in the modulus of elasticity); the weakness of the finite element method is in the modeling of infinite boundaries, which are common in problems relating to underground excavation. However, current programs are enhanced by pre- and post-processors which allow the user to perform parametric analyses quickly and to assess the influence of approximated far-field boundary conditions. Joints can be represented explicitly by specialized elements or may be modeled with the use of constitutive relations.

After the element equations have been derived and the loads have been mathematically applied, the matrix must be solved to find the new equilibrium state. There are two classes of solution techniques; implicit and explicit (with respect to time). Implicit techniques employ standard matrix solution techniques on systems of linear equations. Material nonlinearity is imposed by varying modifying stiffness coefficients and/or by adjusting selected variables. Loads are applied incrementally, each increment being sufficiently small to ensure solution convergence for the increment after only a few iterations. These changes are made such that all constitutive and equilibrium equations are satisfied for each loading increment. Most

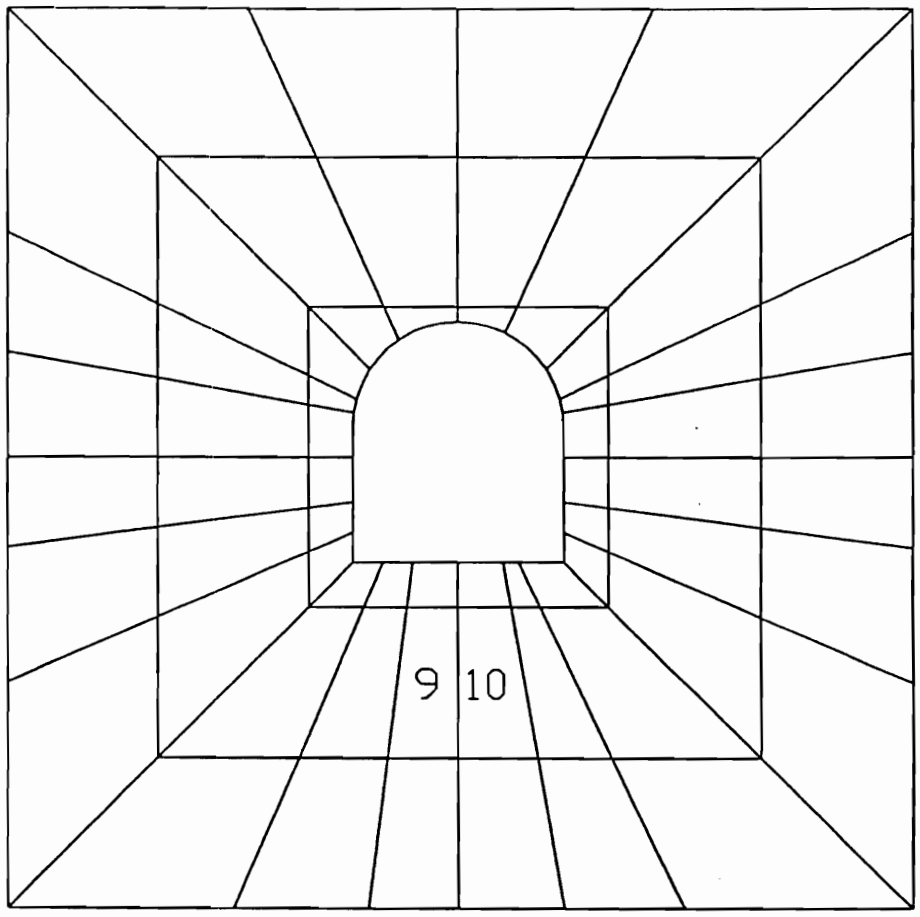

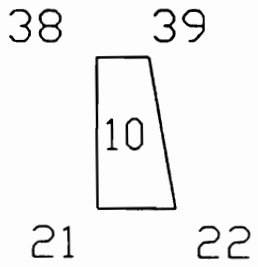

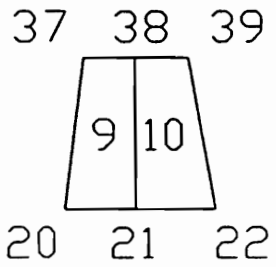

Figure 2.27—Development of finite-element model: finite-element mesh (top), single element (left), and shared nodes (bottom) (After Hoek, et al., 1991).

commercially available finite-element packages use implicit (i.e., matrix) solution techniques (Hoek, et al., 1991).

2.7.3 Distinct-Element Method

In some blocky rock masses pronounced jointing defines wedges and blocks that may be regarded as rigid bodies. These rigid bodies are free to rotate and deform the rock mass along the joints between the blocks. Little, to no deformation occurs within the blocks. Joint systems may be modeled explicitly. However, this highly nonlinear behavior is inefficiently modeled by even a jointed finite-element code employing an explicit solution technique.

Distinct-element methods have been developed which treat each block as a unique free body that interacts with the free bodies surrounding it with minimal deformation of within the blocks (fig. 2.28). Joint surfaces are treated as overlaps of adjacent free bodies and not as joint elements. This approach allows large displacements on the planes of contact between free bodies, a condition that is not easily accommodated with finite-element programs. Distinct-element codes use explicit solution techniques to efficiently solve these highly nonlinear problems.

The relative strengths and weaknesses of the numerical methods just described are summarized in Table 2.2.

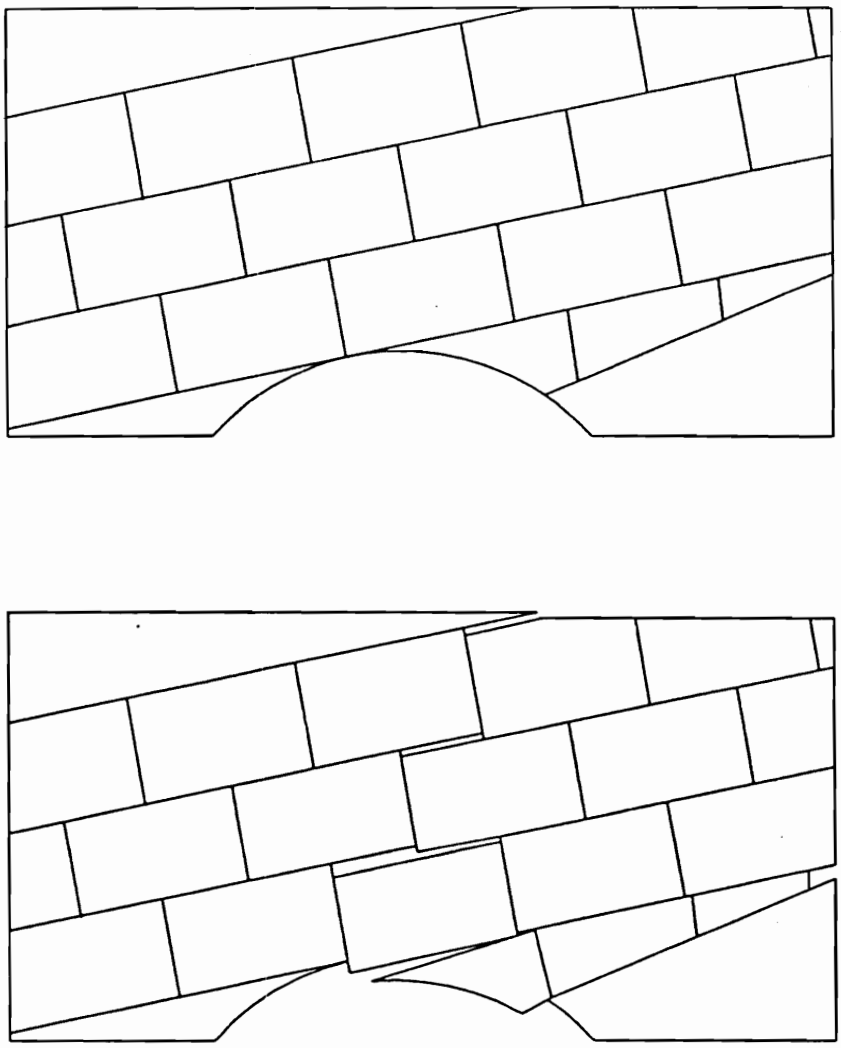

Figure 2.28—Distinct-element modeling of jointed rock mass: before failure (top) and after failure (bottom) (After Vogle, et al., 1978).

Table 2.2 Relative strengths and weaknesses of numerical methods (After Hoek, et al., 1991.)

Methods	Advantages	Disadvantages
Boundary element	Far-field conditions inherently represented	Coefficient matrix fully populated
	Only boundaries require discretization, resulting in smaller number of solution variables than for finite-element methods	Solution time increases exponentially with number of elements used
		Limited potential for handling heterogeneous and nonlinear materials
Finite element	Material heterogeneity easily handled	Entire volume must be discretized, resulting in larger number of solution variables than for boundary-element methods
	Material and geometric nonlinearity handled efficiently, especially when explicit solution technique is used	Far-field boundary conditions must be approximated
	When implicit solution techniques are used matrices are banded	For linear problems, explicit solution techniques are relatively slow
	When explicit solution techniques are used, less skill is required of user in assessing numerical convergence	Solution time increases exponentially with number of elements used for implicit solution techniques
Distinct element	Data structures well suited to modeling systems with high degree of nonlinearity resulting from multiple intersecting joints	Solution times seem much slower than for linear problems
	Very general constitutive relations may be used with little penalty in terms of computational expense	Results can be sensitive to assumed values of modeling parameters (these "disadvantages" are natural consequence of nature of system being modeled; as there is currently no modelling alternative for such problems, the term "disadvantage" must be interpreted accordingly)
	Solution times increase only linearly with number of elements used	

2.7.4 Modeling Considerations

Starfield and Cundall (1988) cited three reasons for the upsurge in geotechnical modeling:

- availability of versatile and powerful computer packages;
- increased ability to include geological detail in the model; and,
- the success of modeling in other branches of mechanics.

Each of these three reasons for increased use of computer modeling in rock mechanics should be accompanied with a warning. The availability of computer packages provides the rock mechanics engineer with a box of tools. Only through an understanding of both the strengths and weaknesses of tools can a worker become a craftsman.Building bigger and faster tools is not the goal; the goal is safer and more efficient mine designs.

Numerical models are built because real life situations are too complex for closed form solutions. One should not unnecessarily complicate models with too much geologic detail.

The success of modeling in other engineering fields has motivated modelers in rock mechanics, but blind imitation of these approaches will fail due to differences between rock mechanics and, for example, aerospace or structural mechanics. The challenge to rock mechanists is to develop a distinctive modeling methodology that is both powerful and useful (Starfield and Cundall, 1988).

2.7.5 Modeling Guidelines

Modelers in ecology have classified problems by the quality of available data and the understanding of the problem to be solved (Holling, 1978). Figure 2.29 graphically displays a method which classifies problems into one of four regions. In region 1, statistics is the appropriate modeling tool when there are good data but little understanding. In region 3, both the data and the understanding are available. Many aerospace and mechanical engineering problems fit this category. In this region, models can be built, validated, and used with conviction. Data-limited problems lie in regions 2 and 4. Problems in rock mechanics usually fall in these data-limited categories.

The availability of ever-increasing volumes of data does not necessarily move rock mechanic problems into region 3. It is, however, fruitful to explore how modeling tools developed for solving region 3 type problems might be applied to rock mechanics problems in regions 2 and 4. Starfield and Bleloch (1986) address the differences between the well-posed problems of region 3 and the data-limited problems of regions 2 and 4 as follows:

- A model is a simplification of reality, an intellectual tool designed for a specific task.
- Design the model to answer specific questions rather than duplicate the details of the modeled system.
- Build multiple simple models rather than one complex model. Simple models can relate to different aspects of the problem.

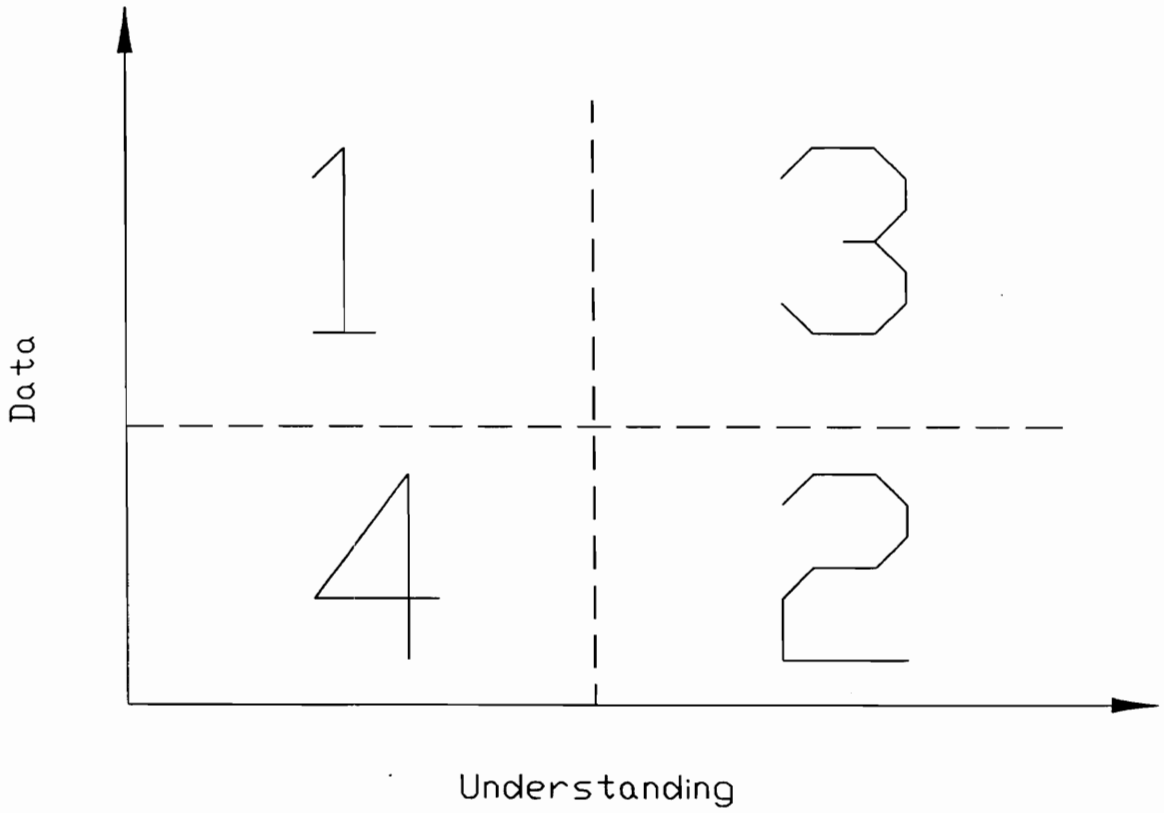

Figure 2.29—Classification of modeling problems (After Holling, 1978).

- Instead of trying to validate a model, aim to gain confidence in it and modify it with use.
- The purpose of modeling data-limited problems is to gain understanding and to explore potential trade-offs and alternatives, rather than make absolute predictions.

2.8 MULSIM/NL Bondary-Element Program

MULSIM/NL is a boundary element method program for calculating stresses and displacements in such tabular deposits as coalbeds. MULSIM/NL was developed to assist in alleviating safety hazards associated with bumps in U.S. coal mines (Zipf 1992a and 1992b). The program provides a means for calculating stress, displacement, and energy changes for various mining configurations in bump-prone conditions. The outputs permit the evaluation of various mine designs that could decrease the occurrence of coal mine bumps.

MULSIM was developed originally to calculate stresses and displacements in the analysis of multiple-seam mining situations (Sinha, 1979). The program neglects the effect of the earth's surface and assumes that the seams are planes at great depth. It can accommodate up to four parallel seams which share a common vertical axis, each modeled by a 12 by 12 array of coarse mesh blocks. Each block can be subdivided subsequently into a 5 by 5 grid of fine-mesh elements (fig. 2.30). The inseam material and the surrounding rock mass are both considered to be linear and elastic.

During the period 1984-85, Bureau upgraded the original program to create MULSIM/BM (Beckett and Madrid, 1988). All of the original capabilities of the program remain in the enhancements. MULSIM/BM includes these major new features: 1) can accommodate up to 26 different linear inseam material properties; 2) includes an inserted material or gob model to represent the layer of broken rock or backfill left behind in retreat mining; 3) can expand permissible coarse-mesh to a 40 by 40 array, the coarse-mesh blocks divisible into fine-mesh elements to a 20 by 20 array, and fine-mesh elements to a 100 by 100 array; 4) fine-mesh and coarse-mesh block stress and displacement output are displayed in the print file; and 5) MULSIM/BM allows the user to specify the extraction ratio of each coarse-mesh block.

Three significant enhancements to MULSIM/BM resulted in the development of MULSIM/NL: 1) nonlinear material models; 2) multiple mining steps; and 3) comprehensive energy release and strain energy computations. Bureau of Mines' coal bump research (Iannacchione, 1988) indicates that highly stressed coal exhibits nonlinear stress-strain behavior. Gob or backfill material left in the wake of coal extraction follows yet other nonlinear stress-strain path. MULSIM/NL has six material models from which to choose including: 1) linear elastic for coal; 2) strain-softening; 3) elastic-plastic; 4) bilinear hardening; 5) strain-hardening; and 6) linear elastic for gob.

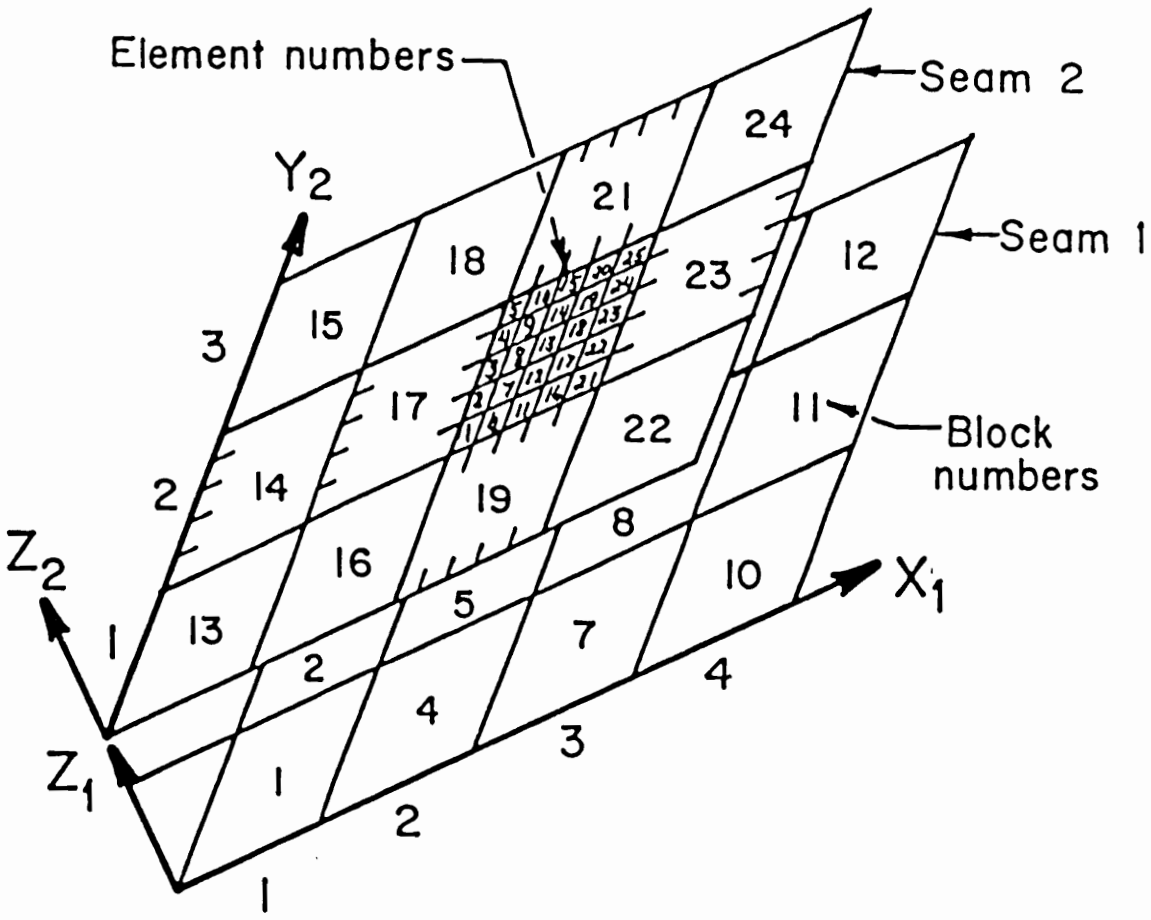

Figure 2.30—Multiple-seam grids for the original MULSIM/NL (After Sinha, 1979).

MULSIM/NL calculates detailed energy changes due to mining. The basis for these calculations, is the energy release rate concept firstadvanced by Cook, et al., (1966), later by Walsh (1977), and more recently by Salamon (1984) and Brady and Brown (1985). The incidence and severity of rock bursts in South African mines has been correlated with the energy dissipation per unit area mined (Hodgson and Joughin, 1966).

MULSIM/NL performs multiple mining steps to examine stress and displacement change as mining progresses. These changes are compatible with displacement and stress change measurements taken during field studies. The energy release rate computations are functions of these stress and displacement changes (Zipf, 1992a).

2.8.1 Displacement Discontinuity Method

The boundary-element method is well suited to the analysis of thin tabular deposits such as coalbeds. Tabular deposits are considered as cracks or discontinuities in an otherwise homogeneous, isotropic, and linear elastic rock mass. The roof-and-floor in underground coal mining operations are the top and bottom surfaces of the crack plane. These planes are the boundaries of the problem. The crack or seam plane is divided into a number of square boundary elements which are assigned material properties or boundary conditions to approximate this geometry. The actual mine plan within this seam plane may have rather complex geometry.

Figure 2.31 shows an actual mine plan where individual elements, either mined or unmined, have assigned material properties.

Closed form solutions derived from elastic theory are the foundation of boundary element methods. An important solution is that of a displacement discontinuity in an infinite solid (fig. 2.32), so named because constant displacement components are applied to the crack walls. Analytic expressions for the stress and displacement components can be found in terms of the displacement discontinuity components D_x and D_z and the spatial coordinates x and z. The concept can be extended to three dimensions. The solution forms, following Zipf (1992a), are:

$$\begin{aligned} \tau_x &= bD_x + cD_y \\ \tau_y &= dD_x + eD_y \\ \sigma_z &= aD_z \end{aligned} \qquad (2.2)$$

where a, b, c, d, and e are influence functions depending on the Young's modulus (E) and Poisson's ratio, (υ) of the host medium and the spatial coordinates (x, y, z). Equation set 2.2 relates an applied displacement discontinuity at the origin to the induced stresses at a point (x, y, z) due to that applied displacement discontinuity. Equation set 2.2 also applies approximately over an element as shown in figure 2.33. Here, constant displacement discontinuities D_x, D_y, and D_z over the source element (k, l) induce stresses τ_x, τ_y, and σ_z at the field element (i, j). Equation set 2.3 reflects the change from point stresses and

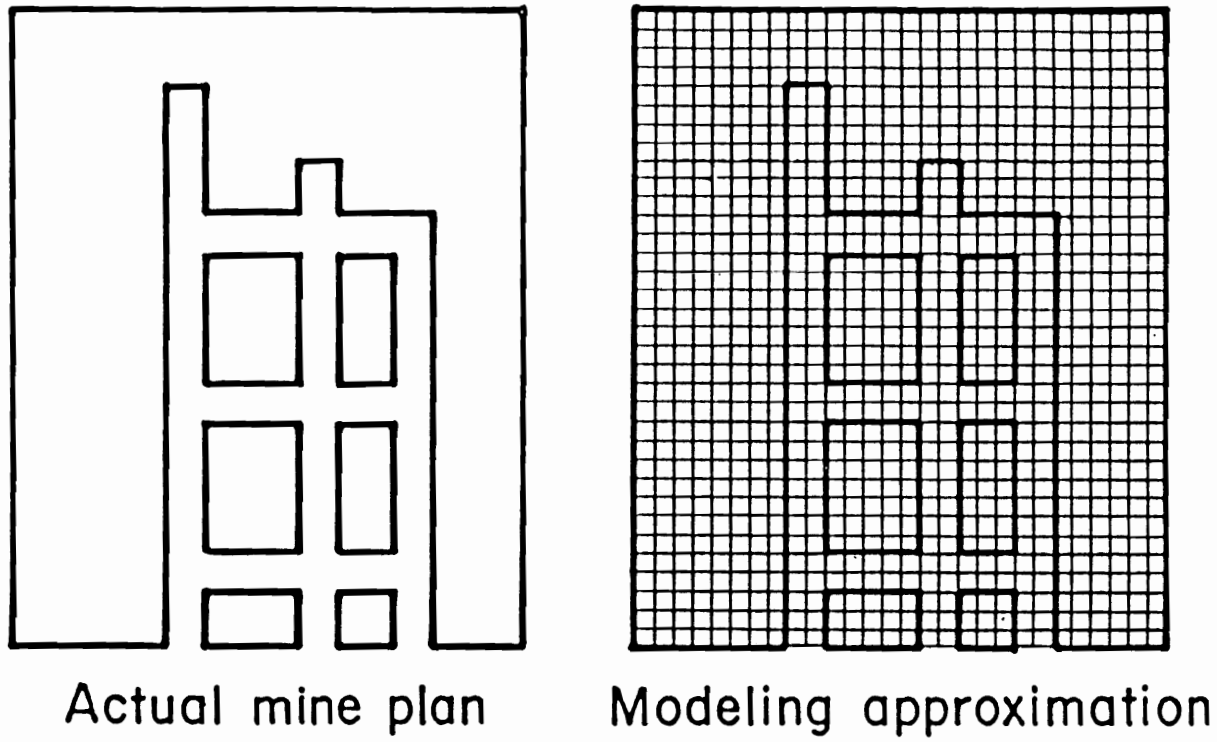

Figure 2.31—In-seam mine plan and gridded modeling approximation (After Zipf, 1992a).

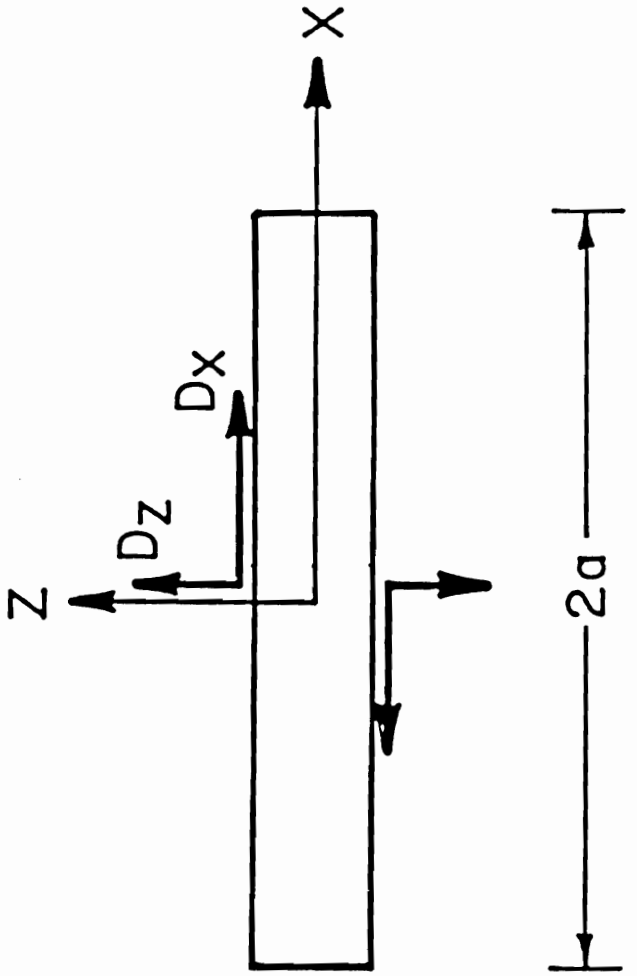

Figure 2.32—Displacement-discontinuity problem in two dimensions (After Zipf, 1992a).

displacement discontinuities to elemental stresses and

$$\tau_x^{i,j} = b_{k,l}^{i,j} D_x + c_{k,l}^{i,j} D_y$$

$$\tau_y^{i,j} = d_{k,l}^{i,j} D_x + e_{k,l}^{i,j} D_y \qquad (2.3)$$

$$\sigma_z^{i,j} = a_{k,l}^{i,j} D_z$$

displacement discontinuities. The total induced stress at element (i, j) is the sum of the induced stresses from all the displacement discontinuities at all the elements (k, l). Taking this summation on equation set 2.3 results in:

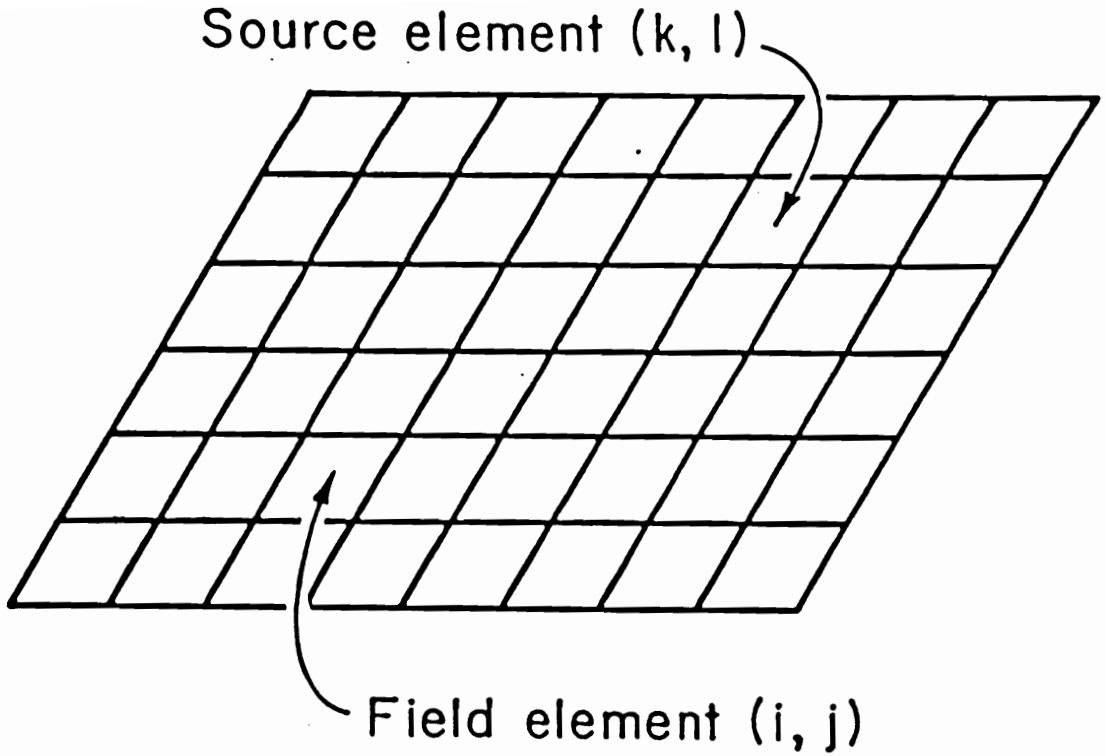

Figure 2.33—Source element (k, l) and the field element (i, j) within the seam plane (After Zipf, 1992a).

$$
\begin{aligned}
{}^{i,j}_{\tau_x} &= \sum_{k,l} \left[{}^{i,j}_{k,l} b\, D_x + {}^{i,j}_{k,l} c\, D_y \right] \\
{}^{i,j}_{\tau_y} &= \sum_{k,l} \left[{}^{i,j}_{k,l} d\, D_x + {}^{i,j}_{k,l} e\, D_y \right] \\
{}^{i,j}_{\sigma_z} &= \sum_{k,l} \left[{}^{i,j}_{k,l} a\, D_z \right]
\end{aligned}
\qquad (2.4)
$$

If N represents the number of elements, then equation set 2.4 represents a system of 3N equations with 6n unknowns--3N stress components τ_x, τ_y, and σ_z, and 3N displacement discontinuities D_x, D_y, and D_z.

A unique solution for the unknowns requires 3N additional independent equations which are generated from the boundary conditions. Figure 2.34 shows an elemental displacement discontinuity and the nature of the applied boundary conditions. For unmined elastic elements, the elemental stresses and displacements are related through the elemental material properties. For simple linear elastic materials, the boundary conditions are:

$$
\begin{aligned}
\tau_x &= G\, D_x / t \\
\tau_y &= G\, D_y / t \\
\sigma_z &= E\, D_z / t
\end{aligned}
\qquad (2.5)
$$

where G = shear modulus

E = Young's modulus

t = element thickness.

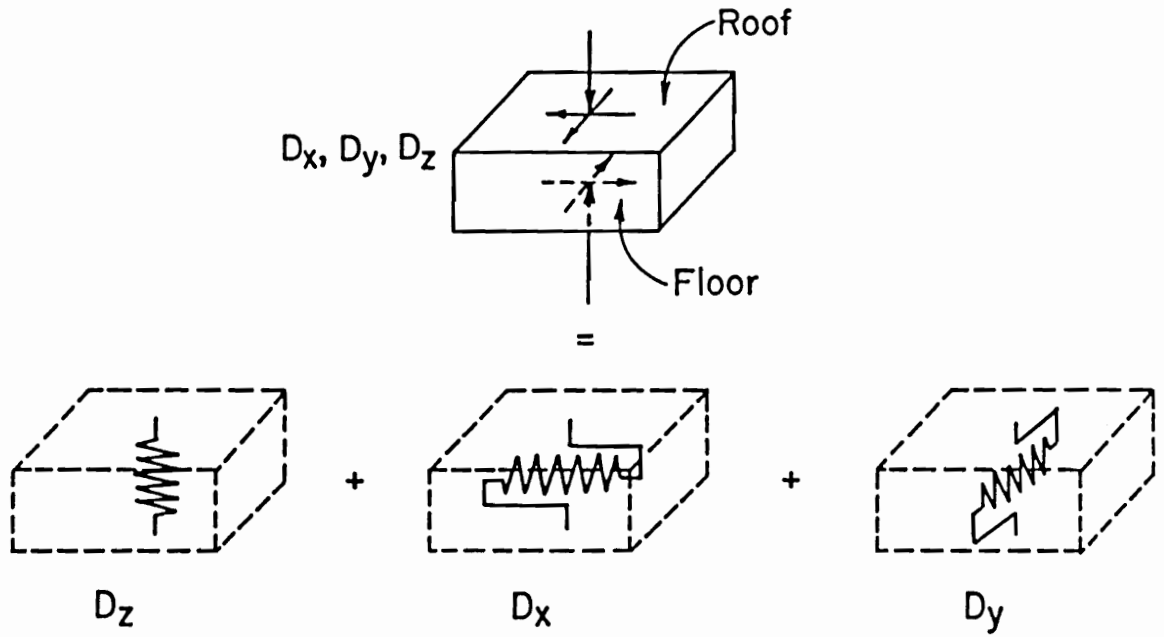

Figure 2.34—Three boundary conditions applied to an elemental displacement discontinuity (After Zipf, 1992a).

The extension of these boundary conditions to more complex nonlinear material properties is straightforward.

For the mined-out areas (open elements), the elemental stresses are zero and the boundary conditions are:

$$\tau_x = 0$$
$$\tau_y = 0 \qquad (2.6)$$
$$\sigma_z = 0$$

Thus, the boundary conditions given by equation sets 2.5 and 2.6 provide the additional 3N relationships which, together with the boundary-element equation set 2.4, enables computating the remaining unknown elemental stresses and displacement discontinuities. Numerical solution of this system of linear algebraic equations is accomplished with a Gauss-Seidel iteration procedure (Zipf, 1992a).

2.8.2 Material Models

Nonlinear inseam material properties are incorporated into the model via the boundary conditions. Implementing the material nonlinearities required a shift from the induced stress approach used in MULSIM/BM. The six stress-strain models for MULSIM/NL are outlined in figure 2.35. Unmined inseam coal material may be represented as linear elastic, strain-softening, or elastic plastic. The gob or backfill material, left in the wake of mining, may be represented as bilinear

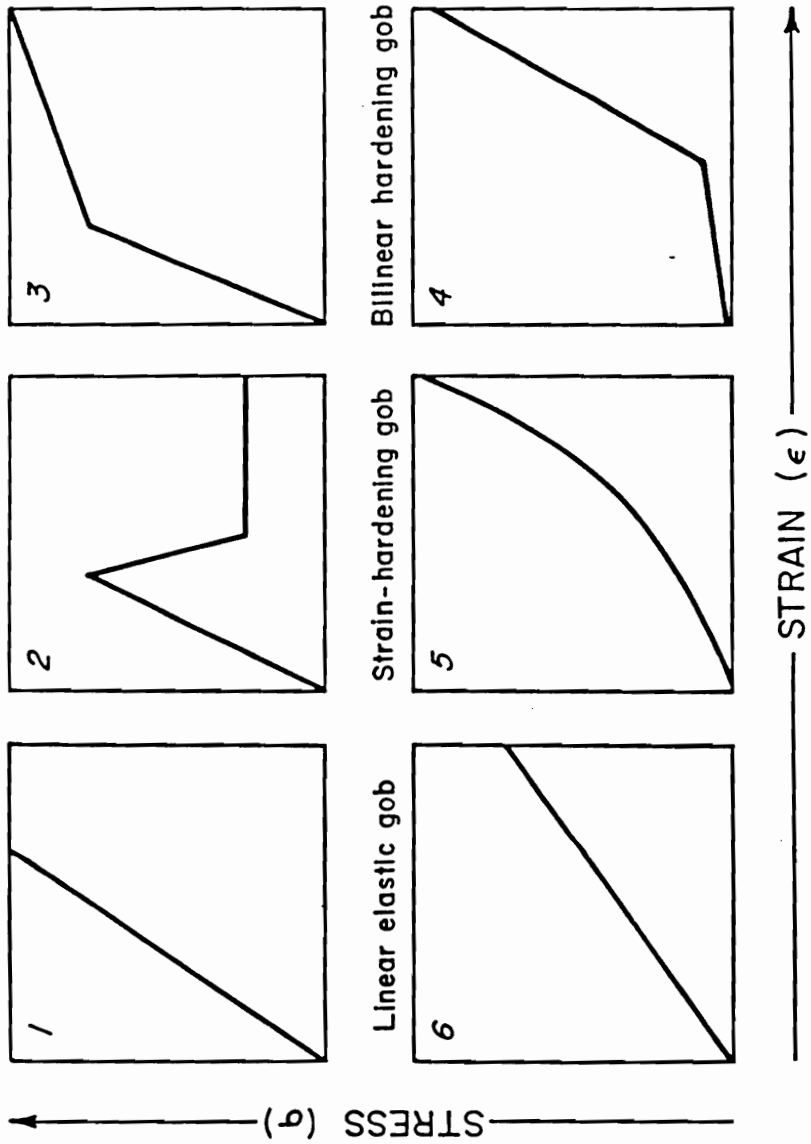

Figure 2.35—The six different stress-strain models available in MULSIM/NL (After Zipf, 1992a).

hardening, strain-hardening, or linear elastic. The distinction between coal material models and gob material models becomes crucial in the subsequent energy calculations.

Linear elastic for coal (1): The required parameters for the model are Young's modulus (E) and shear modulus (G). E relates the normal stress to the normal displacement across an element, whereas, G relates the associated shear stresses to the corresponding shear displacements. With the linear elastic model, MULSIM/NL works internally with a stiffness given by:

$$K = \frac{E}{t} \tag{2.7}$$

where t is the seam thickness.

Linear elastic for gob (6): This model is intended for the gob material left in wake of mining. Required parameters again are E and G plus a gob height factor (n). The factor n is the ratio between the size of broken, rotated gob fragments and the unmined seam height. Typically, values of n range from 2 to 6 and average about 4; beyond a range of 2 to 6, the rock mass surrounding mined-out gob areas remains linear elastic. With linear elastic gob elements, MULSIM/NL uses a stiffness given by:

$$K = \frac{E}{nt} \tag{2.8}$$

The factor n accounts for the bulking of the fractured roof material that fills the void left by mining.

Strain-softening model for coal (2): This model utilizes the stress-strain behavior of coal samples which are loaded through failure by displacement control loading machines (Crouch and Fairhurst, 1973). The model also describes the behavior of moderately sized yield pillars and the perimeters of large pillars. The merits of using a strain-softening model to stimulate the behavior of full-size pillars in coal mines is strongly supported by field observations by Wang, et al., (1976) and Iannacchione (1988).

Peak stress, peak strain, residual stress, residual strain, and Poisson's ratio (υ) are the required input parameters for the strain-softening model. The two shear components are the specified peak and residual stresses scaled by a factor of $1/[2(1+\upsilon)]$. In the linear elastic portion of the strain-softening model, the elastic modulus, computed as $E = \sigma_p/\epsilon_p$, replaces Young's modulus. The residual strain must exceed peak strain and peak stress must exceed residual stress.

Elastic-plastic model for coal (3): This stress-strain model approximates a pseudo-ductile behavior believed to occur in the cores of pillars (Heasley and Barron, 1988). Required input for this model is peak stress, peak strain, the slope of the post

yield portion, and Poisson's ratio (υ). The factor $1/[2(1+\upsilon)]$ scales the amplitude of the normal stress-strain curve to obtain the shear stress-strain relations.

Bilinear hardening model for gob (4): This stress-strain model permits deformation to occur prior to introducing significant element stiffness. Input requirements for the model are stress and strain at the hinge point, modulus in the hardening region past the hinge point, and Poisson's ratio (υ). Again, the stress-strain relations for the normal direction of the element is scaled by the factor $1/2[(1+\upsilon)]$ to obtain the stress-strain relation for the tangential directions of the element.

This gob model also requires the gob height factor (n). The factor n serves as a modulus reduction factor to account for effective seam thickness in the gob area that exceeds seam thickness in the coal areas.

Strain-hardening model for gob (5): Upon gob formation, the roof behind the face fractures and falls into the void left through mining. Broken rock fills a larger volume than solid rock. Once a sufficient amount of rock swells to fill the void, overburden subsidence causes the vertical stress on the gob to increase. The gob consolidation follows a nonlinear, strain-hardening path. Zipf (1992a) provides a complete derivation from this model. This model assumes that the tangent modulus of the gob increases linearly over the stress range 0 to σ_v, where σ_v is the virgin vertical stress. Again, the stress-strain relations for the normal direction of the element is scaled by the factor $1/2[(1+\upsilon)]$ to obtain the stress-strain relation for the tangential directions of the element.

2.8.3 Previous Applications

Zipf and Heasley (1990) demonstrated the superiority of the Olga Mine cut sequence for maintaining a uniform energy release and therefore minimizing bump potential. Zelanko, et al. (1991) used energy methods as part of the analysis of support and strata reaction to longwall retreat mining at a bump prone, multiple seam, eastern Kentucky coal mine. Heasley (1991) advanced the application of energy release calculations as applied to coal bumps through an extensive analysis of an actual bump occurrence. The displacement-discontinuity code, MULSIM/NL, was calibrated with actual field data, and then several alternative energy release values from the model were examined as to their suitability for indicating bump potential. Ultimately, it was determined that prudent application of energy calculations can be used as a tool to investigate the coal bump potential of a mining plan or cut sequence.

Heasley and Zelanko (1992) used the boundary element program MULSIM/NL to evaluate several pillar retreat cut sequences in an effort to determine their relative suitability for use in bump-prone ground. They postulated that the larger the dissipated energy the more likely that the energy will be dissipated dynamically as a coal bump. Therefore, the mining steps associated with the highest dissipated energy are assumed to posses the greatest bump hazard. The energy release methodology is directly tied to vertical stress magnitude; the higher the vertical stress the higher the energy released when that coal is removed.

Chapter III

CASE STUDY ANALYSIS

To determine the primary factors influencing coal mine bumps on continuous miner, room-and-pillar retreat mining sections, a data base was assembled from Bureau of Mines, Mine Safety and Health Administration, and internal coal company documents. The data base contains a total of 58 bump occurrence case histories three of which are described in detail in Appendix A. Analysis of these case studies showed that the most significant factors in bump occurrences are:

A) overburden depth

B) mining method

C) associated strata type

D) geologic structure

E) coalbed characteristics

F) total extraction pillar design.

G) mining rate and time dependent effects

3.1 Overburden Depth

Overburden thickness is a primary consideration in bump control. The overburden in the 58 case histories varied from 625 to 2450 ft. No instances of coal mine bumps could be found under less than 625 ft of overburden, which is considered to be the threshold value for bumps in all types of mining systems. The overburden depth is considered critical as coal mine bumps are primarily due to the release of

excessive pillar stresses. This correlation between overburden depth increases and increased risk of coal mine bumps has been consistently supported by bump researchers (Herd, 1930; Rice,1935; Talman and Schroder, 1958; Goode, et al., 1984; and Campoli, et al., 1993a).

3.2 Mining Method

Comparison of the bump frequency histograms vs depth of overburden for longwall mining (fig. 3.1) and room-and-pillar mining (fig. 3.2) reveals that longwall mining is the dominant method of choice at overburden depths greater than 1600 ft. The frequency of these coal mine bump case studies occurrences vs overburden thicknesses demonstrates the operator preference for longwall over room-and-pillar retreat mining methods as depth increases. This is due to the fundamental difference between the total extraction zones associated with the two mining methods. Continuous miner technology requires the total extraction area be cut into small coal pillars to facilitate ventilation, haulage, and roof support functions during retreat mining. Retreat longwall total extraction zones are very large coal pillars that provide for maximum support. In either case the total extraction zone is required to support the combination of development and gob side abutment loads. The longwall panel is inherently stronger and is thus the preferred method from a ground control stand point. However, longwall sections have very high capital costs and require large and geologically consistent coal reserves to justify their large expense.

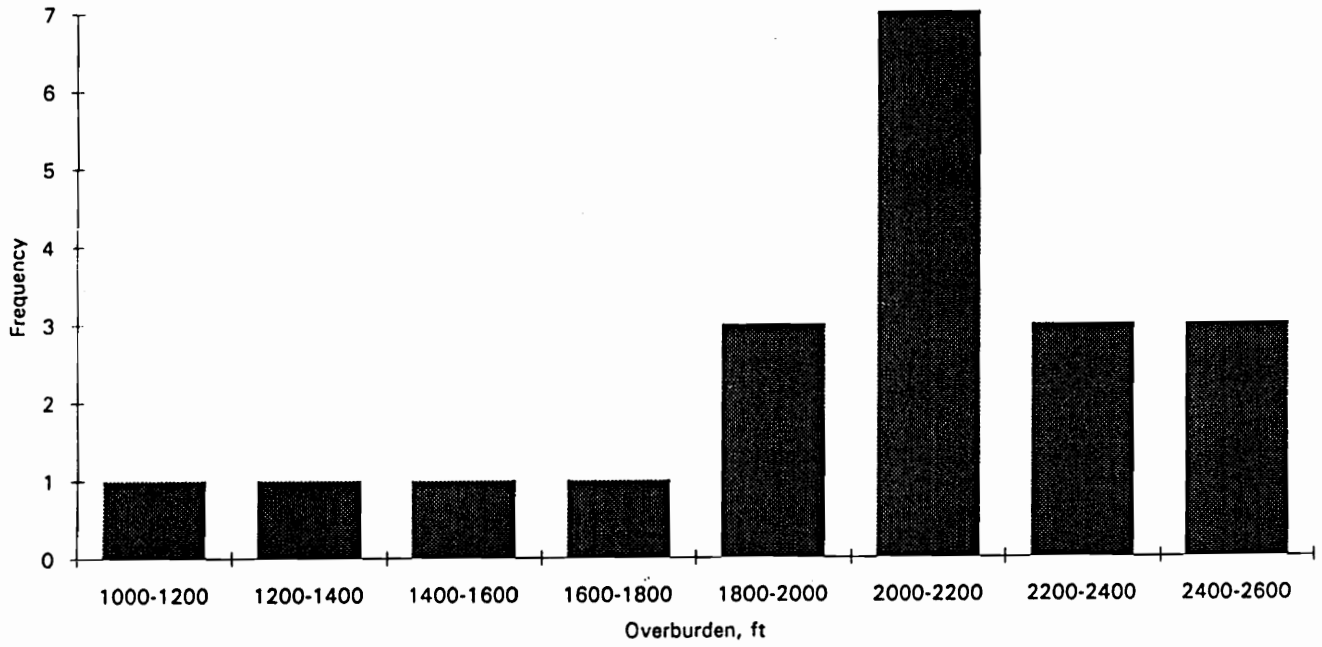

Figure 3.1—Case history frequency of bumps vs depth for longwall mining.

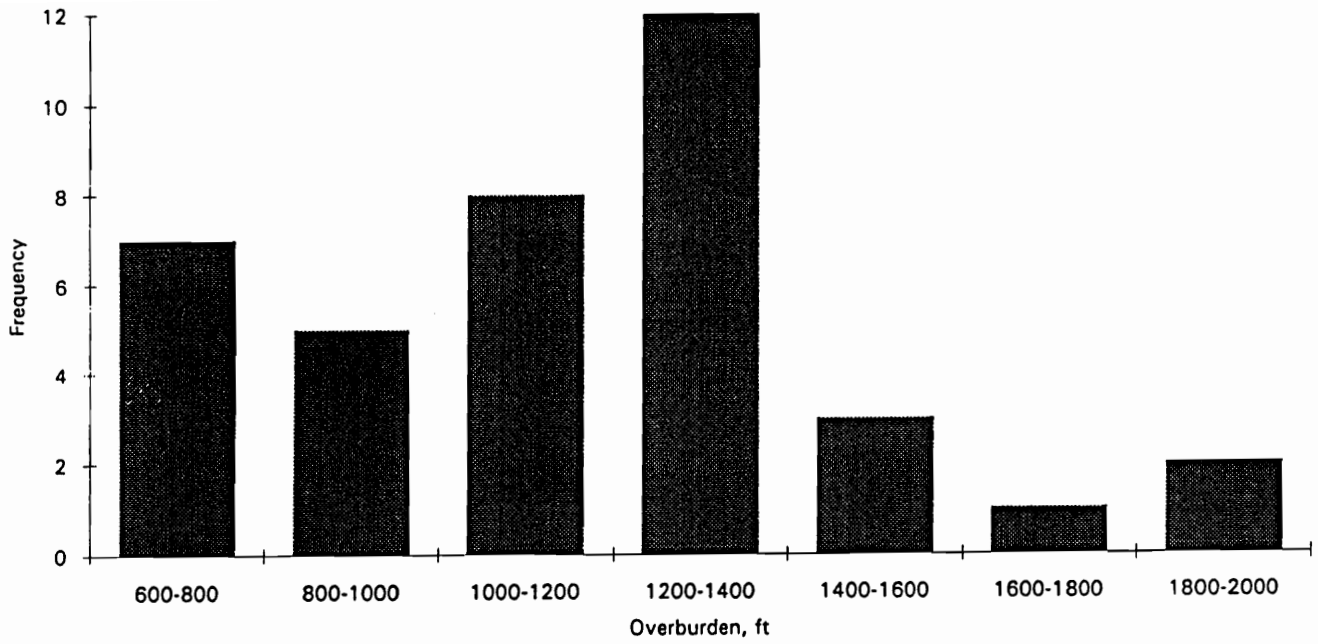

Figure 3.2—Case history frequency of bumps vs depth for room-and-pillar retreat mining.

3.3 Associated Strata

In bump prone coal seams the presence of massive, competent strata in close proximity to the coalbed is a condition noted by numerous observers. (Holland and Thomas, 1954; Goode, et al., 1984; Talman and Schroder, 1958; and Iannacchione, 1988). Analysis of the 58 bump occurrence case studies confirms this tendency, as the immediate roof was either massive sandstone or dense sandy shale. The floor in all but one of the 58 case studies was reported as either sandy shale or shale. This research and the resultant bump hazard assessment model was built on the conclusions that coal mine bumps are a possibility only if:

1) the first 25 ft of roof directly above the coalbed contains greater than 60 percent sandstone

2) the first 10 ft of immediate floor consists of hard shales and sandstones that do not heave readily.

The Olga Mine is the subject of one of the case studies in Appendix A. The mine extracts the Pocahontas No. 3 Coalbed and has been the subjected to numerous coal mine bumps including a double fatality in 1983 (Campoli, et al., 1990). The Upper Pocahontas Sandstone is situated below the Pocahontas No. 4 Coalbed (fig. 3.3). This sandstone unit is laterally discontinuous in the interval 0 to 5 ft below the coalbed. Within this 5 ft interval, the fine to medium grained Upper Pocahontas Sandstone sometimes laterally grades into a competent siltstone and shale units. The Upper Pocahontas Sandstone ranges in thickness from 50 to 75 ft (Hennen, 1915).

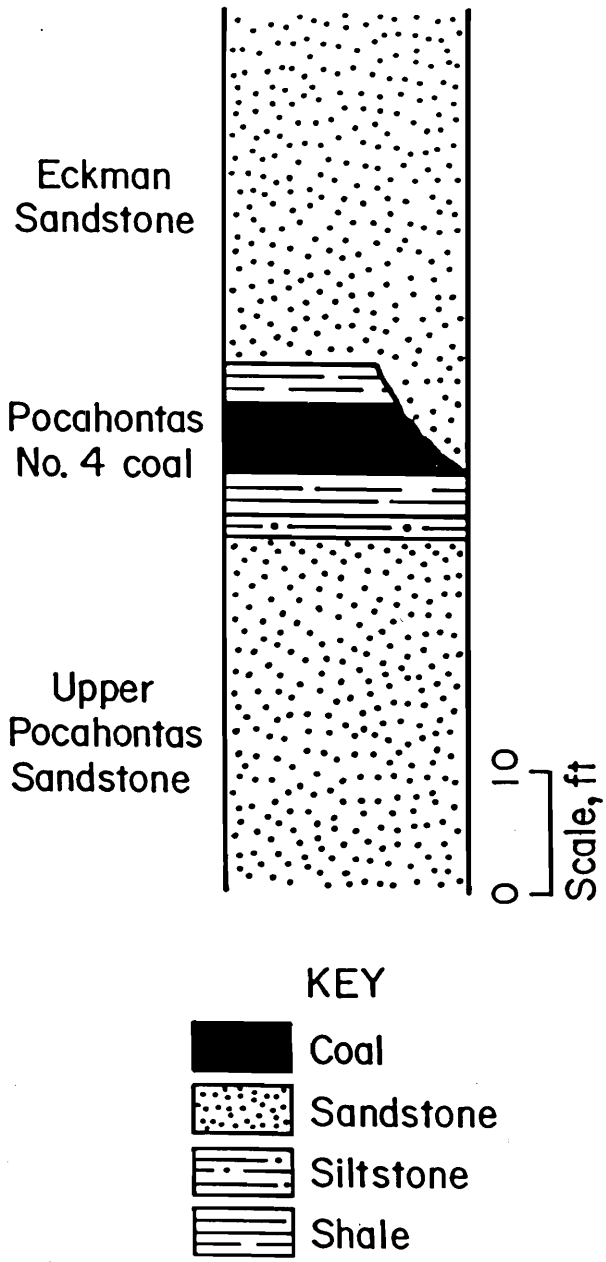

Figure 3.3—Generalized stratigraphic column for the Olga Mine (After Campoli, et al., 1990b).

Under portions of the mine, this sandstone provides a competent and massive floor which does not heave or break readily. As figure 3.4 illustrates, 11 out of 13 bumps associated with injuries or fatalities occurred where the immediate and main floor were 80 to 100 pct sandstone.

The Eckman Sandstone forms the immediate and main roof at Olga and is a very stiff and massive unit. This unit can be 60 or more ft thick and contains a joint system that is unidirectional, extremely pronounced, and widely spaced. The roof has an R.Q.D. of 95 pct and a Final Rock Mass Rating (R.M.R.) of 108 (Newman, 1985). As shown in figure 3.5, every bump occurred where the roof was predominately sandstone (80-100 pct). Therefore, bump-prone areas may be anticipated based on the above geologic correlations. Any area in the mine where the roof-and-floor members are predominately composed of a stiff sandstone should be considered bump-prone. Sames and Zelanko (1994) developed a geology based bump hazard criteria based on the strength of the associated coal strata; the stronger the associated strata the more likely a bump is to occur.

3.4 Geologic Structure

Geologic structure has never been considered a significant factor in bump-prone coalbeds of the eastern coalfields in the United States. Rice (1935), Holland and Thomas (1954), and Talman and Schroder (1958) made little or no reference to

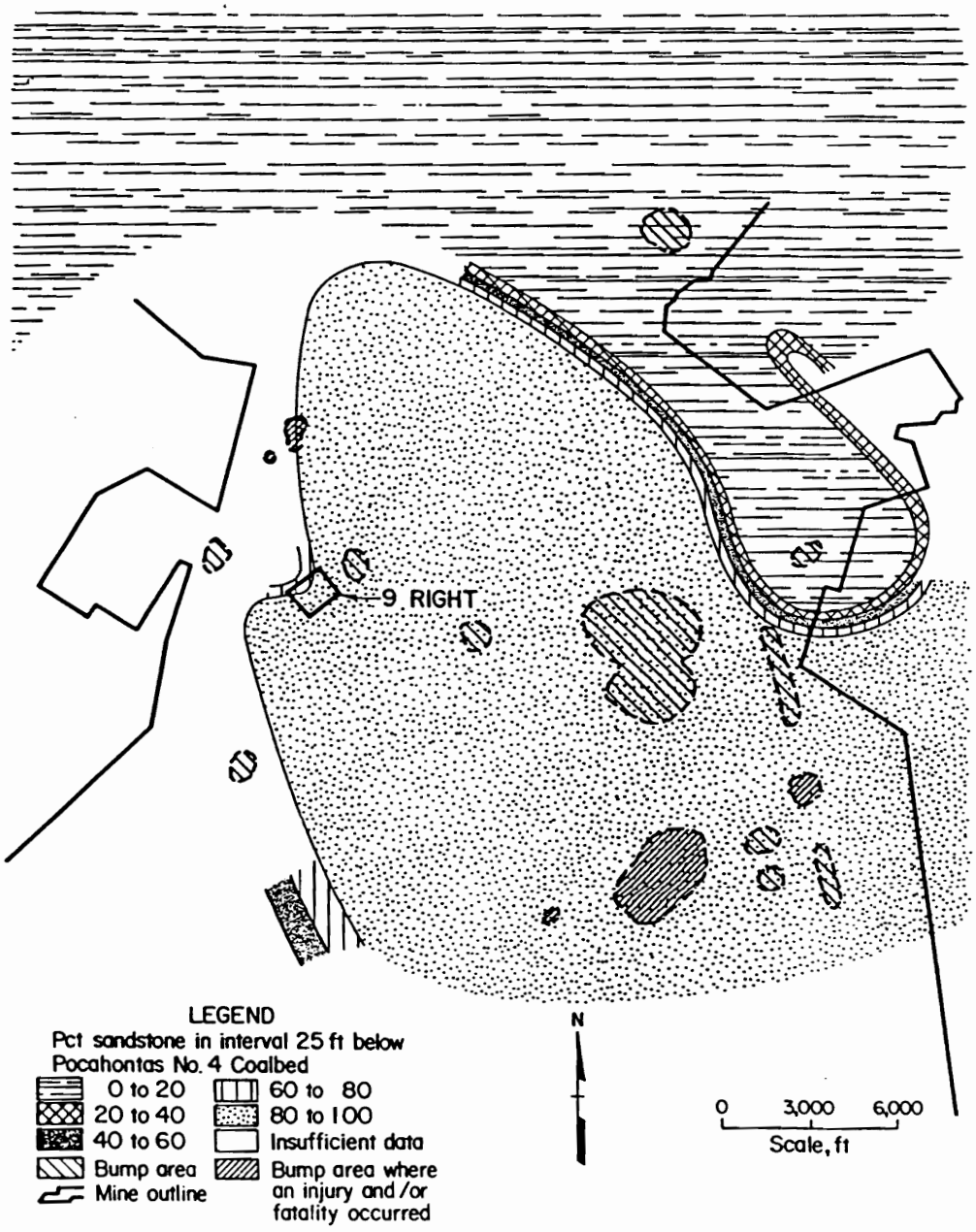

Figure 3.4—Sandstone floor thickness and bump correlation map, Olga Mine (After Campoli, et al., 1990b).

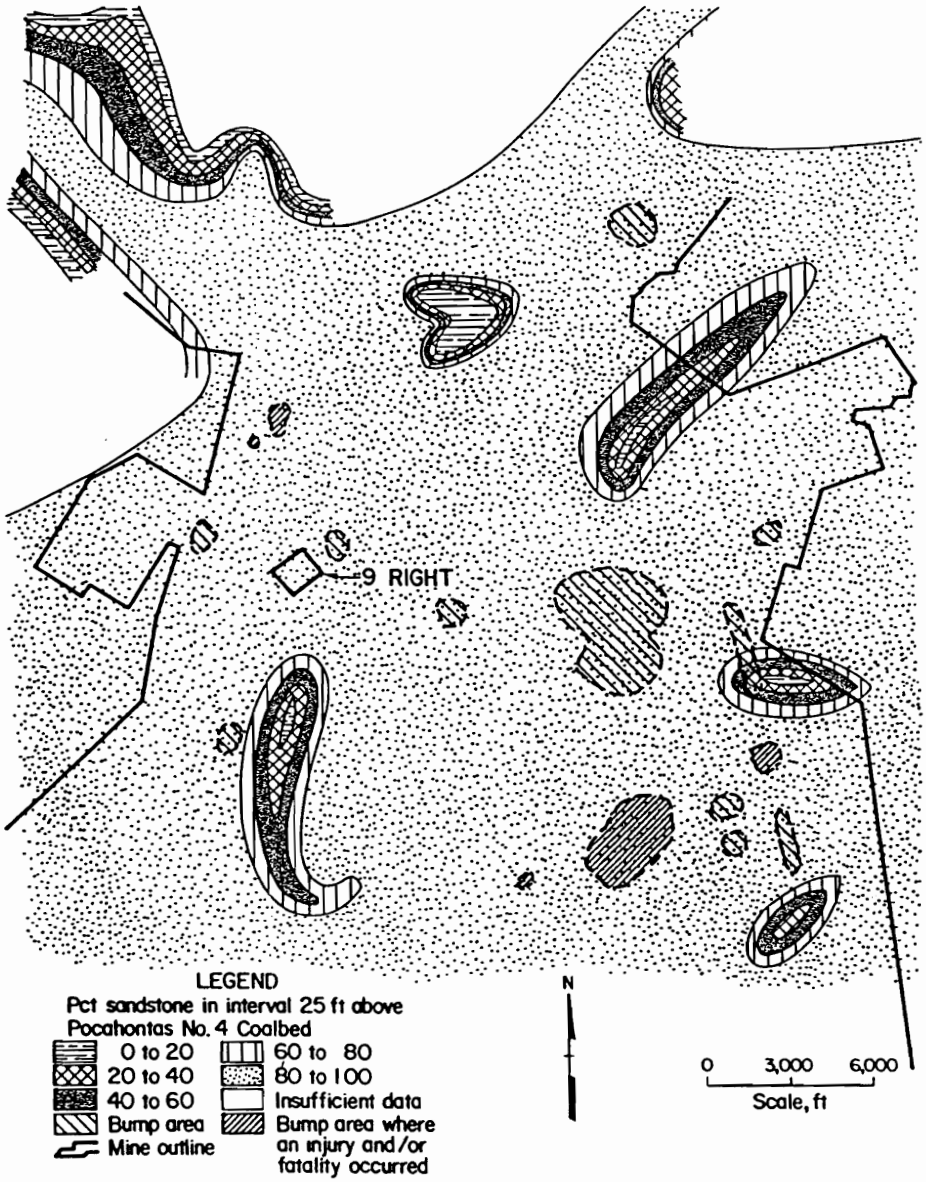

Figure 3.5—Sandstone roof thickness and bump correlation map Olga Mine (After Campoli, et al., 1990b).

the occurrence of faults, folds, or joint structure. In fact, Iannacchione (1988) noted the lack of structure in the bump prone Pocahontas No. 3 and 4 Coalbeds in West Virginia and Virginia. However, small displacement faults and intrusions caused by igneous dikes have been associated with bumps in the Uinta and Piceance Creek Basins in the western United States, where the coalbed is overlain by significant quantities of stiff sandstone (Iannacchione and Demarco, 1992).

Geologic structure and the seismic effects resulting from large scale movement in the main roof were not considered in this research. This simplification of the bump mechanism allows development of the design criteria through manipulation of the mine layout only. However, geologic structure and seismic effects present interesting and fertile areas for future research in the few western United States coalfields that containing significant faulting.

Extensive geological investigations of the Sunnyside District in Utah (Osterwald, 1962) as well as seismic monitoring of rock noises (Dunrud and Osterwald, 1965) indicated that the most numerous and intense bumps occurred within approximately 500 ft of the areas of the mine traversed by the Sunnyside fault system. This however could have resulted from the high tectonic stress field present in the neighborhood of an active fault system.

3.5 Coalbed Characteristics

The relative importance of variations in coalbed physical properties on bump occurrence has been the focus of numerous investigations. Babcock and Bickel (1984) stated " We believe that many, if not most, coals can be made to burst given the necessary conditions of stress and constraint. In cases were the strength is largely produced by constraint, the sudden loss of constraint can produce bursting." The conclusion that most coalbed can be made to burst is supported by the 58 case studies (tab. 3.1). Fifteen coalbeds and a wide variation in coalbed characteristics are represented in the data base, ranging from the soft and friable Pocahontas Coalbeds to the blocky and strong Chilton Coalbed. Each case study represents one bump occurrence and some individual mines were the subject of multiple case studies. The characterization of the coalbed was limited to the impact of coalbed height coalbed height on pillar strength estimation. The height of the coalbed in the case studies ranged from a low of 3.5 ft in the Chilton Coalbed to a high of 9.5 ft in the Harlan Coalbed.

Coal pillar strength prediction schemes have been classified into three categories: empirical formulas, analytical formulas, and numerical models. Empirical formulas are derived from laboratory and/or full-scale testing of coal pillars. These formulas determine a pillar's strength by its geometry in particular, its width-to-height ratio. These empirical formulas treat the entire pillar as a single structural unit. They estimate the average pillar strength, defined as the ultimate load bearing

capacity divided by the bearing area. Empirical formulas have also been devised from statistical analysis of pillar performance.

Analytical formulas assume that the coal pillar consists of an outer yield zone providing constraint to confined core zone. The best known of these mechanics based formulas are the Wilson model (Wilson, 1973), Salamon's squat pillar formula (Salamon, 1990), and the Barron pseudoductile model (Barron, 1984). Both Wilson and Salamon predict an exponential rise in pillar strength with movement away from the mine entry. Barron considered an indefinite exponential stress rise to be unrealistic. By changing the coal fracture criteria from a linear to a gradually decreasing nonlinear Mohr envelope, Barron causes the pillar strength to increase at a decreasing rate to a maximum in the pseudoductile core zone, as illustrated in figure 3.6 (Barron, 1984). A simplified pseudoductile coal pillar strength model has been developed for supercritical width section design criteria. This model was based on in-mine geotechnical evaluations of wide coal pillar behavior in the Pocahontas No. 3 (Campoli, et al. 1990b), Pocahontas No. 4 (Campoli, et al., 1993), and Harlan Coalbeds (Zelanko, et al., 1991). These geotechnical investigations were conducted with borehole platened flatjacks (BPF), coal extensometers, and roof-to-floor convergence instrumentation. Note, these three coalbeds account for 43 of the 58 or 74 percent of the case study data base.

The new coal pillar strength model was necessary because the exponential stress rise was inconsistent with the BPF data and Barron's model was incompatible

Table 3.1-Summary of coalbeds in the case study data base.

State	Coalbed	Pillar retreat	Longwall
Colorado	Coal Basin B		3
	Coal Basin C	1	
Kentucky	Creech	1	
	Harlan	2	4
Utah	Hiawatha		1
	Sunnyside	2	
Virginia	Pocahontas 3		12
	Upper Banner	1	
West Virginia	Beckley	1	
	Cedar Grove	1	
	Chilton	1	
	Eagle	1	
	No. 2 Gas	1	
	Pocahontas 4	25	
	Tiller	1	

with the form of the coal strength assumptions necessary for the supercritical and subcritical section analysis to follow.

The confined pillar core is assumed to reach a maximum stress of 8,000 psi. The stress in the yielded perimeter is assumed to average 3,000 psi. The depth of the yielded perimeter is assumed to be 15 ft in a 6 ft thick coalbed, based on the Olga Mine (Campoli, et al., 1990b) and VP No. 3 Mine (Campoli, et al., 1993) geotechnical evaluations. The depth of the yield zone in the 12 ft thick Harlan Coalbed was shown to be 30 ft in a geotechnical evaluation employing similar instrumentation (Zelanko, et al., 1991). The depth of the yielded perimeter is assumed to vary linearly in the 3 to 12 ft coalbed thickness range (fig. 3.7). Figure 3.8 displays this relationship for a 70 ft square pillar in a 6 ft thick coalbed. The predicted maximum pillar strength for selected total extraction pillar sizes and coalbed thicknesses are displayed in table 3.2. Figures 3.9 and 3.10 compare these predictions to the Bieniawski (Bieniawski, 1986) and all-cell formulas (Mark and Iannacchione, 1992) for 70 and 90 ft square pillars, respectively. The simplified pseudoductile model is the most conservative over the 3 - 6 ft coalbed thickness range, lies between the two other approximations over the 6 - 12 ft coalbed thickness range.

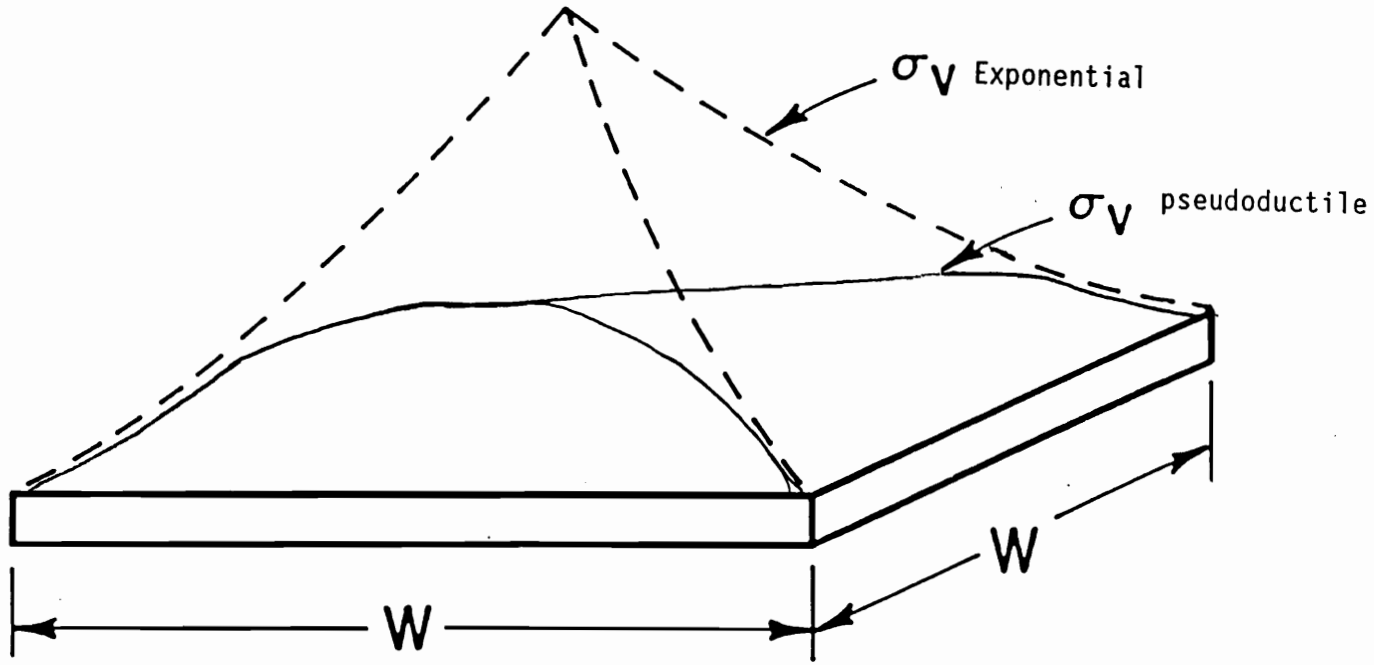

Figure 3.6—Comparison of exponential and pseudoductile assumptions of rise in pillar strength with movement away from the mine entry.

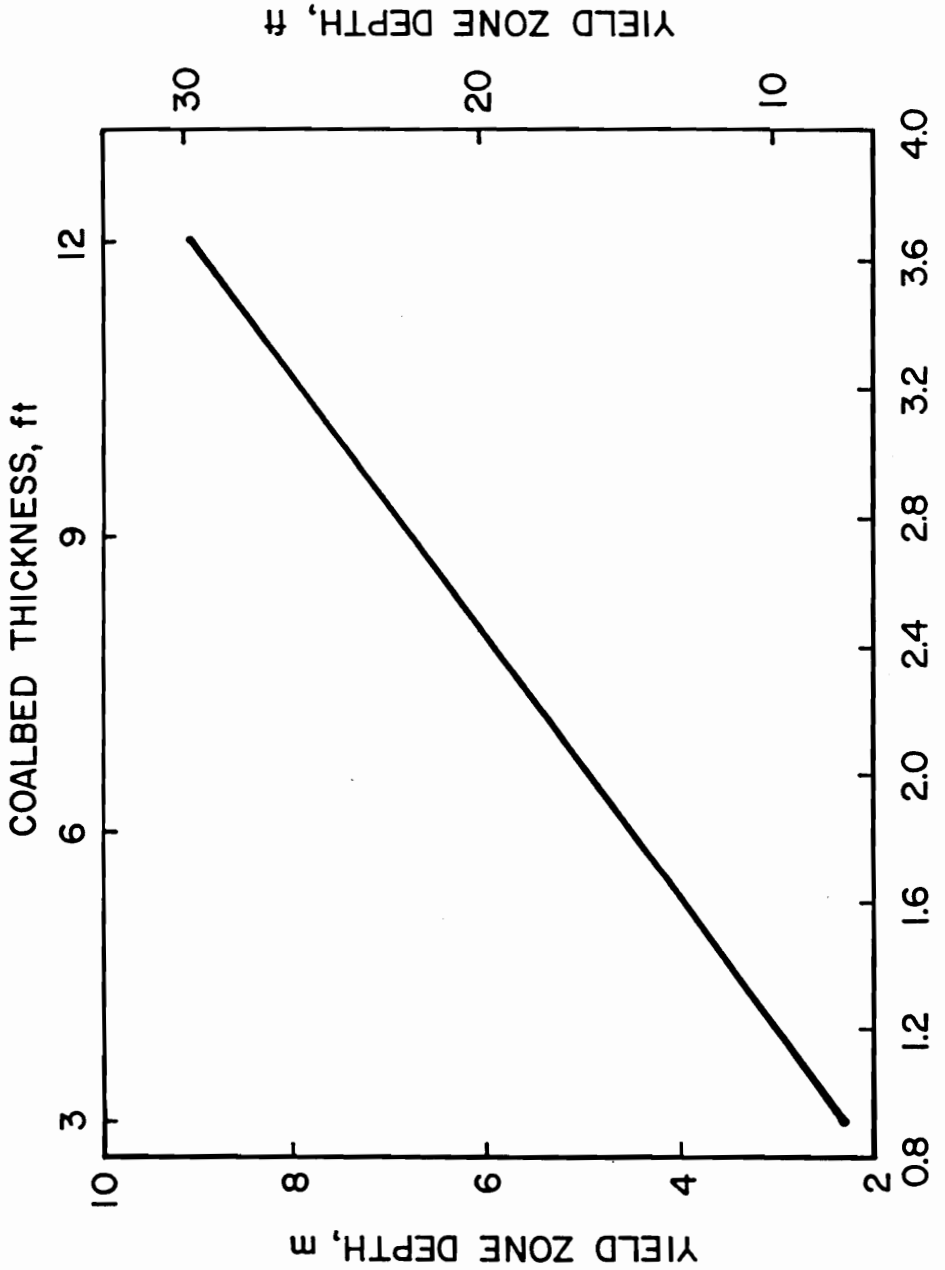

Figure 3.7—Yield zone depth variation with changing coalbed thickness.

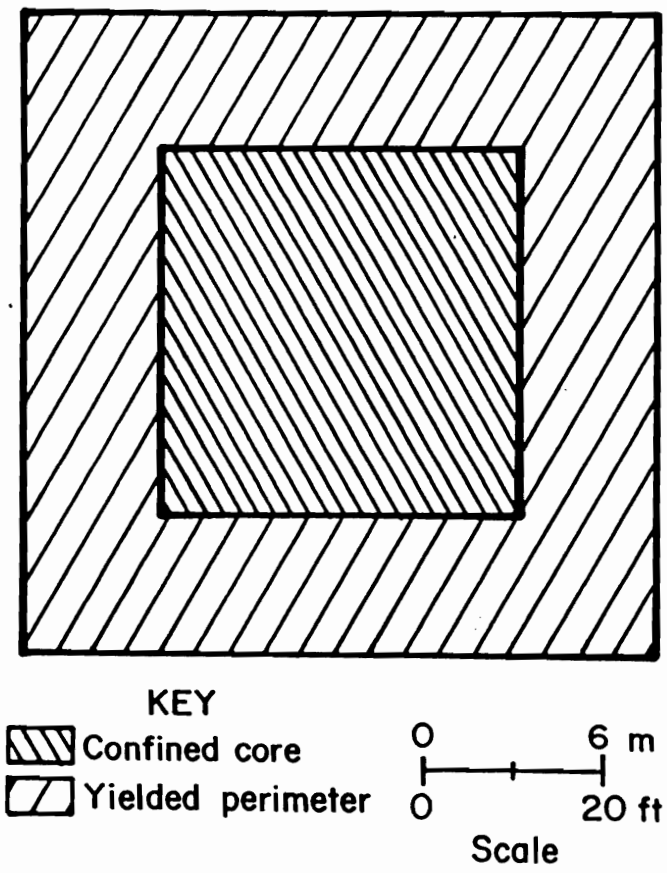

Figure 3.8—Assumed apportionment of yield zone and confined core in a 70 ft square pillar in a 6 ft thick coalbed at maximum load bearing capacity.

Table 3.2—Simplified pseudoductile coal strength model maximum load for selected coalbed thicknesses and total extraction pillar dimensions

Coalbed thickness ft	Pillar dimensions, ft			
	90 x 90	70 x 70	60 x 80	55 x 70
3	7.55[1]	4.29	4.18	3.25
6	6.09	3.27	3.15	2.38
9	4.96	2.57	2.45	1.84
12	4.15	2.19	2.07	1.63

[1] 1 x 10^9 Pounds force (lb)

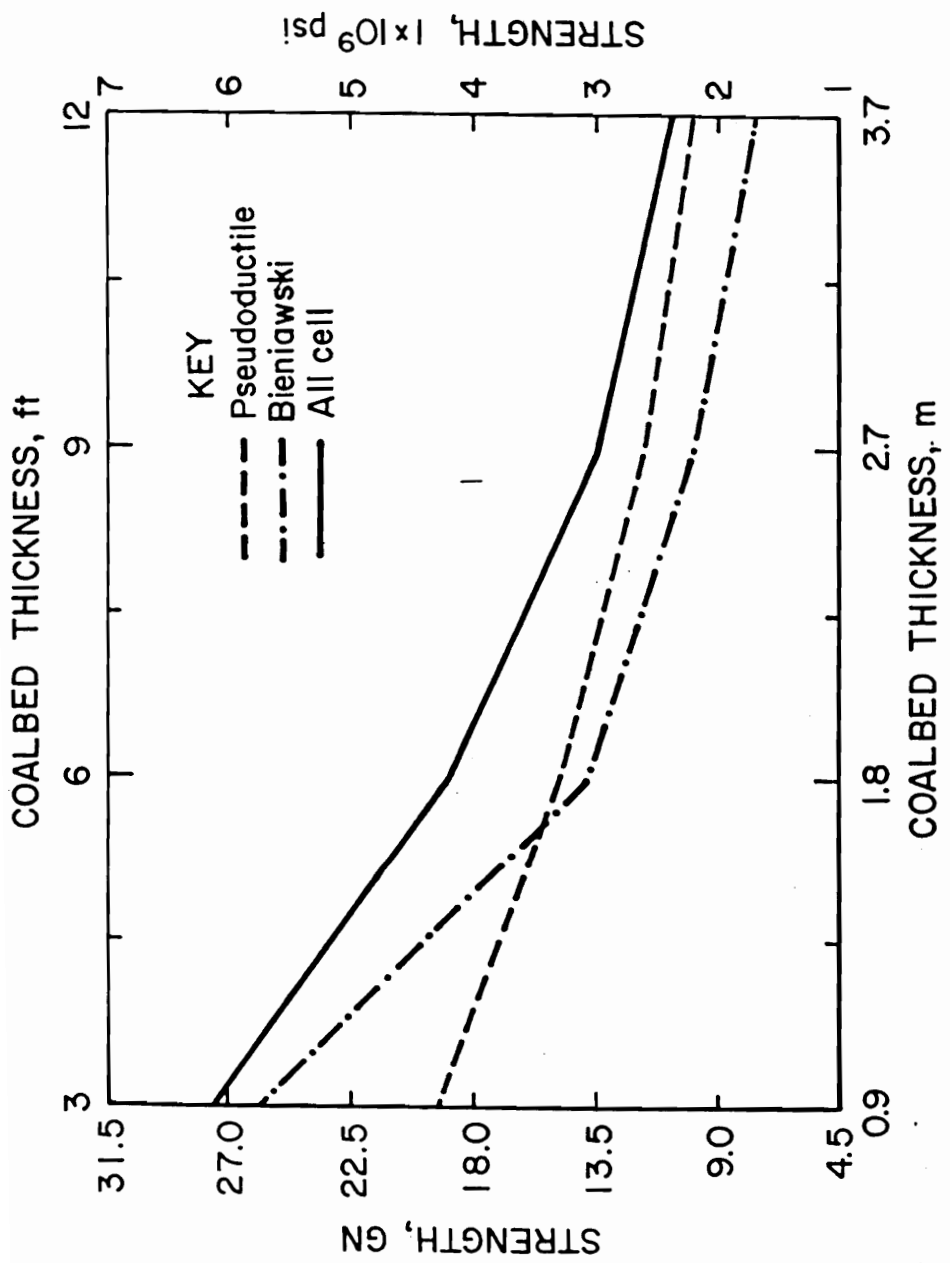

Figure 3.9—Comparison of simplified pseudoductile, Bieniawski, and all-cell pillar strength predictions for a 70 ft square pillar.

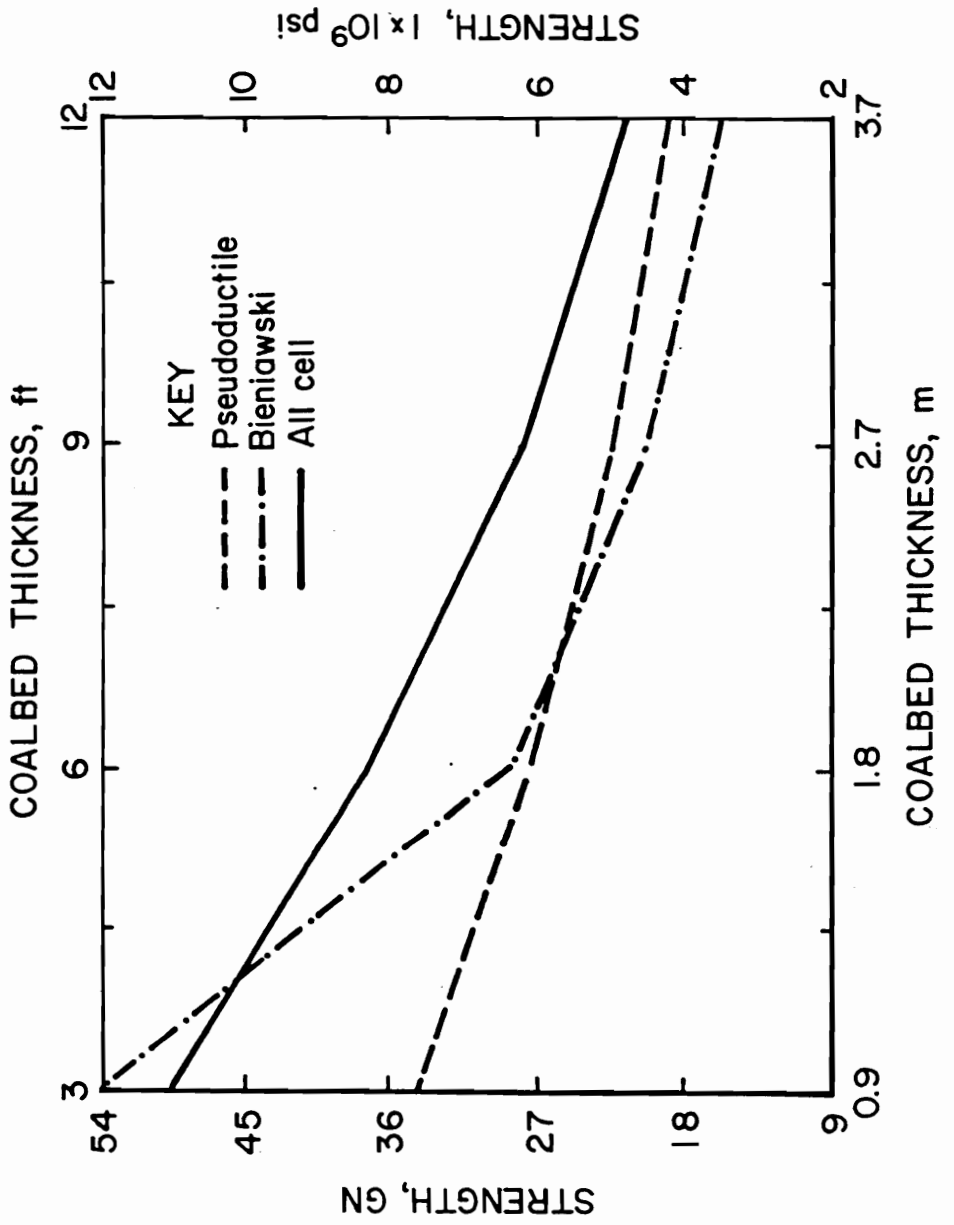

Figure 3.10—Comparison of simplified pseudoductile, Bieniawski, and all-cell pillar strength predictions for a 90 ft square pillar.

3.6 Mining Method Limits Total Extraction Pillar Size

Room-and-pillar retreat mining requires that the pillars intended for total extraction support the combination of development and gob side abutment loads. Total extraction pillar design must also facilitate safe and efficient final mining. The case studies contained in appendix A demonstrate that continuous miner pillar extraction plans for bump-prone coalbeds cannot allow multiple working faces within a pillar as this would place ventilation and roof support personnel in bump hazard areas. The split-and-fender method does not require multiple working places and for that reason has been widely employed in bump prone conditions. The WP-No. 21 Mine employed the method to extract 60 ft square pillars in the 4 ft high Chilton Coalbed (fig. A.4). The Olga mining method employed the split-and-fender method to extract 55 by 70 ft pillars in the 6 ft high Pocahontas No. 4 Coalbed (fig. A.16). Both these designs employ standard 20 ft deep continuous miner cuts.

The ability of the pillar to support the combination of development and abutment loading increases with increases in lateral pillar dimensions. Therefore, pillars should be as large as possible, while allowing for efficient and bump free extraction. However, even nominal pillar size increases can dramatically complicate pillar extraction with the split-and-fender method. Figures 3.11 and 3.12 illustrate possible, 20 ft deep standard cut, pillar extraction plans for 70 by 70 ft and 90 by 90 ft pillars, respectively. Note, the 70 by 70 ft and the 90 by 90 ft pillars require

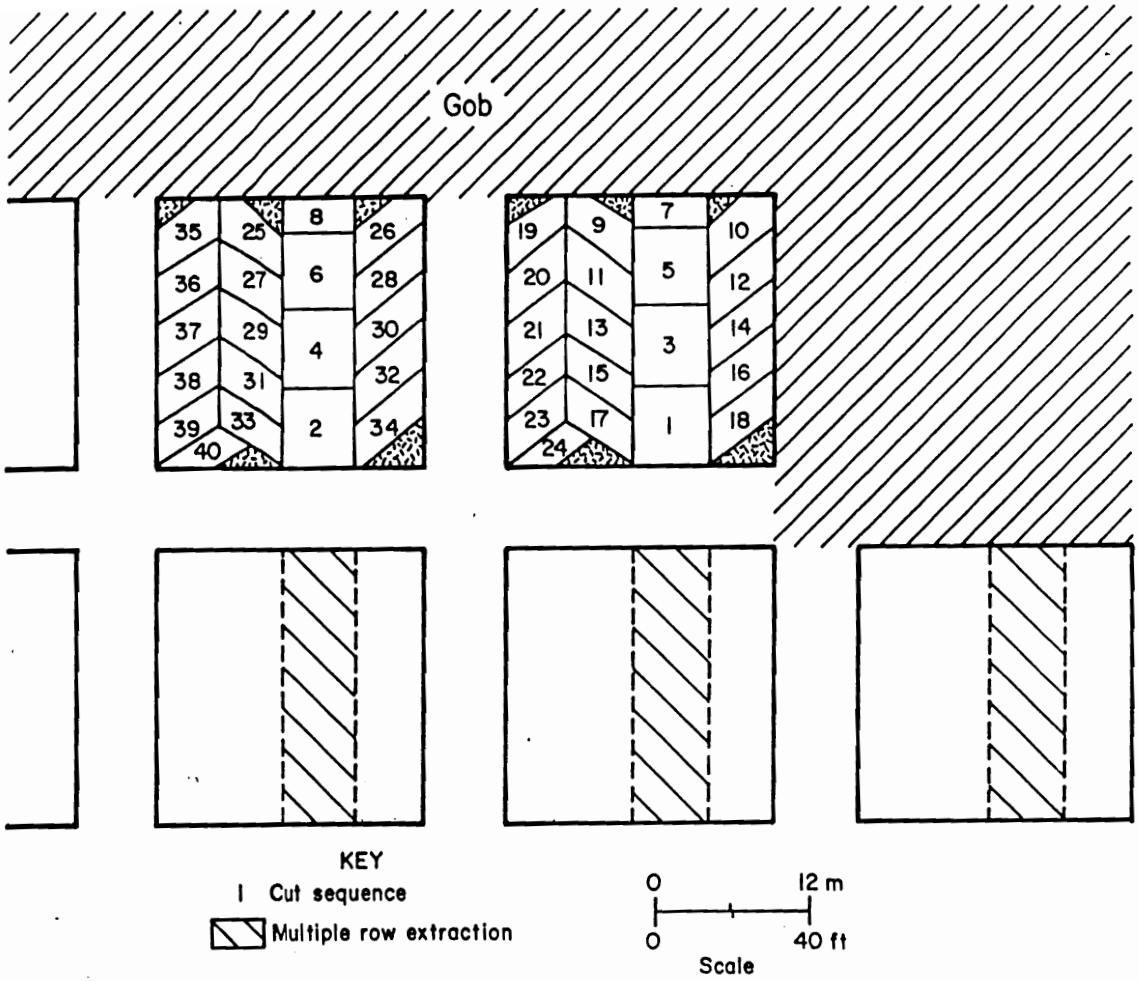

Figure 3.11—Split-and-fender pillar extraction plan for 70 by 70 ft pillar, employing standard deep 20 ft continuous miner cut.

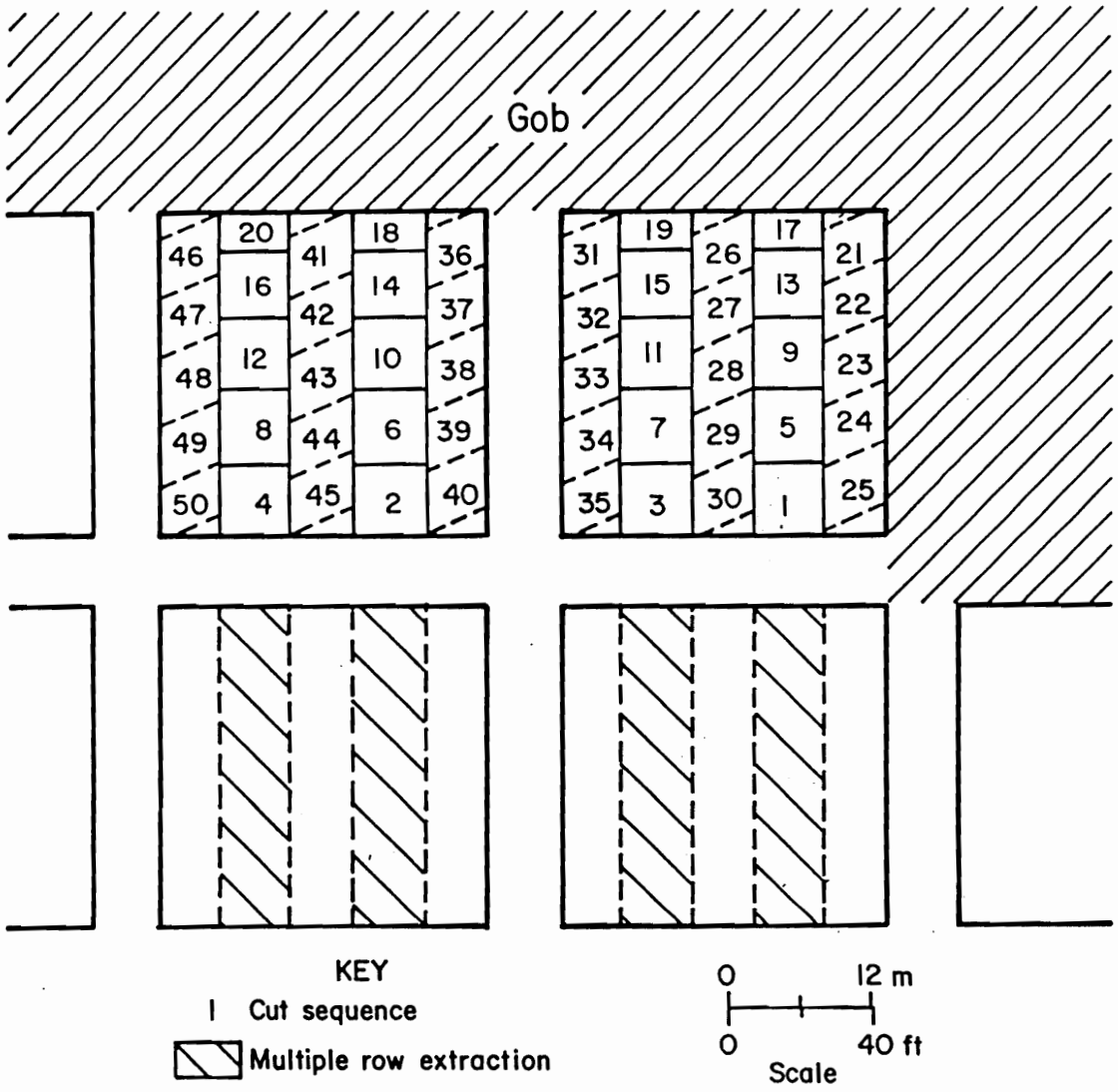

Figure 3.12—Split-and-fender pillar extraction plan for 90 by 90 ft pillar, employing standard deep 20 ft continuous miner cut.

40 and 50 individual miner cuts, respectively. With each additional cut the continuous miner place change time increases. This is especially true if multiple pillar rows are mined simultaneously to distribute abutment loads over multiple pillar rows. Section A.2.2 discusses such a methodology as implemented in the Olga Mine.

Continuous miner pillar extraction design is controlled by ventilation, haulage, and roof control factors. Roof control regulations require that the continuous miner operator never be physically under unbolted or "unsupported" roof (U.S. Code of Regulations, 1989). Previous continuous miner technology translated this limitation into a maximum miner cut of 20 ft. The development of remote control continuous miner technology has allowed for the implementation of pillar extraction plans calling for up to 50 ft deep continuous miner cuts (fig. 3.13). Production increases are realized through reduced continuous miner place change time, because the active cutting time is longer in each cut. Bauer, et al., (1993) estimates changing from a 20 ft standard cut to extended cuts of 30 to 60 ft increases production 4 and 10 pct, respectively. The number of extended cut approvals has dramatically increased since 1985 to a total of 317 in 1991. The standard extended cut depth is considered to be 40 ft with a current maximum depth of 50 ft.

Extended cut implementation could allow the safe and efficient extraction of larger pillars with greater resistance to the combination of development and abutment loading. An Xmas tree extended cut pillar extraction plan, Mine Safety and Health Administration approved and currently in use at the Marrowbone Development

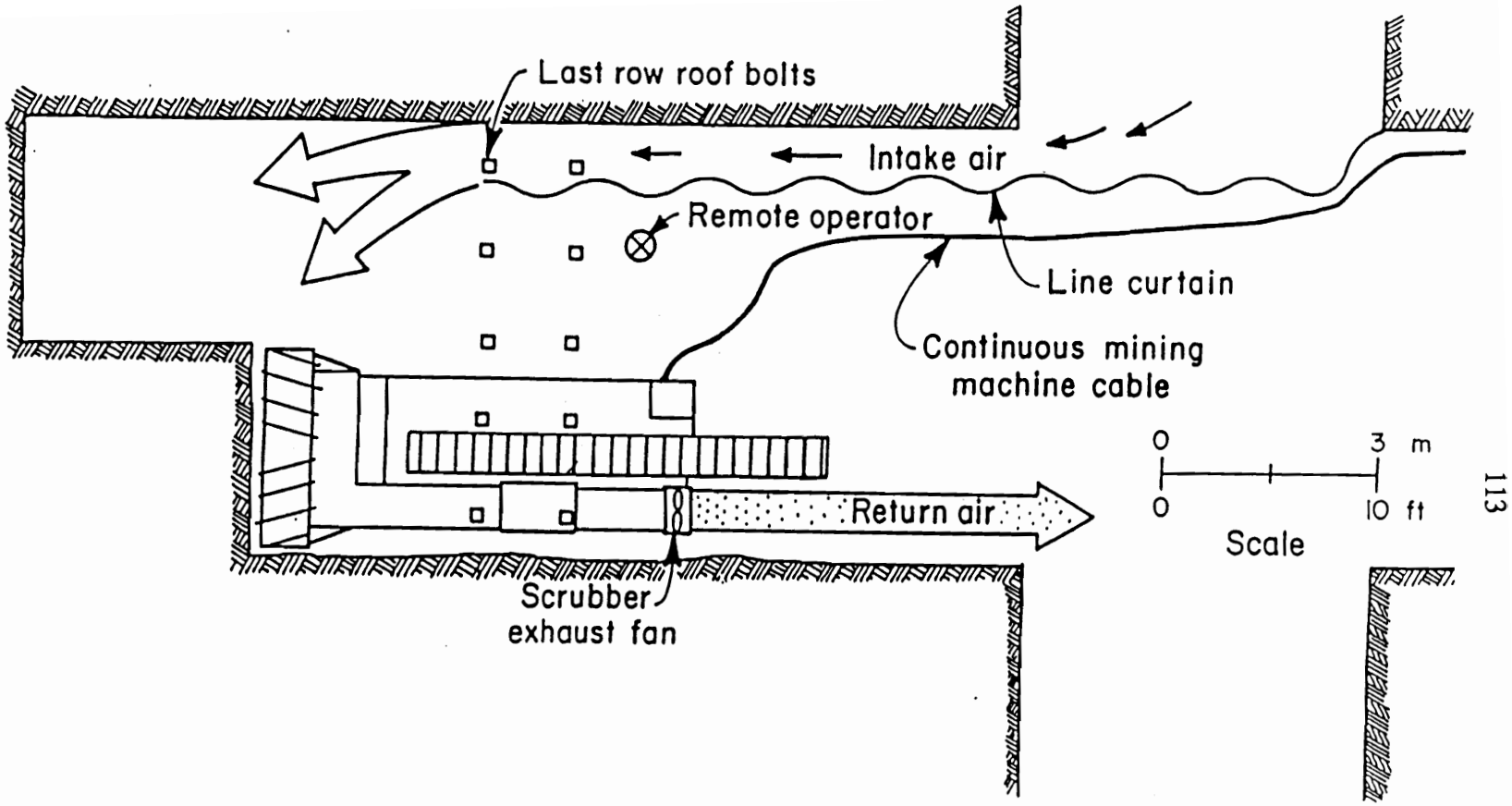

Figure 3.13—Typical extended cut circumstance (After Bauer, et al., 1993).

Company, Naugatuck, West Virginia, employs four mobile roof supports to extract 60 by 80 ft pillars (Chase, 1993). Execution of this pillar extraction plan, employing 40 ft continuous miner cuts, offers a near optimum compromise between load resistance and ease of extraction (fig. 3.14).

3.7 Mining Rate and Time Dependent Effects

The gob side abutment stress distribution over a retreat section may vary with mining rate. The rule of thumb is to maintain a consistent mining rate with minimum section down time for vacation and equipment repair. If a section is allowed to sit idle for weeks or even weekends, the first pillar row outbye the gob is likely to accumulate excessive levels of stress and/or yield. While these considerations are important, they are not considered due to the considerable complications they would bring to this analysis.

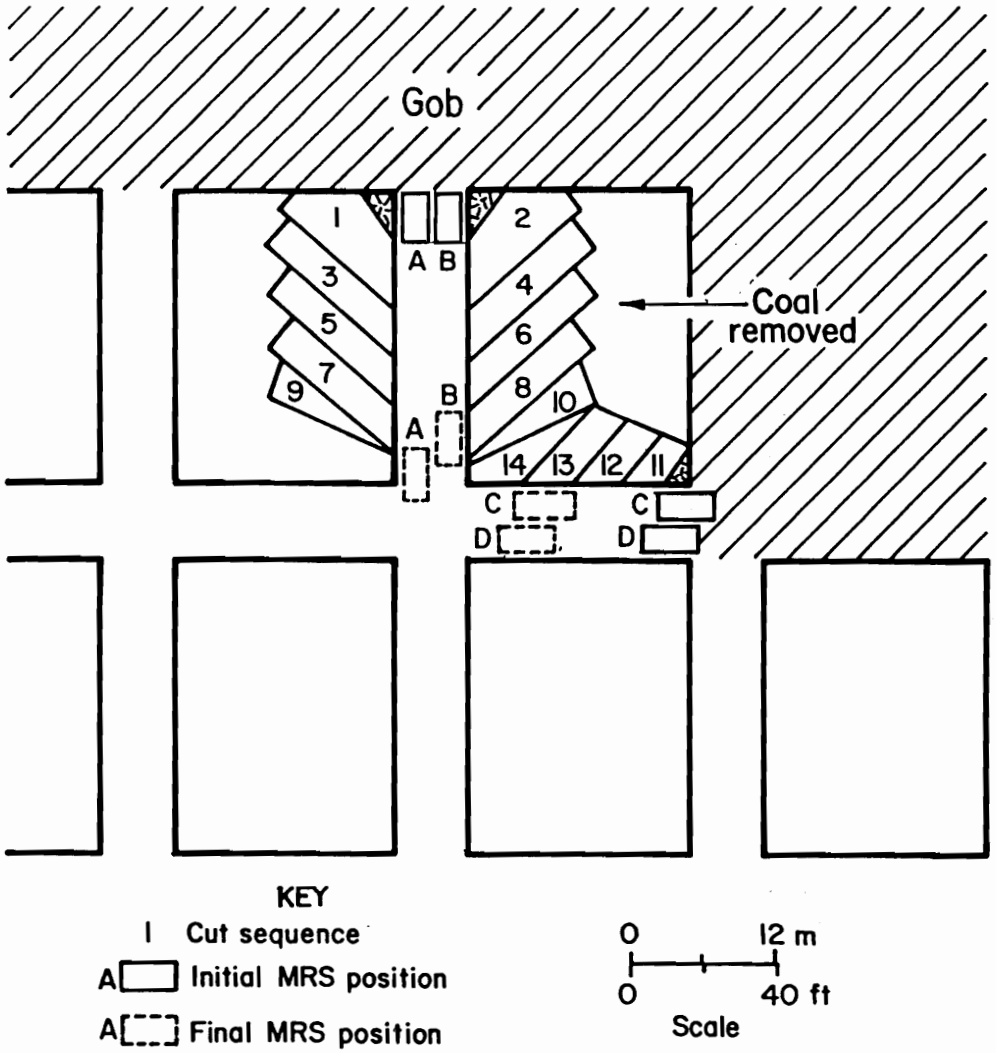

Figure 3.14—Xmas tree pillar extraction plan for 60 by 80 ft pillar, employing 40 ft continuous miner cuts and four mobile roof supports.

Chapter IV

NUMERICAL MODELING

The total extraction pillar designs and the pseudoductile coal strength model are employed in the development of supercritical width and subcritical width section design criteria. A consistent stress limit design criteria is employed for both design procedures. The criteria guides the selection of an appropriate section design for a given overburden thickness. Both design procedures result in total extraction areas, composed of rectangular pillars, separated by continuous abutment pillars. The primary difference between the two design procedures is the width of the total extraction areas. The supercritical design procedure allows for variation in the total pillar size, up to a maximum dimension of 90 ft, within an unlimited total extraction area width. In contrast the subcritical design procedure limits the total extraction pillars to either 60 by 80 ft or 70 ft square designs, within a specified total extraction area width. The supercritical design procedure combines tributary area theory with a linear shear angle concept to estimate the loads applied to total extraction pillars adjacent to gob areas. The subcritical design procedure utilizes the boundary element code MULSIM/NL in the development and implementation of a systematic subcritical design procedure to apply the stress shield concept to retreat room-and-pillar coal mining, under bump hazard. A spreadsheet program summarizes and provides for efficient utilization of the bump control design strategy.

4.1 Stress Limit Design Criteria

The criteria for selecting the appropriate section design for a given overburden thickness was two fold: 1) total extraction pillars at maximum strength must be confined to the first pillar row outbye the expanding gob; and 2) barrier pillar separating the previous gob and the active gob must not yield, until the total extraction panels on both sides of the abutment pillar have been mined.

The first row of total extraction pillars are designed not to yield under the combination of development and abutment loads. The total extraction pillar criteria eliminates the simultaneous mining of multiple rows and the associated inefficient production rates associated with the Olga Mine Method (Campoli, et. al, 1990b).

The abutment pillar criteria insures that the abutment pillar does not yield until it is encompassed by gob on both sides. The abutment pillar is analogous to the tailgate entry in longwall mining. These stress limits were based on in-mine geotechnical evaluations of two successful bump control mine designs; the Olga Mine room-and-pillar (Campoli, et al., 1990b) and the VP No. 3 longwall mine (Campoli, et al., 1990a) designs.

4.2 Supercritical Sections

The supercritical section consists of a very large block of uniformly sized pillars extracted against a very large gob area. The simplified pseudoductile pillar strength assumptions are one half of a supercritical section width model of bump-

prone pillar behavior. Approximations of development and gob side abutment loading are the other half of this model. Development loads are the result of the weight of the overburden directly over the pillar. Tributary area theory predicts these loads by the following equation (1):

$$L_d = (w + \frac{e}{2})\ (l + \frac{e}{2})\ (H)\ (\gamma) \qquad (4.1)$$

where: w = pillar width

l = pillar length

H = depth of overburden

γ = density of rock

e = entry width

Note that the pillar dimensions parallel and perpendicular to the gob line are referred to as the pillar width and length, respectively.

Wilson (1973), King and Whittaker (1971), Mark (1990), and Chase and Mark (1992) have all employed linear shear angle concepts to predict gob side abutment loads. A section becomes supercritical when its gob width exceeds twice the overburden times the tangent of the shear angle (fig. 4.1). It is assumed that increasing gob width beyond supercritical does not increase the side abutment load. Subcritical section gobs are less than twice the overburden times the tangent of the

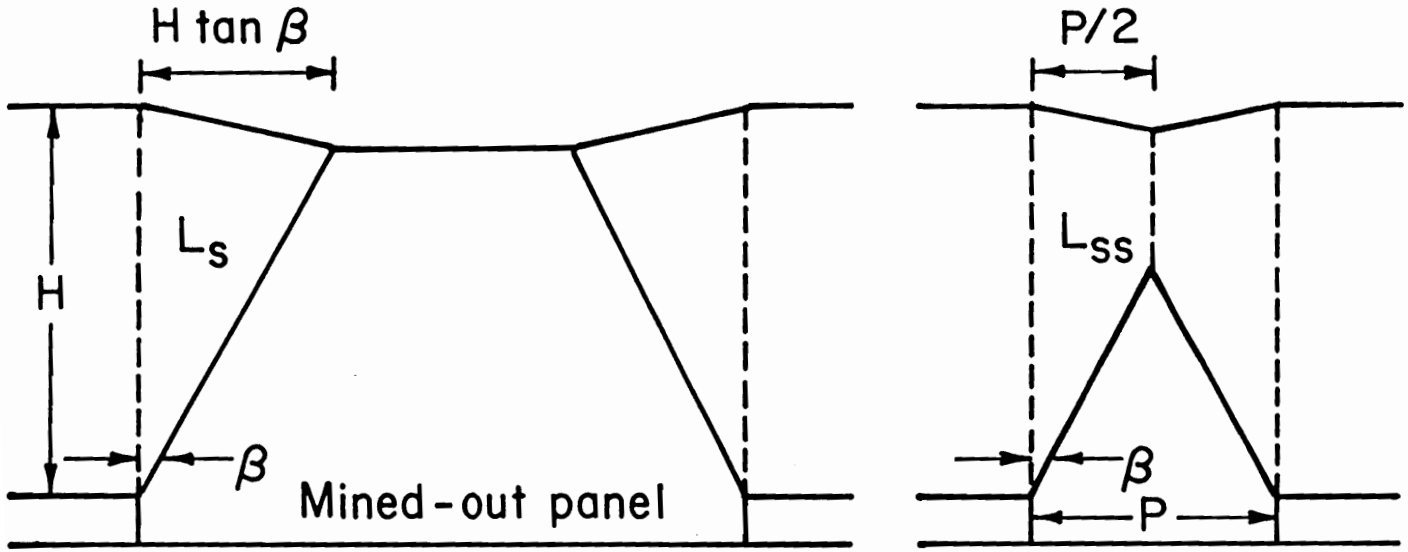

Figure 4.1—Conceptualization of supercritical (L_s) and subcritical (L_{ss}) side abutment load (After Mark, 1990).

shear angle wide. Mark (1990) quantified the supercritical (L_s) and subcritical (L_{ss}) side abutment load with equations 4.2 and 4.3, respectively. The angle beta has been fixed at 21 degrees based on the extensive field studies at over 50 longwalls and over 50 room-and-pillar operations by Mark (1990) and Chase and Mark (1992), respectively.

$$L_s = (H^2)\ (\tan\ \beta)\ (\gamma/2) \tag{4.2}$$

$$L_{ss} = \left[\frac{HP}{2} - \frac{P^2}{8\ \tan\ (\beta)}\right] \gamma \tag{4.3}$$

where:
P = panel width
H = depth of overburden
γ = density of rock
β = shear angle

The distribution of the abutment load on the pillars adjacent to the gob edge has been approximated by Mark (1990). He employed an approximation of the width of abutment influence zone (D) determined by Peng and Chiang (1984) from field measurements. They determined that the D is a function of overburden depth. Mark combined this with an inverse square stress decay function, to form the relationship described in figure 4.2. Integration of the abutment stress distribution function and evaluation over the limits from zero to the pillar length (l), provides an approximation of the portion of the abutment load (L_a) carried by the pillars occupying the first row outbye the gob (L_f).

σ_a Abutment stress distribution function
x Distance from the edge of gob
D Extent of the side abutment influence zone
L_s Total side abutment load
L_f Abutment load on gob side pillar
H Depth of cover
ℓ Pillar length

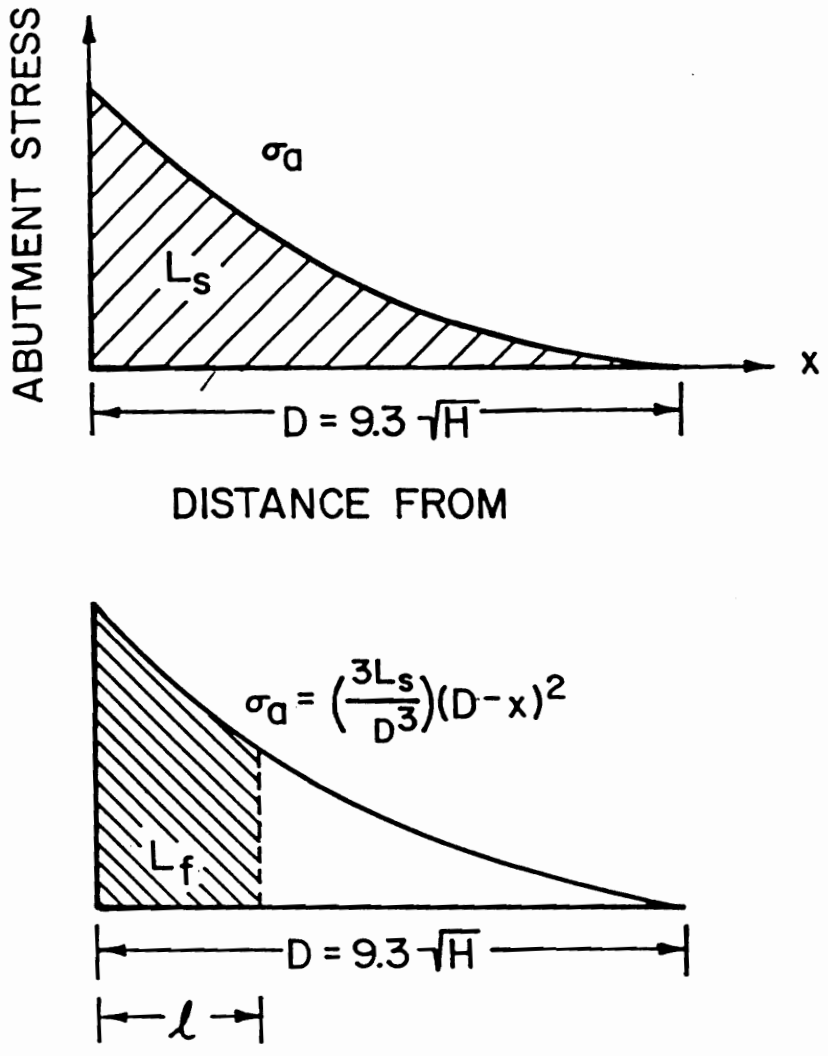

Figure 4.2—Distribution of the side abutment load.

Given the total extraction pillar dimensions, overburden thickness, and coalbed thickness, a stability factor can be calculated for the supercritical width section. The stability factor is the pillar strength as predicted by the simplified pseudoductile model divided by the sum of the development (L_d) and the gob side abutment pillar load (L_f). Thus, the stability factor is unity when the pillar row directly outbye the gob is at maximum load bearing capacity. Figures 4.3 - 4.6 display the variation in stability factor for 55 by 70 ft, 60 by 80 ft, 70 ft square and 90 ft square pillars, respectively. The stability factor is inversely proportional to both coalbed thickness and overburden thickness. These four pillars are representative of the range of pillar sizes that provide considerable load resistance, while allowing high stress extraction under bump-prone conditions.

Setting the stability factor to unity permits direct comparison of the predicted performance of the four pillar sizes (tab. 4.1). The most difficult to extract 90 ft square pillars is predicted to support supercritical designs section up to 1,267 ft of overburden for a 6 ft thick coalbed, while the least difficult to extract, 55 by 70 ft pillar is predicted to support supercritical designs to 960 ft of overburden for a 6 ft thick coalbed. The 60 by 80 ft and 70 ft square pillars are predicted to be near identical in performance (tab. 4.1). The former is recommended when the pillars are to be extracted with mobil roof support and extended cut mining (fig. 4.6).

Due to haulage constraints, economic continuous miner sections cannot be of unlimited width. The supercritical width design procedure assumes that the section is

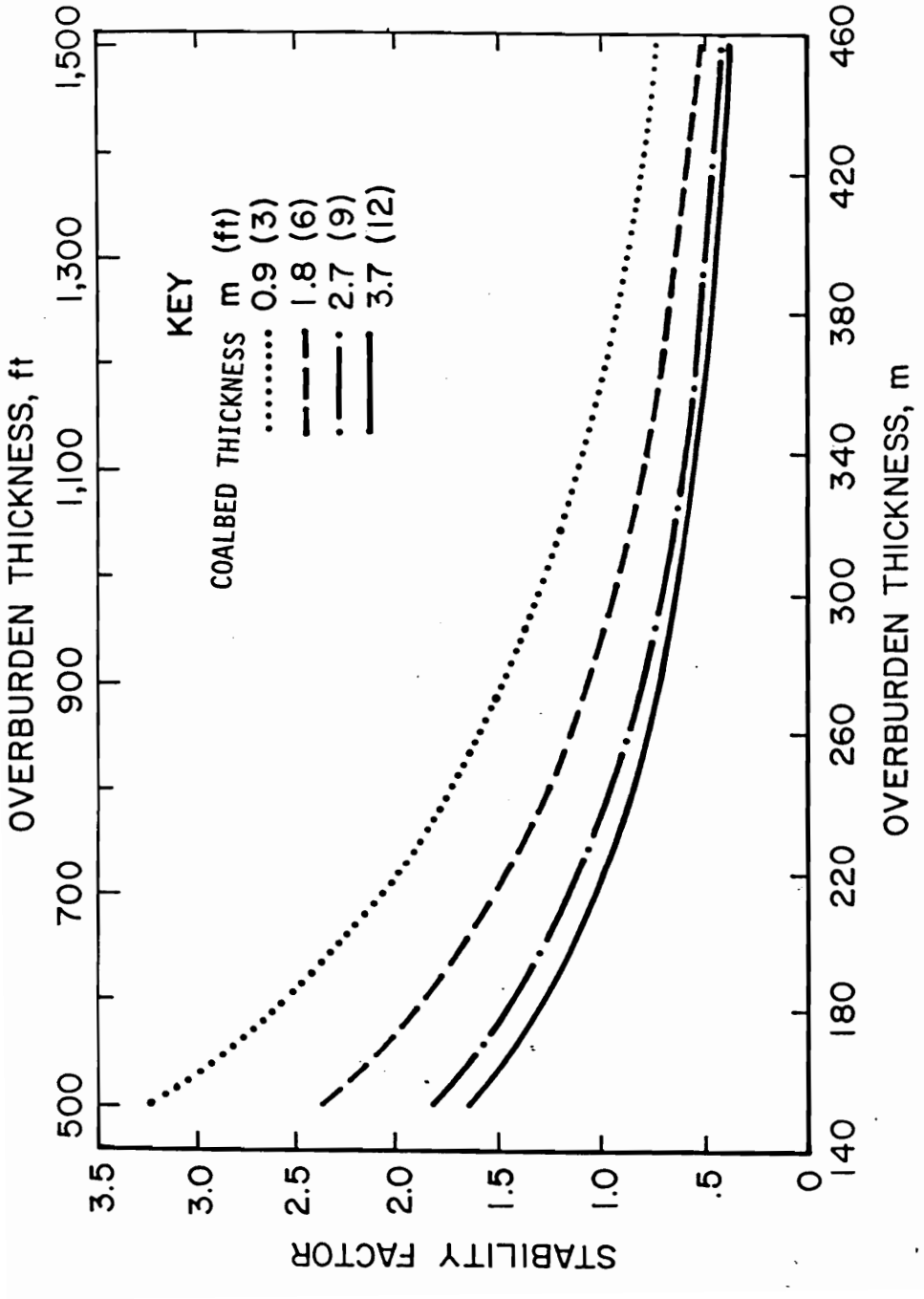

Figure 4.3—Stability factor for 55 by 70 ft pillar at selected coalbed thicknesses.

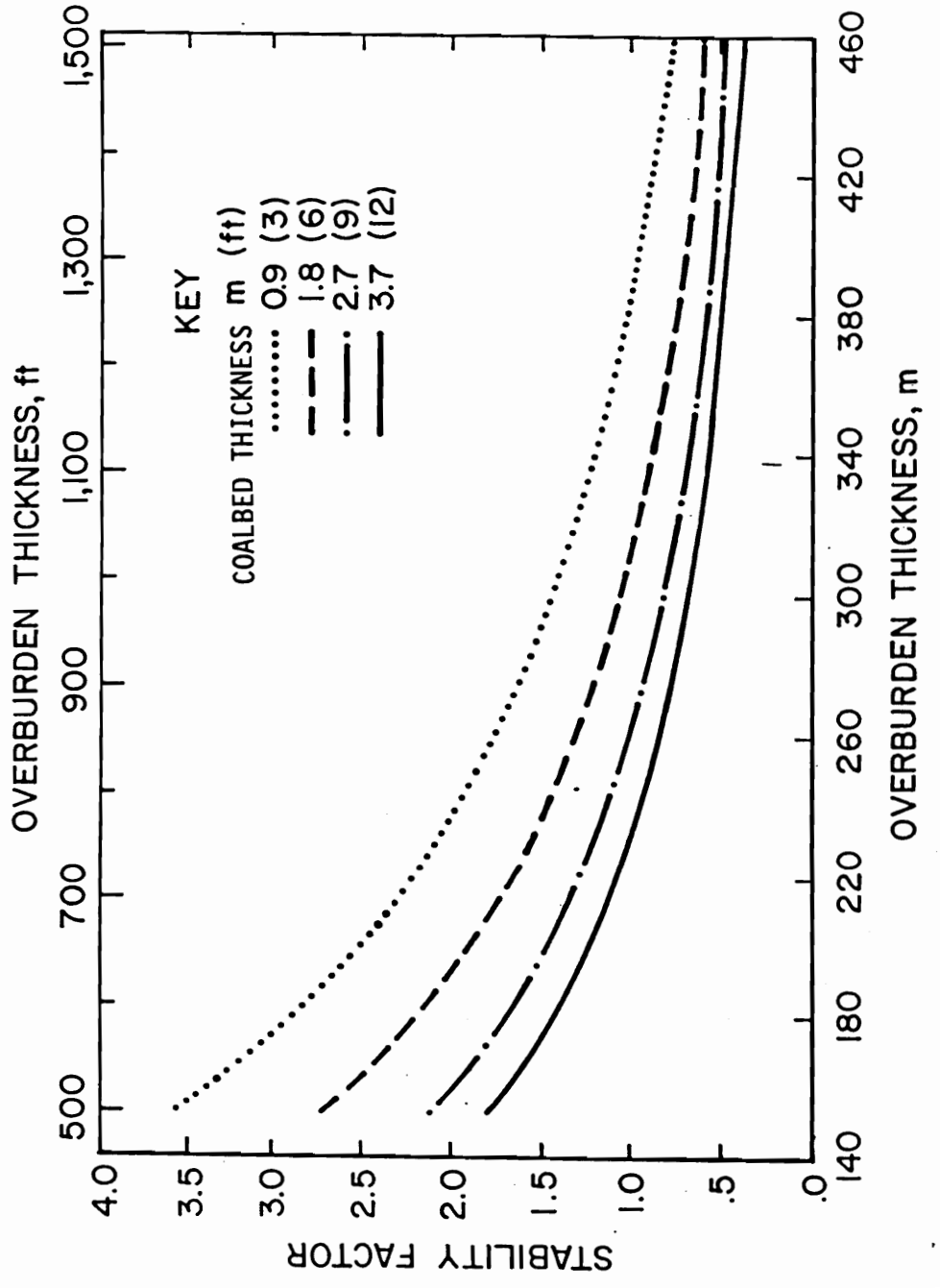

Figure 4.4—Stability factor for 60 by 80 ft pillar at selected coalbed thicknesses.

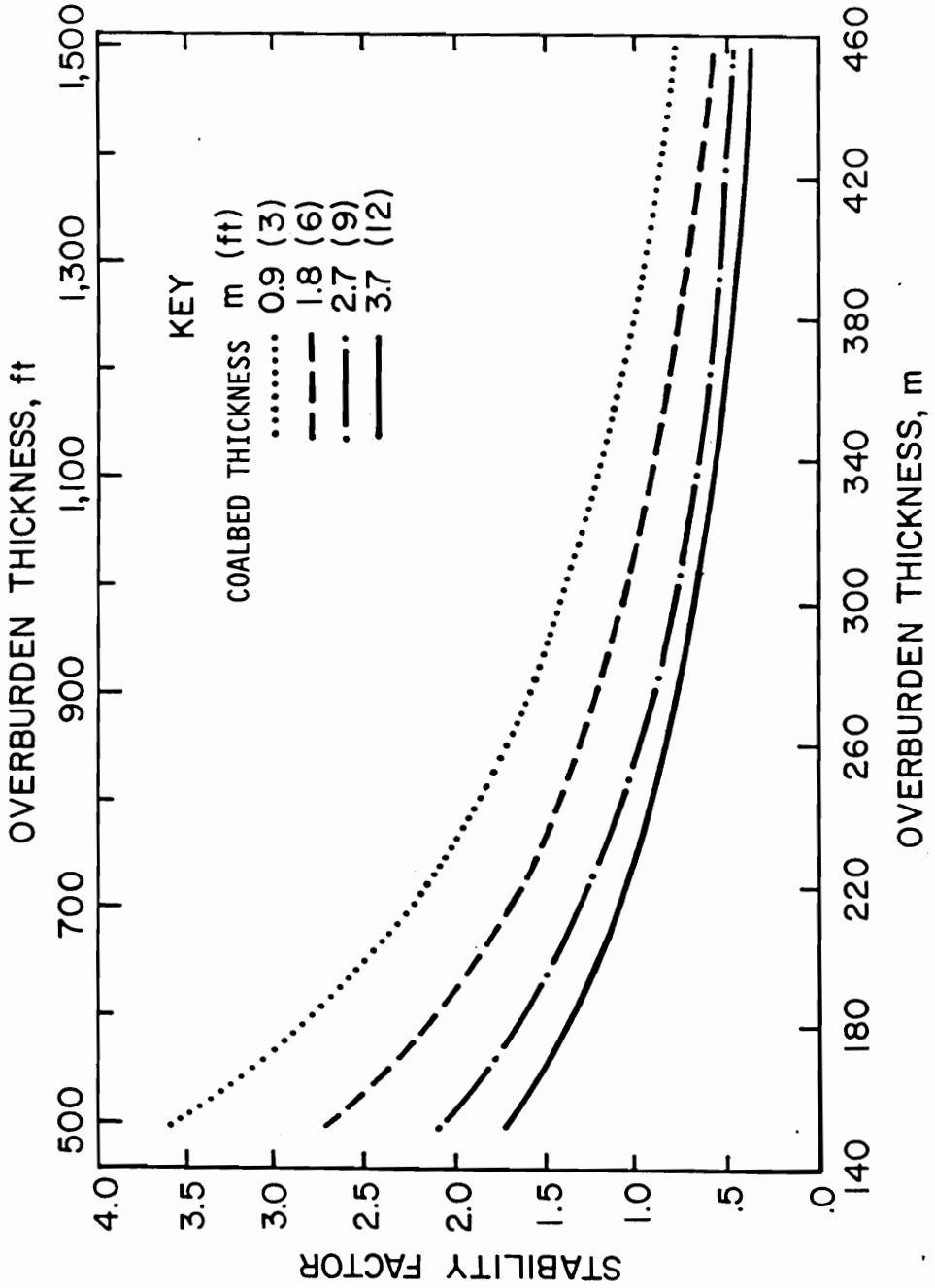

Figure 4.5—Stability factor for 70 ft square pillar at selected coalbed thicknesses.

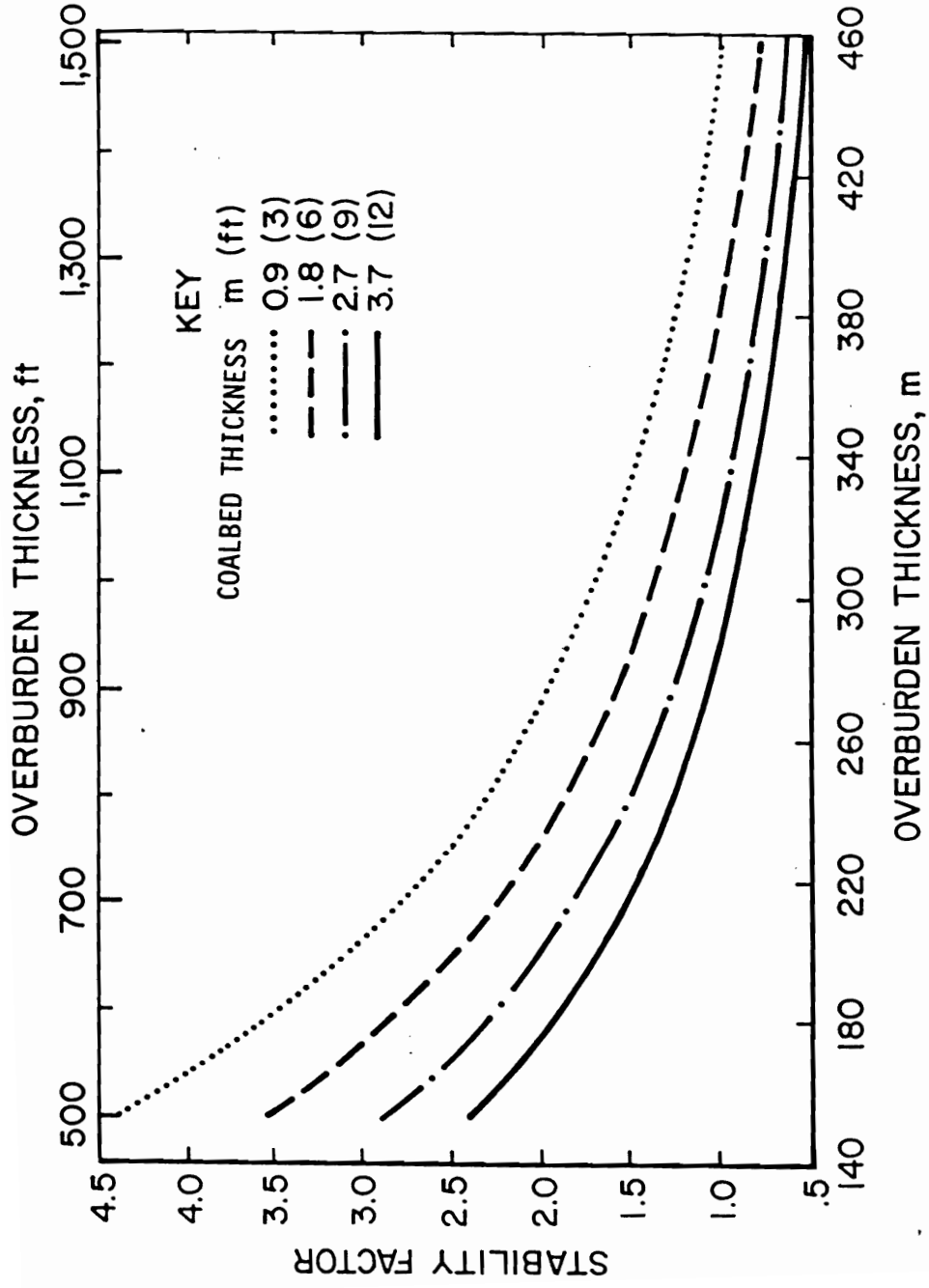

Figure 4.6—Stability factor for 90 ft square pillar at selected coalbed thicknesses.

Table 4.1—Overburden thickness which results in a stability factor of 1.0, for a given pillar size and coalbed thickness

Coalbed Thickness, ft	3	6	9	12
Pillar Size, ft	Overburden thickness, ft			
55 x 70	1,200	960	795	718
60 x 80	1,291	1,054	876	774
70 x 70	1,291	1,062	888	789
90 x 90	1,480	1,267	1,093	960

not subjected to side abutment loads from previously extracted panels. This abutment load interaction can be prevented by separating the total extraction areas with abutment pillars. The Ashley or the Pennsylvania Mine Inspector's formula (Ashley, 1930) has been employed to design barrier pillars for this purpose for many years:

$$W=20+4T+0.1H \qquad (4.4)$$

where W = abutment pillar width

H = depth of overburden

T = coalbed thickness

Figure 4.7 graphically represents the effect of coalbed and overburden variation on the suggested abutment pillar thickness. Recall, that the abutment pillar is required to remain stable only until it is encompassed by gob on both sides. Thus, the abutment pillar are not sterilized, as they may be weakened by mining as total extraction mining progresses. The thin pillar mining method has been employed to extract barrier pillars located between total extraction areas. Figure 4.8 displays this method as conducted by the Gary No. 2 Mine in the Pocahontas No. 4 Coalbed.

4.3 Stress Shielded Subcritical Sections

Mining at overburden thickness greater than those listed in table 4.1 result in a stability factor less than 1.0 for a given total extraction pillar size. Such a stability

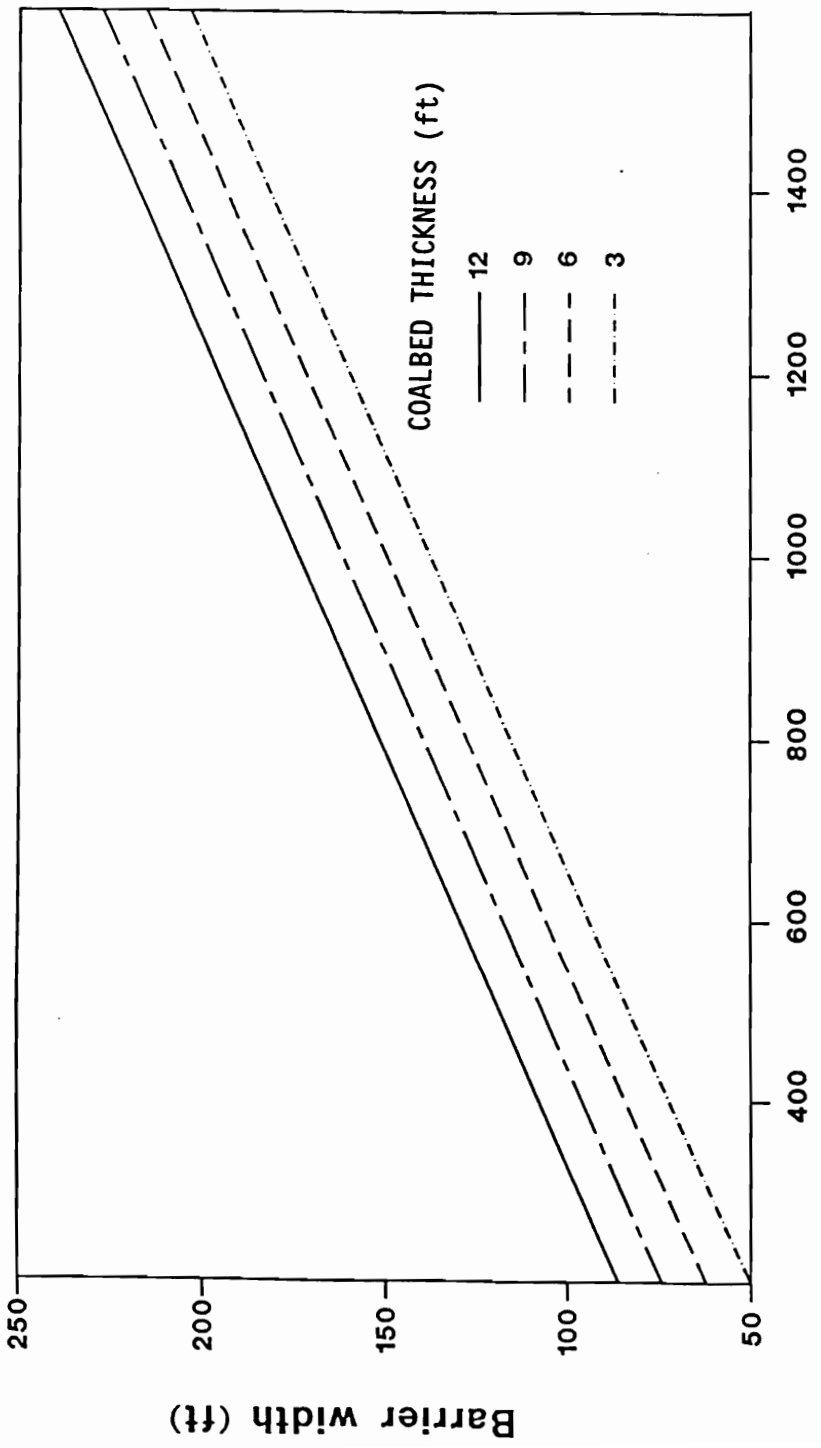

Figure 4.7—Suggested abutment pillar widths for selected coalbed thicknesses.

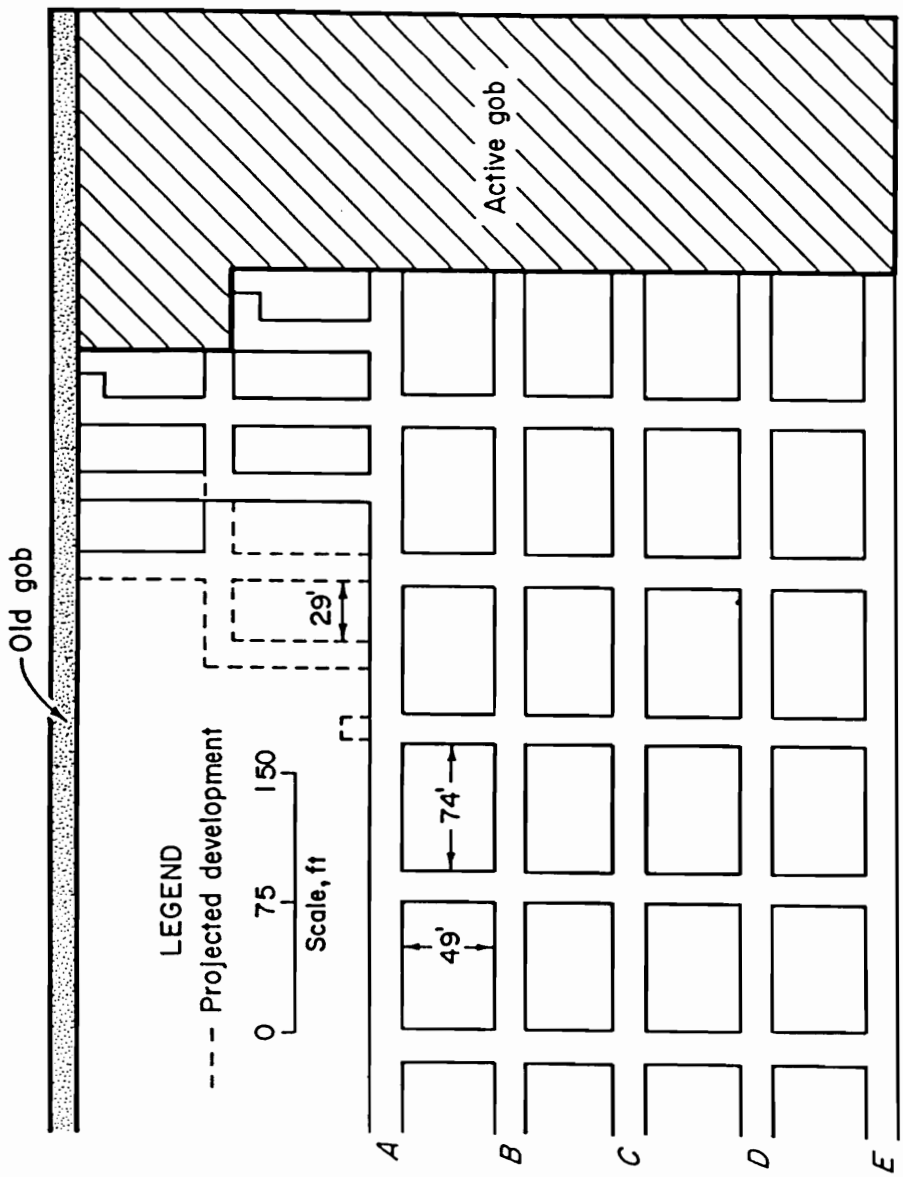

Figure 4.8—Thin pillar abutment pillar extraction method (After Campoli, et al., 1987).

factor indicates that the supercritical design procedure predicts the strength of the gob side pillar row to be insufficient to carry the combined development and abutment load. Successful designs for bump-prone mines too deep to permit supercritical section widths must either shield workings from excessive stress or reduce coalbed bearing capacity directly prior to extraction.

As the goal of this research is to facilitate safe and efficient room-and-pillar retreat mining of bump-prone coalbeds without resorting to costly and hazardous destressing methodologies, a stress shield concept was employed to limit the coalbed stress adjacent to expanding gob areas through variation of the section layout. More specifically, it utilizes the design of subcritical width sections surrounded by permanent barrier pillars. The stress shield concept was advanced with in-mine geotechnical evaluations of two successful mine designs. The Olga Mine room-and-pillar (Chapter 3.2) and the VP No. 3 longwall mine (Chapter 3.3) designs were both implemented under demonstrated bump hazard.

The design criteria for subcritical width sections is more complex than the supercritical width section design criteria. The simple linear geometry of supercritical sections required approximation of in situ tributary load, infinitely wide gob edge behavior, and uniformly sized total extraction pillar strength. The subcritical design criteria requires the prediction of abutment load distributions for rectangular gobs and the apportionment of these loads over mixed pillar sizes. A parametric study of the complicated interaction of various combinations of overburden depths, total extraction

panel widths, and abutment pillar widths was conducted with the boundary element program MULSIM/NL.

4.3.1 MULSIM/NL

MULSIM/NL is a boundary element method program for calculating stresses and displacements in such tabular deposits as coalbeds. MULSIM/NL was developed to assist in alleviating safety hazards associated with bumps in U.S. coal mines (Zipf 1992a and 1992b). The program provides a means for calculating stress, displacement, and energy changes for various mining configurations in bump-prone conditions. The outputs permit the evaluation of various mine designs that could decrease the occurrence of coal mine bumps.

The program neglects the effect of the earth's surface and assumes that the seams are planes at great depth. It can accommodate up to four parallel seams having any orientation with respect to the earth's surface. A continuous, homogeneous, linear elastic rock mass surrounds the seams. MULSIM/NL incorporates six nonlinear inseam material properties via the boundary conditions. Unmined inseam coal material may be represented as linear elastic, strain-softening, or elastic plastic. The gob or backfill material, left in the wake of mining, may be represented as bilinear hardening, strain-hardening, or linear elastic.

The accuracy of calibration determines the accuracy and usefulness of the model predictions. This is especially true in geologic models because of the

uncertainty of the input material properties. Heasley and Pappas (1993) are concluding an extensive model calibration based on in-mine geotechnical evaluation of the strata response to longwall mining in the bump-prone VP No. 3 Mine (Campoli, et al., 1990a) (Campoli, et al., 1993). Longwall gate road pillar failure observed through hydraulic stress-meters was used to calibrate the input failure strength of coal material. The gate road entry convergence was employed to calibrate the elastic moduli of the coal and the surrounding media. The subcritical section parametric studies utilized material property values tested as part of this effort.

The parametric studies varied the overburden depth and section configuration in a 6 ft thick coalbed. The single step models assigned the surrounding media a modulus of elasticity of 1 million psi and a Poisson's ratio of 0.25. The horizontal stress was assumed to be one half of the induced vertical stress.

The coalbed was represented by a strain-softening coal material consistent with the simplified pseudoductile coal pillar strength model utilized in the supercritical design criteria. Peak stress, peak strain, residual stress, residual strain, and Poisson's ratio are the required input parameters for the strain-softening model. The stress-strain response of the four strain softening materials are diagramed in figure 4.9. The distance of the element from the mine entry determines which of the four stress-strain curves represents a particular element. The external coal material makes up the perimeter of the pillar. The peak and residual strength of each coal material increases with the distance from the entry. The core material, the maximum peak, and residual

strength, makes up the center of the pillar. Poisson's ratio was assumed to be 0.3 for all of the strain softening coal materials. These properties were employed with 50 ft square coarse mesh elements, each of which forms a 5 by 5 square of 10 ft square fine mesh elements. Based on these assumptions, a 70 ft square pillar contains only one core material element at its geometric center (fig. 4.10). The numeral "1" represents half of the entry width assumed to be 20 ft. Should the coarse mesh dimensions change, the strain softening material behavior must be altered to reflect the resultant change in fine mesh dimensions. However, the rate of coal strength increase with distance from the entry is consistent with figure 4.9.

Retreat mining allows the roof to cave as the panel is extracted. The volume of broken material is greater than that of the intact rock. This bulking effect, combined with the bending and sagging of the main roof, allows for mechanical loading of the gob floor. The measurement of gob loading during the consolidation cycle is difficult. Accurate characterization of this cycle is very important in the modeling of the complex ground behavior associated with subcritical section design.

A three-prong approach was employed in an effort to develop an accurate representation of the mechanical behavior of gob during the consolidation cycle. First, the properties of simulated gob material were determined in the laboratory and the best form of a stress-strain equation was determined (Pappas and Mark, 1993). Second, a field investigation was conducted to measure longwall gob consolidation in the bump-prone VP No. 3 Mine (Campoli, et al., 1993). Third, MULSIM/NL was

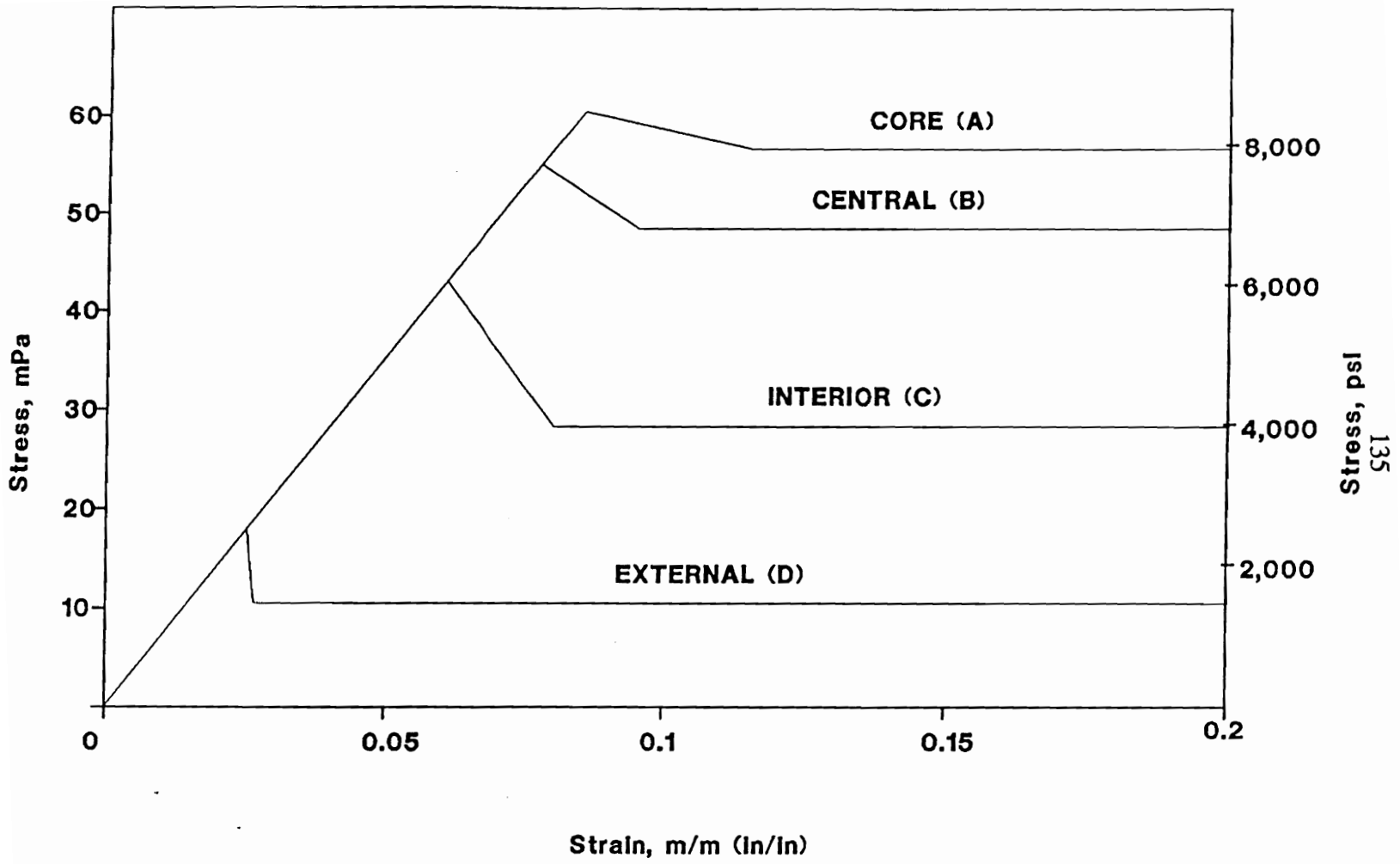

Figure 4.9—Stress-strain response of four coalbed strain softening materials.

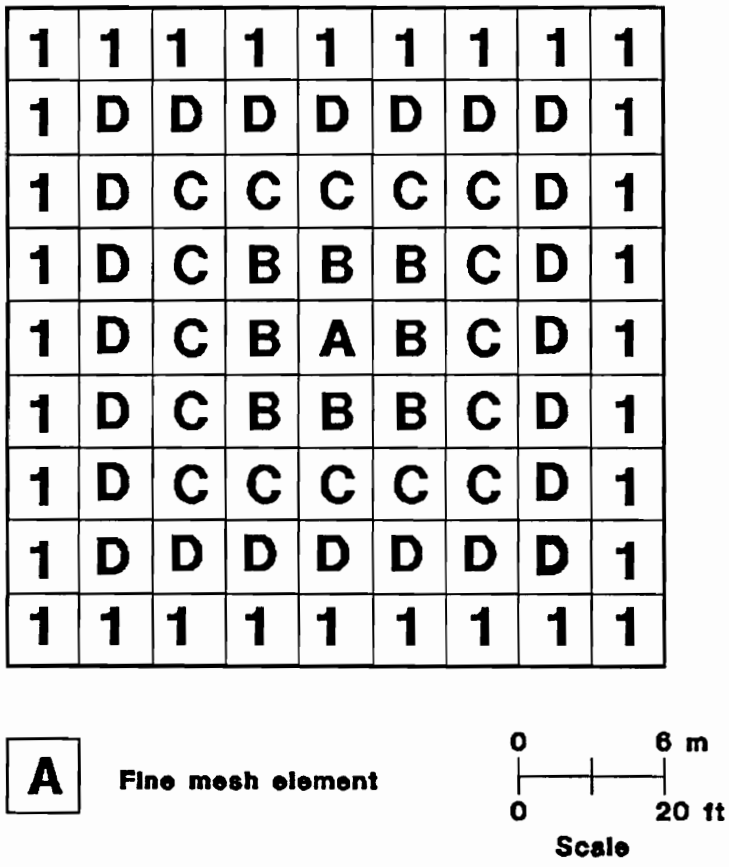

Figure 4.10—Assignment of strain softening material properties in a 70 ft square pillar.

revised to incorporate the laboratory determined stress-strain equation and the new gob material used in an exhaustive calibration of the model based on the in-mine geotechnical response (Heasley and Pappas, 1993).

Laboratory results showed that the stress-strain relationship of the simulated gob material was nonlinear; but the stress-secant modulus relationship was approximately linear. A solution proposed by Salamon (1990) best described the compressive behavior of backfill material with the following stress-strain equation.

$$\sigma = \frac{E_o \epsilon}{(1 - \epsilon/\epsilon_m)} \qquad (4.5)$$

where: σ = the applied stress, psi

E_o = the initial secant modulus, psi

ϵ = the strain, in/in

ϵ_m = the maximum strain, in/in

Solving equation 4.5 for the slope of the stress-strain curve (σ/ϵ) defines the secant modulus (E_s).

$$E_s = \frac{\sigma}{\epsilon} = \left(\frac{1}{\epsilon_m}\right) \sigma + E_o \qquad (4.6)$$

The form of equation 4.6 shows that the secant modulus of Salamon's solution is a linear function of the stress where the Y intercept is the initial secant modulus and the slope of the line is the reciprocal of the maximum strain. This linear relationship

between the secant modulus and the stress agrees with the laboratory gob tests (Pappas and Mark, 1993) and hence this equation was chosen as the most appropriate the data (Heasley and Pappas, 1993).

Implementation and testing of this new gob material in MULSIM/NL proved the material to be an improvement over linear elastic gob material (Heasley and Pappas, 1993) and capable of providing a reasonable fit to measured field data (Campoli, et al., 1990a) (Campoli, et al., 1993). The two major input parameters to Salamon's strain hardening gob model (equation 4.5) are the maximum strain and the initial elastic modulus. The parametric analysis of subcritical section design employed a 0.4 in/in maximum strain and 300 psi initial modulus. The resultant stress-strain curve is diagramed in figure 4.11. The maximum strain parameter determines directly the strain value at which the stress-strain curve goes asymptotic. The magnitude of gob stress is inversely proportional to the maximum strain. The initial modulus is directly proportional to magnitude of gob stress, with maximum effect on the gob edge stress (Heasley and Pappas, 1993).

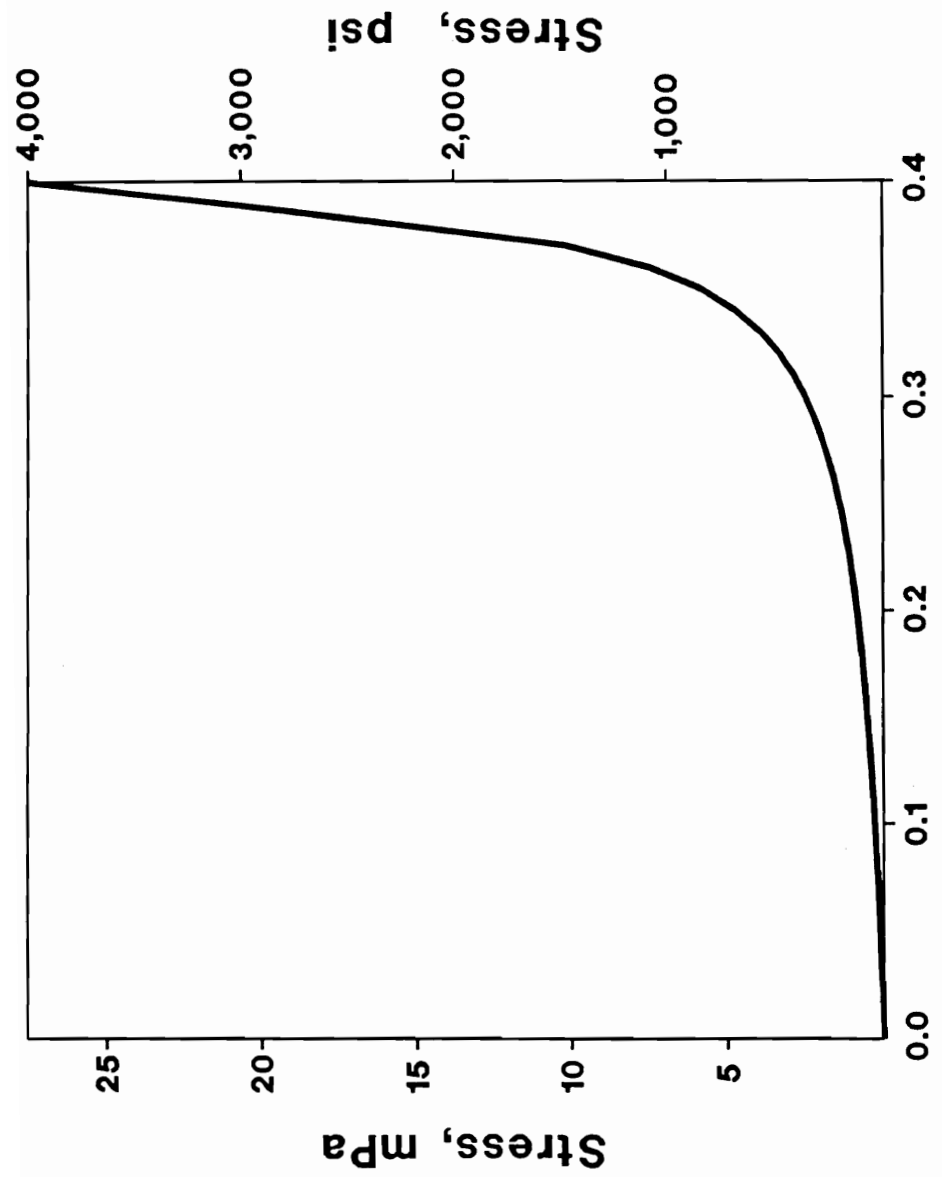

Figure 4.11—Salamon strain hardening gob model stress-strain assumptions.

4.3.2 Parametric Analysis

The strain softening coal strength, strain hardening gob, and host material properties described above were utilized in a MULSIM/NL selection of appropriate subcritical section layouts for seven specific overburden depths. Section designs appropriate for overburden depths from 1,000 to 2,200 ft at 200 ft increments are outlined in figures 4.12 through 4.18. These figures are plots of the 150 by 150 element fine mesh vertical stresses resulting from subjecting the section layout to the indicated depth of overburden. Each fine mesh element is 18 ft square. The fine mesh represents a 2,700 ft square portion of a 6 ft thick coalbed. While the scale of these plots does not facilitate detailed stress pattern analysis, they do provide an insight into the subcritical section parametric analysis. The darker the shading the greater the stress. The solid black areas represent coal at or near the maximum stress of 8,000 psi. The white areas represent entries and gob areas, whose stress is less than 800 psi.

The sections are combinations of 72 ft square pillars, 18 ft wide entries, and 72, 162, and 252 ft wide abutment pillars. These dimensions are mesh generation forced approximations of the 60 by 80 ft pillars and 20 ft entries recommended for ease of extraction under bump-prone conditions. The square pillars are composed of a 4 by 4 block of 18 ft square fine mesh elements whose stress-strain behavior was adjusted to duplicate the distance from the entry behavior diagramed in figure 4.9. The three discrete abutment pillar widths were also

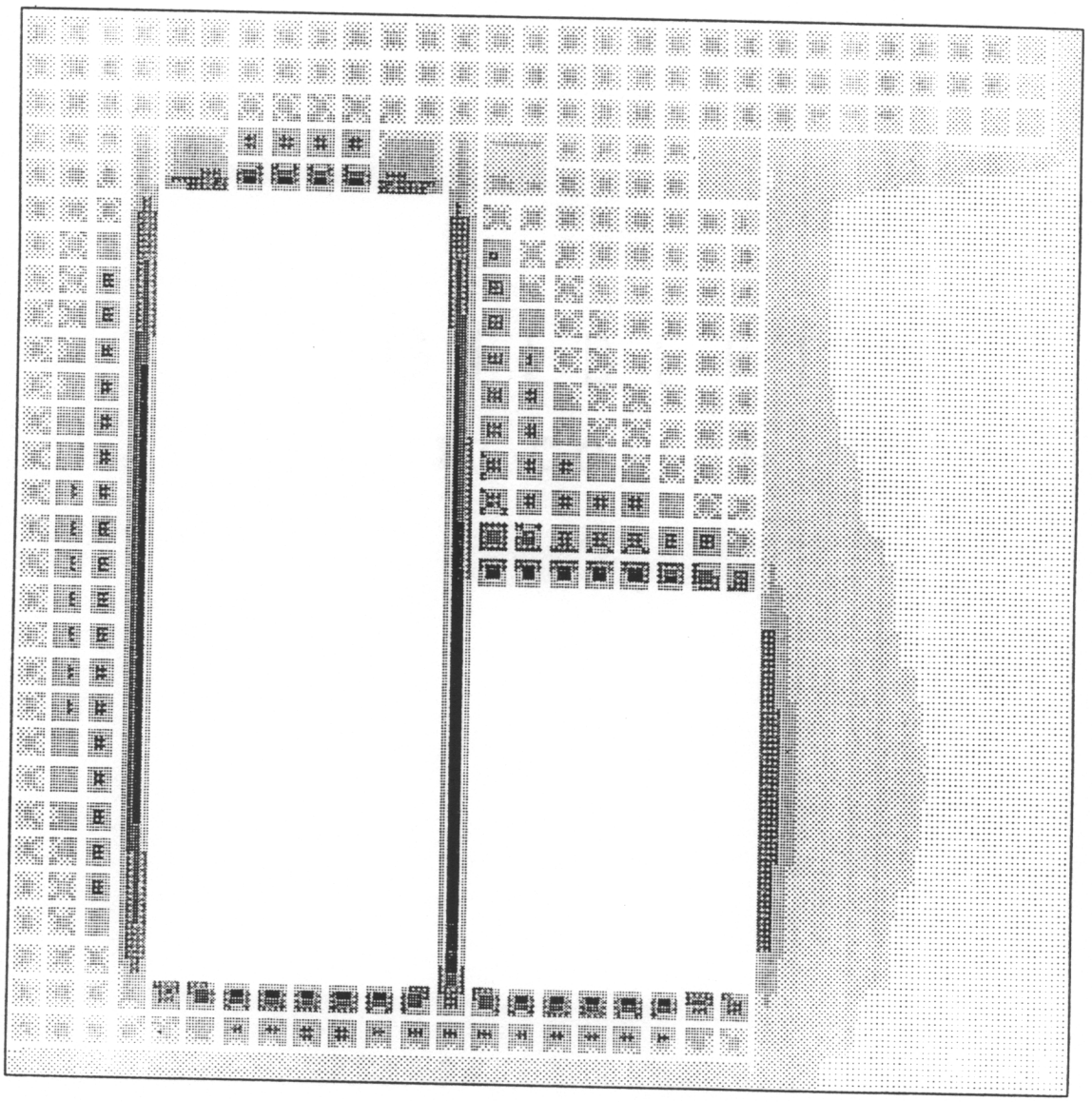

Figure 4.13—Section design B appropriate for 1,200 ft of overburden.

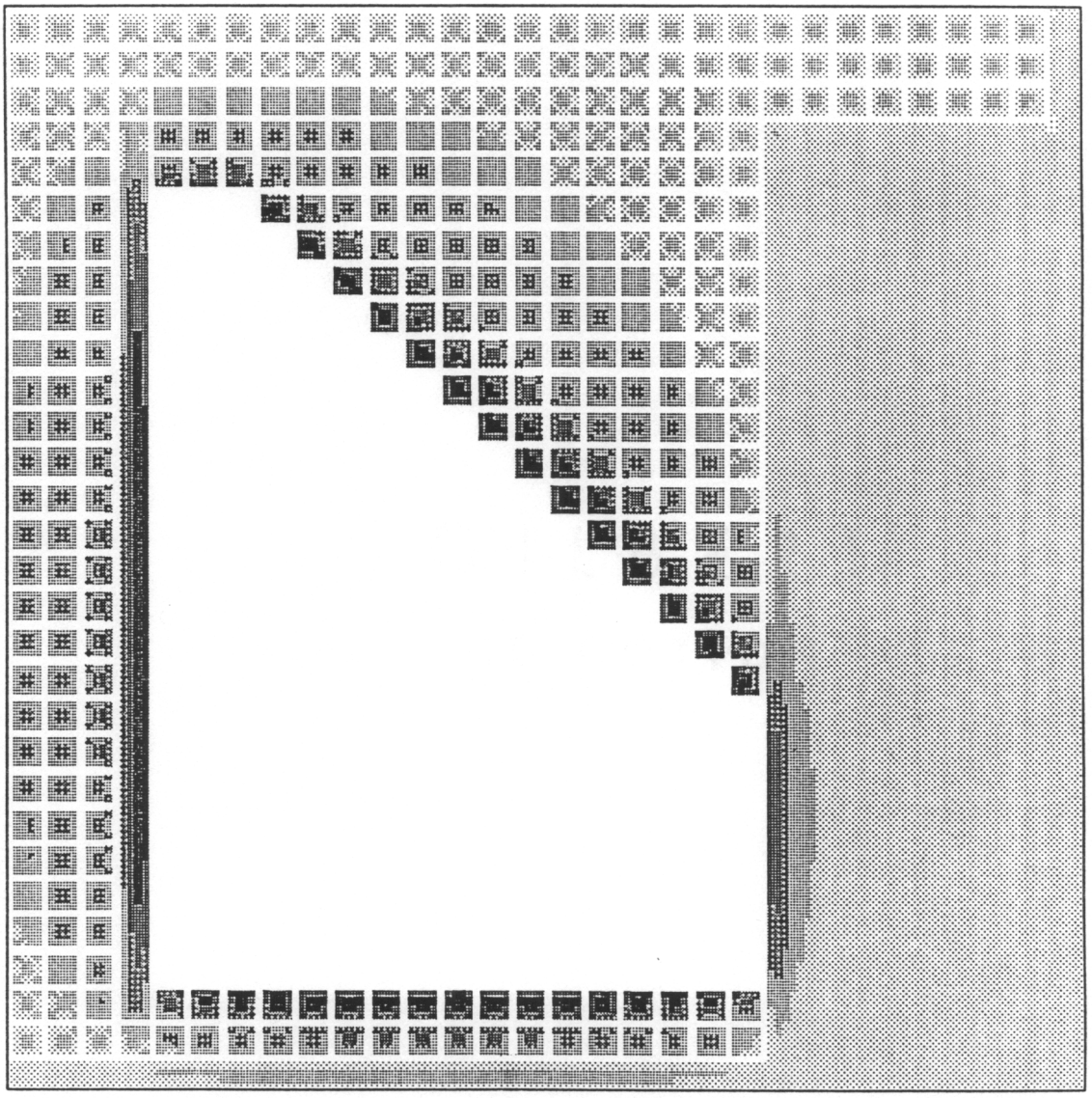

Figure 4.12—Section design A appropriate for 1,000 ft of overburden.

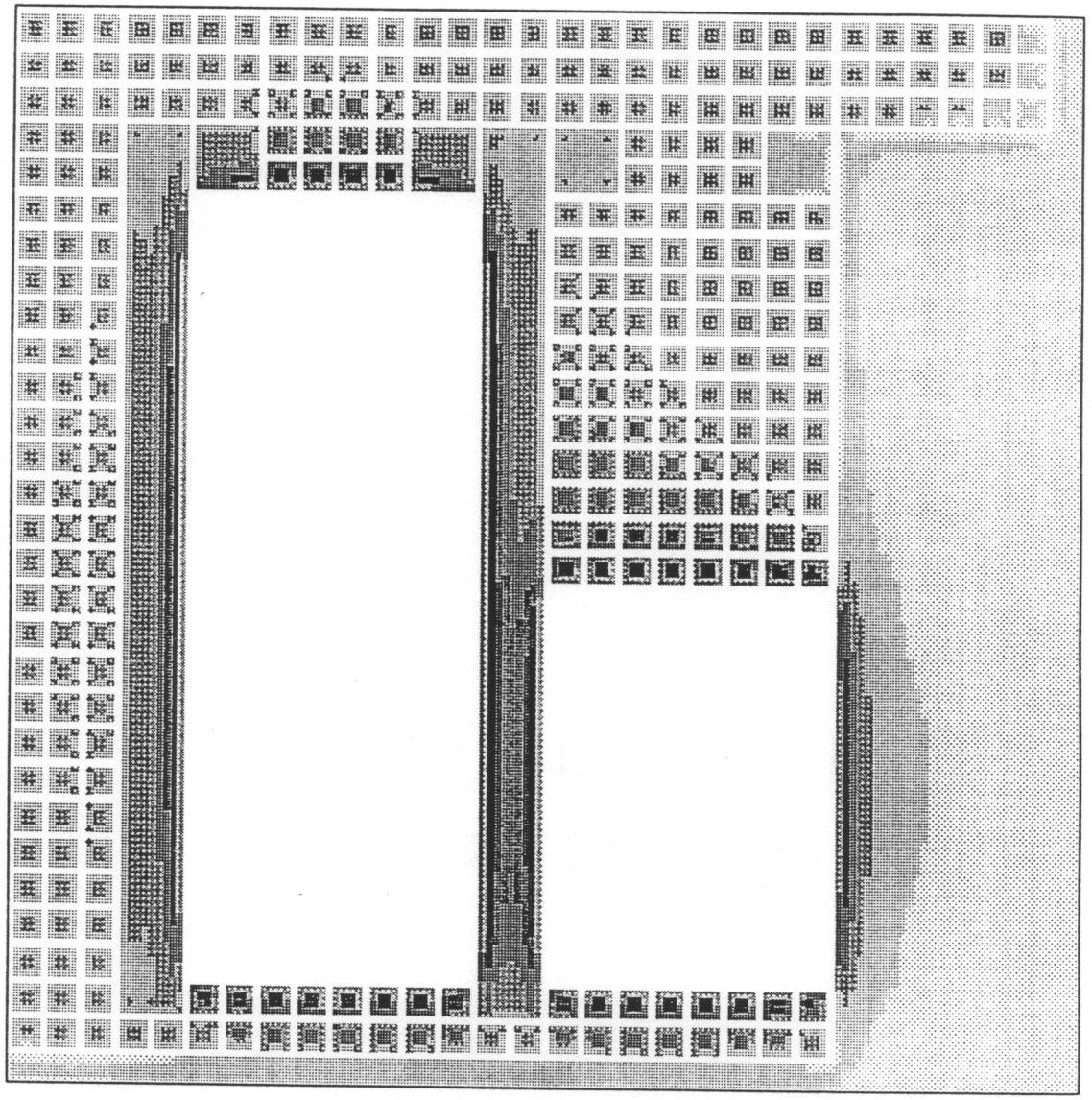

Figure 4.14—Section design C appropriate for 1,400 ft of overburden.

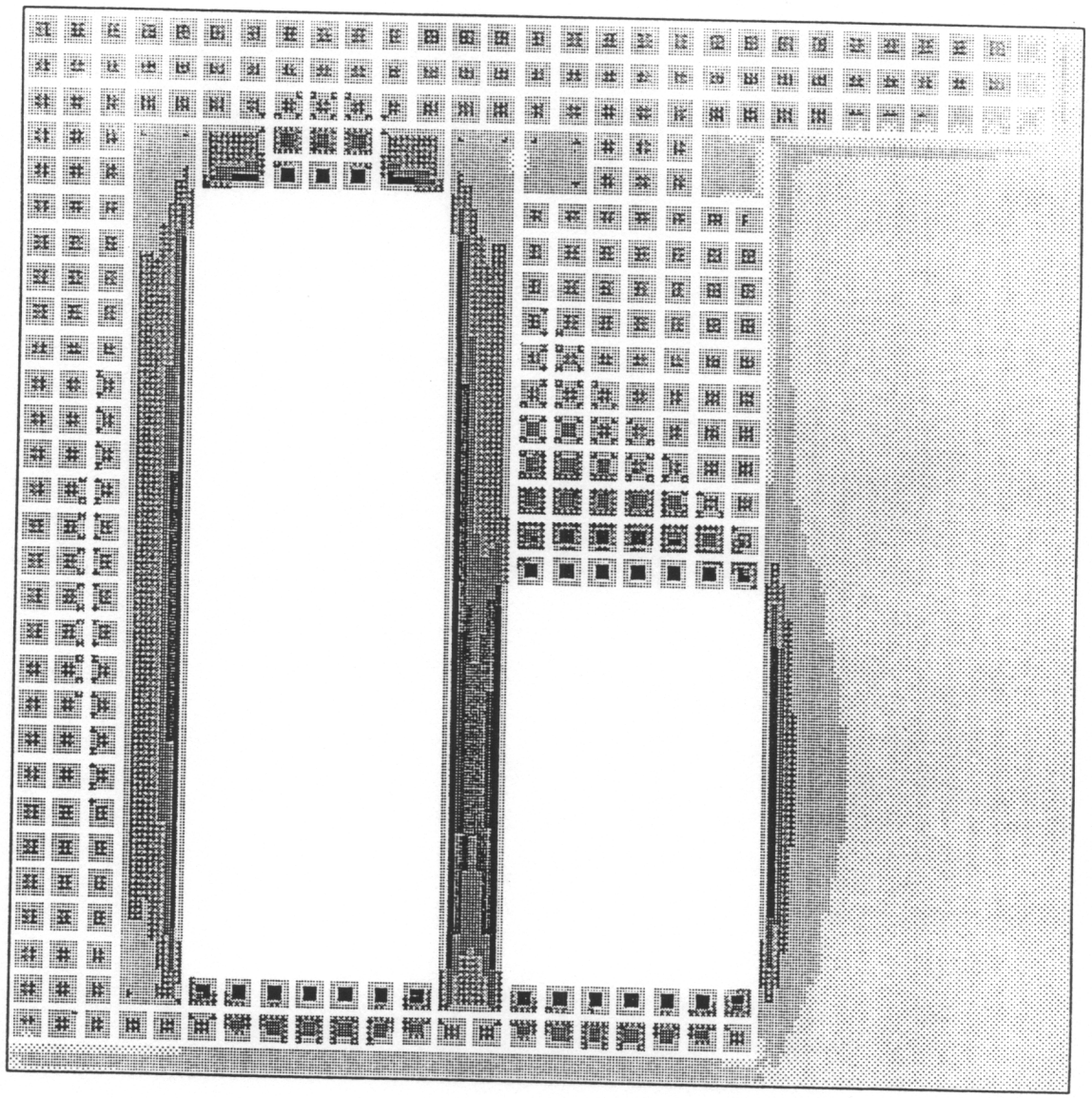

Figure 4.15—Section design D appropriate for 1,600 ft of overburden.

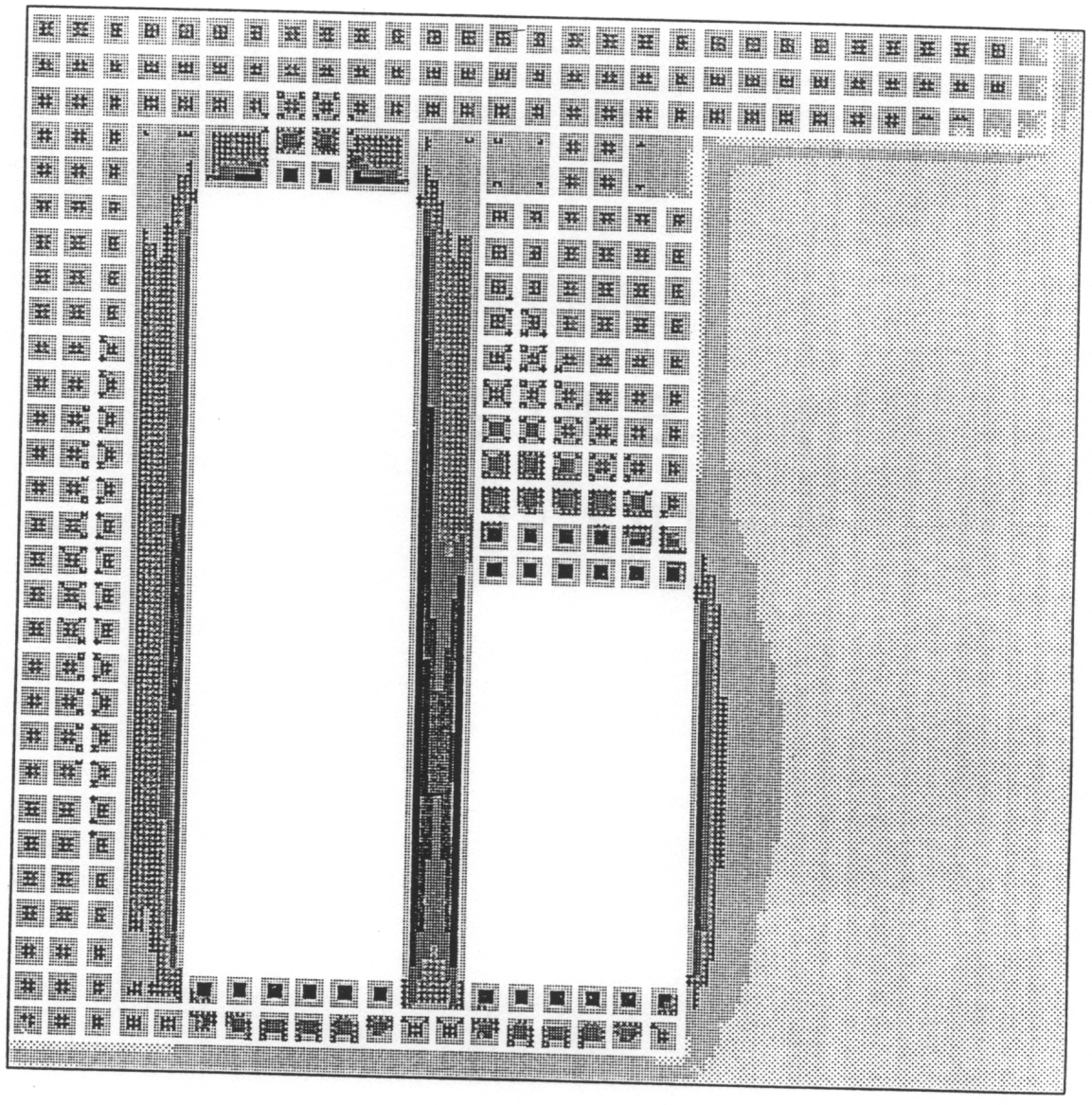

Figure 4.16—Section design E appropriate for 1,800 ft of overburden.

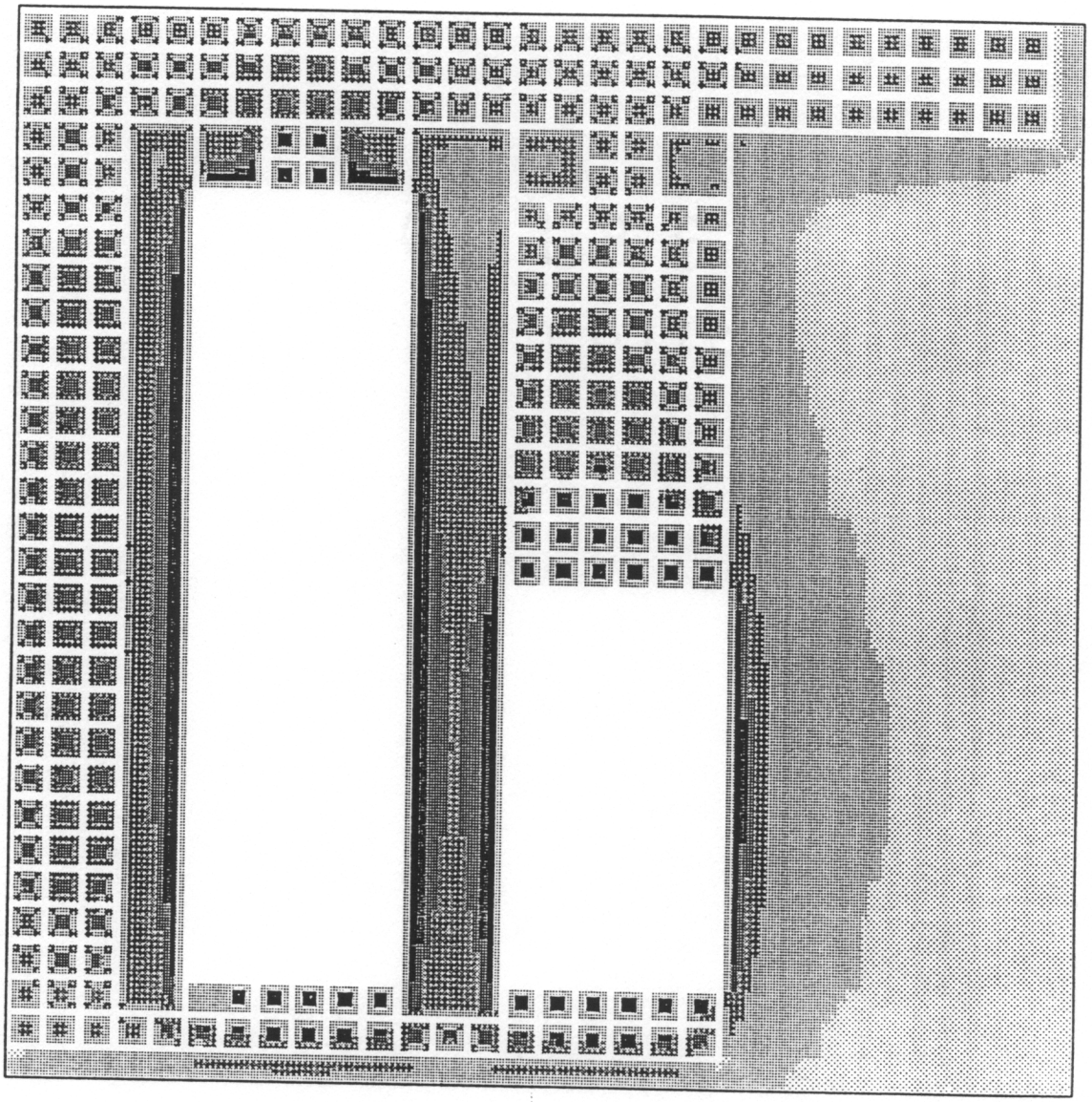

Figure 4.17—Section design F appropriate for 2,000 ft of overburden.

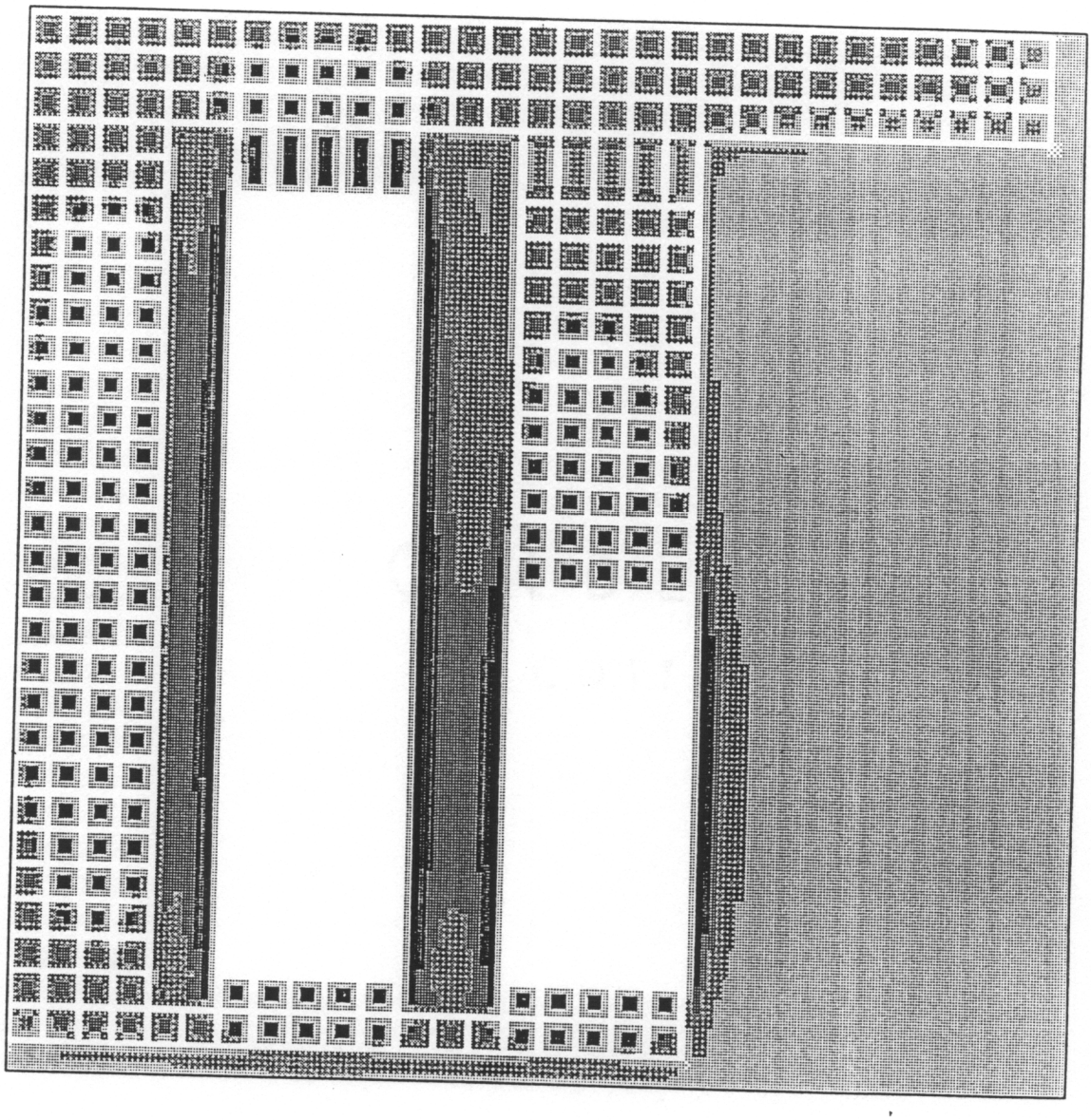

Figure 4.18—Section design G appropriate for 2,200 ft of overburden.

influenced by mesh design considerations and are multiples of the square pillars widths.

The general section configuration is best illustrated in figure 4.14. The square pillars on right and top of the fine mesh form the main and submain haulage of the mine. A two pillar wide barrier protects the main haulage from abutment loads generated from the previous mining of the initial panel. The panels are mined from the bottom up. The two rows of square pillars at the bottom form the bleeder entries. The skin to skin extraction of the panels between continuous barrier pillars is not prohibited by Mine Safety and Health Administration Regulations and should be acceptable as the hard sandstone roof associated with bump-prone mines should bridge over the barrier pillars, forming a void facilitating gob ventilation. Implementation of the above plan would require a gas evaluation plan be established and followed. A two pillar wide barrier pillar is left between the total extraction panels. A worst case stress scenario is evaluated in the one step MULSIM/NL model, one half of the 2,000 ft long second panel has been extracted under 1,400 ft of overburden.

The required abutment pillar width increases with depth, while the permissible section width decreases with depth. Table 4.2 summarizes the suggested section configuration and resultant extraction ratio for each of the seven overburden thickness levels in a 6 ft thick coalbed. Increases in coalbed thickness would decrease coal pillar strength, and thus, reduce the permissible overburden thickness for a given design; decreases in coalbed thickness would have the opposite effect. This

Table 4.2—Summary of section design versus overburden parametric study for subcritical section in 6 ft thick coalbed.

Design	Overburden depth ft	Panel width ft	Barrier width ft	Extraction ratio, %
A	1,000	Unlimited	None required	100
B	1,200	738	70	91
C	1,400	738	158	82
D	1,600	648	158	80
E	1,800	558	158	78
F	2,000	558	246	69
G	2,200	468	246	66

effect would decrease total extraction pillar strength to a greater degree than barrier pillar strength. Subsequent MULSIM/NL parametric analysis could further refine the effect of coalbed thickness variation on subcritical section design.

In excess of forty MULSIM/NL computer runs, configured as described above, were performed in the subcritical design process. Since the criteria for selecting the appropriate subcritical section design for a given overburden thickness was two fold: 1) total extraction pillars at maximum strength must be confined to the first pillar row outbye the expanding gob; and 2) the barrier pillar separating the previous gob and the active gob must not exceed 4,000 psi adjacent the first row of total extraction pillars outbye the expanding gob. Application of the criteria is illustrated by close examination of design E at the 1,800 ft overburden level (fig. 4.19). The fine mesh elements at maximum stress are limited to the first row of pillars outbye the gob and the barrier pillar core stress is less than 4,000 psi adjacent to the first outbye pillar row. Increasing the overburden depth to 2,000 ft causes the design E to fail the abutment pillar stress criteria (fig. 4.20). Design F meets the criteria at an overburden depth of 2,000 ft (fig. 4.21). At an overburden depth of 2,200 ft design F fails to contain the maximum pillar stress to the first outbye pillar row and is found unacceptable (fig. 4.22).

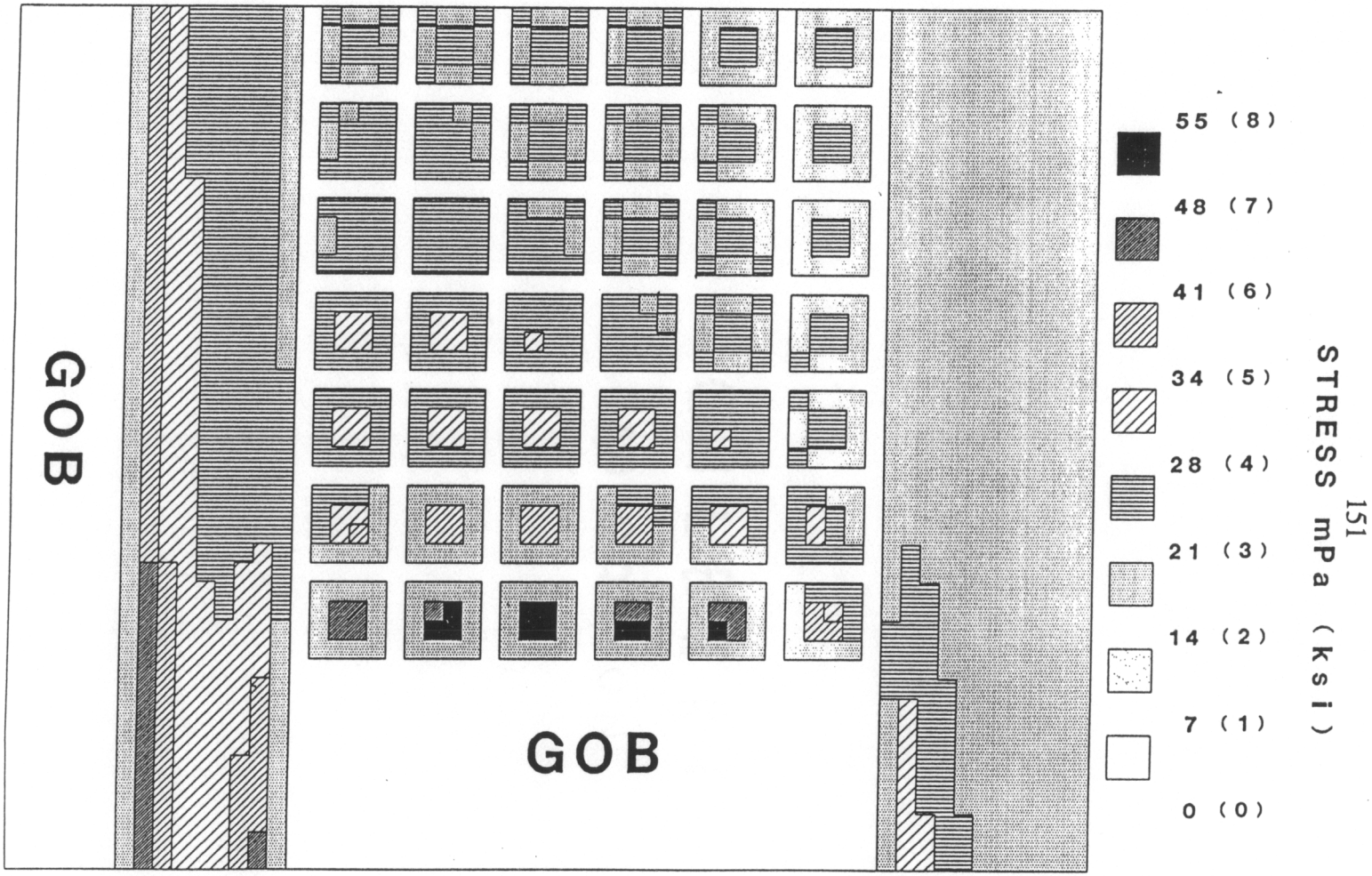

Figure 4.19—In-seam vertical stress for design E at 1,800 ft of overburden.

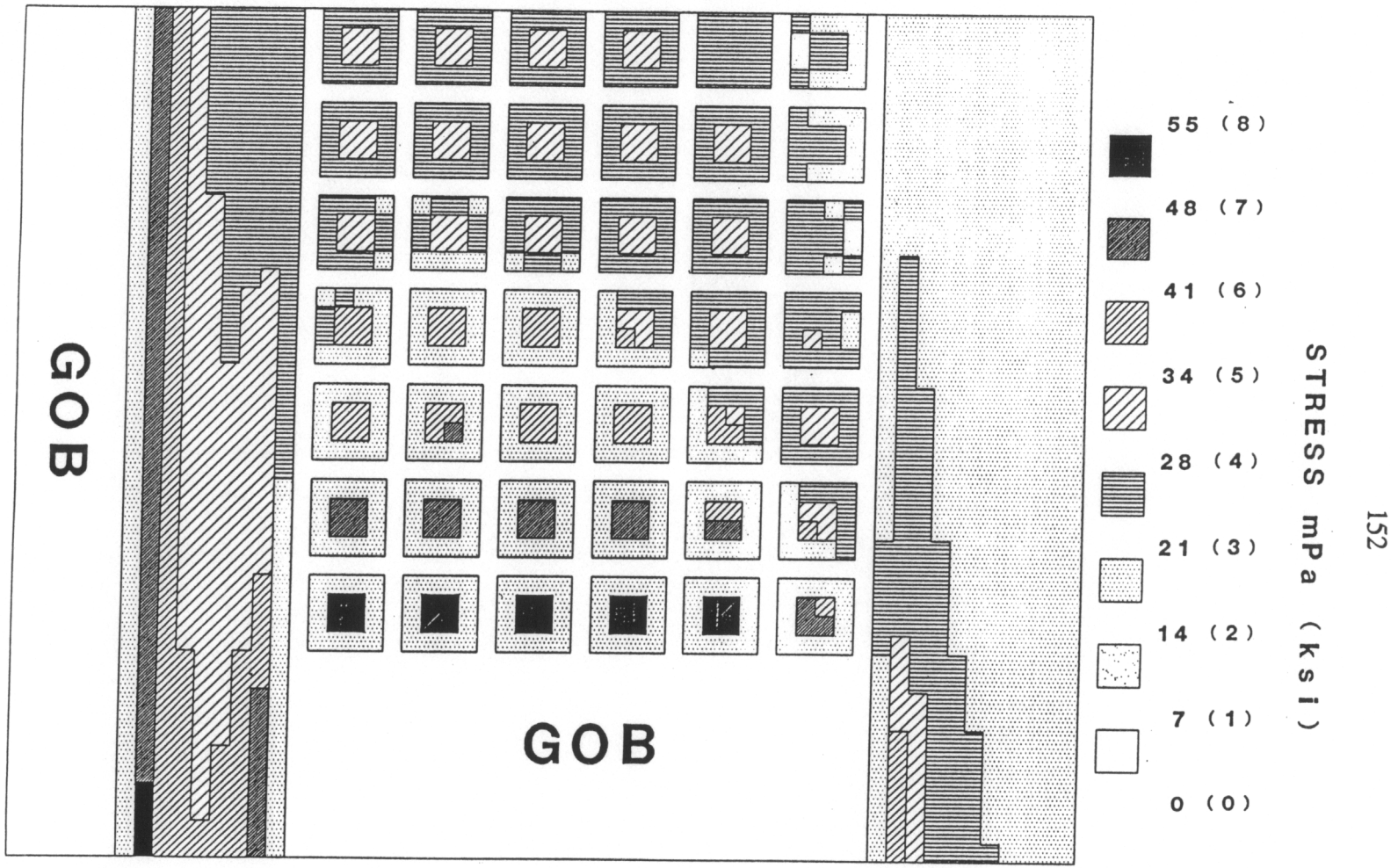

Figure 4.20—In-seam vertical stress for design E at 2,000 ft of overburden.

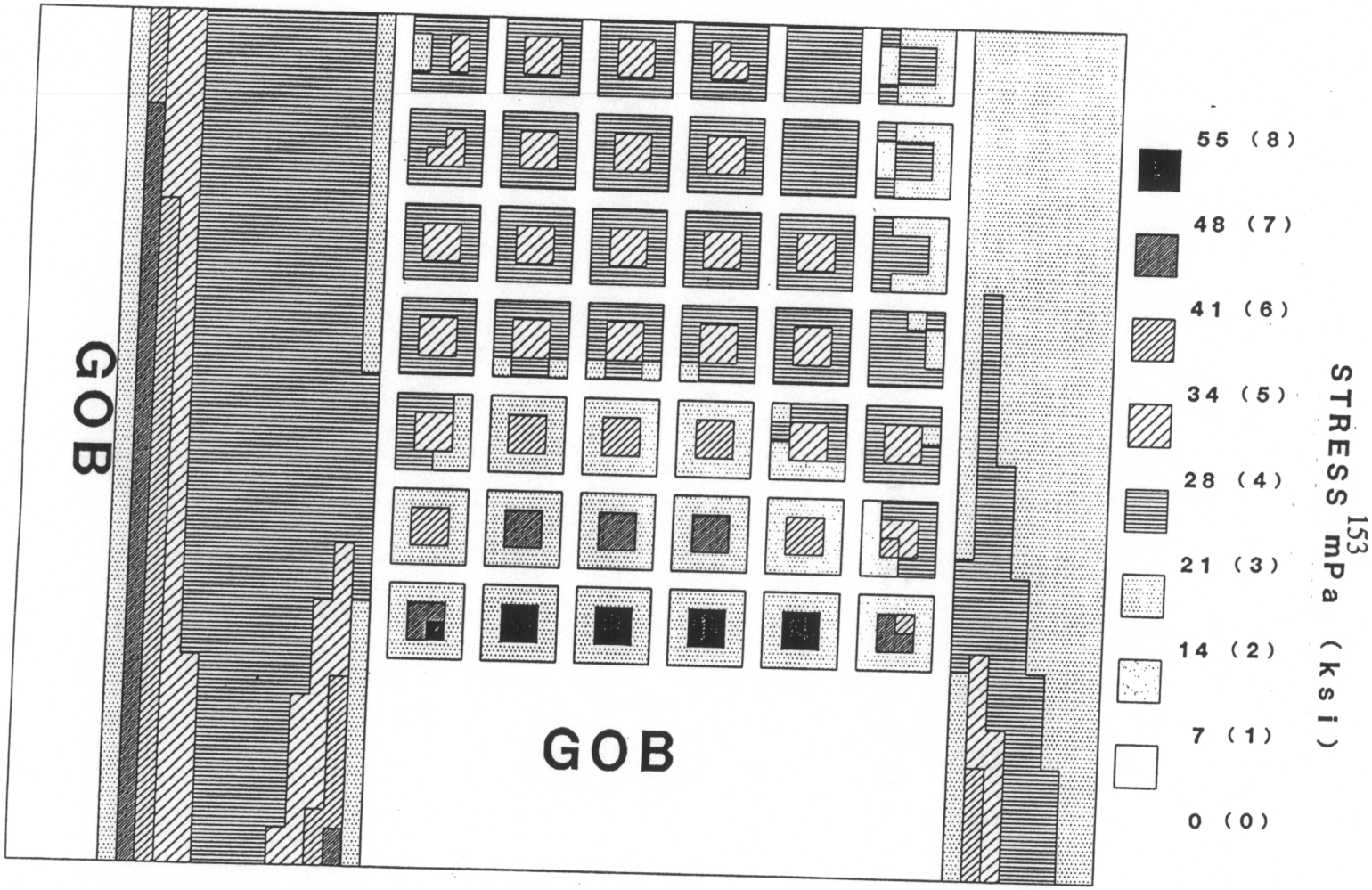

Figure 4.21—In-seam vertical stress for design F at 2,000 ft of overburden.

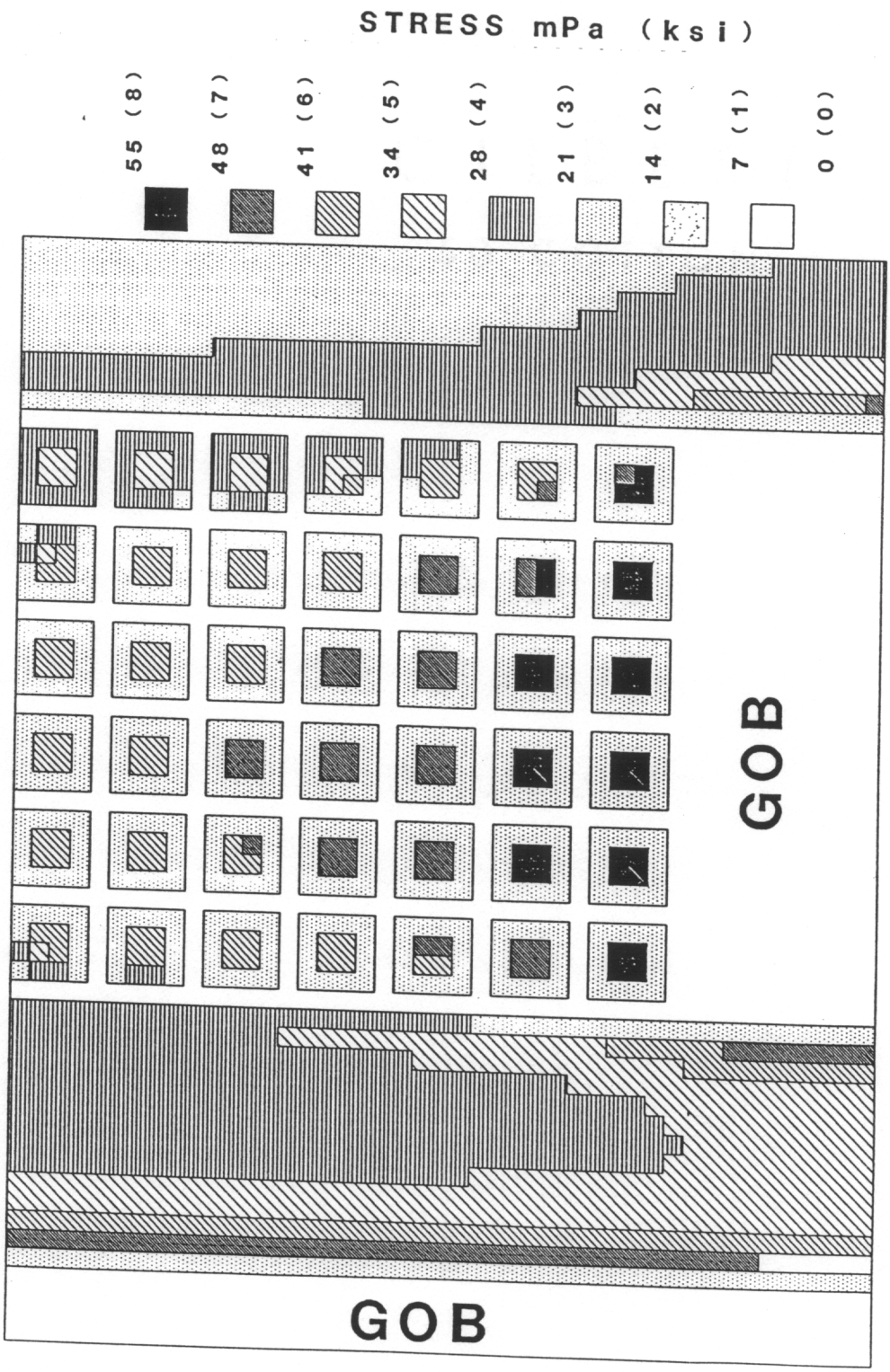

Figure 4.22—In-seam vertical stress for design F at 2,200 ft of overburden.

4.3.3 Generalization of Results

The parametric studies were limited to a 6 ft thick coalbed and seven discrete overburden depths. The results of the parametric study can be generalized to accommodate variation in coalbed thickness and overburden depth. The MULSIM/NL suggested abutment pillar widths are less conservative than those suggested by the Ashley equation for a 6 ft thick coalbed (fig. 4.23). The Ashley equation accounts for variation in coalbed and overburden thicknesses and could be used to suggest barrier pillar width for the subcritical width section.

The width of the subcritical section could be based on a ratio of the total extraction pillar strength in the user specified coalbed thickness to the strength of a total extraction pillar in a 6 ft thick coalbed. The first step in this process is to fit a continuous function to the parametric analysis section width (fig. 4.24). Equation 4.7 accounts for 99.6% of the variation in the 6 ft thick coalbed parametric analysis section width results:

$$P = -0.00321H + 12.1 \tag{4.7}$$

where P = section width in 70 ft square pillars

H = overburden depth, ft

Multiplying the output of equation 4.7 by the ratio of 70 ft square total extraction pillar strength for the specified coalbed thickness over the strength of a 70 ft square pillar in a 6 ft thick coalbed and rounding to the nearest whole number, results in a suggested width of the subcritical section.

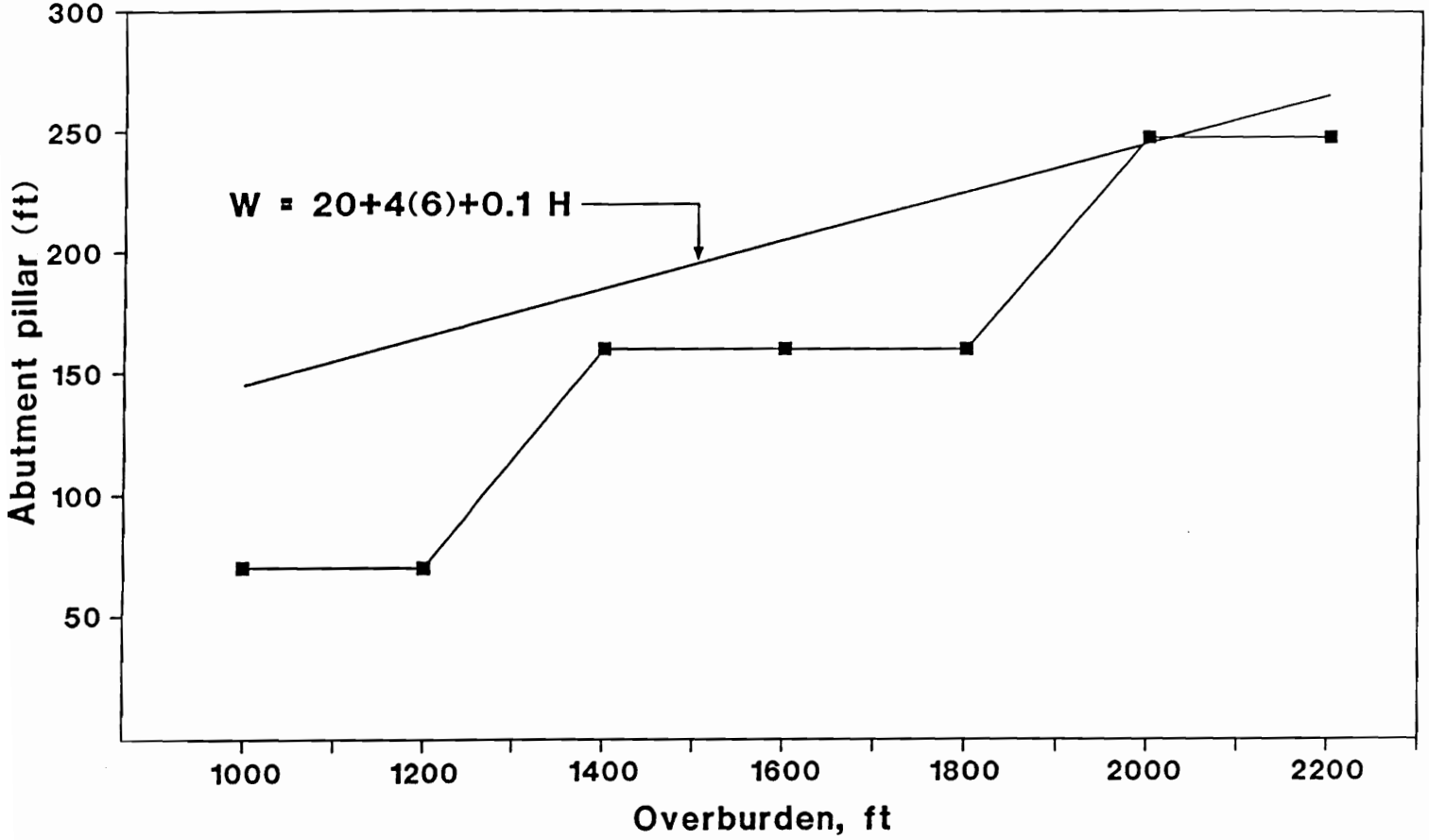

Figure 4.23—Comparison of Ashley and parametric analysis abutment pillar width suggestions, for a 6 ft thick coalbed.

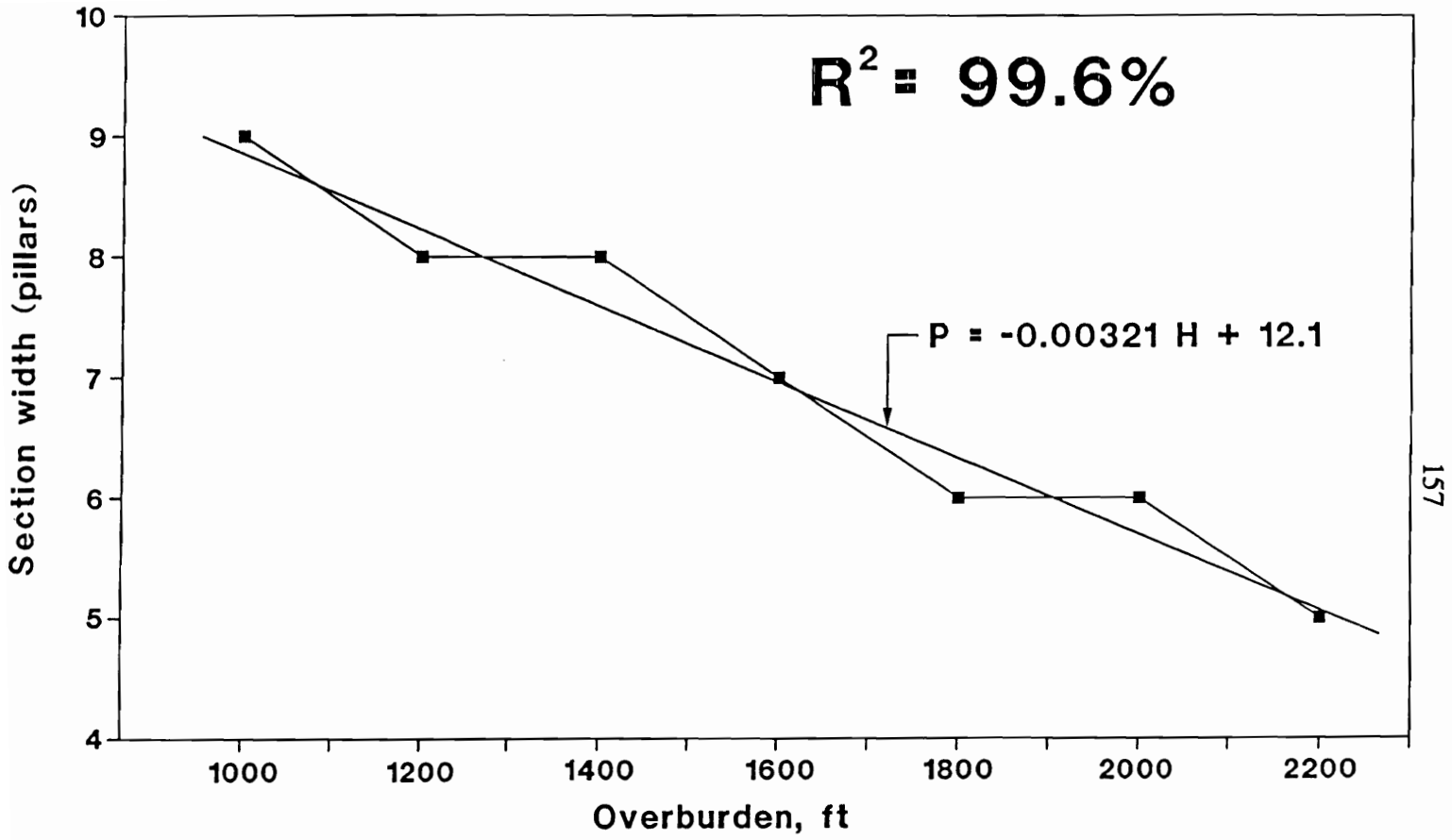

Figure 4.24—Fit of subcritical section width design equation to parametric analysis results.

Chapter V

BUMP HAZARD ASSESSMENT MODEL

A bump hazard assessment model LAYOUT was developed as a spreadsheet template for use in LOTUS or EXCEL, utilizing the supercritical width and subcritical width section design criteria. The model assists the mining engineer in the design of room-and-pillar retreat sections for continuous miner extraction of bump prone coalbeds. The model LAYOUT provides an essential first step in the design process. The basic steps in the model LAYOUT are shown in figure 5.1. LAYOUT questions the user to insure the mined coalbed is contained within bump prone associated strata. If the associated strata is conducive to coal mine bumps the user continues into the supercritical design procedure. The user is asked to specify the overburden depth, coalbed thickness, linear shear angle, and total extraction pillar dimensions. Based on this input, LAYOUT calculates the strength, development load, abutment load, and pillar stability factor for the first two total extraction pillar rows outbye the expanding gob. LAYOUT also calculates a suggested barrier pillar width to separate adjoining supercritical width sections.

LAYOUT assists the user in the evaluation of the pillar stability factors. If the stability factor is unacceptable the user is instructed to return to the beginning of the spreadsheet to change the original input or continue to the subcritical section design procedure.

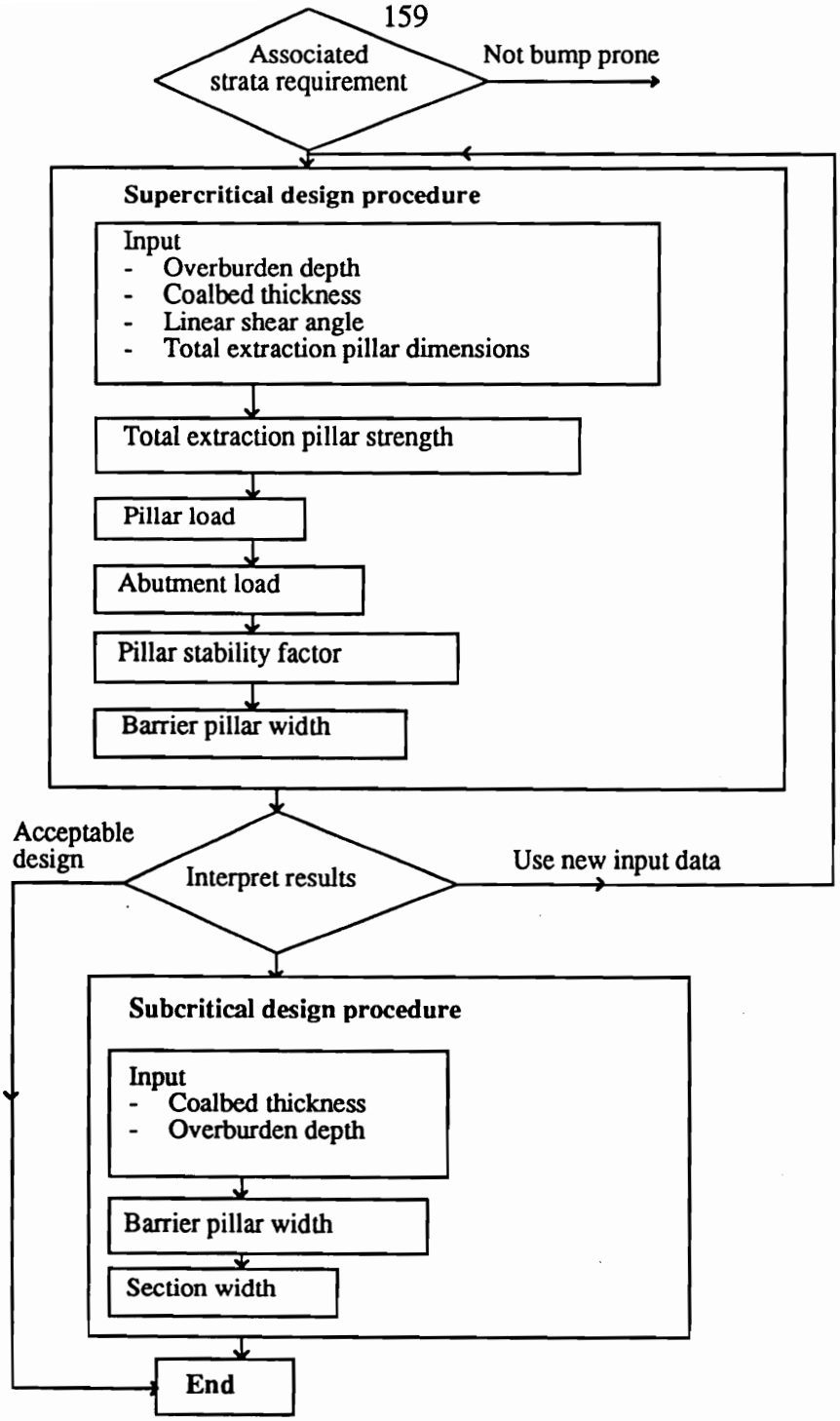

Figure 5.1 - LAYOUT flowchart.

Application of the subcritical section width design procedure results in a suggested section design appropriate for the requested coalbed and overburden thickness input. This is accomplished by interpreting the MULSIM/NL 6 ft thick coalbed parametric study, as previously described above, to accommodate variation in coalbed thickness. Section 5.1 contains an example LAYOUT run as it would appear to the user in LOTUS or EXCEL. Underlined sections are comments on the example which would not appear to the user. LAYOUT contains a complete set of input values, the user changes these values to suit the individual application. The inputs the user may change are in bold type.

While reading through the example contained in Appendix B please consider the following assumptions and limitations associated with LAYOUT:

1) In the supercritical design procedure, the abutment loads are modeled as if sufficient gob has been formed to allow a portion of the overburden weight to be applied to the gob floor, as defined by the linear shear angle chosen by the user. Thus, LAYOUT does not account for first fall effects.

2) After analysis of the few case studies available, it appears that a supercritical stability factor of greater than unity should be applied. However LAYOUT assumes that all of the gob side total extraction pillars are the same size. Care must be taken during advance mining to insure that this is the case.

3) The lack of room-and-pillar retreat mining at depths greater than 1,000 ft limits the available case studies to verify the subcritical design procedure.

4) Layout does not account for faulting or any geologic structure in the mine roof. It is assumed the roof behaves uniformly. If such structure is known to exist the possibility of anomalous stress concentrations should be considered.

5.1 Case Study Model Verification

The model was verified by analysis of the three case studies. In the first case study, W-P No. 21 Mine extracted the 4 ft thick Chilton Coalbed under a maximum overburden of 800 ft. Analysis of LAYOUT output suggests supercritical width sections comprised of 55 by 70 ft total extraction pillars, extracted with the split-and-fender method with a stability factor of 1.57. The mine experienced a fatality in a bump accident during the mining of 60 ft square pillars with the split-and-fender method (fig. 5.2). Analysis using the LAYOUT model resulted in a stability factor of 1.51 for a supercritical section composed of 60 ft square pillars. Thus, either size pillar was sufficient to meet the stress limit design criteria. The case study confirmed this conclusion, see section A-1. The bump was caused by the employment of mixes pillar sizes (fig. 5.2). This case study highlights the need for strict adherence to the design rules of thumb outlines at the in section A-4, in conjunction with the LAYOUT program.

In the second case study, the Olga Mine extracted the 6 ft thick Pocahontas No. 4 Coalbed under 1,300 ft of overburden, see section A-2. Analysis of LAYOUT output suggests the subcritical design procedure, as the 90 ft square total extraction

pillar design results in a safety factor of only 0.98. The subcritical design procedure recommends a eight pillar (738 ft) wide extraction panels separated by 174 ft wide continuous barrier pillars. This is consistent with the successful stress shield layout implemented in the 9 Right study area (fig. 5.3).

In the third case study, the VP No. 3 Mine extracted the 6 ft thick Pocahontas No. 3 Coalbed under 2,000 ft of overburden, see section A-3. Analysis of LAYOUT output suggests the subcritical design procedure, as the 90 ft square total extraction pillar design results in a safety factor of only 0.76. The subcritical design procedure recommends a six pillar (558 ft) wide extraction panels separated by 244 ft wide continuous barrier pillars. The successful stress shield layout implemented in the retreat longwall section extracted 600 ft wide panels separated by 238 ft wide gateroads.

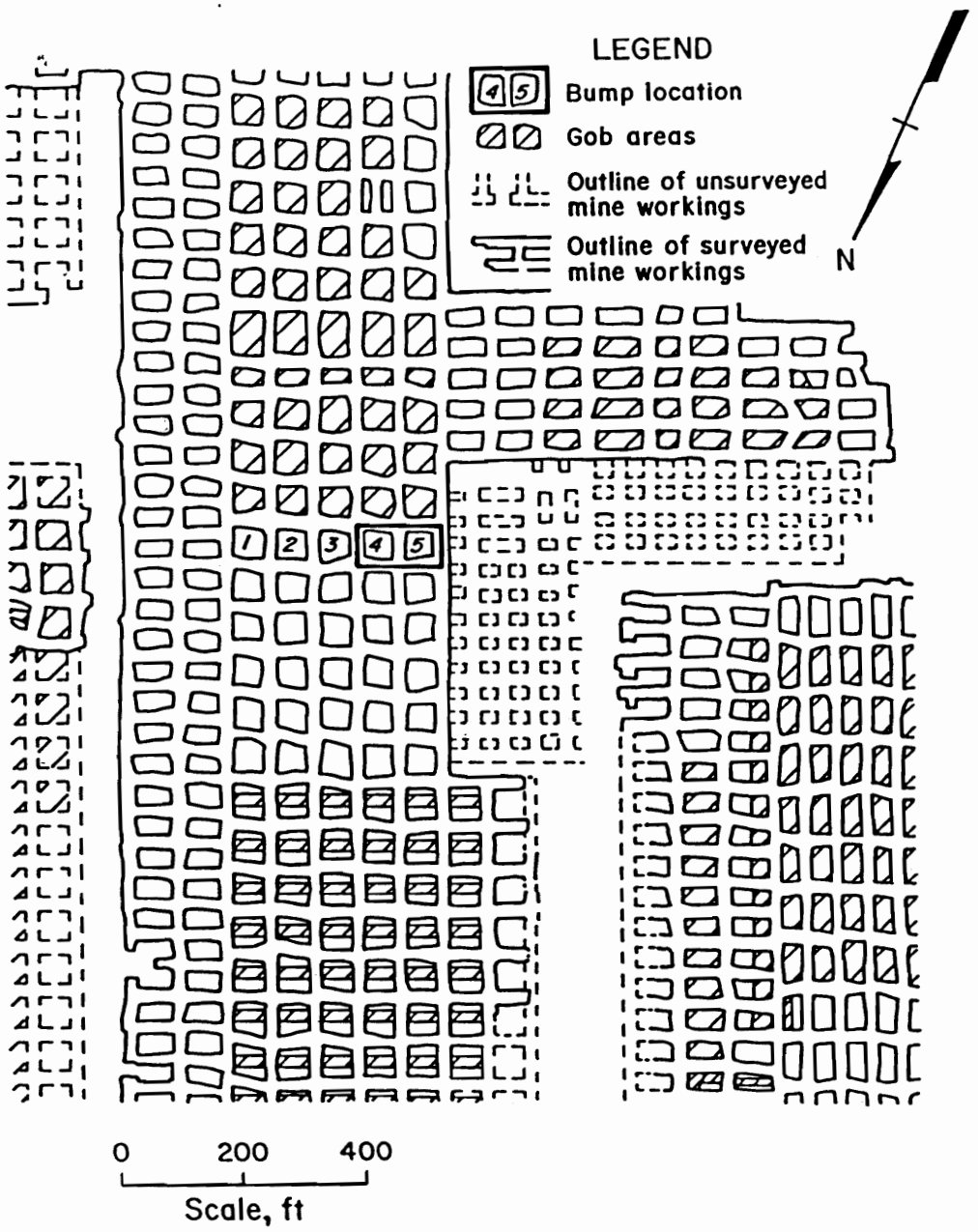

Figure 5.2—Bump accident area W-P No. 21 Mine (After Campoli, et al., 1987).

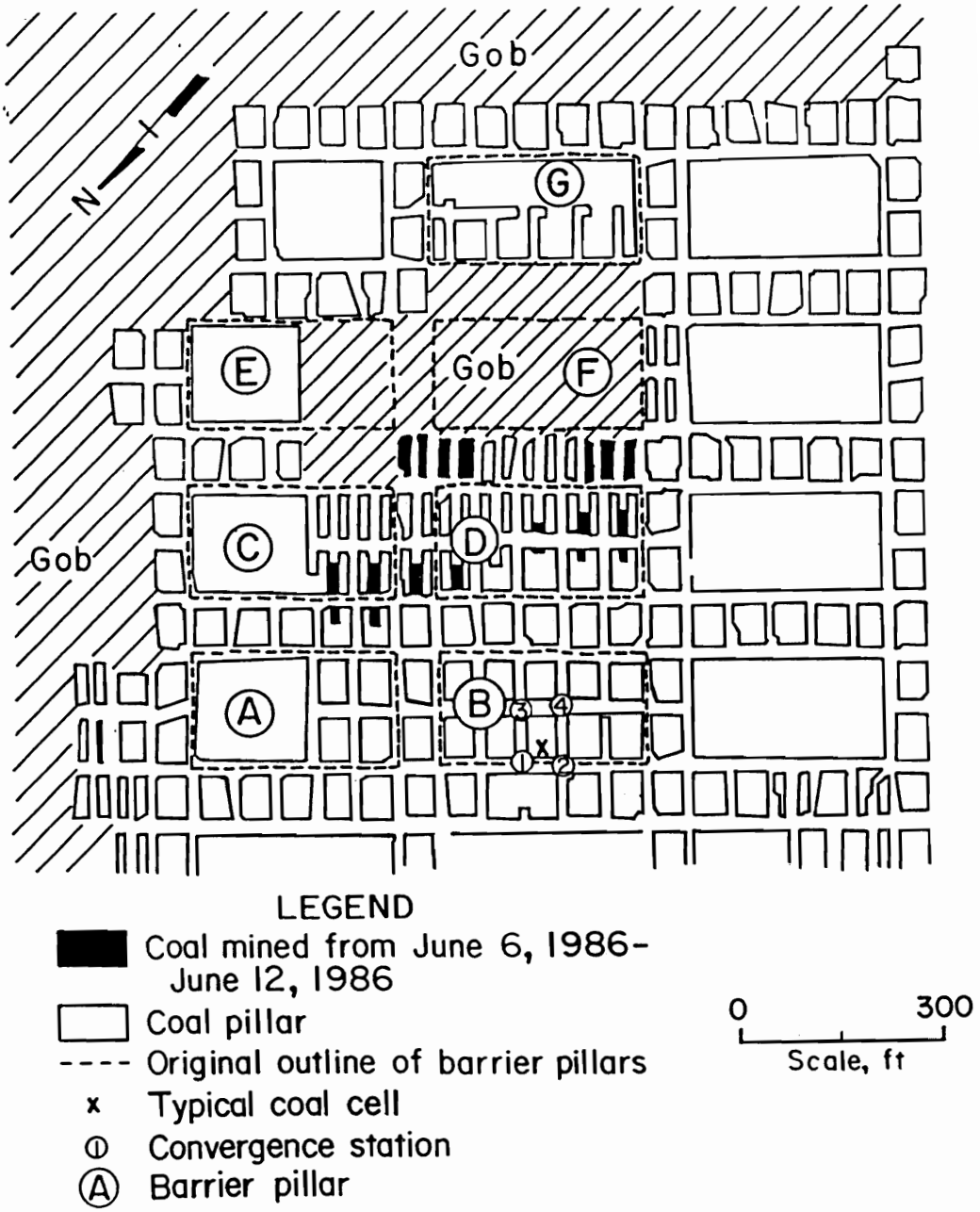

Figure 5.3—Map of the 9 Right study area Olga Mine (After Campoli, et al., 1990b).

Chapter VI

CONCLUSIONS AND RECOMMENDATIONS

6.1 Conclusions

A stress control design protocol for room-and-pillar retreat mining was developed for available continuous miner technology. Based on the assumption that coal mine layout changes are the only factor under significant control of the mine operator, only the configuration of the section was varied.

A stress shield concept was advanced with in-mine geotechnical evaluations of two successful mine designs. A room-and-pillar and a longwall mine design were both implemented under demonstrated bump hazard, under overburden in excess of 1,300 and 2,000 ft, respectively. In both cases, strategic placement of stress shield abutment pillars between adjacent gob areas and total extraction areas eliminated bumps experienced with previous designs.

The ability a coal pillar to support the combination of development and abutment loading increases with increases in lateral pillar dimensions. Therefore, total extraction pillars should be as large as possible, while allowing for efficient and bump free extraction. Continuous miner extraction of 60 by 80 ft pillars with 40 ft with an Xmas tree extended cut pillar extraction plan offers the best compromise

between total extraction pillar strength and ease of extraction.

Supercritical section width design criteria predict that sections comprised exclusively of these 60 by 80 ft total extraction pillars cannot support gob side abutment loads when overburden thickness exceeds approximately 1,050 ft, in a 6 ft thick coalbed. Successful designs for deeper bump-prone mines must either shield workings from excessive stress or reduce coalbed bearing capacity directly prior to extraction.

A confined pillar core coal pillar strength model was developed. The pillar core is assumed to reach a maximum stress when surrounded by a sufficiently wide yielded perimeter. The depth of the yielded perimeter is assumed to vary increase linearly with increased coalbed thickness.

The coal strength model was employed in the development of supercritical width and subcritical width section design criteria. The supercritical design procedure assumes an infinitely long pillar line, composed of uniformly sized pillars, extracted against an infinitely wide gob area. Tributary area theory was combined with a linear shear angle concept to estimate the loads applied to total extraction pillars adjacent to gob areas.

The boundary element code MULSIM/NL was utilized in the development and implementation of a systematic subcritical design procedure to apply the stress shield concept to retreat room-and-pillar coal mining, under bump hazard. The complicated

distribution of gob side abutment load between the side abutment pillars and the chain pillars in the total extraction zone made computer simulation a necessity. MULSIM/NL calibration was based on the longwall and room-and-pillar in-mine geotechnical evaluations. Suggested section layouts were determined for the mining of a 6 ft coalbed under overburden conditions ranging from 1,000 to 2,200 ft at 200 ft increments. The sections consist of 2,000 ft long total extraction areas separated by continuous abutment pillars.

The parametric studies were limited to a 6 ft thick coalbed and seven discrete overburden depths. The results of the parametric study were generalized to accommodate variation in coalbed thickness and overburden depth. The Ashley equation accounts for variation in coalbed and overburden thicknesses and was used to suggest barrier pillar width for the subcritical width section. The width of the subcritical section was based on a ratio of the total extraction pillar strength in the user specified coalbed thickness to the strength of a total extraction pillar in a 6 ft thick coalbed.

LAYOUT, a bump hazard assessment model, was developed as a LOTUS or EXCEL spreadsheet template utilizing the supercritical width and subcritical width section design criteria. LAYOUT was verified with back analysis of three case studies. The model LAYOUT will assist the mining engineer in the design of room-and-pillar retreat sections for continuous miner extraction of bump prone coalbeds.

The model LAYOUT provides an essential first step in the design process. Full scale implementation of the section designs suggested by the design procedure could provide further verification.

6.2 Recommendations

This research effort provides a means of mitigating coal mine bumps through a vertical coalbed stress limit design procedure. The design procedure does not consider variations in the structure of the coalbed and associated strata or variation in main roof caving characteristics and the associated variation in gob side abutment load distribution. These are important geologic characteristics that should be addressed in future research.

A search is underway to find a room-and-pillar retreat coal mine, that employs continuous miner technology under bump prone geologic conditions. The design criteria layout should be used to prescribe section configurations at this cooperative mine, that allow bump free and efficient retreat mining. Geotechnical instrumentation should be employed to evaluate strata behavior through pillar stress and roof-to-floor closure measurements.

REFERENCES

Ashley, G.H., 1930,"Barrier Pillar Legislation in Pennslyvania," Trans., AIME, Coal Division, pp. 76-96.

Babcock, C. O. and D. Bickel, 1984, "Constraint the Missing Variable in the Coal Burst Problem," 25th Symposium on Rock Mechanics, pp. 639-647.

Barron, K., 1984, "An Analytical Approach to the Design of Coal Pillars," CIM Bulletin, v. 77, No. 868, 272 pp.

Barry, A. J., A. Zona, J. L. Gilley, and R. H. Oitto, Jr., 1967, "Investigations of Stress Distributions in Burst Prone Coal Pillars," U.S. Bureau of Mines RI 6971, 42 pp.

Barton, T. M., A. A. Campoli, and M. Gauna, 1992, "Rock Mechanics Research Decreases Longwall Bump Potential at a Southern Appalachian Coal Mine," Mining Engineering, v. 44, No. 4, pp. 347-351.

Bauer, E. R., D. M. Pappas, and J. M. Listak, 1993, "Ground Control Safety Analysis of Extended Cut Mining," U.S. Bureau of Mines IC in Press.

Bauer, E. R., G. J. Chekan, and J. H. Hill, III, 1985, "A Borehole Instrument for Measuring Mining Induced Pressure Changes in Underground Coal Mines," 26th U.S. Symposium on Rock Mechanics, pp. 1075-1084.

Beckett, L. A. and R. S. Madrid, 1988, "MULSIM/BM - A Structural Analysis Computer Program for Mine Design," U.S. Bureau of Mines IC 9168, 302 pp.

Bieniawski, Z. T., 1968, "The Effect of Specimen Size on the Strength of Coal," International Journal of Rock Mechanics and Mining Sciences, v. 5, pp. 325-335.

Blake, W, 1983, "Microseismic Applications for Mining - A Practical Guide," U.S. Bureau of Mines OFR 52-83, 206 pp.

Blake, W., F. Leighton, and W. I. Duvall, 1974, "Microseismic Techniques for Monitoring the Behavior of Rock Structures," U.S. Bureau of Mines Bulletin 665.

Blake, W., 1972, "Rock Burst Mechanics," Quarterly of the Colorado School of Mines, v. 67, No. 1.

Blankenship, C. and A. T. Castanon, 1983, "Multiple Fatal Bump Accident (Outburst)," Mine Safety and Health Administration 4015 Wilson Boulevard, Arlington, VA 22203, 17 pp.

Brady, B. H. G. and E. T. Brown, 1985, "Rock Mechanics for Underground Mining," George Allen and Unwin, London, 527 pp.

Campbell, W. F., 1958, "Deep Coal Mining in Springhill No. 2 Mine," AIME Transactions, v. 211, pp. 987-992.

Campoli, A. A., T. M. Barton, F. C. VanDyke, and M. Gauna, 1990, "Mitigating Destructive longwall Bumps Through Conventional Gate Entry Design," U.S. Bureau of Mines RI 9325, 38 pp.

Campoli, A. A., D. C. Oyler, and F. E. Chase, 1990, "Performance of a Novel Bump Control Pillar Extracting Technique During Room-and-Pillar Retreat Coal Mining," U.S. Bureau of Mines RI 9240, 40 pp.

Campoli, A. A., T. M. Barton, F. C. VanDyke, and M. Gauna, 1993, "Gob and Gate Road Reaction to Longwall Mining In Bump-Prone Strata," U.S. Bureau of Mines RI 9445, 48 pp.

Campoli, A. A., T. M. Barton, F. C. VanDyke, M. Gauna, and M. DeMarco, 1990, "Gate Design Key to Bump Control," Coal, v. 95, No. 9, pp. 54-58.

Campoli, A. A., M. A. Trevits, and G. M. Molinda, 1985, "Coal and Gas Outbursts: Prediction and Prevention," Coal Mining, v. 22, No. 12, pp. 42-47.

Campoli, A. A., 1987, "Evaluating Coal Mine Bump Control Techniques Through Convergence Monitoring," Coal Mining, v. 24, No. 7, pp. 42-46.

Campoli, A. A., C. A. Kertis, and C. A. Goode, 1987, "Coal Mine Bumps: Five Case Studies in the Eastern United States," U.S. Bureau of Mines IC 9149, 34 pp.

Carr, F. E., E. Martin, and B. H. Garden, 1984, "How to Eliminate Roof and Floor Failures With Yield Pillars," Coal Mining, v 21, No. 12, pp. 62-70.

Chase, F. E., 1993, Personal communication available on request, U.S. Bureau of Mines, Pittsburgh Center, Ground and Methane Control Group.

Chase, F. E. and C. Mark, 1993, "Ground Control Design for Pillar Extraction," SME Preprint 93-282, Presentation SME Annual Meeting, Reno, NV, 12 pp.

Coeuillet, R., 1964, "Coal and Gas Outbursts," Proceedings of Symposium on Coal and Gas Outbursts, Economic, pp. 1-14.

Condon, J. L. and R. D. Munson, 1987, "Microseismic Monitoring of Mountain Bumps and Bounces: A Case Study," 6th International Conference on Ground Control in Mining, pp. 1-9.

Cook, N. G. W., 1966, "The Design of Underground Excavations," Proceedings of the Eighth Symposium on Rock Mechanics, pp. 167-193.

Cook, N. G. W., E. Hoek, J. P. G. Pretorius, W. D. Ortlepp, and M. D. G. Salamon, 1966, "Rock Mechanics Applied to the Study of Rock Bursts," Journal of the South African Institute of Mining and Metallurgy, v. 66 (10), pp. 435-528.

Crouch, S. L. and C. Fairhurst, 1973, "The Mechanics of Coal Mine Bumps and the Interaction Between Coal Pillars, Mine Roof-and-Floor," NTIS Report No. PB, pp. 222-898.

Davis, J. E., 1983, "Fatal Outburst of Coal Accident," Mine Safety and Health Administration, P.O. Box 112, Mt. Hope, WV 25880, 26 pp.

Deere, D. U., J. R. Dunn, R. H. Fickies, and R. J. Proctor, 1977, "Geologic Logging and Sampling of Rock Core for Engineering Purposes, Appendix K," West Virginia Geological Survey, 15 pp.

DeMarco, M. J., 1994, "Yielding Pillar Gate Road Design Considerations for Longwall Mining," U.S. Bureau of Mines, Special Pub. 01-94, pp. 19-36.

Dunrud, C. R. and F. W. Osterwald, 1965, "Seismic Study of Coal Mine Bumps, Carbon and Emery Counties, Utah," AIME Transactions, v. 235, pp. 174-182.

Fajklewicz, Z., 1983, "Rock Burst Forecasting and Genetic Research in Coal Mines by Microgravity Method," Forecasting Rock Bursts, Geophysics, Proc., v. 31, pp. 748-765.

Ferm, J. C. and G. A. Weisenfluh, 1981, "Cored Rocks of the Southern Appalachian Coalfields," University of Kentucky (Lexington), 112 pp.

Fine, J., 1964, "Instability of Mine Workings: Bumps, Rockbursts in the Floor and Generalized Collapse," Proceedings of the Fourth International Conference on Strata Control and Rock Mechanics, pp. 46-61.

Gauna, M., H. E. Hamilton, and B. R. Pothini, 1988, "Practical Rock Mechanics for Safety and Productivity Improvements," 7th International Conference on Ground Control in Mining, pp. 126-136.

Goode, C. A., A. Zona, and A. A. Campoli, 1984, "Controlling Coal Mine Bumps," Coal Mining, v. 21, No. 10, pp. 48-53.

Haramy, K. Y., K. Hanna, and J. P. McDonnell, 1985, "Investigations of Underground Coal Mine Bursts," Fourth Conference on Ground Control in Mining, pp. 127-134.

Haramy, K. and J. McDonnell, 1988, "Causes and Control of Coal Mine Bumps," U.S. Bureau of Mines RI 9224, 35 pp.

Haramy, K., J. McDonnell, and L. Beckett, 1988, "Control of Coal Bursts," Mining Engineering, April, pp. 263-267.

Hargraves, A. J., 1958, "Instantaneous Outbursts of Coal and Gas," Proceedings of the Australian Institute of Mining and Metallurgy, No. 186, pp. 21-72.

Heasley, K. A., 1991, "An Examination of Energy Calculations Applied to Coal Mine Bump Prediction," 32nd U.S. Symposium on Rock Mechanics, pp. 481-490.

Heasley, K. A. and D. M. Pappas, 1993, "Gate Road Design Decreases Energy Release and Eliminates Face Bumps," U.S. Bureau of Mines, RI, in Press.

Heasley, K. A. and J. C. Zelanko, 1992, "Pillar Design in Bump-Prone Ground Using Numerical Models with Energy Calculations," Proceedings of the Workshop on Coal Pillar Mechanics and Design, U.S. Bureau of Mines IC 9315, pp. 50-60.

Heasley, K. A., 1989, "Understanding the Hydraulic Pressure Cell," Paper in Rock Mechanics as a Guide for Efficient Utilization of Natural Resources, ed. by A. W. Khair, 30th U.S. Symposium on Rock Mechanics, A. A. Balkema, Boston, pp. 485-492.

Hennen, R. V., 1915, "Wyoming and Mcdowell Counties," West Virginia Geological Survey County Report, 783 pp.

Herd, W., 1930, "Bumps in No. 2 Mine, Springhill, Nova Scotia," AIME Transactions, v. 88, pp. 151-206.

Hodgson, J. and N. C. Joughin, 1967, "The Relationship Between Energy Release Rate, Damage, and Seismicity in Deep Mines," Failure and Breakage of Rock, Proceedings of the Eighth Symposium on Rock Mechanics, pp. 194-203.

Hoek E., M. W. Grabinsky, and M. S. Diederichs, 1991, "Numerical Modeling for Underground Excavation Design," Journal Transactions, Institute of Mining and Metallurgy, v. 100, Section A, pp. A22-A30.

Holland, C. T. and E. Thomas, 1954, "Coal Mine Bumps - Some Aspects of Occurrence, Cause, and Control," U.S. Bureau of Mines Bulletin No. 535.

Holland, C. T., 1958, "Cause and Occurrence of Coal Mine Bumps," AIME Transactions, v. 211, pp. 994-1004.

Holland, C. T., 1942, "Physical Properties of Coal as Related to Causes of Bumps in Mines," AIME Transactions, v. 149, pp. 75-93.

Holling, C. S., 1978, "Adaptive Environmental Assessment and Management," Wiley, Chichester.

Iannacchione, A. T., A. A. Campoli, and D. C. Oyler, 1987, "Fundamental Studies of Coal Mine Bumps in the Eastern United States," Rock Mechanics, Balkema, pp. 1063-1072.

Iannacchione A. T., A. A. Campoli, and D. C. Oyler, 1987, Fundamental Studies of Coal Mine Bumps in the Eastern Portion of the United States," 28th U.S. Symposium on Rock Mechanics.

Iannacchione, A. T. and M. J. DeMarco, 1992, "Optimum Mine Designs to Minimize Coal Mine Bumps: A Review of Past and Present U.S. Practices," New Technology in Mine Health and Safety, Proc. of the Symp., SME Annual Meeting, Phoenix, AZ, Feb. pp. 235-247.

Iannacchione, A. T., 1988, "Behavior of a Coal Pillar Prone to Burst in the Southern Appalachian Basin of the United States," Paper in Proceedings of Second International Symposium of Rockbursts and Seismicity in Mines,
pp. 427-439.

Jacobi, O., 1966, "Occurrence, Causes, and Control of Rock Bursts in the Ruhr District," International Journal of Rock Mechanics, Mineral Science, and Geomechanics Abstracts, v. 3, pp. 205-219.

Kidybinski, A., 1981, "Bursting Liability Indices of Coal," International Journal of Rock Mechanics, Mineral Science, and Geometrics Abstracts, v. 18, pp. 295-304.

King, H. J., and B. N. Whittaker, 1971, "A Review of Current Knowledge on Roadway Behavior," Proceedings of the Symposium on Roadway Strata Control, Institute of Mining and Metallurgy, pp. 73-87.

Krawiec, A. and T. Stanislaw, 1977, "Rock Bursting in Polish Deep Coal Mines in Light of Research and Practical Experience," AIME Transactions, v. 262, pp. 30-36.

Kripakov, N. P., L. A. Beckett, D. A. Donato, and J. S. Durr, 1988, "Computer-Assisted Mine Design Procedures for Longwall Mining," U.S. Bureau of Mines RI 9172, 38 pp.

Lama, R. D., 1967, "Some Aspects of Planning of Deposits Liable to Rock Bursts," Journal of Mines, Metals, and Fuels, pp. 149-158.

Lessley, C. L., 1983, "Investigation of Coal Bumps in the Pocahontas No. 3 Seam," Masters Thesis, Virginia Polytechnical Institute and State University, 302 pp.

Mark, C. and A. T. Iannacchione, 1992, "Coal Pillar Mechanics: Theoretical Models and Field Measurements Compared," Proceedings of the Workshop on Coal Pillar Mechanics and Design, U.S. Bureau of Mines IC 9315, pp. 78-93.

Mark, C., 1990, "Pillar Design Methodology for Longwall Mining," U.S. Bureau of Mines IC 9247, 53 pp.

McCall, T. L., 1934, "Further Notes on Bumps in No. 2 Mine, Springhill, Nova Scotia," AIME Transactions, v. 108,
pp. 41-71.

Newman, D. A, 1985, "The Design of Coal Mine Roof Support and Yielding Pillars for Longwall Mining in the Appalachian Coalfields," Ph.D. Thesis, The Pennsylvania State University, 392 pp.

Neyman, B., A. Szecowka, and W. Zuberek, 1972, "Effective Methods for Fighting Rock Bursts in Polish Collieries," Fifth International Strata Control Conference, 9 pp.

Obert, L. and W. Duvall, 1967, "Rock Mechanics and the Design of Structures in Rock," Wiley, 650 pp.

Obert, L. and W. Duvall, 1945, "Microseismic Method of Predicting Rock Failure in Underground Mining," U.S. Bureau of Mines RI 3797, 14 pp.

Osterwald, F. W., 1962, "USGS Relates Geological Structures to Bumps and Deformation in Coal Mine Workings," Mining Engineering, pp. 63-68.

Oyler, D. C., A. A. Campoli, and F. E. Chase, 1987, "Factors Influencing the Occurrence of Coal Pillar Bumps at the 9-Right Section of the Olga Mine," 6th International Conference on Ground Control in Mining, pp. 10-17.

Pappas, D. M. and C. Mark, 1993, "Behavior of Simulated Longwall Gob Material," U.S. Bureau of Mines, RI 9458, 39 pp.

Peng, S. S. and H. S. Chiang, 1984, Longwall Mining, Wiely, 708 pp.

Peparakis, J., 1958, "Mountain Bumps at the Sunnyside Mines," AIME Transactions, v. 211, pp. 982-986.

Phillips, D. W., 1944, "Rock Bursts or Bumps in Mines," Transactions of the Institute of Mining Engineers, v. 104, pp. 55-91.

Rice, G. S., 1935, "Bumps in the Coal Mines of the Cumberland Field, Kentucky and Virginia, Causes and Remedy," U.S. Bureau of Mines RI 3267.

Salamon, M. D. G., "Mechanism of Caving in Longwall Coal Mining," Paper in Rock Mechanics Contributions and Challenges: Proceedings of the 31st U.S. Symposium, ed. by W. A. Hustrulid and G. A. Johnson (Denver, CO, June 18-20, 1990), A. A. Balkema, 1990, pp. 161-168.

Salamon, M. D. G., 1984, "Energy Considerations in Rock Mechanics: Fundamental Results," Journal of the South African Institute of Mining and Metallurgy, v. 84, pp. 233-246.

Sames, G. P. and J. C. Zelanko, 1994, "Development of Geology Based Bump Hazard Criteria," Computer Methods and Advances in Geomechanics, Balkema, ISBM 90 5410 3809, pp. 1883-1888.

Serta S., 1991, "Recent Advancement of Stress Control Method, Longwall USA, International Exhibition and Conference, June, Pittsburgh, PA, pp. 266-283.

Shepard, R. and W. H. Kellet, 1973, "Strata Behavior: A Study on Faces and Roadways Under a Sandstone Roof Liable to Rock Bumps," Colliery Guardian, pp. 93-102.

Shepherd, J., L. K. Rixon, and L. Griffiths, 1981, "Outbursts and Geological Structures in Coal Mines: A Review," International Journal of Rock Mechanics, Mining Science, and Geomechanics, v. 18, pp. 276-283.

Sikora, W., A. Kidybinski, and K. Saltysec, 1978, "Designing of Hard Roof-Rock Destressing Systems for Safe Warning of Rock Burst Prone Coal Seams," Central Mining Institute Report, Poland, 26 pp.

Sinha, K. P., 1979, "Displacement Discontinuity Technique for Analyzing Stresses and Displacements Due to Mining in Seam Deposits," Ph.D. Thesis, University of MN, University Microfilms International, Ann Arbor, MI, Facsimile No. 7918390, 311 pp.

Starfield, A. M. and A. L. Bleloch, 1968, "Building Models for Conservation and Wildlife Management," Macmillan, NY.

Starfield A. M. and P. A. Cundall, 1988, "Towards a Methodology for Rock Mechanics Modelling," International Journal of Rock Mechanics, Mining Science & Geomechanics, v. 25, No. 3, pp. 99-106.

Talman, W. G. and J. L. Schroder, 1958, "Control of Mountain Bumps in the Pocahontas No. 4 Seam," AIME Transactions, v. 211, pp. 888-891.

U.S. Code of Federal Regulations, "Title 30--Mineral Resources; Chapter I--Mine safety and Health Administration, Department of Labor; Subchapter O--Coal Mine Safety and Health; Subpart C--Roof Support," Part 75, July 1989, p. 494.

Vogle M., C. Fairhurst, and P. A. Cundall, 1978, "Analysis of Tunnel Support Loads Using a Large Displacement, Distinct Block Model," Storage in Excavated Rock Caverns, Oxford, v. 2, pp. 247-252.

Walsh, J. B., 1977, "Energy Changes Due to Mining," International Journal of Rock Mechanics and Mining Science v. 14, pp. 25-33.

Wang, F. D., W. A. Skelly, and J. Wolgamott, 1976, "In Situ Coal Pillar Strength Study," (Contract H0242022, Colorado School of Mines), U.S. Bureau of Mines OFR 107-79, 243 pp.

Wilson, A. H., 1973, "A Hypothesis Concerning Pillar Stability," Mining Engineering, London, v.131, pp. 409-417.

Zelanko, J. C., G. A. Rowell, and T. M. Barczak, 1991, "Analysis of Support and Strata Reactions at a Bump-Prone Eastern Kentucky Coal Mine," 1991 SME Annual Meeting and Exhibit, SME Preprint No. 91-91, 8 pp.

Zipf, R. K., 1992, "MULSIM/NL Theoretical and Programmers Manual," U.S. Bureau of Mines IC 9321, 52 pp.

Zipf, R. K., 1992, "MULSIM/NL Application and Practitioner's Manual," U.S. Bureau of Mines IC 9322, 48 pp.

Zipf, R. K. and Heasley, 1990, "Decreasing Coal Bump Risk Through Optimal Cut Sequencing With a Non-Linear
Boundary Element Program," Proc. 31st U.S. Symp. on
Rock Mechanics, Denver, CO, June, pp. 947-954.

Appendix A

ANALYSIS OF RETREAT MINING CASE HISTORIES

The following case studies document conditions encountered in two room-and-pillar retreat mines and one longwall retreat mine subject to coal mine bumps. The W-P 21 Mine case illustrates the negative impact of mixed pillar sizes on an other wise acceptable design. The Olga Mine case study demonstrates the successful implementation of the stress shield concept following a bump failure due to an under designed supercritical section. The VP No. 3 Mine case study successfully employed the stress shield concept to retreat longwall mining under bump prone conditions. The Olga and VP No. 3 Mines were the subject of intensive in-mine geotechnical evaluations. These results were employed in the development of the principles that support the program LAYOUT.

A.1 W-P 21 Mine

W-P No. 21 Mine worked the Chilton Coalbed of the Kanawha Formation (Pottsville Group, Pennsylvanian System) near Stirrat, Logan County, WV. The coalbed displays irregular thickness, but averages about 4 ft. The Chilton is generally multiple-bedded, with intervening partings of shale and bone (fig. A.1).

Above the coalbed is the solid, light gray Lower Winifrede Sandstone (Hennen, 1915). The sandstone is poorly cemented and brittle and usually breaks at the pillar line. The thickness of the overlying sandstone is fairly uniform. Except for

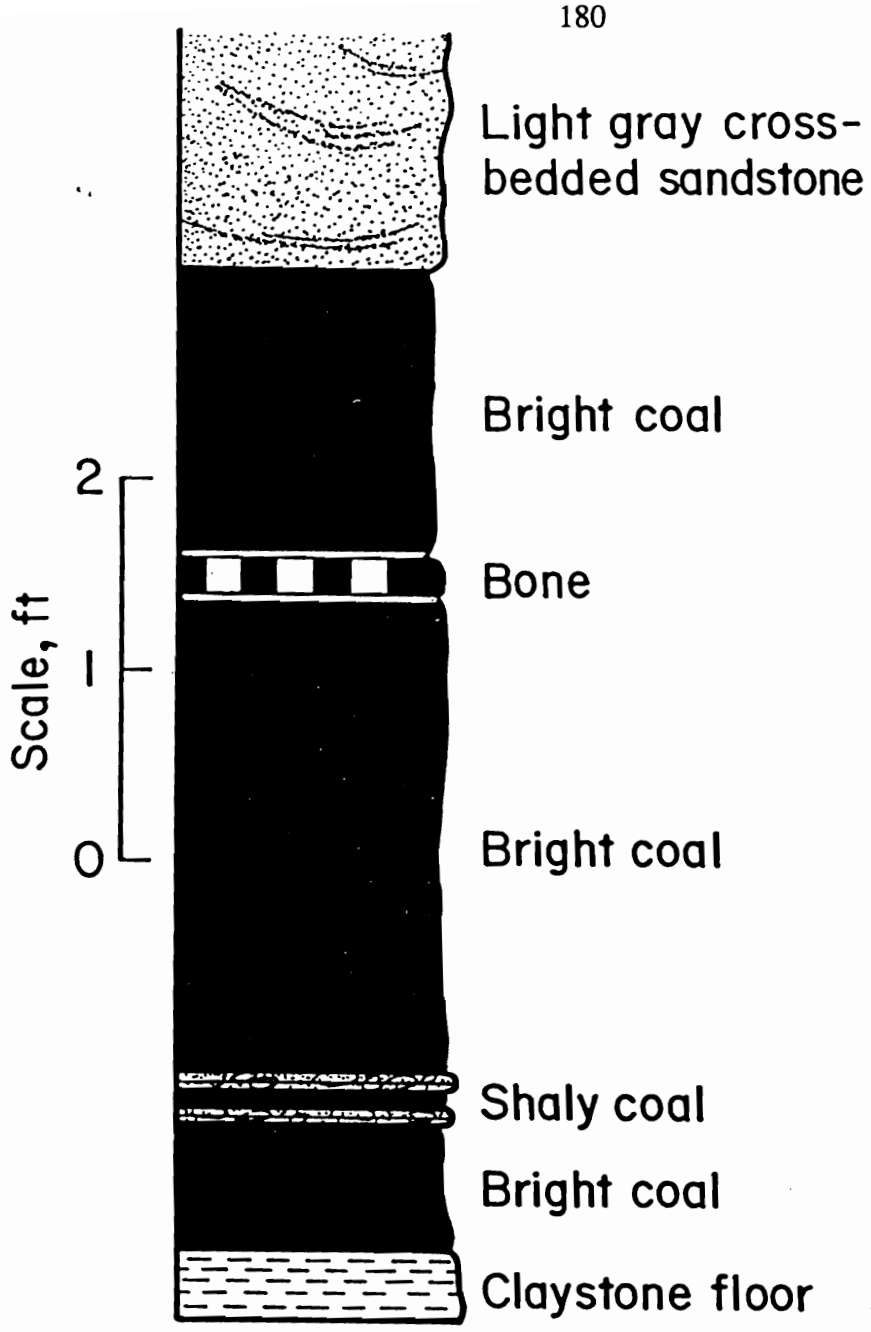

Figure A.1—Stratigraphic column W-P No. 21 Mine (After Campoli, et al., 1987).

one corehole data point in the northeastern most portion of the studied area, the sandstone is generally 40 to 60 ft thick (fig. A.2).

W-P No. 21 Mine, located in the Appalachian Plateau physiographic province, is situated in a relatively uncomplicated structural setting. The mine lies on the east flank of the Handley Syncline, therefore, the coalbed drops in elevation toward the northwest. No faults or clastic dikes have been observed in the area of the mine.

In comparison with other bump-prone mines, overburden depths at the mine are relatively shallow (fig. A.3). The mine is outlined, for the most part, by the outcrop of the Chilton Coalbed. Only under the hilltops does the overburden thickness increase to over 700 ft. A fatal bump occurred in one of these areas of maximum overburden thickness (fig. A.3).

Continuous miners are employed exclusively in W-P No. 21 Mine. Mining is by the room-and-pillar system. When retreat mining is performed, pillars are removed by the split and fender (fig. A.4). Cuts are made in the numbered sequence shown. Each pillar is split, then the outside wings are removed. Finally, the inside wings are mined in tandem, producing a high coal yield and essentially total extraction.

On November 29, 1983, a bump occurred, killing one miner and severely injuring another (Davis, 1983). The depth of cover over this area was 752 ft, which approaches the maximum overburden encountered in the mine. A map of the bump area is shown in figure 5.2. Pillars numbered 4 and 5 bumped with sufficient force to move a 26.5 ton continuous mining machine 15 ft. The miner was cutting the face of

pillar 5 when the accident occurred. Mine officials indicated that a similar bump took place 3 weeks prior to the fatality, during the mining of the pillars inby pillars 4 and 5.

A closer view of the accident area is mapped in figure A.5. Note, the standing gob directly inby and to the left of pillar 4, where the pin machine (roof bolter) was located. The fall of immediate roof only in the gob area of pillars 1 and 2 is also significant. The combination of the stress transferred from the yield pillars directly adjacent to pillar no. 5 (fig. A.5) by the rigid roof and the standing gob led to the bump event. Five rows of pillars were left as a barrier (fig. 5.2), full extraction was discontinued and a partial extraction procedure was instituted. This pillar splitting reduced the extraction rate from nearly total to less than 60 pct (Campoli, et al., 1987).

A.2 Olga Mine

The Olga Mine was closed in early 1987. Prior to that, the mine had been in continuous operation since the early 1900s. The mine has a long history of coal mine bumps. The 9 Right section of the mine was the subject of an extensive geotechnical evaluation by the Bureau (Campoli, et al., 1990b). At the time of this study, mining was conducted exclusively by room-and-pillar methods using continuous miners. The majority of retreat mining involved removing barrier

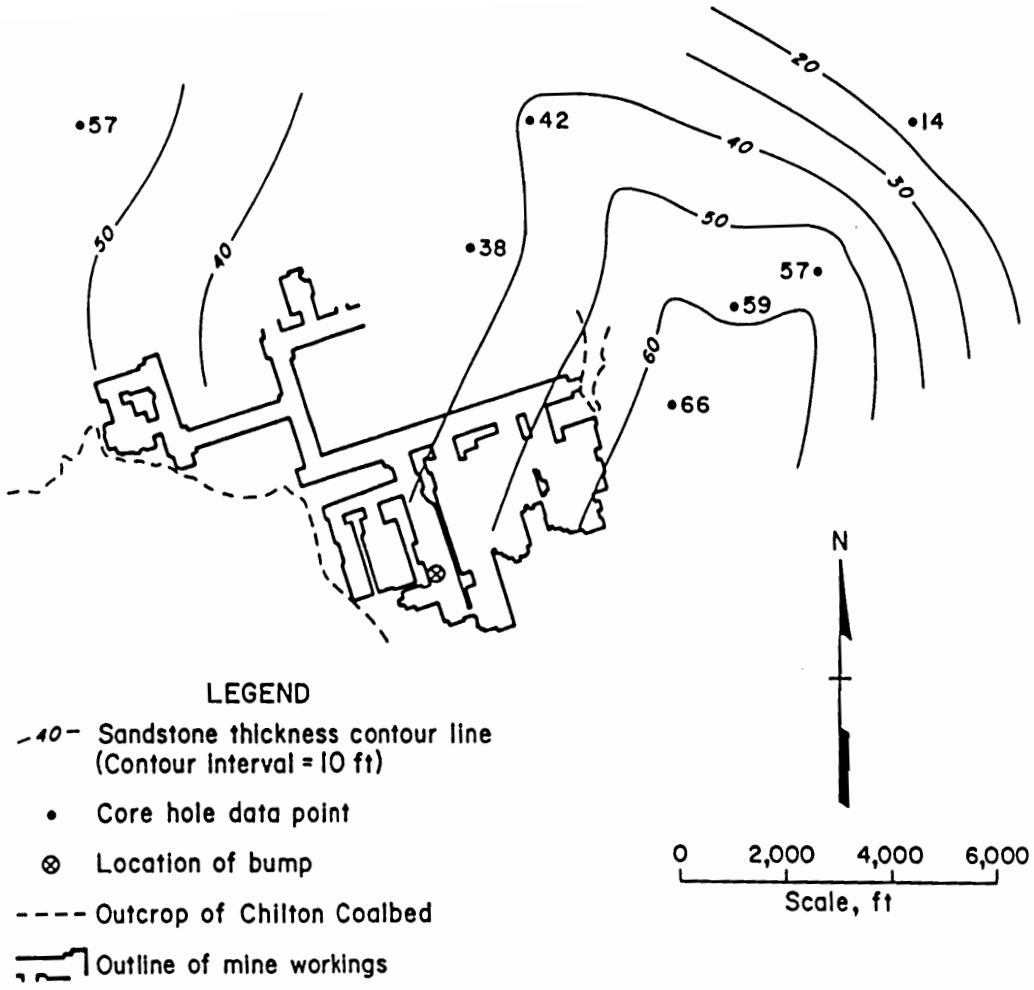

Figure A.2—Sandstone thickness map of the Lower Winifrede Sandstone, which immediately overlies the Chilton Coalbed, W-P No. 21 Mine (After Campoli, et al., 1987).

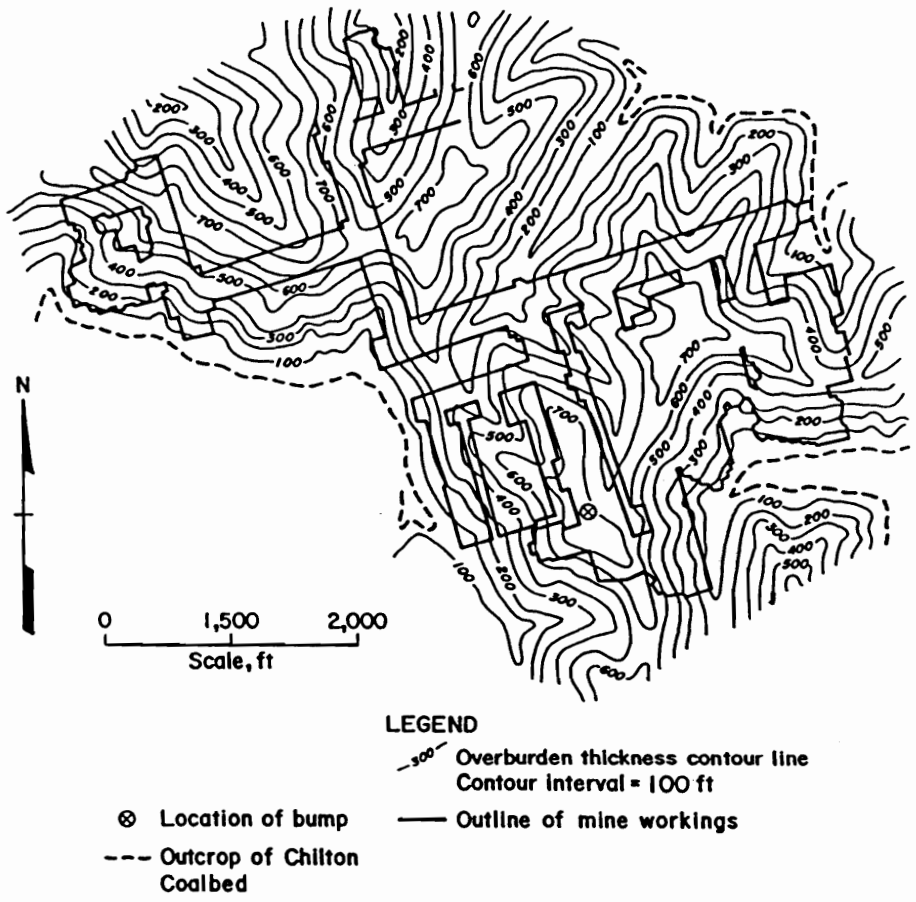

Figure A.3—Overburden map for W-P No. 21 Mine (After Campoli, et al., 1987).

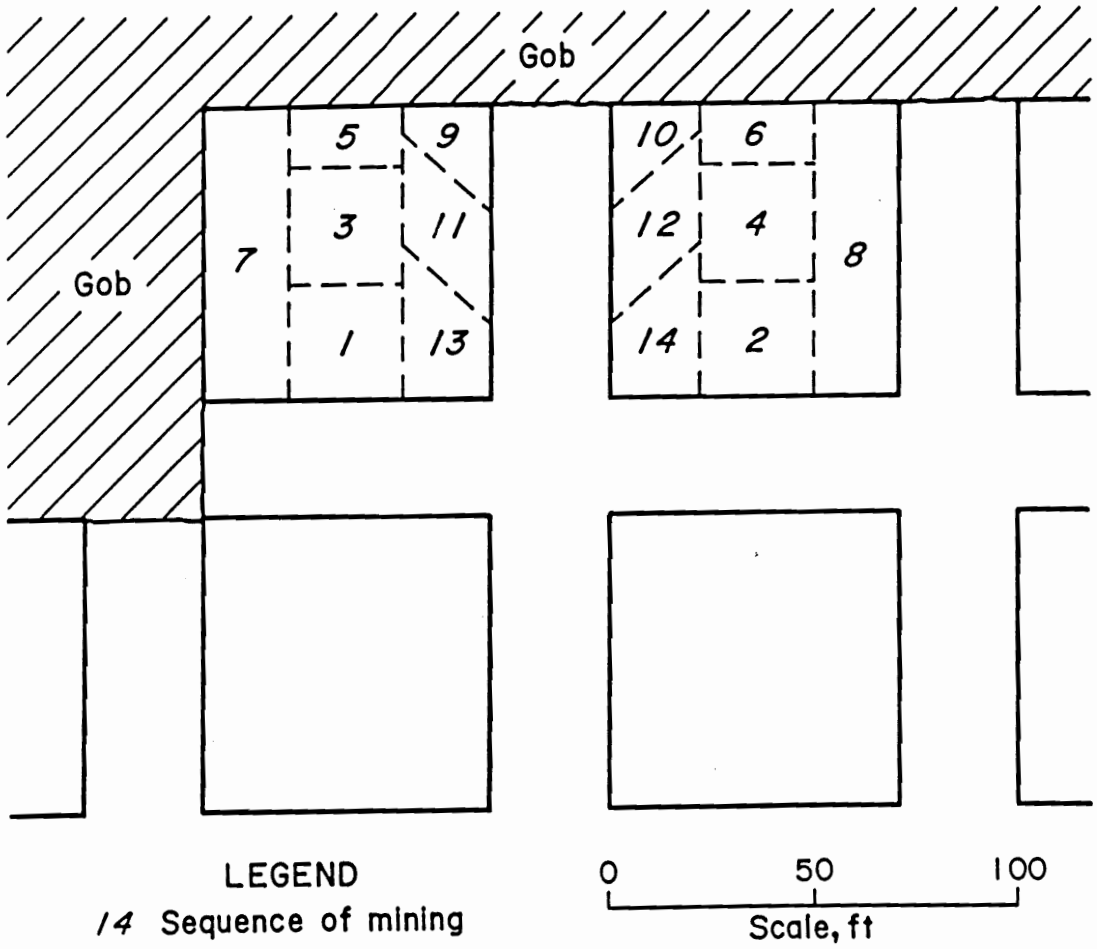

Figure A.4—Split and fender method mining sequence, W-P No. 21 Mine (After Campoli, et al., 1987).

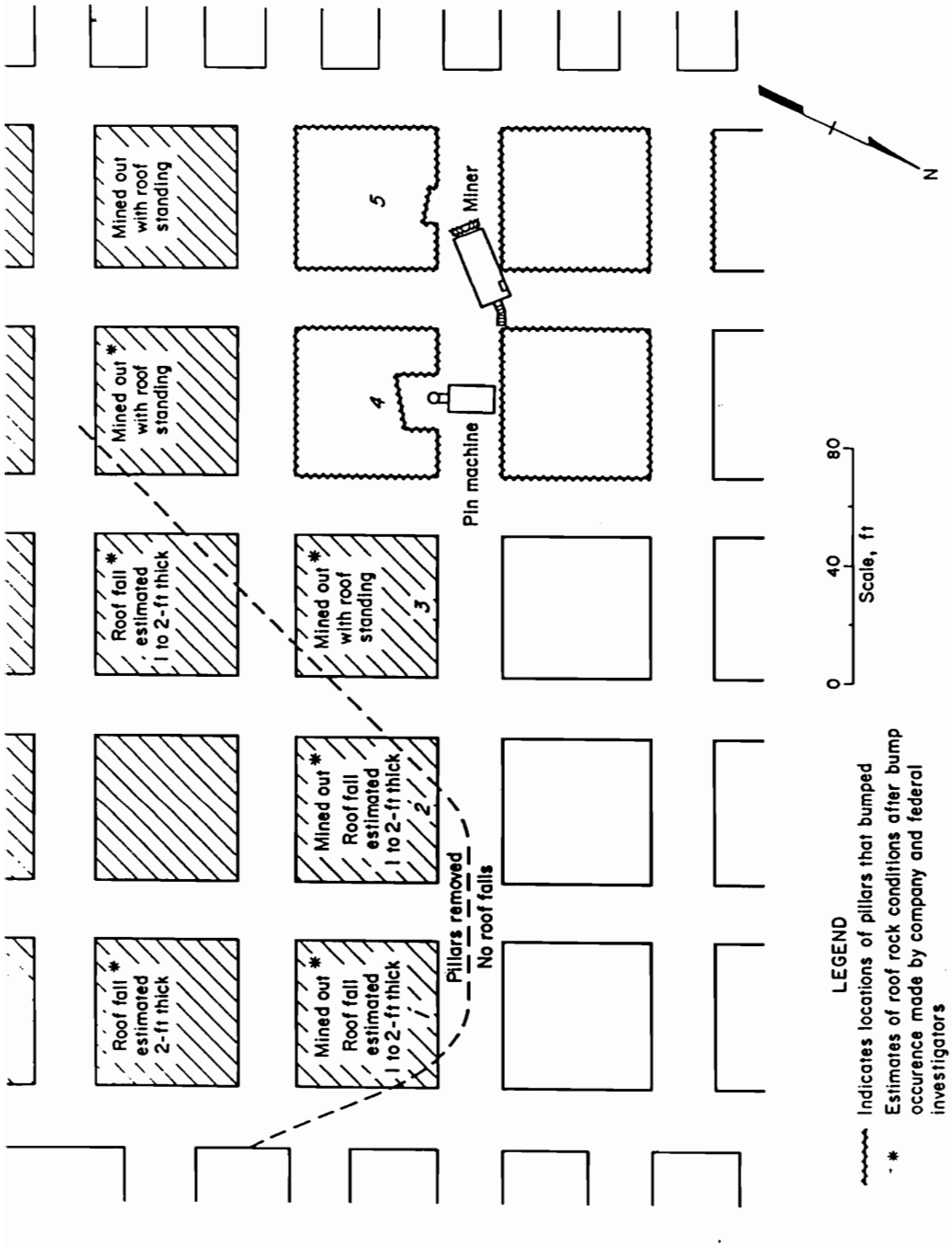

Figure A.5—Plan view of immediate area of bump accident, W-P No. 21 Mine (After Campoli, et al., 1987).

pillars that had been left to protect access roadways driven many years ago. Often, these barrier pillars were adjacent to gob areas.

The Olga Mine extracts the Pocahontas No. 4 Coalbed, which averages 66 in thick (fig. 3.3). The coalbed average compressive strength is estimated at 2,400 psi, as indicated in table A.1 (Iannacchione, et al., 1987b). The 9 Right section is located under the greatest overburden found on the property (fig. A.6). Overburden ranges from 990 to slightly over 1,600 ft in the study area, and from approximately 400 to greater than 1,600 ft mine wide. Major bump sites occurred under overburden greater than 500 ft.

The Upper Pocahontas Sandstone is situated below the Pocahontas No. 4 Coalbed. This sandstone unit is laterally discontinuous in the interval 0 to 5 ft below the coalbed (fig. 3.3) (Hennen, 1915). Within this 5 ft interval, the fine to medium grained Upper Pocahontas Sandstone sometimes laterally grades into a competent siltstone and shale units. Physical properties data for the floor members are listed in table A.1. In addition to being strong relative to other coal measure rocks found in the eastern U.S., the Upper Pocahontas Sandstone in the study area has a high Rock Quality Designation (R.Q.D.) value of 95 to 100 pct (Deere, et al., 1977). The siltstone found in the floor has an R.Q.D. of 90 pct and the shales 64 pct, with fractures on bedding planes. All R.Q.D. data must be considered in the light of the

TABLE A.1 - Mean value of strata physical properties at the 9-Right section of the Olga Mine (After Iannacchione, et al., 1987b).

Strata type	Compressive Strength (psi)	Tensile strength (psi)	Young's modulus[1] (10^6 psi)	Poission's ratio[1]
Sandstone roof	24,200 (40)[2]	1,070 (21)	5.16 (3)	0.30 (3)
Sandstone floor	21,900 (15)	1,010 (12)	5.45 (3)	0.39 (3)
Shale floor	12,600 (18)	970 (6)	3.97 (3)	0.29 (3)
Siltstone floor	16,900 (14)	1,320 (2)	-	-
Coal	2,400 (6)	-	0.61 (6)	0.31 (6)

[1]Tangent (calculated at 50 pct of ultimate strength).
[2]Number of samples tested.

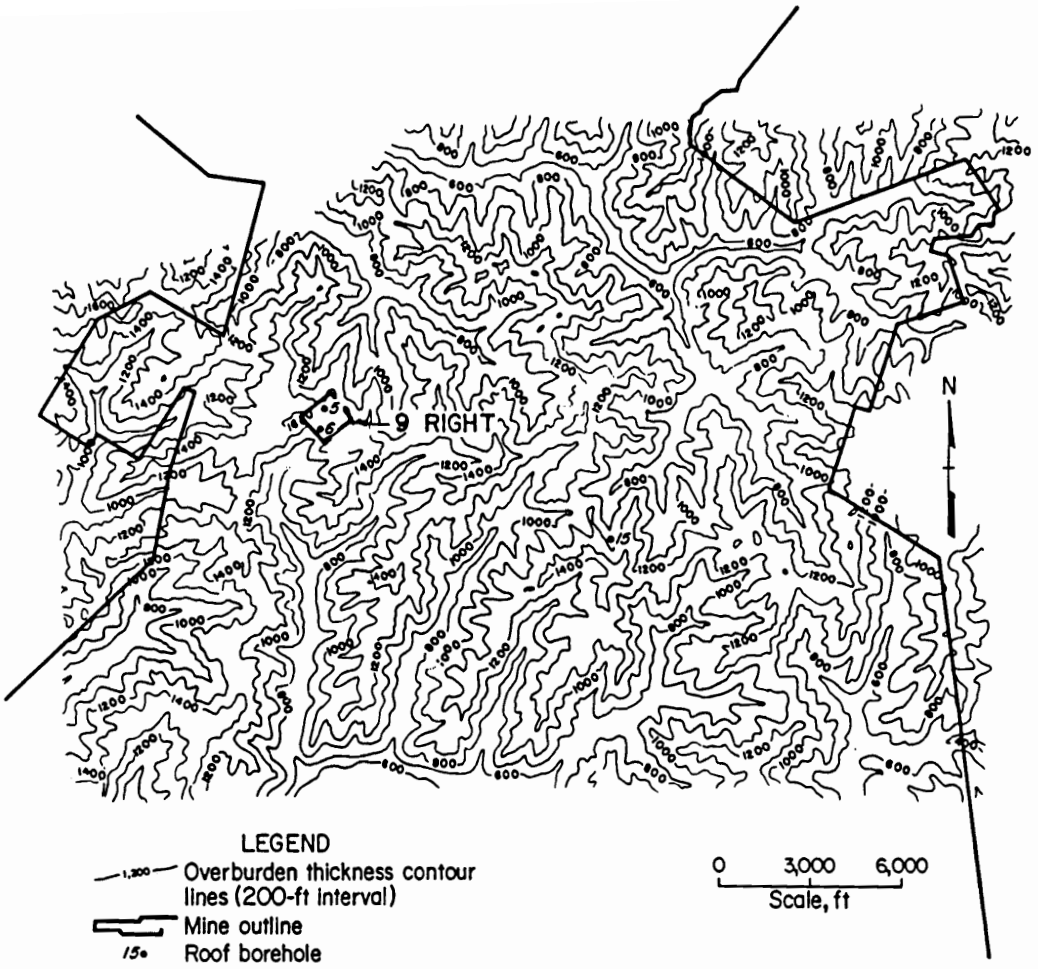

Figure A.6—Overburden map above the Pocahontas No. 4 Coalbed, Olga Mine (After Campoli, et al., 1990b).

fact that the cores were taken from holes drilled from underground entries that were standing for over 50 years. The Upper Pocahontas Sandstone ranges in thickness from 50 to 75 ft (Hennen, 1915). Under portions of the mine, this sandstone provides a competent and massive floor which does not heave or break readily. As figure 3.4 illustrates, 11 out of 13 bumps associated with injuries or fatalities occurred where the immediate and main floor were 80 to 100 pct sandstone.

The Eckman Sandstone forms the immediate and main roof at Olga and is a very stiff and massive unit (table A.1). This unit can be 60 or more ft thick and contains a joint system that is unidirectional, extremely pronounced, and widely spaced. The roof has an R.Q.D. of 95 pct and a Final Rock Mass Rating (R.M.R.) of 108 (Newman, 1985). As shown in figure A.10, every bump occurred where the roof was predominately sandstone (80-100 pct). Therefore, bump-prone areas may be anticipated based on the above geologic correlations. Any area in the mine where the roof-and-floor members are predominately composed of a stiff sandstone should be considered bump-prone.

A.2.1 Fatal Bump

On October 18, 1983, two miners were killed by a bump on a continuous miner section in which a barrier pillar was being extracted under 1,100 ft of overburden (Blankenship and Castanon, 1983). A hard sandstone approximately 60 ft thick was present immediately above the coalbed. The bump occurred during the mining of a 140 by 350 ft barrier pillar (fig. A.7). Eight rooms on 39 ft centers

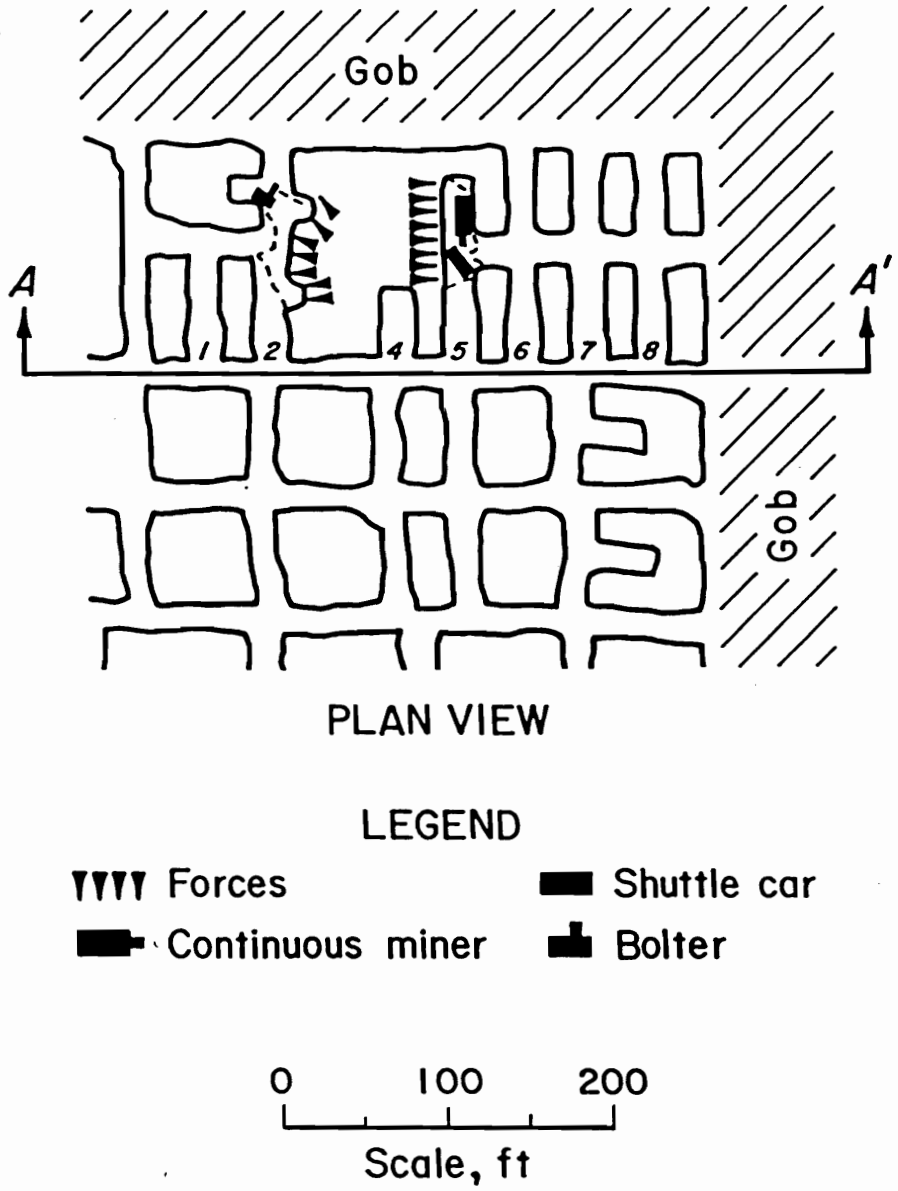

Figure A.7—Plan view of the area of the bump accident of Oct. 18, 1983, Olga Mine (After Campoli, et al., 1987).

were planned to divide the pillar. Forces from the bump moved the continuous miner against the right rib and the shuttle car into the crosscut between rooms 5 and 6 (fig. A.7). The left rib in the No. 5 room was displaced approximately 8 ft and coal filled the remainder of the entry to a depth of 42 in for a distance of approximately 86 ft. The displaced coal is indicated by a dashed line on figure A.7. The roof bolting machine was not moved by the forces, however, coal was expelled filling the No. 2 room with coal from 3.5 to 5 ft deep, for a distance of 60 ft (Blankenship and Castanon, 1983).

According to mine management, the "narrow room method" had been used for several years. However, the specific approach to mining was determined on block-by-block evaluation, based on the knowledge of the miners and mine management (Blankenship and Castanon, 1983). Two inby barrier pillars of similar size and shape were mined prior to the fatal bump pillar (fig. A.8). The No. 2 barrier pillar was also developed using the narrow room method. It bumped expelling several tons of coal and moving the continuous miner during an idle shift. The No. 1 barrier pillar was split into blocks similar in size to the adjacent chain pillars and was retreated without incident.

The change in the projected development of the No. 3 barrier pillar was due to the bump that had occurred in the No. 2 barrier pillar. It was determined by mine management that the No. 2 room should be developed first to create a chain pillar the same size as the inby pillar, which was developed in the 1930s. Rooms 8 through 4

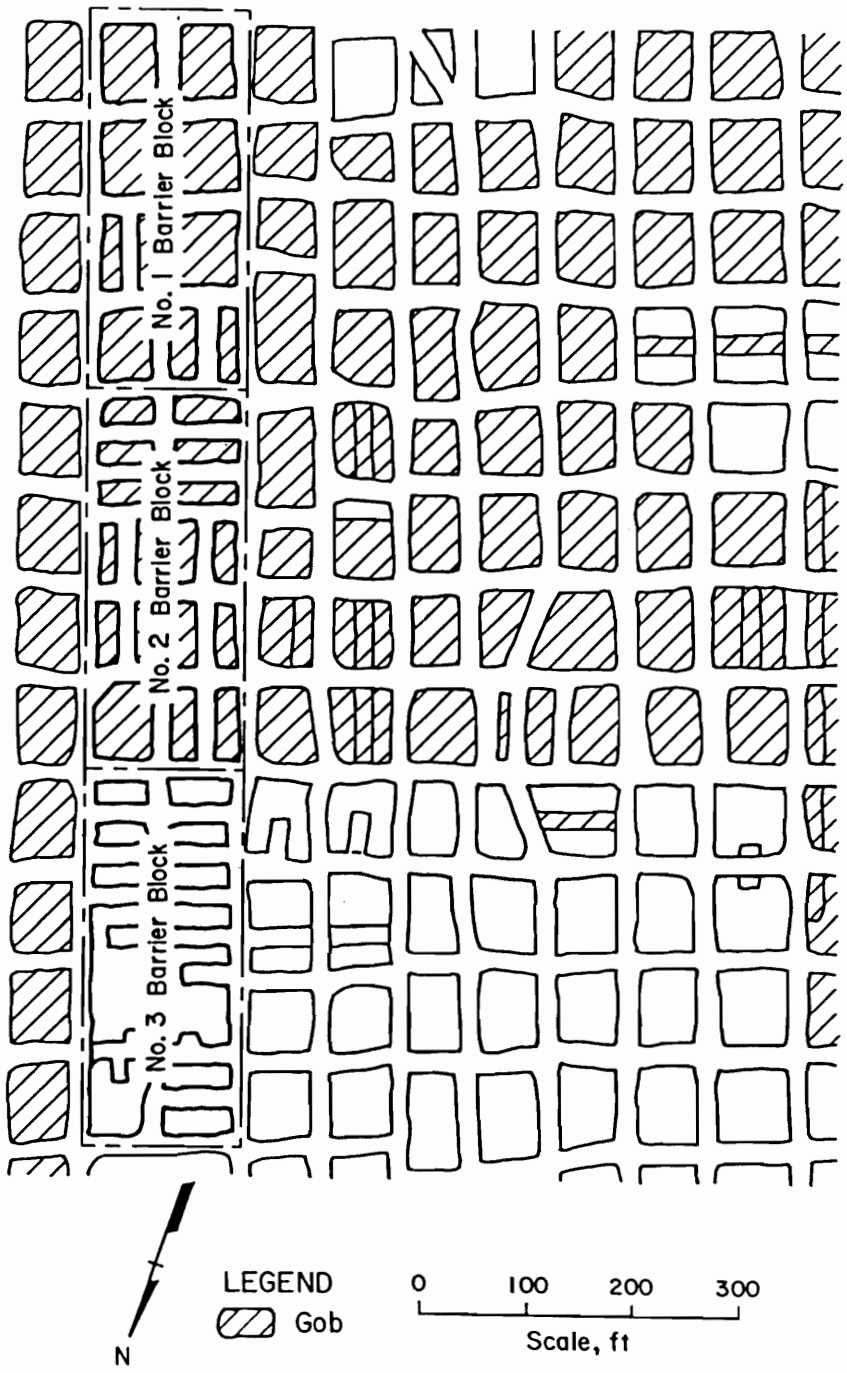

Figure A.8—Plan view of the mining sequence prior to the bump accident, Olga Mine (After Campoli, et al., 1987).

were driven in sequence to form a right to left, stepped pattern of working faces. It was hoped that this plan would allow a gradual release of any stored energy. A cut-by-cut mining plan was formulated and followed by mine management. The No. 3 barrier pillar had been mined down to a 100 by 100 ft block, located between rooms 2 and 6, surrounded by smaller pillars (fig. A.7) when the bump occurred (Blankenship and Castanon, 1983).

The No. 3 barrier pillar was located at the intersection of two gob areas, loads were transferred from both the old gob to the east and the new gob directly inby. Also, the 100 by 100 ft block was surrounded by small yielding pillars on two sides. Figure A.9 presents a theoretical schematic of the load transfer along section A-A (fig. A.7). The smaller pillars, through their convergence, permitted the rigid roof to transfer the load onto the pillar between entries 2 and 5 (fig. A.7). The bump manifested itself when the lateral forces exerted by the pressurized pillar core overcame the confining pressure of the crushed periphery. At that point, the pillar expanded laterally in explosive failure.

A.2.2 Geotechnical Evaluation

The 9 Right section was chosen for this study because it contained barrier pillars of the same size and shape as the pillars (350 by 160 ft) involved in the 1983 fatalities. The configuration of the study area at the onset of the investigation is diagramed in figure A.10. Room-and-pillar retreat mining was underway near the

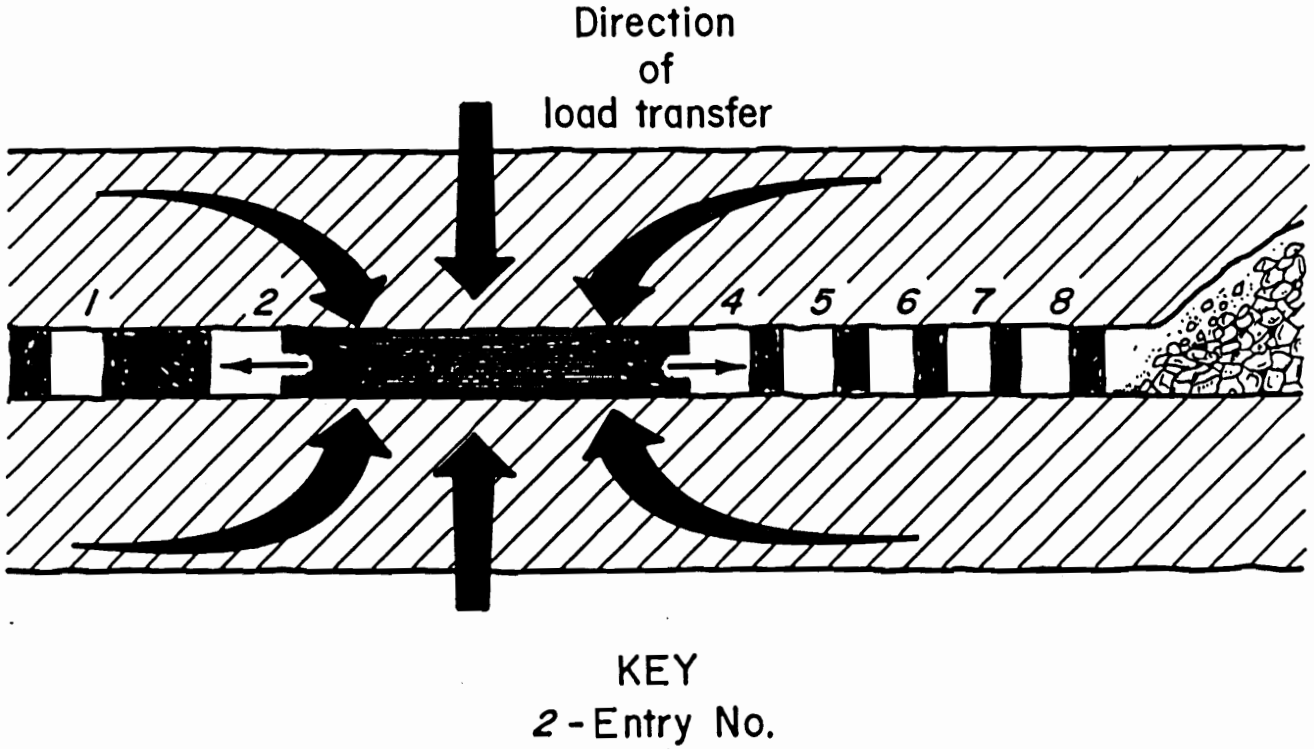

Figure A.9—Idealized diagram of abutment force transfer in the area of the bump accident, Olga Mine (After Campoli, et al., 1987).

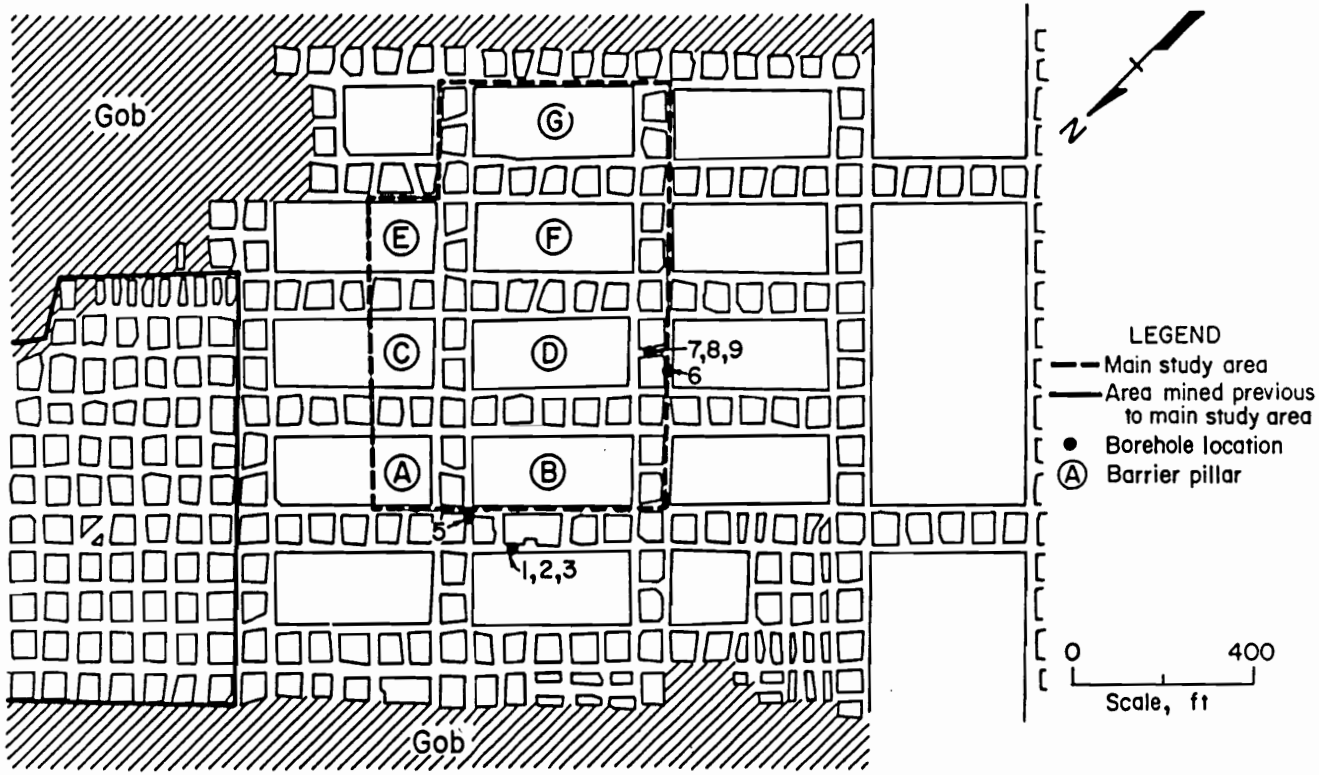

Figure A.10—Map of 9 Right study area, September 1985, Olga Mine (After Campoli, et al., 1990b).

55 by 70 ft chain pillars shown in the left portion of the study area. Upon completion of the room-and-pillar retreat mining in the left portion, barrier splitting began in the main study area. The mining of the study area eventually resulted in the complete extraction of barriers B, D, and F and the partial extraction of barriers A, C, E, and G (fig. A.10).

Barriers B, D, and F were each completely split into ten 55 by 70 ft chain pillars by advance mining. Barriers A, C, and E were each partially split into four chain pillars on the right and a 200 by 160 ft barrier on the left. These 200 by 160 ft barrier pillars shield the new barrier pillar extraction section from the abutment zone pressure originating from the gob formed by the room-and-pillar retreat mining of the left portion, completed in January 1986. Advance mining was discontinued when high stress areas were encountered during the splitting of the barrier G (fig. 5.3). Abutment loads from an old gob area, inby barrier G, caused excessive strain energy to be stored in the rigid barrier, which resulted in a bump that caused a lost time injury. A 9 by 9 block of chain pillars was outlined when the retreat mining of the chain pillars began.

A novel pillar splitting method was the primary bump control technique used in extracting the 55 by 70 ft chain pillars in the outlined block. Three rows of pillars outbye the gob were mined simultaneously to reduce strain energy storage. Generally, the first two rows of pillars outbye the gob were split along their long axes, leaving two 17.5 by 70 ft wings that yielded under abutment zone loading. The splitting of the third row generally was also begun prior to the removal of the wings

adjacent to the gob. An example of this technique is the mining from June 6 through 12, 1986 (fig. 5.3).

Figure A.11 depicts the cut sequence on three rows of chain pillars. Only the cuts taken from a 3 by 3 block of pillars are numbered. Cuts from the inby pillars in the area labeled gob would be in the sequence, as would cuts in the adjacent pillars. Both were not labeled for the sake of clarity. The chain pillars ability to store strain energy and thus bump is destroyed by the time the third center splitting cut is completed. For example, the pillars in row 2 will not bump after cuts 22-24 are extracted.

The reaction of the coal pillars to the barrier pillar mining in the study area was evaluated through measurements of changes in vertical pressures within the pillars, roof-to-floor convergence in adjacent rooms, and dilation of the pillars upon yielding. Measurement of the pressure redistribution within coal pillars was accomplished with hydraulic coal cells, made from a copper flatjack and two aluminum platens (Bauer, et al., 1985). The cells were placed in coal pillars at depths of 15 and 30 ft. These oil filled bladders, were oriented to measure relative pressure changes in the vertical direction. All the cells were initially set at 2,500 psig, this value being the estimated average pressure over the barrier pillars prior to advance mining, calculated from the tributary theory.

Entry height was measured periodically with a portable, telescopic, tube extensometer, capable of an accuracy of plus or minus 0.001 in., over a range from

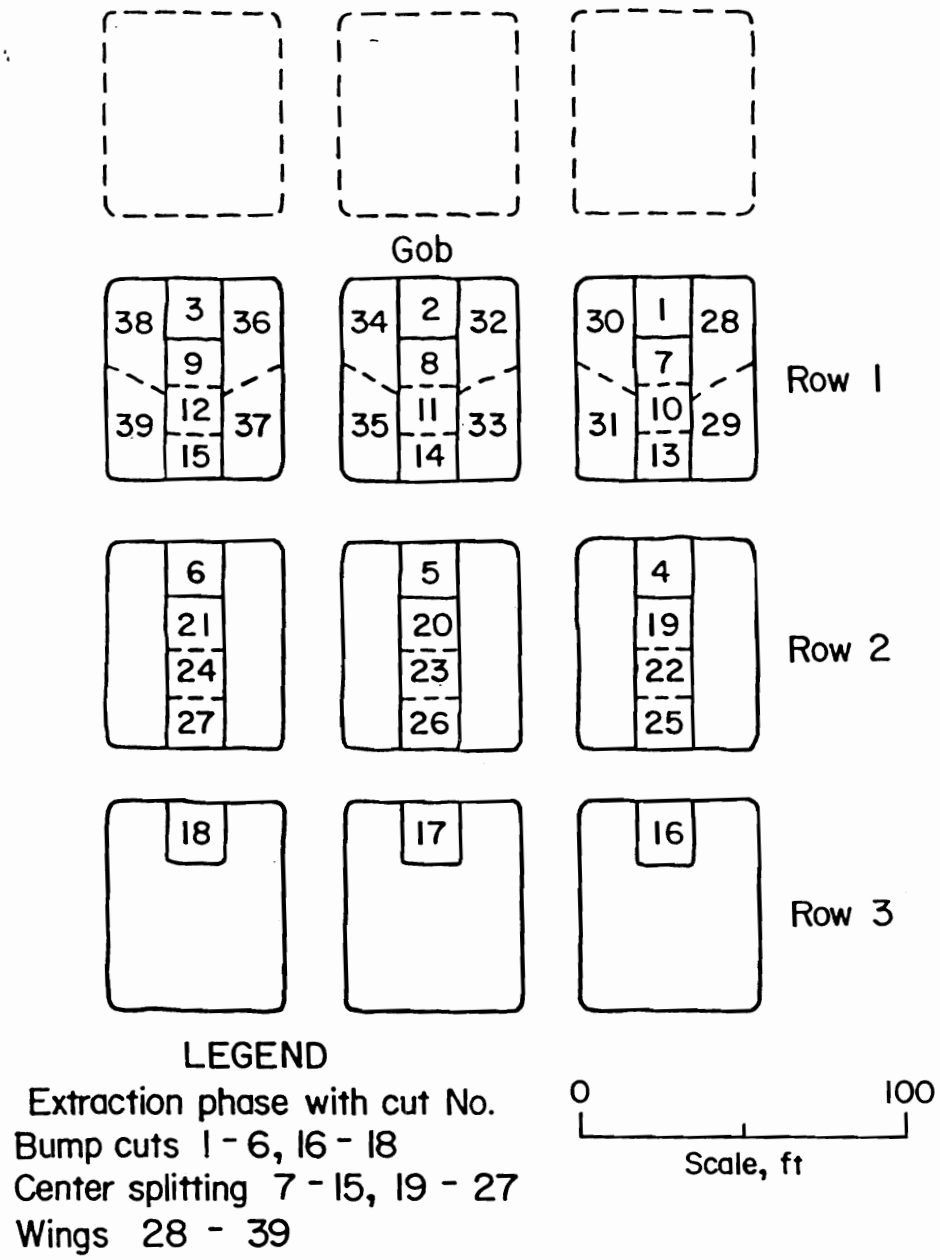

Figure A.11—Generalized pillar splitting extraction sequence, Olga Mine (After Campoli, et al., 1990b).

3 to 7 ft. Permanent anchors were installed in the roof-and-floor at each roof-to-floor convergence station location. The extensometer was moved from station to station. The frequency of readings varied from biweekly to daily depending on the proximity of mining. Dilation of coal pillars upon yielding was evaluated with multipoint extensometers. The wire extensometers were grouted into horizontal drill holes in the coal pillars at mid-seam height. Ten measurement point anchors were spaced 3 ft apart in each drill hole, over the extensometer's 30 ft length.

Analysis of a typical coal cell and the four roof-to-floor convergence stations surrounding the instrumented pillar, provides insight into the relationship between roof-to-floor convergence and coal cell pressure (Oyler, et al., 1987). The representative coal cell was located 30 ft into the center of the first barrier to be split. The coal cell was installed 5 months prior to the initial advance mining of the section. Only slight increases in the pillar pressure (to 3,000 psig from the 2,500 psig setting pressure) occurred prior to advance mining of the main study area (fig. A.12). Dramatic increases in pillar pressure (to 7,500 psig) and roof-to-floor convergence (2.000 in) were associated with the splitting of the instrumented barrier into ten 55 by 70 ft chain pillars. Coal cell pressure and roof-to-floor convergence readings leveled off during the splitting of the inby barriers. Gradual increases in both coal cell pressure and roof-to-floor convergence occurred when retreat mining began, even though mining was nine chain pillar rows inby. The maximum measured

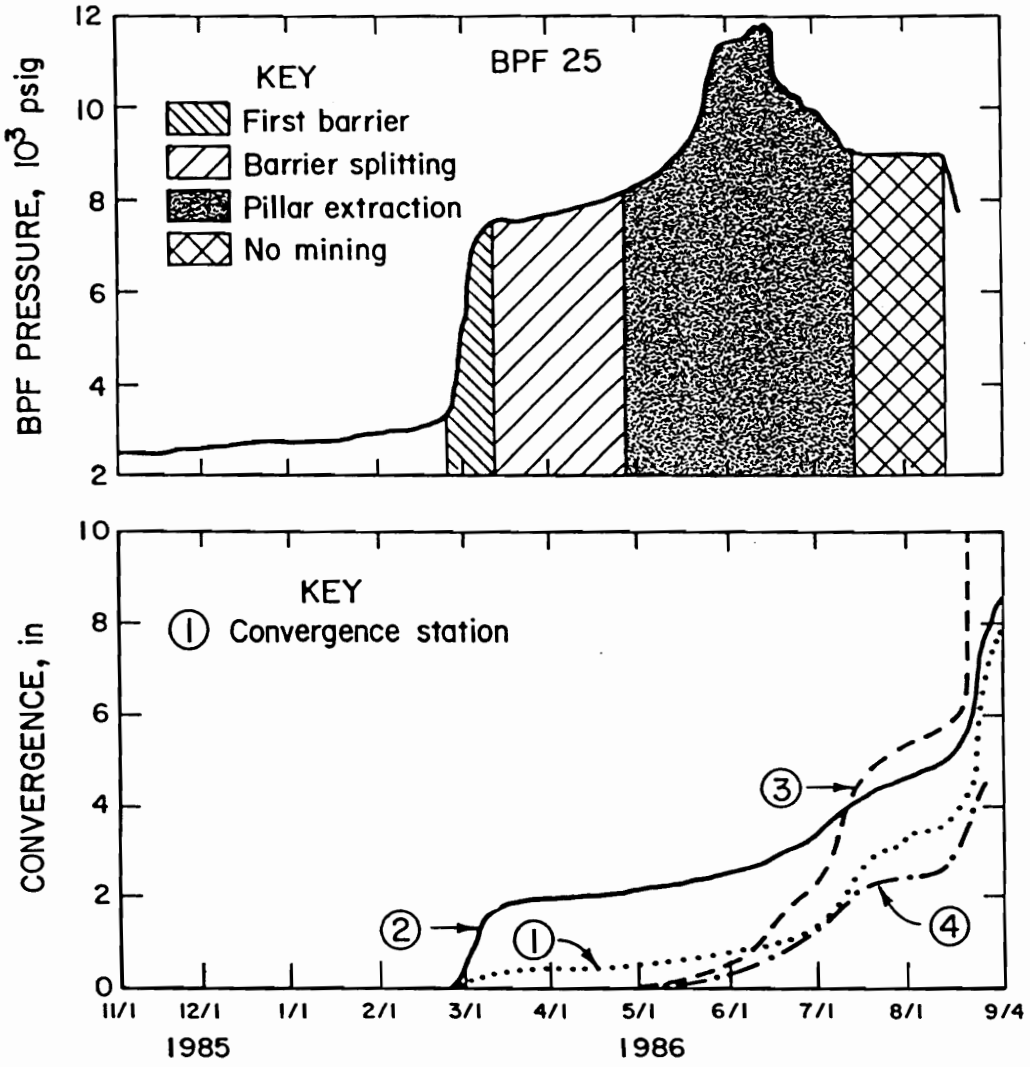

Figure A.12—Coal cell pressure in and roof-to-floor convergence around a typical instrumented chain pillar, from November 1, 1985 to September 4, 1986, Olga Mine (After Campoli, et al., 1990b).

coal cell pressure of 12,000 psig occurred when mining was five pillar rows outbye. Immediately thereafter, the roof-to-floor convergence continued around the instrumented pillar but the coal cell began to fail. Final coal cell failure occurred in mid-September after having remained stable during an idle mining period. Many of the cells were reset with a hydraulic pump when they began to lose pressure. None of the cells held the reset pressure, indicating that their bladders were leaking.

A.3 VP No.3 Mine

Retreat mining of the Pocahontas No. 3 Coalbed by the Virginia Pocahontas Division of the Island Creek Coal Company has long been associated with coal mine bumps. The effect of a gate road design change on the reaction of bump-prone strata to retreat longwall mining was evaluated in the VP No. 3 Mine, Buchanan County, Virginia. A total of 18 longwall panels have been mined at this mine (fig. A.13). Eight successive panels have been mined to the north, and ten successive panels have been mined to the south of twin barrier pillars. The gate entry system between the sixth and seventh panels to the south contained what will be referred to as the 7 development study area. The 7 development study included geotechnical instrumentation designed to document the performance of the original gate road design. The gate entry systems between the seventh and eighth panels to the south, and the ninth and tenth panels to the south contained what will be referred to as the 8 and 10 development study areas, respectively. These two study areas contained geotechnical instrumentation designed to document the performance of the improved

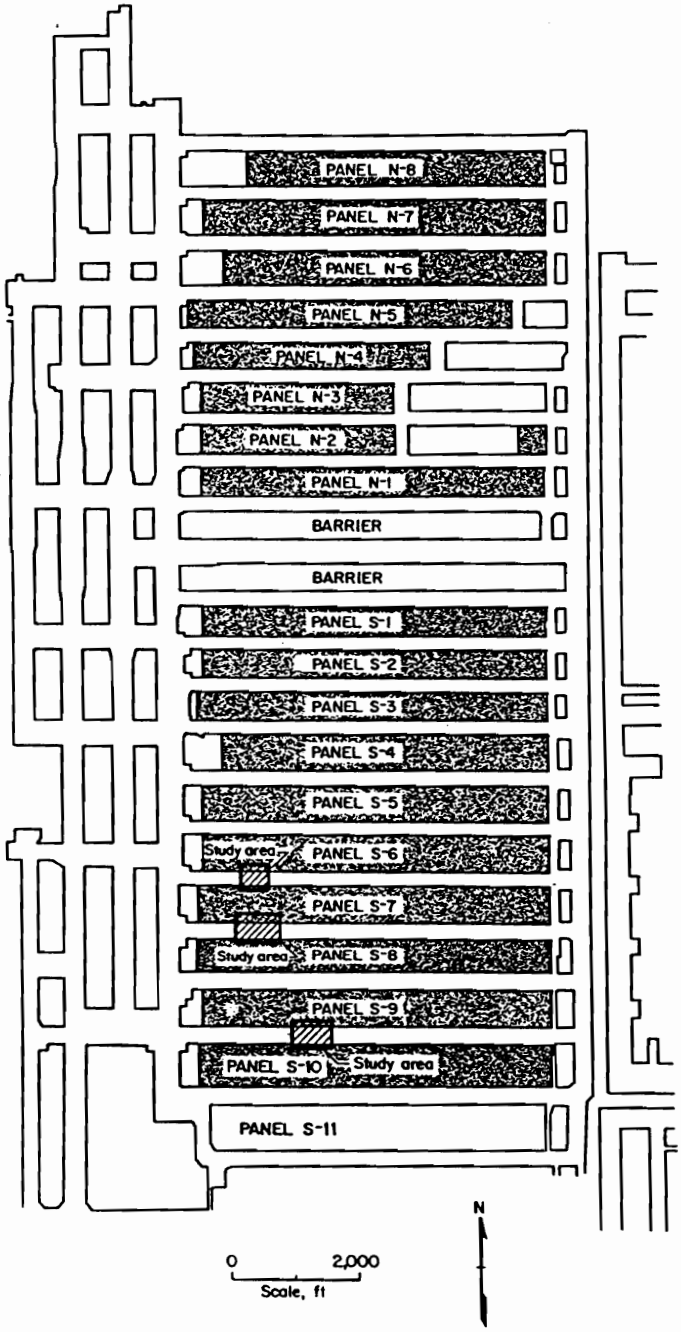

Figure A.13—Mine map, VP No. 3 Mine (After Campoli, et al., 1993).

gate road design. The 10 development instrument array was also designed to measure abutment loads on the floor of longwall gob areas. All three study area locations are indicated on figure A.13.

The VP No. 3 Mine extracts the Pocahontas No. 3 Coalbed, which is located in the Pocahontas Formation and averages 5.5 ft in thickness (fig. A.14). Mine-wide, the coalbed is under overburden ranging from 1,200 to 2,200 ft in thickness and dips 1 degree from east to west. The immediate roof, in the south end of the mine, consists of a widely jointed siltstone overlain by a very stiff, massive sandstone. Mine-wide, the siltstone ranges from a maximum thickness of 110 ft to being nonexistent. The massive sandstone in the main roof varies from a maximum thickness of 450 to a minimum of 135 ft over the mine. The mine floor, in the south end of the mine, consists of a combination of very competent siltstone and sandstone.

Underground observations, in the study area, reported by Iannacchione (1988) indicate a persistent absence of prominent roof-and-floor fractures or joints and that the main roof, dominated by the thick sandstone, is exceedingly difficult to break. Physical property values were determined from ten rock types sampled from a surface corehole. With the exception of the dark grey shale, all of the rock types have a corresponding average uniaxial compressive strength values of between 28,590 and 17,500 psi. Thus, the strength and stiffness of the strata surrounding the Pocahontas No. 3 Coalbed are uncommonly high for coal measure rocks (table A.2). Similarly, high strength and stiffness properties were reported by Iannacchione, et al. (1987) for the strata surrounding the Pocahontas No. 4 Coalbed in bump-prone areas.

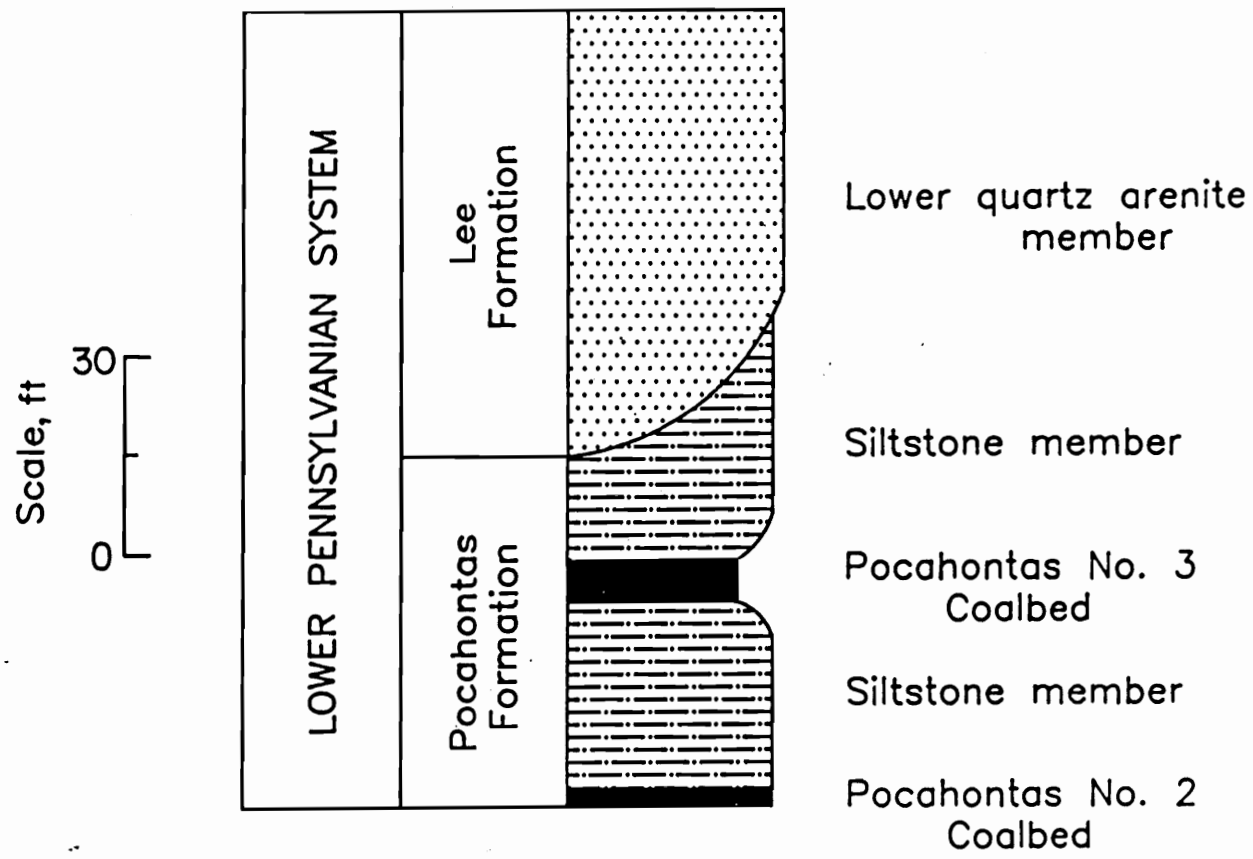

Figure A.14—Generalized stratigraphic column, VP No. 3 Mine (After Campoli, et al., 1993).

A section of the mine plan showing the 6, 7, and 8 development gate entry systems is presented in figure A.15. All of the gate entry systems in this mine are of a conventional design. Conventional designs are intended to support a major portion of abutment load resulting from adjacent gob formation. This is in contrast to an all yield design that immediately transfers abutment load to the longwall panel during adjacent panel mining. Figure A.15 also displays the variations in the overburden, siltstone immediate roof and quartzite main roof thicknesses directly above the 6, 7, and 8 development gate entry systems. The 5, 6, 7, and 8 panels are roughly 600-ft-wide and 6,000-ft-long. The first detailed study area, located in the 7 development gate entry system, is centered approximately 4,700 ft from the start-up entry of panel S-6, under approximately 1,950 ft of overburden. The 8 development gate entry system detailed study area is centered approximately 4,600 ft from the start-up entry of panel S-7, under approximately 2,050 ft of overburden. Thus, the two study areas are located adjacent to each other on opposite sides of panel S-7. This juxtaposition of these two strategically different gate entry system designs in highly stressed strata provided a unique opportunity for obtaining a better understanding of the strata movements and coal behavior associated with the bump phenomena.

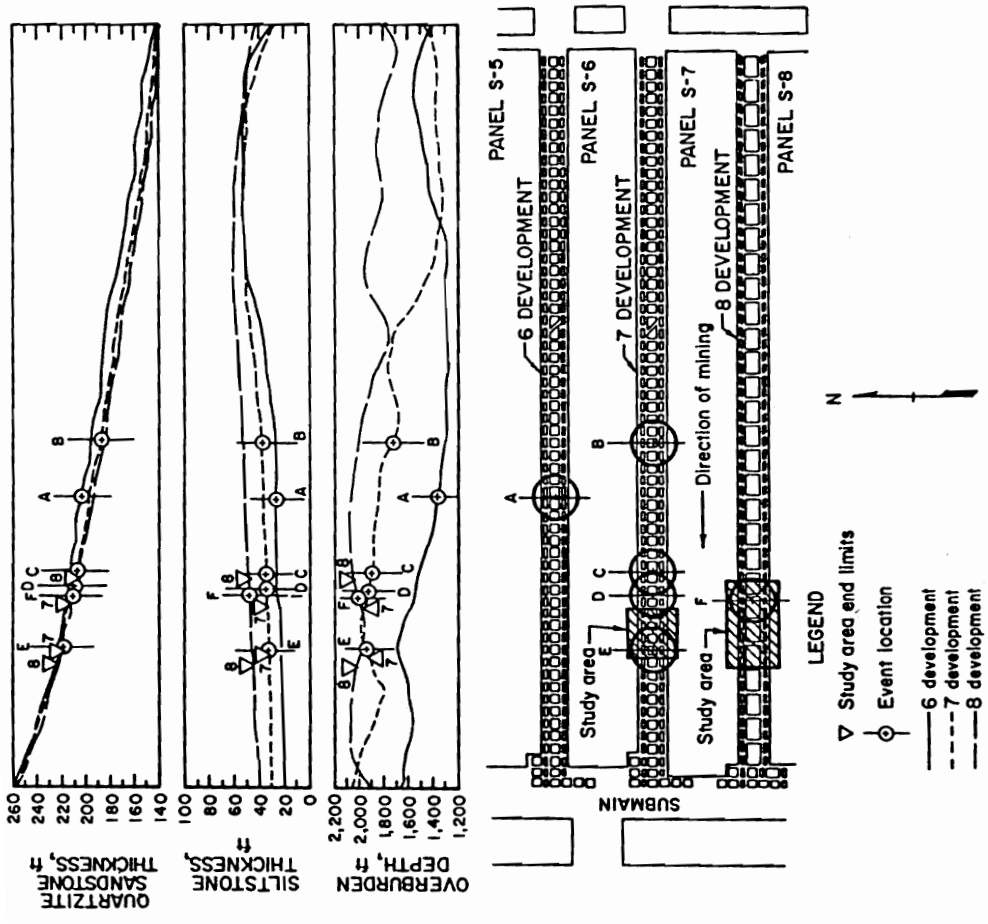

Figure A.15—Superjacent strata conditions over the 6, 7, and 8 development gate entry systems, VP No. 3 Mine (After Barton, et al., 1992).

TABLE A.2—Mean value of strata physical properties from surface corehole, S-9 panel, VP No. 3 Mine.

Strata type	Compressive Strength (psi)	Young's modulus[1] (10^6 psi)	Poission's ratio[1]	RQD %
Crystallized crossbedded sandstone	28,590 (25)[2]	-	-	-
Crystallized massive sandstone	32,210 (4)	-	-	-
Crystallized quartz pebble conglomerate	24,660 (5)	-	-	-
Crystallized sandstone with shale streaks	29,580 (12)	7.67 (3)	0.89 (3)	98.9 (8)
Crossbedded sandstone	20,820 (9)	-	-	100 (4)
Massive sandstone	24,170 (9)	6.12 (3)	0.16 (3)	100 (8)
Sandstone with shale streaks	20,370 (14)	6.03 (3)	0.15 (3)	100 (12)
Sandy shale	18,390 (17)	5.26 (5)	0.29 (5)	100 (10)
Shale with sandstone streaks	17,500 (2)	-	-	100 (4)
Dark grey shale	10,710 (2)	-	-	100 (1)

[1]Tangent (calculated at 50 pct of ultimate strength).
[2]Number of samples tested.

A.3.1 Bump Events in 6 and 7 Development

The 6 and 7 development gate entry systems employed a 218-ft-wide yield-abutment-yield configuration with the yield pillars on 50-ft centers, the abutment pillars on 100-ft centers, and all crosscuts on 100-ft centers. This gate pillar configuration replaced an older yield-yield-abutment design in which the same size pillars were employed; however, in the older design, the tailgate abutment pillar was located directly adjacent to the mined panel. In this previous design, the 80-ft-square pillars frequently experienced heavy bumps directly adjacent to the tail drive causing coal to be thrown into the face area (Campoli, et al., 1987). However, in the yield-abutment-yield design, the 80 by 30 ft pillars reached their maximum load bearing capacity and began to yield during the headgate pass of the face, thereby, eliminating their potential to bump. The yielded pillars effectively shield workmen from coal thrown in the event the 80 by 80 ft tailgate abutment pillar bumps during the subsequent tailgate pass.

Abutment pillar bumps began to occur adjacent to the tail drive within the 6 development gate entry system when 3,650 ft of panel S-6 had been mined. The bump area, labeled A, was under 1,350 ft of overburden, 27 ft of sandy shale immediate roof, and 230 ft of quartzite main roof (fig. A.15). Only slight movement of the face was observed on the tailgate end of the face line. Dramatic coal displacements were observed within the tailgate (fig. A.16). No coal was disturbed in the headgate, in this, or any of the bumps investigated during this study. The tailgate entry contained a double row of wooden cribs. The fresh air intake entry, labeled as

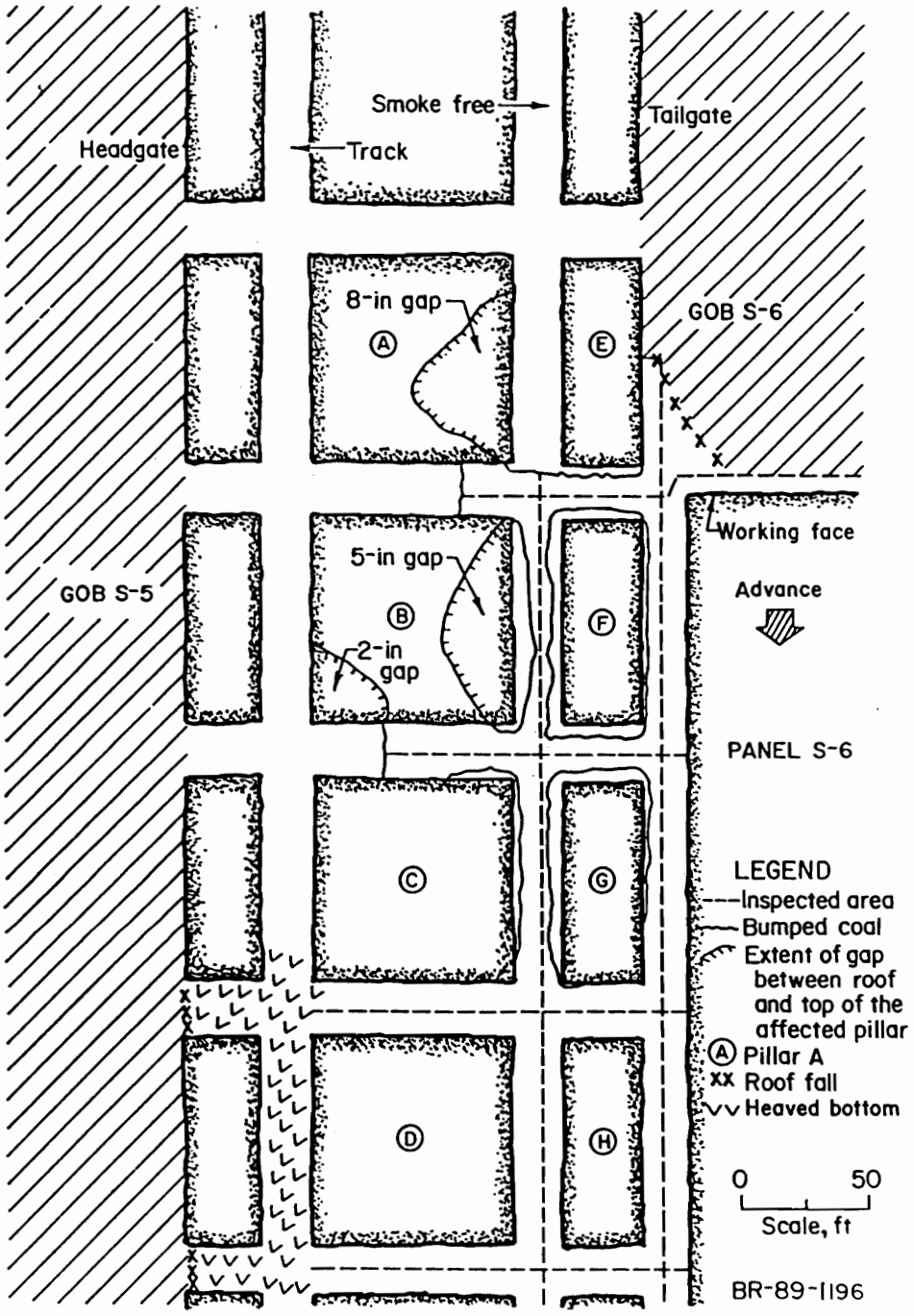

Figure A.16-Plan view of bump A within the 6 development gate entry system, VP No. 3 Mine (After Campoli, et al., 1990a).

the smoke-free, was supported by a double row of wooden posts which allowed the area to be explored to the extent noted on figure A.16.

The shearer was cutting coal, near the tailgate side of panels S-6 when bump A took place. None of the members of the face crew were injured; but they reported experiencing the shock wave released by the bump. Ventilation devices located at the mouth of 6 development over 2,000 ft away, were damaged.

Tailgate abutment pillar bumps, similar in magnitude to the 6 development event (bump A) just described, occurred during the mining of panel S-7. However, abutment pillar bumping (bump B) began approximately 450 ft earlier in panel mining. The B bump area was under 1,720 ft of overburden, 37 ft of sandy shale immediate roof, and 188 ft of quartzite main roof (fig. A.15) while the A bump area was under 1,350 ft of overburden, 27 ft of sandy shale immediate roof, and 203 ft of quartzite main roof.

As the mining of panel S-7 progressed, the tailgate abutment pillars began progressively bumping 500 ft in advance of the longwall face. This violent failure of the tailgate abutment pillars transferred load to panel S-7, initiating the occurrence of bumps on the tailgate corner of the longwall panel. Two of the face bumps, labeled C and D, were significant events which affected normal operations (fig. A.15). The C and D bump events occurred after panel S-7 was mined to 4,240 and 4,430 ft, respectively. Also, it is interesting that these bumps occurred at the crosscut in the tailgate. A plan view of the C bump site is presented as figure A.17. Both face bumps happened when the shearer was cutting from the head to the tail, in the area 20

to 40 ft from the tailgate corner of panel S-7. In bump D, the force of the bump lifted the panline and thrust it toward the gob. In both the C an D bumps, the rib of panel S-7 panel threw coal into the tailgate entry for approximately 40 ft. Ventilation devices in the tailgate were not affected in either the C or D face bumps, indicating that abutment pillar bump events in the tailgate did not occur simultaneously with the face bumps.

A visual inspection of the pillar conditions in the tailgate after face bump C indicates that the load-bearing capacity of abutment pillars A through F was destroyed prior to face bump C's occurrence (fig. A.17). This failed condition is assumed for pillar C, as it could not be inspected. The entry between pillars B and I was completely closed by abutment pillar B's bumping, making travel down the smoke-free entry impossible. The area containing abutment pillars G, F, and E was inspected by approaching the C bump site from the submain. The entry between pillars D and K was not traveled. Figure A.18 shows the condition of the completely closed entry between abutment pillars F and E. Note, that the posts in neither entry were broken by roof-to-floor convergence indicating the main overburden load is supported by panel S-7. Consequently, the abutment pillars would not be expected to deform or punch into the bottom.

After the D bump, the tail of the face was kept 10 ft in advance of the head as much as possible. This procedure was implemented to decrease the stress concentration on the tail by redistributing stresses toward the head. It cannot be ascertained if the tail advancement procedure had the desired effect. Subsequent to

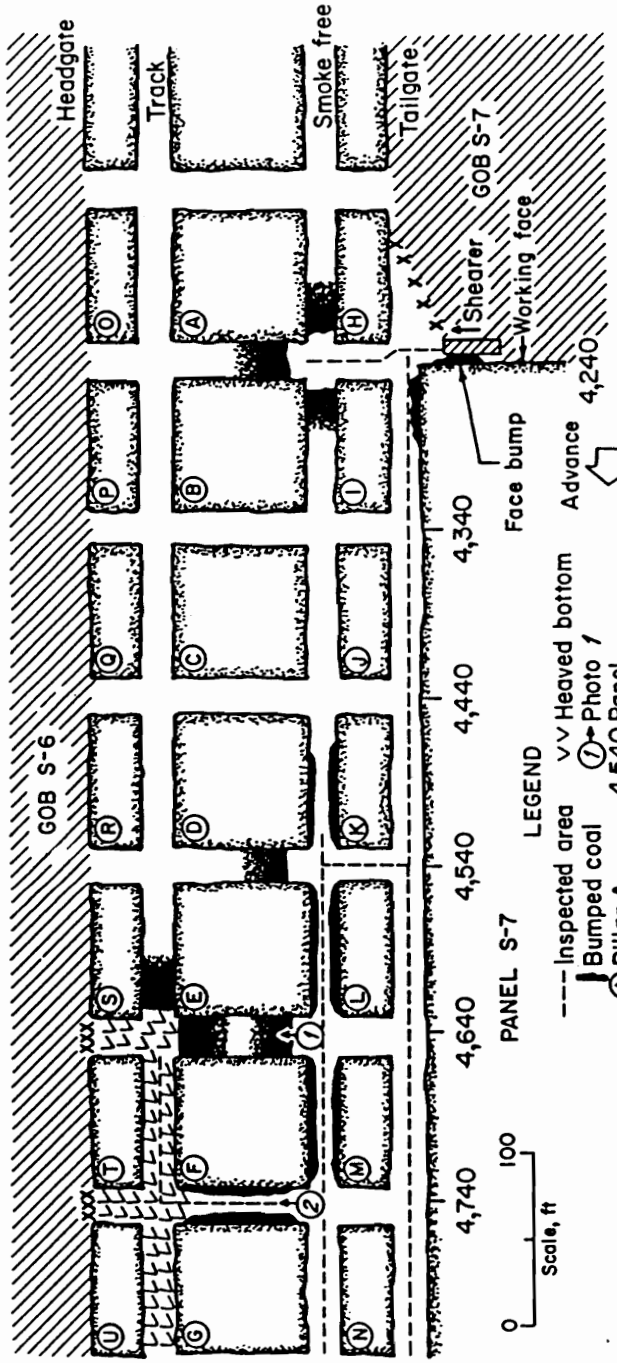

Figure A.17—Plan view of bump C within the 7 development gate entry system. Circled italic numbers denote location from which photographs were taken, VP No. 3 Mine (After Campoli, et al., 1990a).

Figure A.18—Condition of crosscut between pillars E and F, location 1, fig. A.17, VP No. 3 Mine (After Campoli, et al., 1990a).

the D bump, the shearer was operated remotely during panel S-7 mining. This procedure was a very positive step, as it allowed the longwall to advance to the completion of panel S-7 without further major face bump delays.

An abutment pillar bump (bump E) similar to bumps at sites A and B was experienced after 4,860 ft of panel S-7 had been mined. Tailgate ventilation devices were affected. This bump is significant, in that, it marks the return to tailgate abutment pillar failure adjacent to or on the gob side of the longwall face. This reduction in the magnitude of the bump events may be due to the now nearby barrier pillars. These barriers are left to protect the submain entries from gob abutment loading.

A.3.2 Ground Control Experience in 8 Development

In an attempt to better control ventilation between previous and active gobs, to improve tailgate entry stability, to control tailgate bumps, and to standardize gate entry system design, the mine modified the yield-abutment-yield configuration for the 8 development gate entry system. This new 238-ft-wide design consists of yield pillars on 40 ft centers and abutment pillars on 140 ft centers. Between the yield pillars, the crosscuts were driven at a 60-degree angle on 100-ft centers, whereas between the abutment pillars the crosscuts were driven at a 90-degree angle on 200-ft centers. This layout results in 20 by 80 ft yield pillars on either side of a 120 by 180 ft abutment pillar. The larger abutment pillars in this new design are intended to support the applied abutment loads, and thus, prevent the ground stresses from

overriding the longwall face. Gauna, et al., (1988) reports the new design requires less entry be mined to advance the entire section which represents an improvement through reduced mining requirements. However, leaving a larger pillar in the gob decreases slightly the extraction rate. Continuous miner coal production rates were not affected negatively by the design change.

The comparison of the geologic and mine geometry conditions at the 6 development A bump site and the 7 development B bump site, pointed to the importance of overburden thickness as the major factor determining bump-proneness. This factor indicates a more severe tailgate bump problem should have developed during the mining of panel S-8 than was experienced during the just described mining of panel S-7 (fig. A.15). The quartzite thickness in the main roof is extremely consistent over the 6, 7, and 8 development gate entry systems. Siltstone immediate roof thickness is greatest over the 8 development gate entry system. However, a 37 pct increase in siltstone immediate roof thickness from bump site A to B apparently did not have this effect. Furthermore, the immediate roof-and-floor within the 8 development gate entry system are comprised of extremely competent rock types which can be classified as bump prone (Campoli, et al., 1990a).

The structural rigidity of the immediate roof and bottom within the 8 development gate entry system was confirmed by the conditions at site F (fig. A.19). The length of active gob at site F is equivalent to that at bump site D in the 7 development gate entry system (fig. A.15). Excellent roof and minimal bottom heave were encountered in the tailgate entry even with the face (fig. A.20). Spalling of the

8 panel rib into the tailgate entry was evident over approximately the first 40 ft in advance of the face. Minor instability was encountered during the mining of the face, in the area 20 to 40 ft from the panel S-8 tailgate corner (fig. A.19). Coal cutting induced cracking and minor spalling of the face, indicating stress readjustment was taking place. While this minor face instability was slight as compared with face bumps C and D, it is important to the subsequent analysis of pillar behavior under high stress. The tailgate entry 200 ft in advance of the face was undisturbed by the mining of panel S-8.

Heaved bottom was found at or behind the face in the smoke-free entry (fig. A.21). Bumping of abutment pillar A was noted approximately 100 ft behind the face (fig. A.19). It appears that the 120 by 180 ft abutment pillars form a solid column that punches into the mine floor, when they are subjected to high abutment zone stresses. However, the bottom appears to fail in a brittle fashion (fig. A.21). The smoke-free entry and the abutment pillar crosscut, 200 ft in advance of the face, were undisturbed by the mining of panel S-8. Continuous roof-to-floor convergence data, obtained by a data acquisition system, confirmed that abutment pillar bumping did not close the smoke-free entry, as far as 200 ft behind the face. The majority of the crosscut between abutment pillars B and C, unchanged since the completion of panel S-7, displayed minimal bottom heave (fig. A.22). However, the last 15 to 20 ft of the crosscut on the gob side experienced bottom heave, which resulted in approximately 15 in of roof-to-floor convergence, during the mining of panel S-7. Similar bottom heave behavior was found in the track entry and the yield pillar

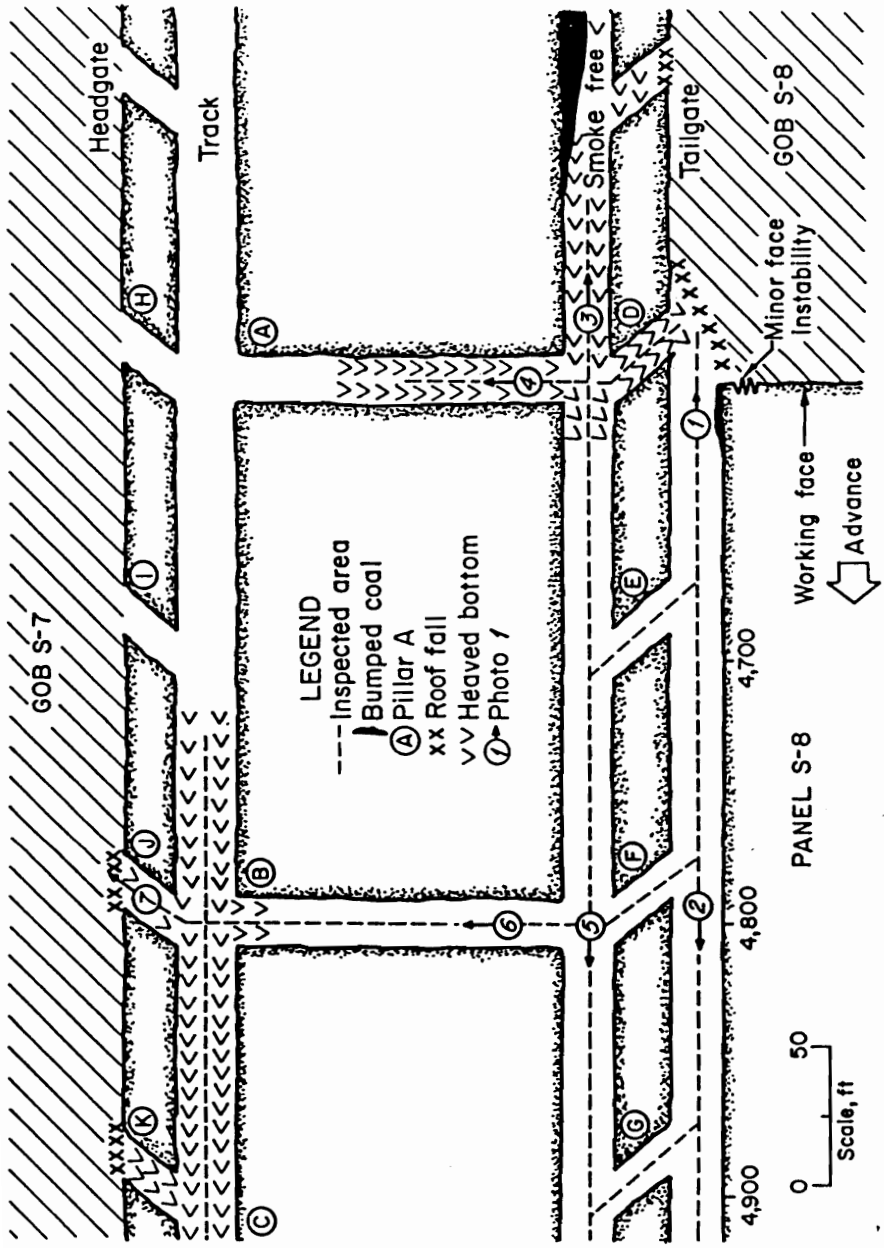

Figure A.19—Plan view of conditions at site F, within the 8 development detailed study area. Circled italic numbers denote location from which photographs were taken, VP No. 3 Mine (After Campoli, et al., 1990a).

Figure A.20—Tail entry directly in advance of tail shield, location 1, fig. A.19, VP No. 3 Mine (After Campoli, et al., 1990a).

crosscuts. The good roof conditions directly adjacent to the panel S-7 gob, at the crosscut between yield pillars K and J (fig. A.23), are representative of the entire study area.

The superior performance of the 8 development gate entry system design over the previous design was confirmed by inmine observations. Under worst case conditions, the 120 by 180 ft abutment pillars did not begin to bump until they were approximately 100 ft behind the face. The previously employed 80-ft-square abutment pillars bumped 500 ft in advance of the face, allowing load transfer to the mined panel. Thus, the 180 by 120 ft abutment pillars, within the 8 development gate entry system, effectively shielded the panel S-8 from the excess loads that resulted in the face bumps at the tailgate corner of panel S-7. The performance of the subsequent gate entry systems employing the improved design equaled success of the 8 development gate entry system.

A.3.3 Instrumentation Response

The effect of the two designs on gate road stability and bump occurrence was evaluated through the three instrument arrays and inmine observations. The state-of-the-art instrumentation arrays consisted of stainless steel borehole platened flatjacks (BPF) for indicating changes in pillar stress, coal extensometers for measuring

Figure A.21—Brittle failure of bottom in smoke-free entry adjacent to mining of panel S-8, location 3, fig. A.19, VP No. 3 Mine (After Campoli, et al., 1990a).

Figure A.22—Abutment pillar crosscut 200 ft in advance of mining panel S-8, location 6, fig. A.19, VP No. 3 Mine (After Campoli, et al., 1990a).

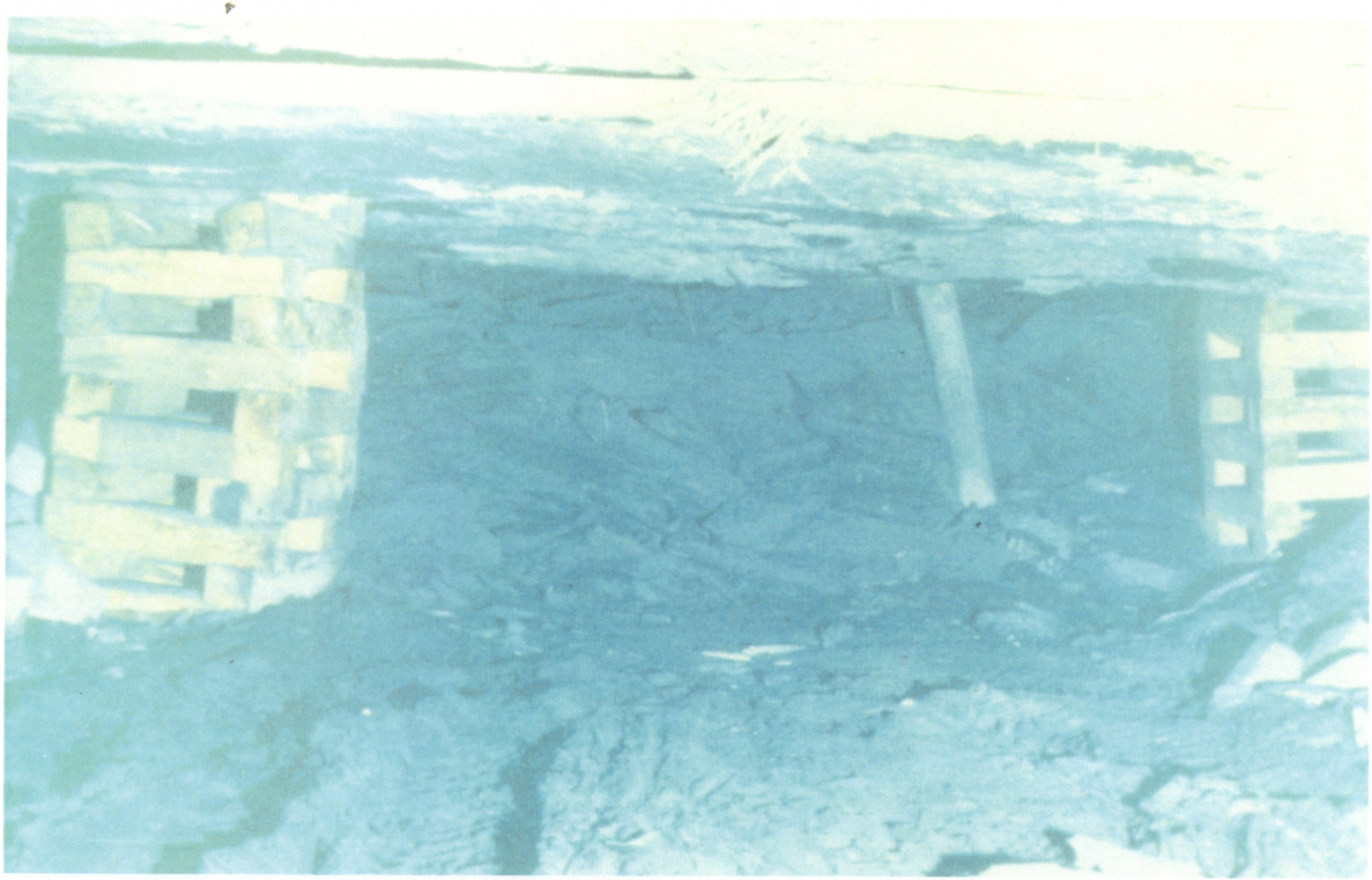

Figure A.23—Edge of panel S-7 gob 200 ft in advance of mining panel S-8, location 7, fig. A.19, VP No. 3 Mine (After Campoli, et al., 1990a).

pillar dilation, convergence stations for measuring roof-to-floor closure, differential roof-sag indicators, and differential floor-heave indicators. Permissible data acquisition systems were employed to continuously monitor coalbed stress and roof-to-floor convergence instrumentation in hazardous areas.

Coalbed stress change data revealed that the yield pillars in both designs failed during the extraction of the headgate panel. Roof-to-floor convergence, coal extensometer response, and coalbed stress change data effectively isolated the timing of abutment pillar failure in both gate road designs. The 80 ft square abutment pillars within the 7 development study area partially failed after the headgate pass was complete, reached their maximum load bearing capacity 1,000 ft in advance of the tailgate pass, and began bumping 500 ft in advance of the longwall face. This violent failure of the tailgate abutment pillars resulted in load transfer to panel 7, and the occurrence of bumps on the tailgate corner of the longwall face. The 120 by 180 ft abutment pillars within the 8 and 10 development study areas reached their maximum load bearing capacity 200 ft in advance of the mining of the tailgate pass and did not bump until they were approximately 100 ft into the gob. Thus, the new design effectively shields the working face from excessive loading. This was confirmed by coalbed stress change data taken from the tailside edge of panel 8 and the lack of face bumps during the mining of panels 8, 9, and 10.

The hydraulic pressure output from the BPF were converted to an approximation of the in situ coalbed stress by the BPFCAL computer program developed by Heasley (1989). The average change in abutment pillar stress induced

by the headgate pass was approximately 6,000 psi for both designs. The peak core stress of both designs was approximately 8,000 psi. However, the yielding of the inner core of the 120 by 180 ft abutment pillars occurred long after the yielding of 80 ft square abutment pillars.

Coal extensometers demonstrated that the abutment pillars of both designs formed a 15-ft-wide yielded perimeter zone. The coalbed stress instrumentation also indicated that the depth of the yield zone was 15 ft. The average stress across the yield zone was approximately 3,000 psi. It is suggested by this study, that 15 ft is the width of the yield zone in Pocahontas No. 3 Coalbed pillars at ultimate strength and that width does not significantly change when the two dimensional size is increased. Therefore, any increase in pillar size should result in a direct increase in confined core size. Based on the 15-ft-wide confinement zone, the ratio of maximum stress core area to original pillar area for the 80 ft square and 120 by 180 ft abutment pillars is 0.39 and 0.63, respectively. A 270 pct increase in confined core functional bearing area per lineal ft of gate road length reduced abutment pillar stress and deformation, mitigated load transfer to the tailgate corner of the mined panel, and successfully eliminated the anticipated face bumps similar to those experienced during the mining of panel 7 (Campoli, et al., 1990a).

3.4 Case Study Conclusions

The following conclusions can be drawn from the above case studies:

1) Room-and-pillar retreat mining under bump prone geologic conditions can present a severe and life threatening hazard.

2) Stiff immediate associated strata, especially the first 25 ft of mine roof and first 10 ft of mine floor are associated with coal mine bumps.

3) Pillars greater than 90 by 90 ft require multiple working places in a single pillar and should be avoided, as bumps are triggered by mining induced stress adjustment.

4) Pillars within total extraction areas must be uniform in size and shape.

5) Coalbeds of many thicknesses and strength characteristics can be made to bump if overstressed and confined within stiff immediate associated strata.

6) Pillar lines should be as straight as possible, avoiding stress concentration points at the intersection of gob areas.

7) Simultaneous mining of multiple pillar rows can spread abutment loads outbye the pillar line, at the expense of productivity and efficiency.

8) The yield zone in 6 ft thick Pocahontas No. 3 Coalbed and Pocahontas No. 4 Coalbed pillars at ultimate strength is 15 ft wide, and this width does not significantly change with changes in lateral pillar size.

9) The yield zone surrounded a confined pillar core and the size of this area was the primary consideration in determining coal pillar strength.

10) The stress of the yield zone and confined core at peak strength were approximately 3,000 and 8,000 psi, respectively.

11) Abutment pillars placed between total extraction zones can successful shield total extraction zones.

Appendix B

EXAMPLE LAYOUT RUN

LAYOUT is a design procedure for room-and-pillar retreat mining which results in supercritical or subcritical width sections separated by continuous barrier pillars. Both the supercritical and subcritical sections contain uniformly sized total extraction pillars. However, the width of subcritical sections are limited due to ground control considerations.

SUPERCRITICAL WIDTH SECTION DESIGN

Data Input

Immediate roof

If first 25 ft of the roof directly above the coalbed contains greater than 60 percent sandstone, continue.

If first 25 ft of the roof directly above the coalbed consists of laminated siltstones and shales and/or clay layers that break easily, coal mine bumps are not a design criteria: exit program now.

Immediate floor

If the first 10 ft of immediate floor consists of hard shales and/or sandstones, that do not heave readily, continue.

If the first 10 ft of immediate floor consists of soft shales and/or clays that readily heave coal mine bumps are not a design criteria: exit program now.

Overburden

Enter the depth of overburden to the nearest foot in cell C59.

1500 ft

Coalbed

Enter the thickness of the coalbed to the nearest tenth of a foot in cell C64.

7 ft

Abutment load approximation

Enter the linear shear angle to the nearest degree in cell C69.

21 degrees

Pillar dimensions

Enter the pillar dimension parallel to the gob line, to the nearest foot, in cell C74.

70 ft

Enter the pillar dimension perpendicular to the gob line, to the nearest foot, in cell C82.

90 ft

Total Extraction Pillar Strength

Perimeter

The area of the yielded perimeter is calculated based on the pillar dimensions and the coalbed height. The perimeter area is displayed in cell C96, to the nearest square foot.

4375 sq. ft

Enter the assumed strength of the yielded pillar perimeter, to the nearest psi, in cell C100.

3000 psi

Core

The area of the confined core is calculated based on the pillar dimensions and the coalbed height. The confined core area is displayed in cell C107, to the nearest square foot.

1925 sq. ft

Enter the assumed strength of the confined pillar core, to the nearest psi, in cell C111.

8000 psi

Peak Strength

The load bearing capacity of the total extraction pillar at peak strength is displayed, in pounds, in cell C117.

4.11e+09 lb.

Pillar Loads

Development Load

The tributary area method is employed to approximate the development load. Based on the overburden depth and pillar dimensions the development load is displayed, in pounds, in cell C129.

2.41e+09 lb.

Abutment Load

A linear shear angle concept is employed to approximate the front abutment load. Based on the overburden depth, overburden mechanical, properties, and pillar dimensions. The total abutment load, in pounds, is displayed in cell C137.

6.30e+09 lb.

The distance the total abutment load is spread is dependent on the depth of overburden and is displayed, in feet, in cell C142.

360.2 ft

First Pillar Row

The abutment load on the first pillar row outbye the expanding gob, in pounds, is displayed in cell C148.

3.92e+09 lb.

Second Pillar Row

The abutment load on the second pillar row outbye the expanding gob, in pounds, is displayed in cell C154.

1.92e+09 lb.

Pillar Stability Factor

The load bearing capacity at peak strength divided by the combination of development load and abutment load is called the stability factor. A stability factor of unity indicates the strength of the pillar equals the load applied. A stability factor greater than unity indicates the strength of the pillar exceeds the load applied and thus will not yield or bump.

First Pillar Row

Stability factor =0.65

PILLAR ROW UNSTABLE

Second Pillar Row

Stability factor =0.95

PILLAR ROW UNSTABLE

Barrier Pillar Width

Suggested barrier pillar widths were determined from the Ashley or Mine Inspectors formula:

$$W = 20 + 4T + 0.1D$$

Where W is the barrier pillar width, T is the coalbed thickness, and D is the overburden thickness.

The barrier pillar width suggested for the above input data is displayed, to the nearest ft, in cell C187.

198 ft

If the above supercritical design procedure results in stability factor less than one, push the [home] key to return to the beginning of the program to investigate the effect of larger pillars or continue to investigate a possible subcritical width design.

THE STABILITY FACTORS OF_ FOR THE FIRST AND SECOND PILLAR ROWS ARE BOTH LESS THAN ONE. THUS, THE EXAMPLE CONTINUES INTO THE SUBCRITICAL DESIGN PROCEDURE

SUBCRITICAL WIDTH SECTION DESIGN

The MULSIM/NL parametric studies varied the overburden depth and section configuration in a 6 ft thick coalbed. Sections composed of 70 by 70 ft total extraction pillars separated by continuous barrier pillars were prescribed for overburden depths from 1,000 to 2,200 ft, at 200 ft intervals. The required abutment pillar width increases with depth while the section width decreases with depth.

Overburden Depth (ft)	Panel Width (# pillars)	Barrier Width (ft)
1000	unlimited	70
1200	8	70
1400	8	158
1600	7	158
1800	6	158
2000	6	246
2200	5	246

Increases in coalbed thickness decrease coal pillar strength and thus reduce the permissible overburden thickness for a given design; decreases in coalbed thickness have the opposite effect.

LAYOUT extrapolates the 6 ft thick coalbed results to account for variation in coalbed thickness. This is accomplished in a two step process. First, the barrier pillar width is assumed to follow a linear relationship with depth. Second, the width of the section is controlled by the strength of the total extraction pillar (70 by 70 ft) as compared to the 6 ft thick coalbed case.

Data Input

Overburden

Enter the depth of overburden to the nearest foot in cell C239.

1500 ft

Coalbed

Enter the thickness of the coalbed to the nearest tenth of a foot in cell C244.

7 ft

Barrier Pillar Width

The barrier pillar widths suggested by the MULSIM parametric study are less conservative than the Ashley or Mine Inspector's formula:

$$W = 20 + 4T + 0.1D$$

Where W is the barrier pillar width, T is the coalbed thickness, and D is the overburden thickness.

To view a graph comparing the two approximations of barrier pillar width required, for a 6 ft thick coalbed, enter [/gv]. Because the Ashley formula is more conservative, it is employed in this analysis.

The barrier pillar width suggested for the above input data is displayed, to the nearest ft, in cell C263.

198 ft

Section Width

The MULSIM parametric study was conducted with 70 by 70 ft total extraction pillars. The section width was specified in multiples of these pillars. The 70 by 70 ft pillar was shown to be interchangeable with the 60 by 80 ft pillar, as the strength of these pillars are near identical. Thus, the 60 by 80 ft design may be substituted if mobile roof supports are to be employed.

A linear equation was fit to the MULSIM parametric study output with a R squared correlation of 99.6%. The equation is:

$$P = 0.00321D + 12.1$$

Where P is the number of pillars across the section width and D is the overburden thickness. Recall, this equation applies in a 6 ft thick coalbed.

LAYOUT modifies the output of the above equation to account for variation in coalbed thickness. This is accomplished by multiplying the equation's prediction by the ratio of the total extraction peak pillar strength for the specified coalbed thickness and a 6 ft thick coalbed.

Total Extraction Pillar Strength Ratio

The peak strength of a 70 by 70 ft pillar, based on the assumptions employed in the supercritical design section and the specified coalbed thickness, is displayed in cell C298 in pounds.

3.00e+09 lb

The peak strength of a 70 by 70 ft pillar, based on the assumptions employed in the supercritical design section in a 6 ft thick coalbed is displayed in cell C304 in pounds.

3.27e+09 lb.

Section Width

The width of the section, in multiples of either 70 ft square or 60 by 80 ft, in displayed in cell C310.

7 Pillars

The suggestions of Layout should be considered to be the first step in the design process, a guide to formulating the initial full scale underground section design. Once a specific design is implemented, the in-mine strata reaction to panel extraction becomes the crucial input for subsequent section design.

VITA

Alan A. Campoli, the son of Angelo D. and Rita M. Campoli, was born in Kane, PA on July 4, 1956. Mr. Campoli received his secondary education in Greensburg, PA at Hempfield Area High School, graduating in 1974. Immediately thereafter, he began part-time studies at the University of Pittsburgh. He graduated Cumlaude with a B.S.E. in Mining Engineering in 1981 and Summa Cumlaude with a M.S.E. in Engineering Management in 1984, both from the University of Pittsburgh. Mr. Campoli was a coal miner at the Crescent Hills Coal Company in California, PA from 1977 to 1979. He has been an employee of the United States Bureau of Mines, Pittsburgh Research Center, Ground and Methane Control group since 1979. Mr. Campoli is a Registered Professional Engineer in Pennsylvania; a former Chairman of the Pittsburgh Section of the Society for Mining, Metallurgy, and Exploration, Inc.; and a Certified Mine Foreman in Virginia and West Virginia. He has been a technical project leader for research on coal mine bump control, cross-measure methane drainage systems, coal and gas outbursts, and methane drainage pipeline safety. He became a PhD Candidate in Mining Engineering at Virginia Polytechnic Institute and State University in January 1992, and will complete the requirements of that degree in May 1994.